



UNIVERSIDAD  
DE BURGOS

DEPARTAMENTO DE BIOTECNOLOGÍA Y CIENCIA DE LOS ALIMENTOS

# Fish oil valorization using supercritical carbon dioxide technologies

PHD THESIS

Valorización de aceite de pescado mediante  
tecnologías de dióxido de carbono supercrítico

TESIS DOCTORAL

Rodrigo Melgosa Gómez

Burgos, 2018

# Fish oil valorization using supercritical carbon dioxide technologies

Valorización de aceite de pescado mediante tecnologías de dióxido de carbono supercrítico

MEMORIA QUE PARA OPTAR AL GRADO DE DOCTOR POR LA UNIVERSIDAD DE BURGOS EN EL PROGRAMA DE AVANCES EN CIENCIA Y BIOTECNOLOGÍA ALIMENTARIAS PRESENTA:

Rodrigo Melgosa Gómez

Burgos, 2018



**UNIVERSIDAD  
DE BURGOS**

LA PRESENTE TESIS DOCTORAL QUEDA  
REGISTRADA EN EL FOLIO N° ..... DEL  
CORRESPONDIENTE LIBRO DE REGISTROS,  
CON EL N° .....

En Burgos, a ..... de ..... de 2018

El Encargado del Registro



UNIVERSIDAD  
DE BURGOS

DEPARTAMENTO DE BIOTECNOLOGÍA Y CIENCIA DE LOS ALIMENTOS

Dña. MARÍA TERESA SANZ DÍEZ y Dña. SAGRARIO BELTRÁN CALVO,  
Profesoras del Departamento de Biotecnología y Ciencia de los Alimentos de la  
Universidad de Burgos,

CERTIFICAN:

que el graduado en Ciencia y Tecnología de los Alimentos y Máster en Seguridad y Biotecnología Alimentarias D. Rodrigo Melgosa Gómez ha realizado bajo su dirección el trabajo titulado “Fish oil valorization using supercritical carbon dioxide technologies”, cuyo título en castellano es: “Valorización de aceite de pescado mediante tecnologías de dióxido de carbono supercrítico”.

Considerando que dicho trabajo reúne los requisitos exigidos para ser presentado como Tesis Doctoral, expresan su conformidad con dicha presentación.

Para que conste y surta los efectos oportunos, firman el presente certificado.

En Burgos, a 12 de marzo de 2018

Fdo.: María Teresa Sanz Díez

Fdo.: Sagrario Beltrán Calvo

Profesoras del Dpto. de Biotecnología y Ciencia de los Alimentos



**UNIVERSIDAD  
DE BURGOS**

**DEPARTAMENTO DE BIOTECNOLOGÍA Y CIENCIA DE LOS ALIMENTOS**

D. JOSÉ MANUEL BENITO MORENO, Coordinador del programa de Doctorado  
“Avances en Ciencia y Biotecnología Alimentarias” de la Universidad de Burgos,

**CERTIFICA:**

que la memoria titulada “Fish oil valorization using supercritical carbon dioxide technologies”, presentada por D. Rodrigo Melgosa Gómez, graduado en Ciencia y Tecnología de los Alimentos y Máster en Seguridad y Biotecnología Alimentarias, ha sido realizada en el Departamento de Biotecnología y Ciencia de los Alimentos bajo la dirección de las Dras. María Teresa Sanz Díez y Sagrario Beltrán Calvo, y en representación de la Comisión Académica del programa de Doctorado, autoriza su presentación para ser defendida como Tesis Doctoral.

Para que conste, y surta los efectos oportunos, firmo el presente certificado.

En Burgos, a 12 de marzo de 2018

Fdo.: José Manuel Benito Moreno

Coordinador del programa de Doctorado

## Acknowledgements

This work has been performed within the research group Industrial and Environmental Biotechnology, which is recognized by the University of Burgos (GIR-UBU BIOIND) and Junta de Castilla y León (Unidad de Investigación Consolidada UIC-128), in the frame of the research projects detailed below:

- SUPERCRITICAL FLUID PROCESSES APPLIED TO THE PRODUCTION AND SEPARATION OF ACYLGLYCERIDES ENRICHED IN OMEGA-3, financed by the Ministry of Economy and Competitiveness of Spain and the European Regional Development Fund.

**Ref.: CTQ2012-39131-C02-01**

- APPLICATION OF EMERGING TECHNOLOGIES TO THE FORMULATION OF BIOACTIVE COMPOUNDS OF INTEREST TO THE FOOD INDUSTRY, financed by Junta de Castilla y León and the European Regional Development Fund.

**Ref.: BU055U16**

Financial support of these public institutions is gratefully acknowledged.

I also owe my gratitude to the Ministry of Economy and Competitiveness for financing my predoctoral contract.

**Ref.: BES-2013-063937**

## Agradecimientos

Este trabajo ha sido realizado en el seno del grupo de investigación Biotecnología Industrial y Medioambiental reconocido por la Universidad de Burgos (GIR-UBU BIOIND) y por la Junta de Castilla y León como Unidad de Investigación Consolidada UIC-128, en el marco de los proyectos de investigación que a continuación se detallan:

- PROCESOS CON FLUIDOS SUPERCRÍTICOS APLICADOS A LA PRODUCCIÓN Y SEPARACIÓN DE ACILGLICÉRIDOS ENRIQUECIDOS EN OMEGA-3, financiado por el Ministerio de Economía y Competitividad y el Fondo Europeo de Desarrollo Regional.

**Ref.: CTQ2012-39131-C02-01**

- APLICACIÓN DE TECNOLOGÍAS EMERGENTES A LA FORMULACIÓN DE COMPUESTOS BIOACTIVOS DE INTERÉS PARA LA INDUSTRIA ALIMENTARIA, financiado por la Junta de Castilla y León y el Fondo Europeo de Desarrollo Regional.

**Ref.: BU055U16**

He de agradecer el apoyo económico recibido de estas instituciones públicas.

También he de expresar mi gratitud por el apoyo económico recibido del Ministerio de Economía y Competitividad a través de la financiación de mi contrato predoctoral.

**Ref.: BES-2013-063937**

*A las Dras. Sagrario Beltrán y María Teresa Sanz por su gran labor como directoras de esta Tesis. Gracias, sobre todo, por ser mucho más que eso. A Tere, por todo lo que me ha enseñado, por su enorme dedicación y su inestimable ayuda. A Sagrario, por darme la oportunidad de participar en este proyecto y creer en mí como futuro investigador.*

*A todos los compañeros del Área de Ingeniería Química que, desde que llegué para realizar mi TFG, me acogieron como un miembro más. En especial a Beti por su ayuda en el apartado analítico. También a Orlando por introducirme en el mundo supercrítico. A Sarai y María, por su apoyo técnico (y moral) y su disposición. A toda la gente con la que he coincidido durante estos años y han colaborado de una u otra forma en este trabajo. A Sara, Ángela, Liliana, Alba, Helios, Almudena, Daniela, Esther y Óscar.*

*A mis padres por inculcarme los valores de esfuerzo, constancia y humildad. A mi hermana Lara y a Dani por sus sabios consejos y, sobre todo, por su apoyo en los momentos más difíciles. A mi familia que siempre ha confiado en mi capacidad y me ha animado a afrontar este reto. En especial a mi abuelo, al que siempre tendré presente.*

*A mis amigos: Javi, Chavi, Jairo, Dani y Félix, por estar cerca en los momentos buenos y también en los menos buenos, aunque nos separen muchos kilómetros.*

*A Vanesa, por los nuevos comienzos.*

*A todos ellos, quiero dedicar esta Tesis.*

*Rodrigo*

Fish oil valorization using supercritical carbon dioxide technologies

# Table of Contents



## Table of contents of the PhD Thesis

Summary of the PhD Thesis .....	1
Introduction.....	7
Objectives .....	67
Results.....	73
Effects of supercritical carbon dioxide treatment on four commercial lipases.....	77
Phase behavior of the pseudo-ternary system carbon dioxide + ethanol + fish oil at high pressures.....	121
Supercritical carbon dioxide as solvent in the lipase-catalyzed ethanolsis of fish oil: kinetic study.....	159
Omega-3 encapsulation by PGSS-drying and conventional drying methods. Particle characterization and oxidative stability .....	209
Conclusions and Future Challenges.....	265
Appendix: Analytical Methods .....	273

Fish oil valorization using supercritical carbon dioxide technologies

# Summary



## Summary of the PhD Thesis

This PhD Thesis is focused on the application of supercritical fluid (SCF) technologies to the production and formulation of concentrates of omega-3 polyunsaturated fatty acids ( $n-3$  PUFAs).

In the last decades,  $n-3$  PUFAs have drawn the attention of pharmaceutical and food industries due to their well-known healthy effects. The main  $n-3$  PUFAs, namely eicosapentaenoic acid (C20:5  $n-3$ ; EPA) and docosahexaenoic acid (C22:6  $n-3$ , DHA), have demonstrated cardioprotective and anti-inflammatory effects. Besides, an adequate intake of  $n-3$  PUFAs, especially DHA, has been related to the normal function of brain and eyes in adults, and is recommended for the normal development of these organs in children. For these reasons, many food supplements and nutraceuticals are nowadays marketed, and the demand for  $n-3$  PUFA concentrates has steadily increased in the last years.

The main natural source of  $n-3$  PUFAs is fish oil, which is usually obtained as a low-value by-product in the fishery industry and primarily serves as feeding in fish farms. Therefore, valorization of fish oil, in order to obtain nutraceuticals and food supplements with high added value, constitutes a great yet challenging opportunity, since production of high-quality fish oil suitable for human consumption requires not only searching for raw materials rich in  $n-3$  PUFAs, but also developing industrially-feasible production and concentration methods that could yield less oxidized, highly-purified  $n-3$  PUFA concentrates.

Conventional production of  $n-3$  PUFA concentrates make use of non-environmentally friendly organic solvents and high temperatures that are detrimental to the easily-oxidizable  $n-3$  PUFAs. Alternatively, a biorefinery approach using SCF technologies can overcome these drawbacks. The latest advances in supercritical extraction and refining of fish oil, production of  $n-3$  PUFAs, concentration and purification, as well as formulation using SCF technologies enable the possibility of obtaining  $n-3$  PUFAs without solvent residues at mild, non-oxidative conditions.



Taking into account these considerations and the advantages of enzymatic and SCF technologies combined, this Thesis mainly investigates the production of *n*-3 PUFA by means of lipase-catalyzed ethanolysis of fish oil in supercritical carbon dioxide (SC-CO<sub>2</sub>) media.

The work is comprised both of basic and applied research, including the potential effects of SC-CO<sub>2</sub> exposure on several lipases that can be used in lipid biotransformations in SC-CO<sub>2</sub> media (Chapter 1), the experimental determination and modeling of phase equilibrium data of the carbon dioxide + ethanol + fish oil reaction system (Chapter 2), and a kinetic study of the enzymatic ethanolysis of fish oil in SC-CO<sub>2</sub>, catalyzed by the commercial lipase Lipozyme RM IM (Chapter 3). Additionally, this work provides an insight into the formulation of a commercial omega-3 concentrate by the supercritical encapsulation technology Particles from Gas-Saturated Solutions (PGSS)-drying, obtaining a solid powder with better stability against oxidation compared to conventional spray-drying (Chapter 4).

## Resumen general de la Tesis Doctoral

La presente Tesis Doctoral se centra en la aplicación de la tecnología de fluidos supercríticos (FSCs) para la producción y formulación de concentrados de ácidos grasos poliinsaturados omega 3 (AGPI  $n-3$ ).

En las últimas décadas, los AGPI  $n-3$  han captado la atención de las industrias farmacéutica y alimentaria debido a sus conocidas propiedades saludables. Numerosos estudios han demostrado que los principales AGPI  $n-3$ , concretamente los ácidos eicosapentanoico (C20:5  $n-3$ ; EPA) y docosahexanoico (C22:6  $n-3$ , DHA) presentan efectos cardioprotectores y antiinflamatorios. Además, una adecuada ingesta de AGPI  $n-3$ , especialmente DHA, es necesaria para la función normal de los ojos y el cerebro en adultos y está especialmente recomendada para el normal desarrollo de estos órganos en niños. Debido a esto, hoy en día se comercializan numerosos alimentos funcionales, suplementos alimenticios y nutracéuticos, y la demanda de concentrados de AGPI  $n-3$  no ha dejado de crecer en los últimos años.

La principal fuente natural de AGPI  $n-3$  es el aceite de pescado, que normalmente se obtiene como un subproducto en la industria de procesado de pescado y se destina principalmente para alimentación animal en piscifactorías, constituyendo un producto de bajo valor añadido. Por lo tanto, la valorización de aceite de pescado para obtener alimentos funcionales, suplementos alimenticios y nutracéuticos, constituye una gran oportunidad de negocio, pero también un importante desafío ya que la producción de aceite de pescado de alta calidad destinado a consumo humano no solo requiere de la búsqueda de buenas fuentes de AGPI  $n-3$ , sino también del desarrollo de métodos de obtención y concentración capaces de producir AGPI  $n-3$  con alta pureza y baja oxidación, y que además sean fáciles de implementar a escala industrial.

Los métodos convencionales de obtención de concentrados de AGPI  $n-3$  hacen uso de disolventes orgánicos perjudiciales para el medio ambiente, así como de altas

temperaturas que pueden degradar los fácilmente oxidables AGPI  $n-3$ . Alternativamente, el concepto de biorrefinería usando tecnologías de FSCs puede salvar estos inconvenientes. Los últimos avances en extracción y refinado supercrítico de aceite de pescado, en la producción, concentración y purificación de AGPI  $n-3$ , así como en la formulación de concentrados de AGPI  $n-3$  con FSCs, hacen posible la obtención de AGPI  $n-3$  sin residuos de disolventes y en condiciones suaves y no oxidativas.

Teniendo en cuenta estas consideraciones y las ventajas combinadas de las tecnologías enzimática y de FSCs, el principal objeto de investigación de la presente Tesis Doctoral es la producción de AGPI  $n-3$  mediante etanolisis de aceite de pescado catalizada enzimáticamente, utilizando dióxido de carbono supercrítico (CO<sub>2</sub>-SC) como medio de reacción.

El presente trabajo incluye tanto investigación básica como aplicada. Se han evaluado los efectos potenciales de la exposición al CO<sub>2</sub>-SC en varias lipasas comerciales usadas en la biotransformación de lípidos en CO<sub>2</sub>-SC (Capítulo 1), se han obtenido y modelado datos experimentales de equilibrio entre fases del sistema de reacción dióxido de carbono + etanol + aceite de pescado (Capítulo 2) y se ha realizado un estudio cinético de la reacción de etanolisis de aceite de pescado en CO<sub>2</sub>-SC catalizada por la lipasa inmovilizada comercial Lipozyme RM IM (Capítulo 3). Adicionalmente, en este trabajo se ha profundizado en la encapsulación supercrítica de un concentrado comercial de AGPI  $n-3$  mediante la tecnología *Particles from Gas-Saturated Solutions* (PGSS)-*drying*, obteniendo una formulación en forma de polvo sólido con una estabilidad oxidativa mejorada en comparación con la técnica convencional de spray-drying (Capítulo 4).

Fish oil valorization using supercritical carbon dioxide technologies

# Introduction





## Tables

<b>Table I-1.</b> EPA and DHA contents in some fish species (adapted from [22]). ....	20
<b>Table I-2.</b> Main fatty acids in fish oils from different species (adapted from [24]). .....	22
<b>Table I-3.</b> Comparison of most common techniques for $n-3$ PUFA fractionation and purification (adapted from [31]). .....	28
<b>Table I-4.</b> Comparison of physical properties of gases, liquids and supercritical fluids (SCF) (adapted from [74]). .....	32
<b>Table I-5.</b> Critical properties of different solvents (adapted from [76]) .....	33



## Figures

<b>Figure I-1.</b> Structural formulas for <i>all-cis</i> -9,12,15-octadecatrienoic acid ( $\alpha$ -linolenic acid, ALA, C18:3 <i>n</i> -3), <i>all-cis</i> -docosa-5,8,11,14,17-eicosapentaenoic acid (EPA, C20:5 <i>n</i> -3), and <i>all-cis</i> -docosa-4,7,10,13,16,19-hexaenoic acid (DHA, C22:6 <i>n</i> -3).....	16
<b>Figure I-2.</b> Essential fatty acid metabolism desaturation and elongation of <i>n</i> -6 and <i>n</i> -3 series (adapted from [3]). .....	17
<b>Figure I-3.</b> Flow diagram of the conventional wet pressing method to obtain crude fish oil at industrial scale (adapted from [25]). .....	21
<b>Figure I-4.</b> Transesterification reaction of triacylglycerides (TAG) with an alcohol producing fatty acid alkyl esters (FAAE) and glycerol. ....	26
<b>Figure I-5.</b> Schematic representation of lipid peroxidation (adapted from [1,45]). .....	29
<b>Figure I-6.</b> Phase diagram of carbon dioxide illustrating the supercritical region above the critical temperature ( $T_C$ ) and pressure ( $p_C$ ) (data taken from [75]). .....	31
<b>Figure I-7.</b> Global process to obtain <i>n</i> -3 PUFA concentrates from fish by-products as a solid powder. FFA: free fatty acids, SFA: saturated fatty acids. (adapted from [77]).....	34
<b>Figure I-8.</b> Schematic representation of the RESS process (adapted from [72]). .....	45
<b>Figure I-9.</b> Schematic representation of the SAS process (adapted from [155]). .....	46
<b>Figure I-10.</b> Schematic representation of the SFEE process (adapted from [157]). .....	47
<b>Figure I-11.</b> Pressure <i>vs.</i> composition (p-x) diagram of the fish oil + CO <sub>2</sub> system (experimental data taken from [80]). .....	48



## Figures (*continued*)

**Figure I-12.** Schematic representation of the PGSS process (adapted from [72]).....49

**Figure I-13.** Temperature vs. composition (T-x) diagram of the CO<sub>2</sub> + H<sub>2</sub>O system at p = 1 atm, calculated assuming ideal behavior of the gas phase. Operating conditions in the spray tower should lie above the dew line (adapted from [166]).....51



## 1. $n-3$ polyunsaturated fatty acids

Fatty acids are organic compounds formed by a carboxylic acid with a long aliphatic chain. Depending on the presence or absence of double covalent bonds between adjacent carbon atoms (e.g., saturations), fatty acids can be unsaturated or saturated (SFA), respectively. The former can be monounsaturated (MUFA) if they only present one double bond along its aliphatic chain, or polyunsaturated (PUFA) if they present two or more saturations [1].

The two carbon atoms in the chain that are bound next to either side of the double bond can occur in a *cis* or *trans* configuration.

### *cis*

A *cis* configuration means that the two hydrogen atoms adjacent to the double bond are on the same side of the chain. The rigidity of the double bond freezes its conformation and causes the chain to bend. The effect of this is that, in restricted environments, such as when fatty acids are part of a phospholipid in a lipid bilayer, or triglycerides in lipid droplets, *cis* bonds limit the ability of fatty acids to be closely packed, and therefore can affect the permeability of lipid membranes or the melting temperature of oils and fats.

### *trans*

On the other hand, a *trans* configuration means that the two hydrogen atoms adjacent to the double bond lie on opposite sides of the chain. As a result, they do not cause the chain to bend, being its shape similar to straight saturated fatty acids.

In most naturally occurring unsaturated fatty acids, each double bond in the aliphatic acid chain has three  $n$  carbon atoms after it, and all are *cis* bonds. The differences in geometry between saturated and unsaturated fatty acids, as well as the various types of unsaturated fatty acids, play an important role in biological processes and the construction of biological structures such as cell membranes. The *cis* unsaturated

fatty acids provide fluidity to triacyl-glycerol reserves and phospholipid membranes, and many serve as eicosanoid precursors (prostaglandins, prostacyclins, thromboxanes, and leukotrienes) with important biological functions [2]. Most fatty acids in the *trans* configuration are not found in nature and are the result of human processing (e.g., hydrogenation).

$n-x$  ( $n$  minus  $x$ ; also  $\omega-x$  or omega- $x$ ) refers to the location of the first double bond in unsaturated fatty acids, counting from the terminal methyl carbon of the compound (designated as  $n$  or  $\omega$ ) (Fig. I-1). The human metabolism cannot form double carbon bonds before the 9th carbon from the omega position ( $n-9$ ), so that essential fatty acids always present a double bond before the  $n-9$  position [2].

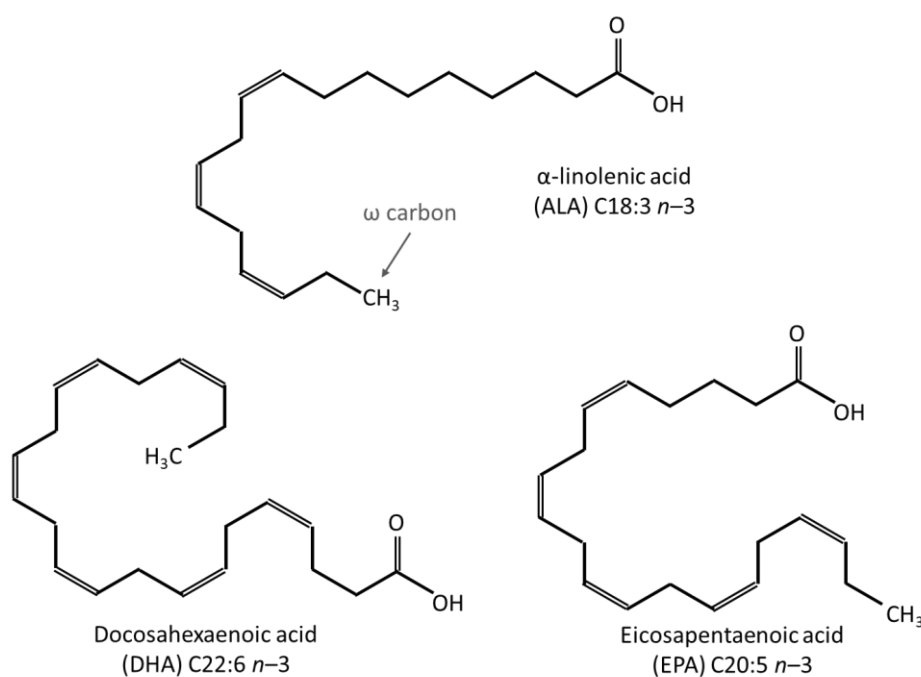


**Figure I-1.** Structural formulas for *all-cis*-9,12,15-octadecatrienoic acid ( $\alpha$ -linolenic acid, ALA, C18:3  $n-3$ ), *all-cis*-docosa-5,8,11,14,17-eicosapentaenoic acid (EPA, C20:5  $n-3$ ), and *all-cis*-docosa-4,7,10,13,16,19-hexaenoic acid (DHA, C22:6  $n-3$ ).



From a nutritional point of view, both  $n-3$  and  $n-6$  PUFAs are therefore essential fatty acids, and their requirements should be completely fulfilled from the diet in order to promote and preserve human health [3]. The parent omega-6 fatty acid is linoleic acid (C18:2  $n-6$ , LA) and the parent omega-3 fatty acid is  $\alpha$ -linolenic acid (C18:3  $n-3$ , ALA). Omega-6 fatty acids as arachidonic acid (C20:4  $n-6$ ; AA) can be synthesized by humans from LA, and omega-3 fatty acids, as eicosapentaenoic acid (C20:5  $n-3$ ; EPA), docosapentaenoic acid (C22:5  $n-3$ , DPA) and docosahexaenoic acid (C22:6  $n-3$ , DHA), from ALA (Fig. I-2); however, the conversion of ALA into its longer-chain homologues is too low to cover the requirements of the human metabolism, especially in developmental or disease conditions, thus EPA and DHA are considered as conditionally essential fatty acids.

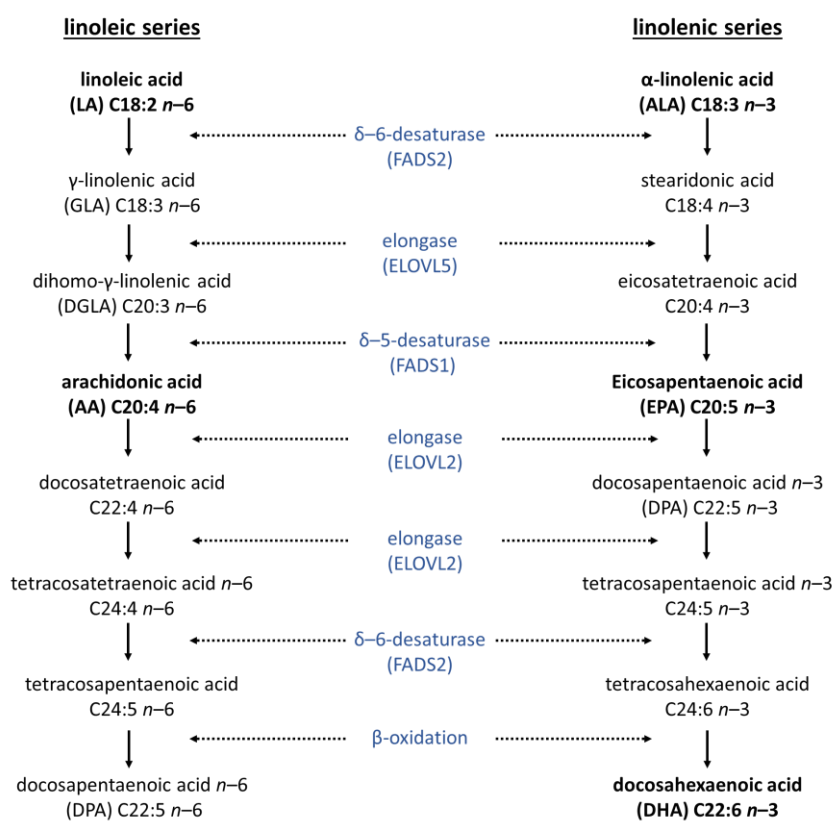


**Figure I-2.** Essential fatty acid metabolism desaturation and elongation of  $n-6$  and  $n-3$  series (adapted from [3]).



EPA and DHA have demonstrated a cardioprotective role through antiarrhythmic, blood-triglyceride-lowering, hypotensive, and antithrombotic effects [4]. Research has also shown anti-inflammatory effects including reduction of rheumatoid arthritis and Chron's disease symptoms [5]. DHA consumption is specially related to reduced risk of developing mental illnesses such as depression, Alzheimer's disease, and dementia, as well as certain forms of cancer [6–9]. Furthermore, the role of DHA in pre-natal, infant, child and adolescent development is well known [3]. An adequate intake of DHA has been associated with fewer allergic diseases such as asthma, rhinitis, and eczema in children and gestational females, and with a normal neural and retina development and function in children [10].

Several authors have pointed out that a proper balance between  $n-3$  and  $n-6$  families should be maintained to maximize the healthy effects of essential fatty acids [11]. This is because  $n-3$  and  $n-6$  PUFAs compete for the same enzyme systems involved in elongation and desaturation to form longer-chain, more unsaturated, and more biologically active fatty acids (Fig. I-2) [11]. Maximum conversion of EPA and DHA is achieved with an  $n-6:n-3$  ratio of 1:1 [12]. However, excessive intake of  $n-6$  PUFAs derived from high consumption of meat, vegetable oils, fast food and snacks in western societies may increase the  $n-6:n-3$  ratio up to values of 15-20:1 [13]. Nutrition experts recommend reducing the  $n-6$  PUFAs intake and increase  $n-3$  PUFAs in the diet of adults and infants to an ideal  $n-6:n-3$  ratio around 2:1 and advise of the necessity of consuming fish and green vegetables for an optimal brain and cardiovascular health and function and to prevent disease [14].

Dietary recommendations for  $n-3$  PUFA are often given separately for ALA and for EPA plus DHA due to the aforementioned low conversion of ALA into its highly-unsaturated counterparts, and to their different biological functions [11]. Authorities have set the recommended intake for PUFA at 6-10% of the total energy intake (E), with a total omega-3 intake that can range between 0.5-2 % E. The recommended daily intake of EPA plus DHA in adults is 250 mg/day and should



not reach 2 g/day to avoid lipid-peroxidation adverse effects, while ALA recommendation is 2 g/day. For pregnant and lactating females, the minimum intake for optimal adult health and foetal and infant development is 0.3 g/day EPA+DHA, of which at least 0.2 g/day should be DHA. [15,16].

## 2. Production of $n-3$ PUFAs from fish

The most important natural sources of essential  $n-3$  PUFAs are marine organisms such as fish, seafood, and algae. EPA and DHA are synthesized by marine phytoplankton, which is the primary producer of  $n-3$  PUFAs in the trophic chain. Fish is the most common source of  $n-3$  PUFAs in human diet, and oily fishes such as those from Scombridae, Clupeidae and Salmonidae families content the highest percentage of DHA and EPA in the foodstuff portion (Table I-1). Fish oil therefore, as the fatty liquid obtained from fish that contains high amounts of  $n-3$  PUFAs, has become a valuable product not only as raw material to produce  $n-3$  PUFA concentrates, but also as an ingredient itself in  $n-3$  PUFA-enriched foods [17]. For these reasons, this section will consider fish oil as the primary source of omega-3.

Nevertheless, it is important to point out that some fish species may contain significant levels of toxic compounds such as methylmercury, polychlorinated biphenyls (PCBs), dioxins, heavy metals and other environmental pollutants, compromising the health benefits provided by omega-3 intake if contaminated fish is consumed in a frequent basis [4]. These toxic compounds are present at relatively low levels in fresh water and oceans, but they easily enter the aquatic trophic chain and, since they have long half-lives, they bioaccumulate reaching high levels in old, large, predatory fish and marine mammals [18]. From this point of view, small oily fish with short life-cycles such as sardines and anchovies are preferable as source of  $n-3$  PUFAs. Some algal and fungal sources of DHA have been discovered in recent years without some of the potential pollutants such as methylmercury [19,20].



Seaweed constitutes a vegan source of omega-3. However, the low lipid content in these marine vegetables (2 g/100 g) should be also pointed out [21].

**Table I-1.** EPA and DHA contents in some fish species (adapted from [22]).

Species	Common name	g/100 g of foodstuff portion	
		C20:5 <i>n</i> -3 (EPA)	C22:6 <i>n</i> -3 (DHA)
<i>Scomber scombrus</i>	Mackerel	1.10	2.56
<i>Mullus surmuletus</i>	Red mullet	0.91	1.66
<i>Sardina pilchardus</i>	Sardine	0.62	1.12
<i>Salmo salar</i>	Salmon	0.50	1.00
<i>Thunnus thynnus</i>	Tuna	0.24	0.98
<i>Engraulis encrasicolus</i>	Anchovy	0.14	0.80
<i>Pagellus bogaraveo</i>	Sea bream	0.12	0.61
<i>Gadus morrhua</i>	Cod	0.23	0.47
<i>Merluccius merluccius</i>	Hake	0.10	0.54
<i>Conger conger</i>	Conger eel	0.15	0.43
<i>Luvarus imperialis</i>	Swordfish	0.15	0.30
<i>Galeorhinus galeus</i>	Dogfish	0.04	0.30

Nowadays, fish oil is almost exclusively produced from small and oily species such as menhaden, sardine, sprat, herring and mackerel; and from the liver of lean fish, mainly cod [23]. These fishes or fish parts are often considered as unappetizing for human consumption and therefore constitute a by-product in the fishery industry [24]. Fish oil composition varies markedly depending on the species of origin (Table I-2) and other factors including sex and season, as well as the production process and the quality of the raw material.

At industrial scale, the most common process to obtain crude fish oil from fresh fish is the wet pressing method, as described by the Food and Agriculture Organization of the United Nations [25] (Fig. I-3). The wet pressing method consists of two main

steps: (1) cooking the raw material for coagulation of protein and release of bound water and oil, and (2) separation by pressing of the coagulate into a solid phase (presscake) containing 60-80% of the oil-free dry matter, and a liquid oily phase (press liquor) containing oil, water and the rest of the solids (suspended and solubilized). After screening and decantation for removal of suspended solids, the press liquor is separated by 3-phase centrifuges into crude fish oil, stickwater and small solids.

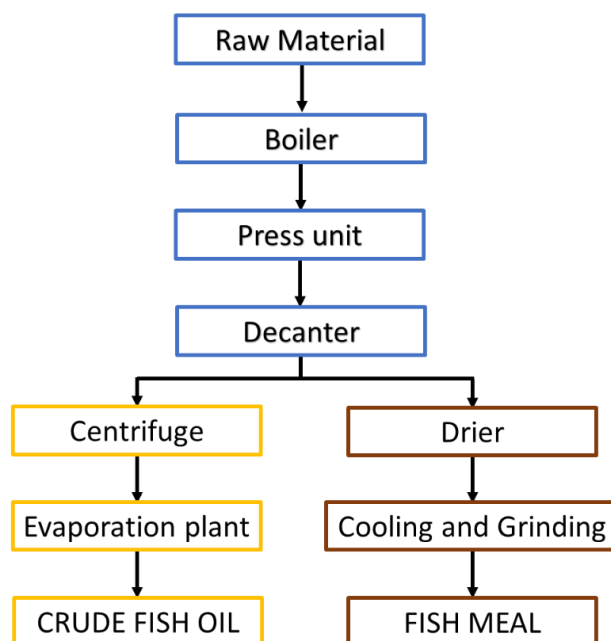


**Figure I-3.** Flow diagram of the conventional wet pressing method to obtain crude fish oil at industrial scale (adapted from [25]).

Crude fish oil is then filtered, stabilized and stored in tanks for further refining. Stickwater is concentrated in multiple-effect evaporators and mixed with the presscake. After gentle drying of the mixture and milling, a protein-rich powder is obtained (fish meal), constituting the other major by-product of the fishery industries.

**Table I-2.** Main fatty acids in fish oils from different species (adapted from [24]).

Fatty acid		(% total lipid)					
		Capelin	Norway Pout	Mackerel	Sardine	Horse mackerel	Anchovy
Myristic	C14:0	7	6	8	8	8	9
Palmitic	C16:0	10	13	14	18	18	19
Palmitoleic	C16:1 <i>n</i> -7	10	5	7	10	8	9
Oleic	C18:1 <i>n</i> -9	14	14	13	13	11	13
Eicosenoic	C20:1 <i>n</i> -11	17	11	12	4	5	5
Cetoleic	C22:1 <i>n</i> -11	14	12	15	3	8	2
Eicosapentaenoic (EPA)	C20:5 <i>n</i> -3	8	8	7	18	13	17
Docosahexaenoic (DHA)	C22:6 <i>n</i> -3	6	13	8	9	10	9



Crude fish oil is not suitable for human consumption since it contains a wide range of undesirable compounds such as free fatty acids (FFAs), phospholipids, pigments, lipid peroxidation products, and environmental pollutants. A refining process is therefore necessary to remove fish oil impurities, consisting on several steps such as degumming to separate phospholipids, neutralization to eliminate FFAs, bleaching to adsorb pigments and some pollutants, and deodorization to remove smelly compounds [26]. The refined fish oil obtained through this process is a complex mixture of fatty acids, being 20-30 % wt.  $n-3$  PUFAs [27], which are bonded to glycerol in the natural occurring form of triacylglycerides (TAGs). Studies about the positional distribution of fatty acids in TAGs of several fish oils have shown that most PUFA are linked to the  $sn-2$  position of the glycerol backbone [28], which is related to a higher stability against oxidation [29], as well as higher bioavailability.

In 2016, the major producers of fish oil were Peru, Scandinavian countries, and Chile, with a total production of around 425000 tonnes. Production decreased from previous years, although it is expected to have increased in 2017 due to the end of El Niño phenomenon and better fishing seasons [30].

Fish oil is mostly used as fish feeding in aquaculture, especially for carnivorous fish from the Salmonidae family. Fish oil is commonly fed to farmed fish during the middle period of growth to ensure that the fatty acid profile and especially the  $n-3$  PUFA content stays similar to that in wild fish. In the last years, fish oil usage in aquaculture has increased at around 4-6% per year [24]. Other non-food applications of fish oil include formulation of pesticides and paints, and leather making [24].

On the other hand, the use of fish oil as a food supplement or nutraceutical is only around 5 % of total fish oil production [31], although it has been increasing even more rapidly than in aquaculture, at around 15% per year [24]. Fish oil has become the most popular food supplement in Europe, where it is used by around 20 % of adult population, and USA [17,32]. This makes the use of fish oil as source of  $n-3$  PUFAs a fantastic opportunity for valorization of this fish by-product. However, the production of high-quality fish oil suitable for human consumption requires not only

searching for raw materials rich in  $n-3$  PUFAs, but also developing production and concentration methods feasible at industrial scale that could yield less oxidized, highly-purified  $n-3$  PUFA concentrates.

Alternative non-thermal processes for fish oil production include enzymatic methods using food-grade proteases to break tissues and cell membranes and release the fish oil, or supercritical extraction, which is a green technology that able to extract fish oil from dehydrated (e.g., freeze-dried) fish by-products [33,34].

### 3. Production of $n-3$ PUFA concentrates

The most popular ways to increase  $n-3$  PUFA intake are: (1) direct fish or fish oil consumption, (2) ingestion of capsules and tablets containing these compounds, and (3) functional foods fortified with  $n-3$  PUFAs. Either in one way or another, it is important to fulfil daily recommendations for  $n-3$  PUFAs without increasing the ingestion of SFA too much. For this reason, high-purity  $n-3$  PUFA concentrates are preferable to formulate nutraceuticals as well as for functional food supplementation.  $n-3$  PUFA concentrates can be found either as TAGs, diacylglycerides (DAGs), monoacylglycerides (MAGs), phospholipids (PL), ethyl esters (EE), or FFAs, as well as their mixtures [23].

Bioavailability and stability against oxidation of  $n-3$  PUFAs should be also considered. These two parameters are closely influenced by the chemical structure in which  $n-3$  PUFA concentrates are produced. Researchers have demonstrated that  $n-3$  PUFAs are better absorbed by human organism in acylglyceride forms (TAG, DAG, MAG, PL) rather than in EE forms [35]. The same is true for the stability against oxidation, which is also higher for acylglycerides than for EE [36]. Although FFAs present higher bioavailability than EE and even TAG forms of  $n-3$  PUFAs, they are usually not considered because they can present irritant effects and low stability against oxidation [35,37]. Latest research in this field points to emulating the best conditions for the  $n-3$  PUFAs to be absorbed at the intestinal mucosa level.



This way, structured lipids with  $n-3$  PUFAs in the  $sn-2$  position, and medium-chain (MC) fatty acids (C8-C14) in the  $sn-1,3$  extremes of the glycerol backbone are the best substrate in terms of increasing human pancreatic lipase activity, which is  $sn-1,3$ -specific and presents higher activity towards MC fatty acids. This strategy would ultimately result in  $n-3$  PUFAs being directly assimilated after pancreatic lipase digestion, increasing its absorption rate [23].

In the last years, many processes have been developed to obtain concentrates of  $n-3$  PUFA from fish oil. Most of them consist on (1) transesterification reactions followed by (2) fractionation and purification of  $n-3$  PUFA. Formulation of the concentrated  $n-3$  PUFA (3) is also required to obtain a stable final product.

### 3.1. Transesterification

Transesterification consist on exchanging the organic group  $R_i$  of an ester (triacylglyceride, TAG) with the organic group  $R'$  of an alcohol, yielding a different ester and a different alcohol (Fig. I-4) [1]. Transesterification may occur spontaneously at high temperatures ( $> 200$  °C). However, thermal degradation of lipids is likely to occur under these conditions; therefore, the use of chemical or enzymatic catalysts, which allow the transesterification reaction to take place at lower temperatures, is common in the food industry.

Chemical transesterification of lipids is widely used in the food industry. Most commonly used chemical catalysts are strong acids and bases, as well as sodium or sodium/potassium alkylates. Chemical transesterification can be applied in the manufacturing of shortenings and margarines from different fats such as palm oil, palm kernel oil and milk fat. Production of low-calorie fat substitutes such as Salatrim and Olestra is also achieved through chemical transesterification. However, due to the lack of specificity of the catalysts, usually randomized products are obtained, and many studies have shown that chemical transesterification can negatively affect oxidative stability of fats and oils [1].

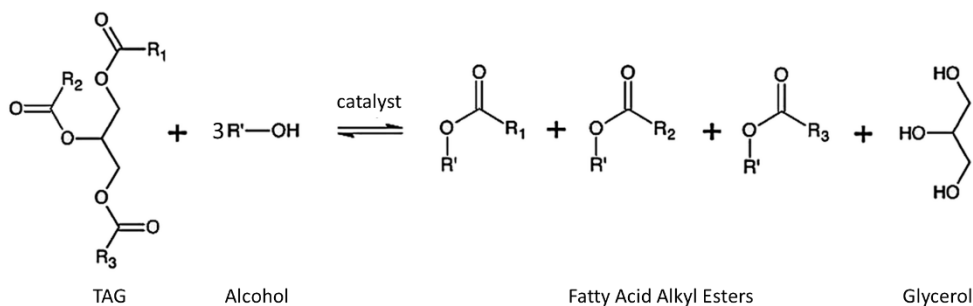


**Figure I-4.** Transesterification reaction of triacylglycerides (TAG) with an alcohol producing fatty acid alkyl esters (FAAE) and glycerol.

Enzyme-catalyzed transesterification exploits the regio- and stereo-specificity of lipases to prepare structured lipids with interesting properties, such as in the industrial production of cocoa butter and human milk fat substitutes [1]. The use of lipases in the transformation of fish oil into *n*-3 PUFA-enriched derivatives is an attractive alternative to conventional chemical methods since lipases can operate under mild conditions, which is preferable to avoid oxidation [17,38]. Enzymatic ethanolysis of fish oil has been widely studied as a simple method to obtain *n*-3 PUFA EE [17]. Partial acylglycerides (DAGs and MAGs) significantly enriched in EPA and DHA can be also obtained by enzymatic ethanolysis with *sn*-1,3-specific lipases and adequate reaction conditions [38]. Other food-grade alcohols such as glycerol can be also used as acyl donors [39]. Glycerolysis of fish oil is advantageous because, using a *sn*-1,3-specific lipase, it offers the possibility of obtaining 2-MAGs in a one-step process [39]. The main limitation of enzymatic alcoholysis of fish oil, especially glycerolysis, is the poor miscibility of the substrates, which reduces the contact between them and the catalysts and leads to low *n*-3 PUFA conversion. To overcome this drawback, use of organic solvents such as tertiary alcohols and/or surfactants is needed, which increases material costs as well as operating costs since separation and purification steps are required for solvent removal [39].



As an alternative to conventional organic solvents, supercritical fluids have been also proposed as a good medium to carry on enzymatic reactions, providing good transport properties that may result in higher reaction rates. The most widely used solvent is supercritical CO<sub>2</sub>, which is a gas under atmospheric conditions and, as such, no solvent residues are left in the reaction products after simple depressurization. Besides, oxygen displacement prevents the *n*-3 PUFAs to undergo oxidation [114–117].

### 3.2. Concentration

Concentration of *n*-3 PUFA derivatives obtained by enzymatic transesterification into a highly purified form is not easily achieved due to the complex nature of fish oils. The main properties of each fatty acid or fatty acid family, such as boiling and melting temperatures, molecular size and degree of unsaturation are considered in the development of separation techniques for *n*-3 PUFAs.

Several methods have been investigated for *n*-3 PUFA fractionation and purification [40,41], but only a few are suitable for industrial-scale production. The most commonly used are molecular distillation, low-temperature crystallization, urea complexation, and supercritical fluid fractionation. Each method has its own advantages and drawbacks (Table I-3) [31].

In addition, combined fractionation techniques can be applied, depending on the chemical form of the *n*-3 PUFAs, and the desired concentration and purity in the final product [42], but currently, molecular distillation is the most industrially applied process for *n*-3 PUFA fractionation and purification [41], together with supercritical fluid fractionation, which will be briefly explained later in section 4.4.

**Table I-3.** Comparison of most common techniques for *n*-3 PUFA fractionation and purification (adapted from [31]).

	<b>Molecular distillation</b>	<b>Low-temperature crystallization</b>	<b>Urea complexation</b>	<b>Supercritical fluid fractionation</b>
<b>Selective towards</b>	Boiling point	Melting point	Saturated fats	Chain length and degree of saturation
<b>Operating T (°C)</b>	140 to 220	-70 to 0	-10 to 90	35 to 50
<b>Operating p (bar)</b>	10 <sup>-6</sup>	1	1	>140
<b>Use of toxic solvents</b>	No	Possible	No	No
<b>Max EPA+DHA concentration (%)</b>	65-75	> 90	45-65	75-85
<b>Decontamination efficiency</b>	Very high	Low	Low	Medium
<b>Mode of operation</b>	Continuous	Batch	Batch	Continuous
<b>Risk of oxidation</b>	Low	Possible	Possible	Low
<b>Capital investment</b>	Low	Low	Low	High

### 3.3. Formulation

As we have previously mentioned, one of the major drawbacks of oils containing high amount of *n*-3 PUFAs, such as fish oils, is their high susceptibility to oxidation. Lipid oxidation involves the formation of lipid hydroperoxides and free radicals which negatively affect sensory properties, since they can decompose into low-molecular-weight volatile compounds causing non-desirable off-flavours, and what is more, they present potentially cytotoxic, carcinogenic and mutagenic effects [43,44].

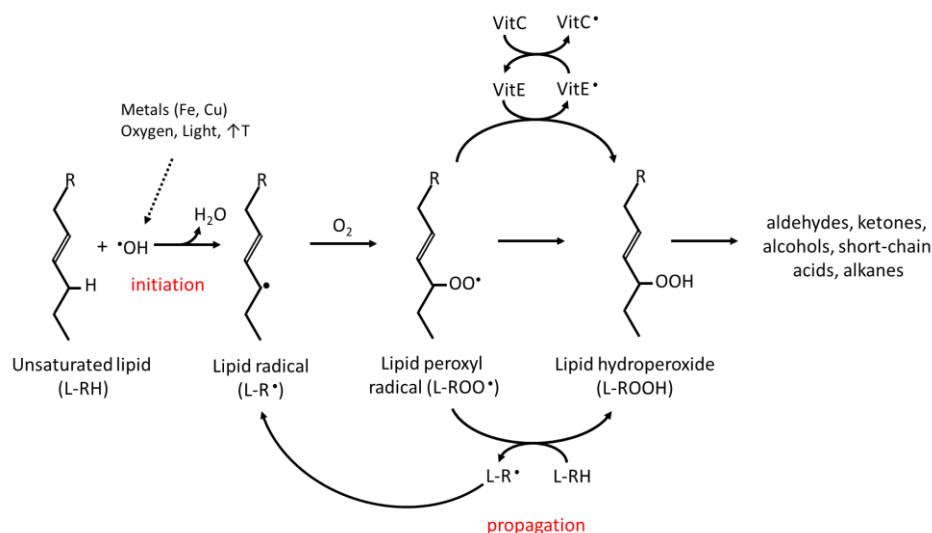


**Figure I-5.** Schematic representation of lipid peroxidation (adapted from [1,45]).

Polyunsaturated fatty acids are converted to lipid radicals in the initiation step. This highly reactive species attack other polyunsaturated fatty acids, thereby initiating a chain reaction (propagation). Antioxidants such as vitamin E scavenge lipid peroxy radicals and break the chain reaction. Vitamin E can be regenerated by ascorbic acid (vitamin C).

For these reasons, preventing lipid oxidation is a key factor in  $n-3$  PUFA-containing oils in order to preserve their food-quality properties, such as color, texture, flavour, and nutritional value [43]. However,  $n-3$  PUFAs in food products are difficult to protect from oxidation because it follows complex mechanisms that depend on the structural organization of the fatty acids in TAG and other lipids [29], as well as their presentation (bulk oil, water-in-oil or oil-in-water emulsion, encapsulated or microencapsulated), and can be catalyzed by different factors such as temperature, light exposure, oxygen concentration or presence of transition metals (e.g., iron and copper) [17] (Fig. I-5).

Optimal processing conditions throughout the whole supply chain, from ensuring the quality of raw material to storage in adequate conditions and protective packaging, passing through suitable production and purification strategies, are essential to preserve  $n-3$  PUFA from oxidation [17]. In addition, other mechanisms to improve fish oil stability and prolong its shelf-life are necessary [46].



Addition of antioxidants is one of the most common strategies to prevent or delay oxidation in  $n-3$  PUFA-enriched oils. There is a great number of available antioxidants, such as BHA, BHT, EDTA, tocopherols, ascorbic acid, ascorbyl palmitate, propyl gallate, gallic acid, lactoferrines, etc., whose protective effect against lipid oxidation has been studied both in bulk fish oil [46] and in fish oil-in-water emulsions [47]. Due to consumer's preference for additives from natural sources, the last trends point to the use of natural antioxidants and plant extracts, such as oregano, rosemary, parsley, or olive mill and winery by-products, on the stabilization of bulk fish oil and fish oil-in-water emulsions [48–51].

Encapsulation or microencapsulation of  $n-3$  PUFA with coating materials of different nature has been also proposed as a strategy to delay lipid oxidation, enhance oil stability and avoid the appearance of off-flavours [1,52]. Carriers of different nature have been applied to encapsulate oils rich in  $n-3$  PUFA, such as gelatin [53], starch [54],  $\beta$ -cyclodextrin [55], whey protein isolate [56], barley protein [57], chitosan [58], or fully-hydrogenated soybean oil [59]. Different physical and chemical processes have been also developed to encapsulate and stabilize active compounds such as  $n-3$  PUFA from fish oil [60]. Among these, spray-drying is the most common and economical method [61–66], although other processes such as freeze drying [67–69], ultrasonic atomization [70], enzymatic gelation [53], nano-precipitation [54], inclusion complexation [55], or electro-spinning [71] have been also developed as alternatives to reduce  $n-3$  PUFA oxidation since they avoid the use of high temperatures during the drying step.

Alternative encapsulation processes using supercritical fluids can be also used to protect bioactive compounds such as  $n-3$  PUFAs from oxidative degradation, thanks to the mild temperature and inert atmosphere process conditions [72]. Encapsulation and co-precipitation processes such as Rapid Expansion of Supercritical Solutions (RESS), Supercritical Anti Solvent Precipitation (SAS), Supercritical Fluid Extraction of Emulsions (SFEE), Particles from Gas Saturated Solutions (PGSS), and PGSS-drying will be later discussed in section 4.4.4.

## 4. Supercritical fluid technology

### 4.1. Introduction to supercritical fluids

A supercritical fluid (SCF) is any fluid whose reduced temperature and pressure (defined as in Eqs. I-1, I-2) are above unity, pressure being below the necessary to solidify the fluid [73]. Considering SCF applications as solvents, reduced density should be also above unity (Eq. I-3).

$$p_r = \frac{p}{p_C} \quad (\text{I-1})$$

$$T_r = \frac{T}{T_C} \quad (\text{I-2})$$

$$\rho_r = \frac{\rho}{\rho_C} \quad (\text{I-3})$$

In the supercritical region (Fig I-6), the fluid presents intermediate properties between a gas and a liquid, e.g., liquid-like density and gas-like viscosity and diffusivity (Table I-4). That is, SCFs have at the same time good solvent power and good transport properties [74].

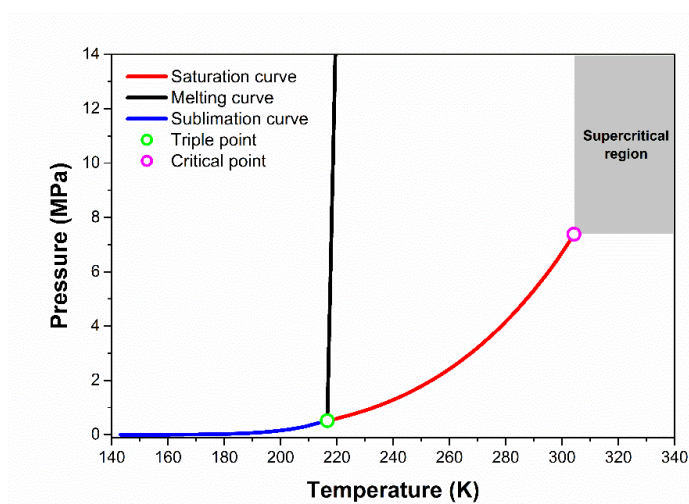


**Figure I-6.** Phase diagram of carbon dioxide illustrating the supercritical region above the critical temperature ( $T_C$ ) and pressure ( $p_C$ ) (data taken from [75]).



Moreover, since SCFs also possess gas-like compressibility, density-related properties such as solvent power can be tuned through pressure and temperature variation in order to dissolve different solutes.

**Table I-4.** Comparison of physical properties of gases, liquids and supercritical fluids (SCF) (adapted from [74]).

Physical state	Physical properties				
	p, T conditions (MPa, K)	Density (kg/m <sup>3</sup> )	Viscosity (Pa·s)	Diffusivity (m <sup>2</sup> /s)	Surface tension (mN/m)
Gas	<b>0.1, 298</b>	0.5-2	10 <sup>-5</sup>	10 <sup>-5</sup>	0
SCF	p <sub>c</sub> , T <sub>c</sub>	200-500	1.3·10 <sup>-5</sup>	0.7·10 <sup>-5</sup>	0
	4p <sub>c</sub> , T <sub>c</sub>	400-900	3.9·10 <sup>-5</sup>	0.2·10 <sup>-7</sup>	0
Liquid	<b>0.1, 298</b>	600-1600	10 <sup>-3</sup>	10 <sup>-9</sup>	25-80

Among the several fluids that can be used as supercritical solvents (Table I-5), the most widely used SCF is carbon dioxide; the main reason being that supercritical carbon dioxide (SC-CO<sub>2</sub>) is considered a green solvent. SC-CO<sub>2</sub> is inert, non-toxic, and non-flammable. Besides, CO<sub>2</sub> is a gas at ambient conditions, so it is completely released from the processed products after depressurization. Economical aspects are also advantageous for SC-CO<sub>2</sub>, since it is readily available in the atmosphere and inexpensive to obtain at high purity. Additionally, CO<sub>2</sub> presents mild critical conditions (T<sub>c</sub>=304.15 K, p<sub>c</sub>=7.38 MPa [75]) which allow processing of thermolabile compounds, such as omega-3 PUFAs. From an industrial point of view, the accessibility of CO<sub>2</sub> and its moderate critical conditions make operational costs affordable. A wide variety of processes that take advantage of the interesting features of SC-CO<sub>2</sub> have been developed in the last decades. Among them, extraction, enzymatic reactions, fractionation, chromatography, particle formation, impregnation, inactivation of enzymes and microorganisms, etc. [17].

**Table I-5.** Critical properties of different solvents (adapted from [76])

Solvent		Critical properties		
		T <sub>c</sub> (K)	p <sub>c</sub> (MPa)	ρ <sub>c</sub> (g/cm <sup>3</sup> )
<b>Carbon dioxide</b>	CO <sub>2</sub>	304.1	7.38	0.469
<b>Water</b>	H <sub>2</sub> O	647.1	22.06	0.322
<b>Methane</b>	CH <sub>4</sub>	190.4	4.6	0.162
<b>Ethane</b>	C <sub>2</sub> H <sub>6</sub>	305.3	4.87	0.203
<b>Propane</b>	C <sub>3</sub> H <sub>8</sub>	369.8	4.25	0.217
<b>Ethylene</b>	CH <sub>2</sub> =CH <sub>2</sub>	282.4	5.04	0.215
<b>Propylene</b>	CH <sub>3</sub> CH=CH <sub>2</sub>	364.9	4.6	0.232
<b>Methanol</b>	CH <sub>3</sub> OH	512.6	8.09	0.272
<b>Ethanol</b>	CH <sub>3</sub> CH <sub>2</sub> OH	513.9	6.14	0.276
<b>Acetone</b>	CH <sub>3</sub> COCH <sub>3</sub>	508.1	4.7	0.278

#### 4.2. Supercritical processing of fish oil

The development of supercritical fluid technologies has made possible to propose a global process for obtaining fish oil concentrates rich in omega-3 as a solid powder using SC-CO<sub>2</sub>. A scheme of this process is presented in Fig. I-7. In this figure, we can see that alternative processes with SC-CO<sub>2</sub> can be used in each step (e.g., fish oil extraction, refining, concentration and fractionation, and formulation). Furthermore, CO<sub>2</sub> can be recycled, thus reducing operational costs.

Few years ago, Rubio-Rodríguez *et al.* [17] summarized the advances in fish oil processing alternatives, focusing on the use of SC-CO<sub>2</sub> as an extracting solvent in the fish oil industry. More recently, Ciriminna *et al.* [32] have made an overview of new methods for fish oil production, pointing at three milestones that have been reached at industrial scale, significantly enhancing omega-3 production: (1) molecular distillation, (2) supercritical fluid extraction and purification, and (3) development of omega-3 supplements in TAG form.

Nowadays, research on the field aims to the biorefinery concept, such as the case study presented by Fiori *et al.* [78] for the industrialization of a valorization plant of fish processing residues in order to obtain omega-3 concentrates for the nutraceutical sector.

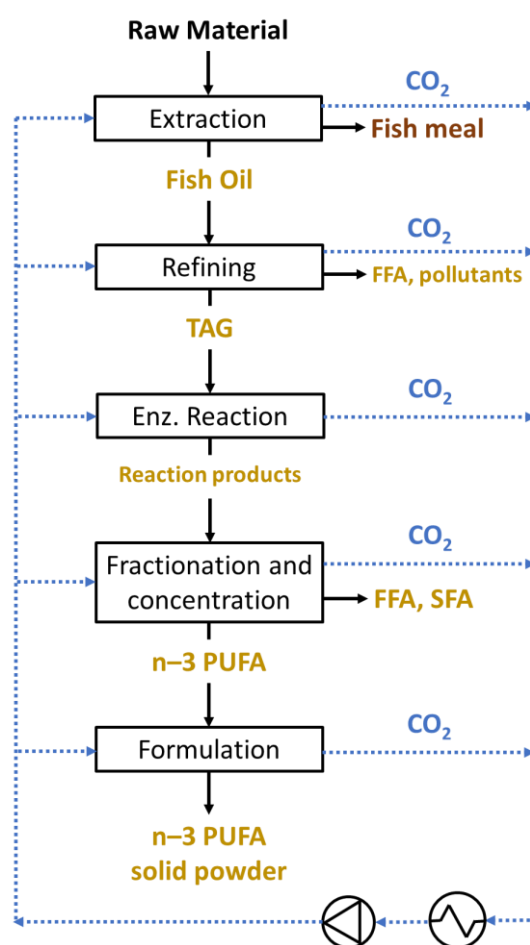


**Figure I-7.** Global process to obtain *n*-3 PUFA concentrates from fish by-products as a solid powder. FFA: free fatty acids, SFA: saturated fatty acids. (adapted from [77]).

In the next sections, the supercritical alternatives to the conventional methods for fish oil extraction, refining, concentration and fractionation, and formulation will be discussed.



#### 4.2.1. Supercritical extraction of fish oil

Fish oil is a natural mixture of different lipid compounds, mostly TAGs, liquid at room temperature, soluble in non-polar solvents as hexane or petroleum ether, and insoluble in polar solvents as water. Due to its low polarity, SC-CO<sub>2</sub> has been also found to be a good solvent of fats and oils, such as fish oil components and related compounds. Experimental phase equilibria of different components of fish oil and SC-CO<sub>2</sub>, as well as co-solvents such as ethanol, has acquired great relevance in the last years because this knowledge is essential to design processes such as supercritical fluid extraction (SFE), fractionation (SFF) or supercritical fluid chromatography (SFC), which are involved in fish oil production, refining, and concentration.

The first studies about fish oil solubility in SC-CO<sub>2</sub> were carried out with sardine oil in a pressure range of 20 to 35 MPa at four different temperatures (313, 333, 343 and 353 K) [79], revealing that, at constant temperature, fish oil solubility increased significantly with pressure, whereas, at constant pressure, oil solubility decreased with temperature up to a pressure value from which it began to increase as temperature increased. This behavior was also observed in other natural fish oils from sand eel [80], orange roughy, spiny dogfish liver or cod liver [81]. It was explained considering that, at constant pressure, a temperature increase has a double effect: the density of the solvent decreases, which would decrease solubility, yet the vapor pressure of the solute increases, which would have the opposite effect. At low pressures the first effect predominates and at high pressures is the solute vapor pressure effect which becomes stronger, resulting in a cross-over of the fish oil-CO<sub>2</sub> dew lines when increasing pressure [74]. It was also found that fish oil solubility increases by adding polar co-solvents such as ethanol [81]. In the early 1990s, Staby and Mollerup measured phase equilibrium data of acylglycerides, free fatty acids, fatty acid methyl and ethyl esters, and other minor components such as cholesterol,  $\beta$ -carotene,  $\alpha$ -tocopherol, squalene or phospholipids in supercritical fluids [82]. More recently, Güçlü-Üstündağ and Temelli published a compilation of solubility



data for the main pure lipid classes such as fatty acids, fatty acid esters and mono-, di- and triglycerides [83] and for other minor lipids such as  $\beta$ -carotene,  $\alpha$ -tocopherol, stigmasterol and squalene in SC-CO<sub>2</sub> [84].

Based on the good solubility of fish oil and its derivatives in SC-CO<sub>2</sub>, abundant research has been made dealing with SFE of fish oil from different fish by-products. Letisse *et al.* [85] optimized the extraction conditions for SFE of fish oil from sardine, finding  $p = 30$  MPa,  $T = 75$  °C, and CO<sub>2</sub> rate of 2.5 mL/min during 45 min as the optimum conditions. Fish oil yield was around 10 % of the dried raw material, with EPA and DHA contents of 10.95 and 13.01%, respectively. Rubio-Rodríguez *et al.* studied the influence of different process parameters on the extraction yield and oil quality for the SFE of fish oil from hake [33,34], orange roughy, salmon, and jumbo squid freeze-dried by-products [34], and compared SFE to other extraction methods (e.g., cold extraction, wet reduction and enzymatic extraction), showing that SFE may be a useful method to prevent oxidation in fish oils rich in omega-3, and to reduce certain pollutants such as polar derivatives of heavy metals [34]. Similar results have been reported by Bucio *et al.* [86] for the SFE of fish oil from rendered fish meal with liquid and SC-CO<sub>2</sub>, in which most toxic compounds (e.g., heavy metals) remained in the raffinate. A recent review of fish oil extraction using green methods such as SFE, ultrasound-assisted extraction, microwave-assisted extraction, and enzymatic hydrolysis, points at SFE with CO<sub>2</sub> as the most promising green extraction method [87]. Latest research on SFE of fish oil investigates the potential bioactivity of fish oils extracted from different sources, such as yellow croaker [88], African catfish [89], striped weakfish [90], Indian mackerel [91], sturgeon [92], longtail tuna [93], rainbow sardine [94], sardine [95], tuna [96–99], Pacific saury [100], salmon [101,102], or common carp [103]. Mathematical modeling of the extraction process has been recently revisited by Adeoti *et al.* [101], finding the local adsorption equilibrium model proposed by Goto *et al.* [104] as the most suitable for the SFE of fish oil, since it addresses intraparticle diffusion and external mass transfer of SFE in a fixed solid bed.



Nowadays, SFE is considered a mature technology able to replace traditional extraction processes in certain applications, such as hop extraction and coffee decaffeination [74]. Compared to conventional extraction processes in the fish oil industry such as steam distillation or solvent extraction, SFE has shown good results in the production of fish oil with no solvent residues and lower amounts of impurities, especially heavy metals. Therefore, SFE is a promising technology to produce good-quality fish oil, suitable as raw material to produce omega-3 concentrates at industrial scale. However, in some cases other components such as FFAs are also extracted together with fish oil, and the proportion of *n*-3 PUFAs is still low to be used as food ingredient or in pharmaceutical applications; hence subsequent refining, fractionation and concentration steps are required.

#### 4.2.2. Fish oil refining using supercritical fluids

Supercritical fluid refining, together with membrane and enzymatic processes, is one of the most recently proposed alternatives to conventional oil refining with chemical products or high temperatures [17].

Several studies have taken advantage of the benefits of SC-CO<sub>2</sub> as a green solvent in degumming and bleaching [105], and deacidification [106,107] of different seed oils, as well as in fish oil refining, where the major challenge is the removal of toxic contaminants such as dioxins and PCBs [108]. Jakobsson *et al.* [109] studied the semi-continuous and simultaneous deacidification and removal of dioxins from cod liver oil in using SC-CO<sub>2</sub> and ethanol as co-solvent. The different polarities of FFAs and dioxins did not allow to remove both types of compounds simultaneously, although it was possible to separate dioxins from deacidified fish oil by using pure SC-CO<sub>2</sub> at low pressure. In subsequent studies, the same authors implemented a countercurrent extraction column to improve dioxin removal up to 80 % with the first 17 % of the oil [110]. A pilot countercurrent fractionation plant was also used by Catchpole *et al.* to remove impurities such as peroxides, fatty acids or odour



components, from crude fish oils from different sources (orange roughy oil, deep sea shark liver oil, spiny dogfish oil and cod liver oil), by using SC-CO<sub>2</sub> and ethanol as co-solvent (5 % wt.) [111]. Kawashima *et al.* studied SFE of fish oil coupled with adsorption on activated carbon to remove PCBs, polychlorinated dibenzo-p-dioxins (PCDD), and polychlorinated dibenzofurans (PCDF), finding the SFE process to effectively remove PCBs, and the adsorption method more efficient for the removal of PCDDs and PCDFs; combining both methods, they could achieve a reduction of the total toxicity of almost 100% [108]. A continuous countercurrent SFE-adsorption process was implemented in following studies using 40% less CO<sub>2</sub> and yielding 30 % more refined oil [112].

Nowadays, the major drawback of supercritical fluid refining is the high cost of the equipment. However, fish oil refining with SC-CO<sub>2</sub> looks promising when oil purity and quality, as well as avoiding the use of toxic solvents, are the main goals [113].

#### 4.2.3. Enzymatic modification of fish oil in supercritical fluids

Supercritical fluids have been also proposed as a good media to carry on enzymatic reactions. Several reviews on the matter have been published [114–117], showing the possibilities of enzymatically-catalyzed reactions in supercritical and expanded media, including oil hydrolysis and transesterification. SC-CO<sub>2</sub> is again the most widely used solvent for enzymatic reactions in SCFs, since it is considered a green solvent, non-toxic, and it can be easily and completely removed from the reaction products. In addition, SC-CO<sub>2</sub> physical properties such as density, diffusivity or viscosity, which can be changed by changing pressure or temperature, may affect the selectivity of the catalyst towards a certain substrate, or it can be tuned to produce the desired isomeric form of a certain product [117]. Moreover, enzymatic reactions in SC-CO<sub>2</sub> can be easily coupled with other supercritical processes such SFE, SFF, SFC, or microencapsulation techniques, which minimizes the oil manipulation and, therefore, prevents its oxidation [17].



Because of these advantages, different enzymes, usually immobilized lipases, have been used to successfully conduct different reactions in SC-CO<sub>2</sub>. Among them, the non-specific lipase Novozyme 435 from *Candida antarctica* [118–122], and the *sn*-1,3-regiospecific lipases Lipozyme TL-IM from *Thermomucor lanuginose* [123,124] and Lipozyme RM IM from *Rhizomucor miehei* [125,126] are the most widely used.

Marty *et al.* presented a first approach to lipase catalyzed reactions in SC-CO<sub>2</sub> comparing the esterification of oleic acid and ethanol in SC-CO<sub>2</sub> and in hexane by an immobilized lipase from *R. miehei* (Lipozyme) [125,126]. Yu *et al.* firstly reported the enzymatic modification of natural lipid sources in SC-CO<sub>2</sub> using an immobilized lipase from *C. cylindracea* in the transesterification of canola oil with anhydrous milk fat [127]. Ethanolysis of cod liver oil in SC-CO<sub>2</sub> by Novozym 435 from *C. antarctica* was investigated in continuous and semi-continuous mode, continuously extracting the final products of the reaction, fatty acid ethyl esters (FAEEs) dissolved in the flowing CO<sub>2</sub>-rich vapor phase [118–120]. Thus, it was found that CO<sub>2</sub> flowrate and phase behavior of the system influenced the reaction rate and product composition [118–120]. To investigate the influence of the catalyst, including the characteristics of the enzyme carrier, ethanolysis of cod liver oil in batch mode was also performed using lipases from *Humicola lanuginosa* and from *C. antarctica* immobilized on supports of different properties [128]. Hydrophobicity of the carrier was found to possibly affect the specificity of the catalysts against DAGs and MAGs [128]. Ethanolysis of palm kernel oil in SC-CO<sub>2</sub> by Lipozyme IM from *R. miehei* and Novozym 435 was studied by Oliveira and Oliveira [121,122]. Transesterification of menhaden oil and a concentrate of free *n*-3 PUFA from the same source by Lipozyme IM-60 was also evaluated by Lin *et al.* [129]. A similar reaction with borage oil and a concentrate of free *n*-3 PUFA from menhaden oil was also investigated by Lin and Chen [130], finding that enzymatic transesterification in SC-CO<sub>2</sub> was 40% higher than in conventional solvents and proving that biocatalysis in supercritical fluids may be an interesting strategy to



produce structured lipids enriched in omega-3 from fish oil under mild conditions and with a high yield. Ma *et al.* [131] have studied the enrichment of DHA from tuna oil via esterification of free *n*-3 PUFA from tuna oil and ethanol, assessing the effects of lipase type, enzyme loading, pressure, temperature, reaction time, and water addition on DHA enrichment in the residual fatty acid fraction. Roh *et al.* [132] have recently investigated the transesterification of menhaden oil with excess ethanol in SC-CO<sub>2</sub>, finding that reaction rates were enhanced and inhibition by excess ethanol was reduced in SC-CO<sub>2</sub> when compared to a solvent-free system, achieving the maximum conversion at 10.0 MPa and 50 °C with 3 % wt. of Lipozyme TL-IM and 3.0 ethanol:menhaden oil molar ratio.

As observed, enzymatic modification of fish oil in SC-CO<sub>2</sub> provides enhanced reaction rates and even higher total conversion than solvent-free media, with the advantage of not using toxic organic solvents. This application will be further discussed in the Results section, where the effects of SC-CO<sub>2</sub> exposure on different lipases and the kinetics of lipase-catalyzed ethanolysis of fish oil in SC-CO<sub>2</sub> (chapters 1 and 3, respectively) will be investigated in more detail.

On the other hand, reaction products obtained by enzymatic modification of fish oil are not usually highly concentrated in omega-3; hence, this technology is often coupled with other concentration methods that will be discussed in the following section.

#### 4.2.4. Supercritical fluid fractionation and concentration of *n*-3 PUFAs

In the last years, the use of SCFs in *n*-3 PUFA fractionation and concentration has acquired great interest, and several processes have been developed based on supercritical fluid fractionation (SFF), and supercritical fluid chromatography (SFC) technologies, which will be further discussed in the following sections.

*i) Supercritical fluid fractionation*

Most of the studies on SFF of fish oil related compounds have been performed over FAEEs; hence, phase equilibrium involving this type of compounds, especially EPA-EE and DHA-EE has been also widely studied [82,83]. Few research has been done about SFF of natural fish oil in TAG form. Antunes-Corrêa *et al.* [133] measured solubility of natural fish oil in SC-CO<sub>2</sub> by a dynamic method, finding that most compounds presented distribution coefficients between extract and raffinate close to unity, leaving SFF of natural fish oil with little prospect of development.

In 1978, Dr. Kurt Zosel firstly reported and patented SFF of fish oil FAEE with supercritical ethane [134]. Some years later, several authors took advantage of the interesting features of SC-CO<sub>2</sub> to fractionate fish oil FAEEs [135–137]. Since then, investigation on SFF of fish oil FAEEs with SC-CO<sub>2</sub> has continued. In many cases, research has simultaneously dealt with experimental determination of phase equilibria of the mixtures involved, which is essential for the design and modelling of SFE and SFF. This was reflected in the early review by Staby and Mollerup, which collected phase equilibrium data of fish oil constituents and SC-CO<sub>2</sub> together with experimental applications in SFE, SFF and SFC [82].

In the late 1990s and 2000s, technological development led to continuous counter-current SFF (CC-SFF) in multi-stage columns [138–140]. Advances in CC-SFF of FAEEs from fish oil until the 2010s decade are comprehensively reviewed in the works of Sahena *et al.* [141], and Rubio-Rodríguez *et al.* [17]. Pressure, temperature, solvent to feed ratio, and residence time/number of stages are considered as the most important parameters for the optimization of the CC-SFF process [141].

In most recent years, Maschietti *et al.* studied the influence of these operating parameters (e.g., number of theoretical stages, reflux ratio and solvent-to-feed ratio) and developed a predictive model for CC-SFF of FAEE from fish oil [142]. They simulated a CC-SFF process with internal reflux generated by operating the top



stage of the column at a higher temperature ( $T_1$ ) than that of the body ( $T$ ), and predicted a recovery of 95 % of long-chain FAEE (C20 and C22) with 95 % purity, operating at  $p = 13.3$  MPa,  $T = 50$  °C,  $T_1 = 66-70$  °C, and number of stages and solvent-to-feed ratio of 16-30 and 88-120, respectively [142]. Few years ago, Fiori *et al.* [143] made a practical approach to CC-SFF of FAEEs from fish oil. They optimized process conditions ( $T = 80$  °C,  $p = 19.5$  MPa, external reflux ratio = 0.92, solvent to feed ratio = 63), and investigated the economic feasibility of a CC-SFF plant. Operating cost were estimated on 2.30-2.50 €/kg for an 85 % wt. omega-3 concentrate, and investment costs in the range 2-15 €/kg<sub>concentrate</sub> depending on plant capacity (from 10 to 300 kg/h of FAEE feed). Pieck *et al.* have recently developed a simplified equilibrium-stage model for CC-SFF of FAEE from fish oil [144]. The model, validated with their own experimental data, successfully predicts the effect of varying the solvent-to-feed ratio on the concentration of the major compounds present either in the feed or in the extract and raffinate, which are the most important variables for economic analysis [144].

Research on SFF of fish oil and its derivatives is still open with the aim of achieving industrial-scale production [17]. Although recent reviews [145] have shown that CC-SFF is widely spread among leading research institutions, the actual number of industrial-scale CC-SFF applications is still low [146], the main reason being that competitive processes such as vacuum distillation and short path distillation are well known and readily available, whereas CC-SFF needs to be designed for each specific application [146]. Knowledge of the phase behavior of the mixtures involved and mathematical models to describe the CC-SFF process are essential for its large-scale implementation, yet they have not diffused to all members of the chemical engineering community, and even less to decision-making executive boards [146].

*ii) Supercritical fluid chromatography*

Supercritical fluid chromatography (SFC) is an attractive alternative to traditional techniques such as gas chromatography (GC) or high-performance liquid chromatography (HPLC) for analytical, preparative or production purposes [147].

Thanks to the beneficial and tuneable properties of SCFs, which have been mentioned at the beginning of this section, they can be used as a mobile phase in chromatography, together with packed or capillary columns filled with a suitable stationary phase. Several materials, such as octadecyl silane, aluminium oxide, or silica gels from different nature are mainly used as the column stationary phase, whereas SC-CO<sub>2</sub> is the eluent solvent of choice due to its green characteristics. Co-solvents are often incorporated, most of the times with changing proportion over time [147]. The high selectivity of the supercritical mobile phase, combined with a suitable stationary phase, make SFC especially indicated for separation of omega-3 PUFAs. Since the inventions from Perrut *et al.* [148], and Brunner and Reichmann [149], many studies have been published about SFC applied to fish oil derivatives, mainly FAEE, to obtain omega-3 PUFAs with a high purity and recovery not only in the laboratory but also at large scale [17]. For a very recent insight on the SFC technique and its main applications, the reader is referred to the book edited by Prof. Poole [150].

From the point of view of pharmaceutical and food industries, preparative SCF constitutes a very promising technique able to satisfy the growing demand for EPA and/or DHA products with more than 95% purity and without solvent residues [31]. SFC processes, often combined with SFE and SFF, are already installed at production scale, and pharmaceutical companies as KD-Pharma or Solutex, produce concentrates of omega-3 PUFA in proportions higher than 90 % of EPA and/or DHA, and both in FAEE and TAG forms.

#### 4.2.5. Supercritical fluids in the formulation of $n-3$ PUFAs

Formulation of omega-3 PUFA concentrates is one of the most challenging tasks of their production. Several encapsulation techniques using SCFs have been developed in recent years and constitute a good alternative to stabilize bioactive compounds such as fish oil concentrates and protect them against oxidation during shelf-life, taking advantage of favourable processing conditions (e.g., mild temperature and inert atmosphere) to preserve, and even enhance, nutritional and health properties. Encapsulation processes such as Rapid Expansion of Supercritical Solutions (RESS), Supercritical Anti Solvent Precipitation (SAS), Supercritical Fluid Extraction of Emulsions (SFEE), Particles from Gas Saturated Solutions (PGSS), and PGSS-drying are examples of this technology [72].

##### *i) Rapid Expansion of Supercritical Solutions (RESS)*

Rapid Expansion of Supercritical Solutions (RESS) was developed in the mid-1980s as the first formulation technique using SCFs [72]. Since then, many experimental and theoretical investigations [151,152] have proven that RESS is a suitable technique to produce submicrometric organic particles without additional solvents or surfactants to induce precipitation. Besides, RESS allows processing of heat-sensitive materials at mild temperatures and inert atmosphere.

Basically, the RESS process consists on a SFE step at  $T_E$  and  $p_E$ , in which the SCF (usually SC-CO<sub>2</sub>) is saturated with the material of interest. Subsequently, the fluid is brought to pre-expansion conditions ( $T_0$ ,  $p_0$ ). Finally, the mixture is expanded down to post-expansion conditions ( $T_P$ ,  $p_P$ ) through a nozzle (Fig. I-8). The sudden depressurization produces a large decrease in density (and solvent power), which creates a supersaturation condition and particle formation at high nucleation rates.

RESS process has been used in the pharmaceutical industry for the formulation of several drugs, either alone if they are solid at ambient temperature, or co-precipitated with solid bio-degradable polymers used as carriers. Its main

limitation is the low solubility of polar substances in SC-CO<sub>2</sub>, which can be overcome by incorporating liquid or solid co-solvents in the extraction step, although they need to have a high vapor pressure in order to easily separate them from the dried particles by evaporation or sublimation.

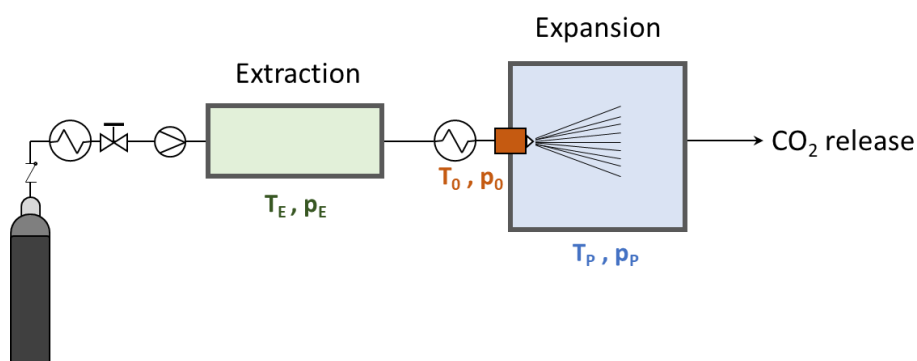


**Figure I-8.** Schematic representation of the RESS process (adapted from [72]).

There are not many studies referred to RESS process applied to lipid-related compounds in the literature. Oum *et al.* [153] investigated the influence of various expansion parameters on the formation of cholesterol, among other different organic substances, obtaining particle sizes around 190-250 nm at  $T_0 = 348\text{-}423$  K and  $p_0 = 20\text{-}30$  MPa, using SC-CO<sub>2</sub> as solvent.

#### ii) *Supercritical Anti-Solvent Precipitation (SAS)*

In the Supercritical Anti Solvent (SAS) process, the SCF (usually SC-CO<sub>2</sub>) or compressed gas and the organic solution containing the solute to be precipitated are fed to a precipitator. Here, the organic solution is dispersed in the SC-CO<sub>2</sub>, resulting in the precipitation of the solute by an antisolvent effect (Fig. I-9). Depending on the mode of operation, the supercritical phase can be static (batch) or continuously fed, as the so-called PCA (Precipitation with Compressed Antisolvents) or ASES techniques (Aerosol Solvent Extraction System) [154].



SAS process usually operates at pressures between 9-15 MPa in order to achieve a fast dissolution of the organic solvent into the supercritical phase. In this pressure range, several organic solvents such as ethanol or acetone are completely miscible with SC-CO<sub>2</sub> [72]. The organic solution is commonly sprayed through a nozzle into the precipitation chamber, enhancing the mass transfer due to droplet formation and producing small particles with narrow size distribution. Coaxial nozzles with an additional pre-mixing region at the end of the nozzle are the most commonly used [72].

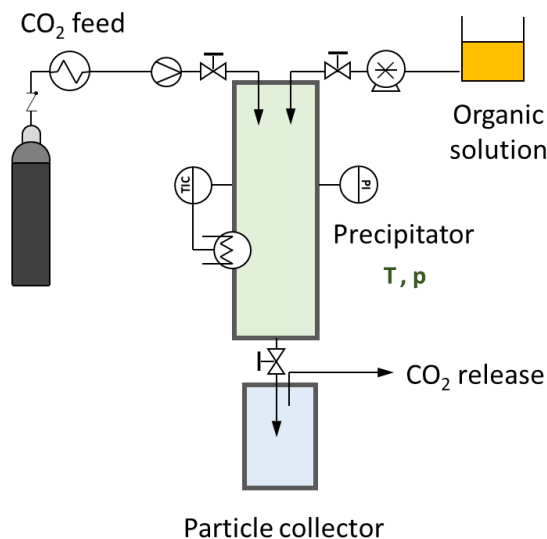


**Figure I-9.** Schematic representation of the SAS process (adapted from [155]).

The SAS process has been recently applied to encapsulate fish oil by Karim *et al.* [156], using hydroxypropyl methyl cellulose as a carrier. The study optimizes particle size by varying temperature, pressure, and feed emulsion rate using response surface methodology, although neither fish oil characterization nor the organic solvent used are reported. Optimum conditions were found at 60°C, p =15 MPa, and emulsion feed rate of 1.36 mL/min, obtaining particles with 58.35 μm mean diameter.

*iii) Supercritical Fluid Extraction of Emulsions (SFEE)*

The Supercritical Fluid Extraction of Emulsions (SFEE) process uses SC-CO<sub>2</sub> to rapidly extract the organic solvent from an oil-in-water emulsion, promoting the precipitation of the bioactive compounds (and surfactants or coating polymers) previously dissolved in the organic phase. During the extraction, each solvent drop behaves as a miniature SAS precipitator, thus allowing particle sizes in the sub-micrometric or nanometric scale and very narrow size distribution. The result is an aqueous dispersion of poorly water-soluble active compounds, stabilized by a surfactant to avoid agglomeration. Fig. I-10 shows a scheme of the SFEE process.

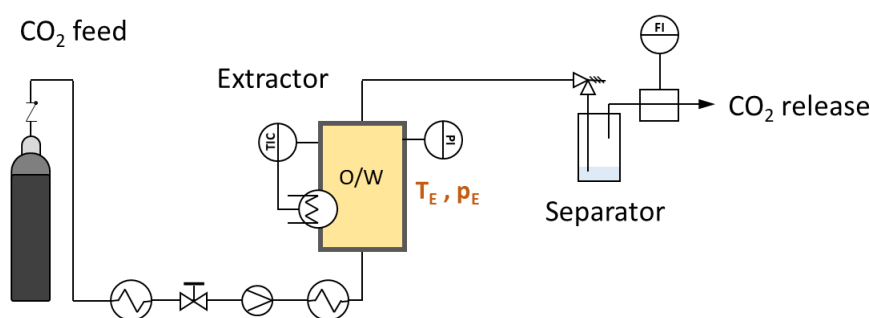


**Figure I-10.** Schematic representation of the SFEE process (adapted from [157]).

The SFEE process can be implemented at large scale by means of a countercurrent packed column [158]. Existing research has involved the encapsulation of solid pharmaceutical compounds in different matrices, although this technique can be also applied for encapsulating nutraceuticals in the food industry, such as vitamin E in polycaprolactone (PCL) [159],  $\beta$ -carotene in OSA-starch [160] and quercetin in Pluronic L64<sup>®</sup>, soy-bean lecithin, and  $\beta$ -glucan [161,162]. Fish oil with high EPA and DHA content has been recently encapsulated by SFEE process using an acetone-in-water emulsion, Tween 80 as surfactant, and PCL as the encapsulating polymer [157]. SFEE at 313 K, 8.0 MPa and CO<sub>2</sub> mass flow of 0.6 g/min achieved non-aggregated spherical nanoparticles of fish oil with a size below 100 nm.

*iv) Particles from Gas-Saturated Solutions (PGSS), and PGSS-drying*

Particles from Gas-Saturated Solutions (PGSS) was developed in 1995 by Weidner *et al.* [163,164], its main feature being that it works on the other side of the solubility isotherm in a p-x diagram (Fig I-11), taking advantage of the fact that the solubility of a compressed gas (usually SC-CO<sub>2</sub>) in liquids and/or molten high-molecular weight compounds (e.g., polymers) is much higher than the solubility of these substances in SC-CO<sub>2</sub>. This way, PGSS overcomes the drawbacks of the previously discussed technologies such as solubility limitations and high gas consumption.

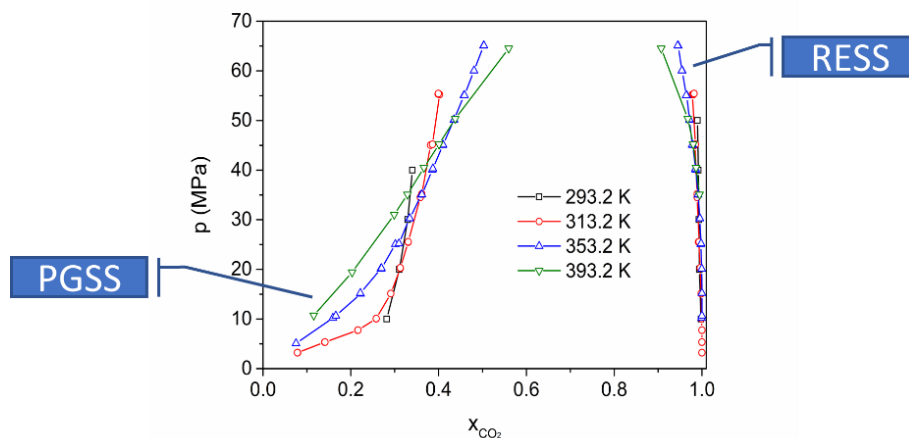


**Figure I-11.** Pressure vs. composition (p-x) diagram of the fish oil + CO<sub>2</sub> system (experimental data taken from [80]).

PGSS can operate in batch or continuous mode. A schematic representation of the process is provided in Fig. I-12. In this process, SC-CO<sub>2</sub> at T<sub>M</sub>, p<sub>M</sub> dissolves into the liquid or molten high-molecular weight polymer, giving an expanded gas-saturated solution with reduced viscosity. After intensive mixing (e.g., static mixer), the gas-saturated solution is expanded through a nozzle into a spray-tower to a lower (usually atmospheric) pressure. The sudden vaporization of the dissolved CO<sub>2</sub> provides a high atomization of the sprayed droplets, as well as solidification and precipitation of the particles due to the temperature decrease caused by the Joule-Thomson effect [165,166]. Solid particles are then separated from the gas by means

of filters and/or a cyclone. Final product properties, such as particle size and morphology, can be controlled by adjusting the process parameters, such as SC-CO<sub>2</sub> concentration in the liquid or molten polymer, pre-expansion conditions ( $T_0$ ,  $p_0$ ), nozzle geometry, and post-expansion conditions ( $T_{\text{spray}}$ ,  $p_{\text{spray}}$ ).

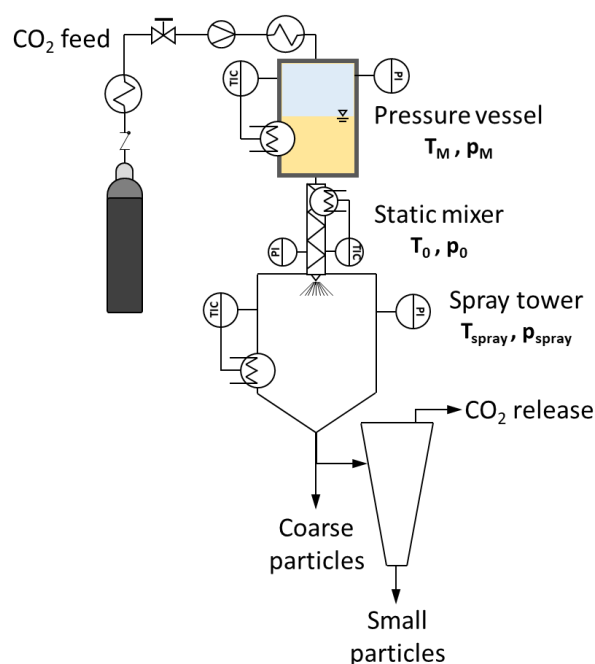


**Figure I-12.** Schematic representation of the PGSS process (adapted from [72]).

The PGSS process can produce particles from different substances, especially high-molecular weight polymers which are able to dissolve large amounts (up to 40 % wt.) of CO<sub>2</sub>. Mixtures of one or more bioactive compound(s) and one or more polymer(s) can be also processed, achieving composite particles and encapsulated bioactive compounds. In contrast with SAS or SFEE processes, no organic solvents are required, enabling the production of a solvent-free powder. Compared to RESS process, PGSS operates at lower pressure and consumes less gas. Typical pressures are in the range 3-25 MPa, with gas consumptions of 0.1-2 kg CO<sub>2</sub>/kg solute [72].



PGSS process has been recently applied by Tanbirul-Haque and Chun [167] to microencapsulate FAEEs obtained by enzymatic ethanolysis of SFE-extracted menhaden oil into polyethylene glycol 8000 (g/mol). Irregular particles with 16.7 % wt. FAEE load and particle size distribution centered around 120  $\mu\text{m}$  were obtained with operating pressures ranging from 10 to 20 MPa, temperatures between 45-55°C, and nozzle diameter of 200 and 300  $\mu\text{m}$ . Oil quality before and after PGSS process was measured through FFA determination, acid value, and peroxide value, finding almost no changes and enabling PGSS process as a suitable technique to formulate *n*-3 PUFA-enriched oils. However, no stability studies after storage were performed.

The PGSS process has been further modified in order to process aqueous solutions and dispersions (e.g., natural extracts, O/W emulsions) [168–172], leading to the so-called PGSS-drying process. Typically, the PGSS-drying process operates at pressures from 10 to 15 MPa and temperatures between 373 and 393 K, which are best to dissolve CO<sub>2</sub> in an aqueous solution or dispersion. Similar to classical PGSS, CO<sub>2</sub> is intensively mixed with the aqueous solution or dispersion in a static mixer and, subsequently, the saturated mixture is expanded through a nozzle into the spray tower, which operates at ambient pressure. Temperature in the spray tower and gas-to-product ratio (GPR) must be adequately controlled in order to operate above the dew line of the carbon dioxide + water system (Fig. I-13) and ensure the complete drying of particles [166].

The PGSS-drying technique can be used as an alternative to conventional spray-drying process, especially for processing of thermolabile compounds. Besides the enhanced atomization, the sudden depressurization from supercritical to atmospheric conditions causes an intense and deep cooling effect (Joule-Thomson effect) that allows drying at lower temperatures than spray-drying. Additionally, the intrinsically inert ambient conditions due to oxygen displacement, prevent or at least delay oxidative degradation of the encapsulated bioactive compounds [165].

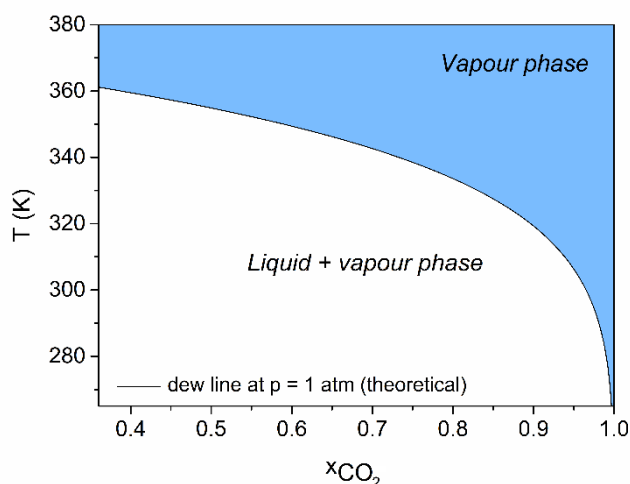


**Figure I-13.** Temperature vs. composition (T-x) diagram of the CO<sub>2</sub> + H<sub>2</sub>O system at p = 1 atm, calculated assuming ideal behavior of the gas phase. Operating conditions in the spray tower should lie above the dew line (adapted from [166]).

Fish oil encapsulation in a maltodextrin coating using PGSS-drying was carried out by Rubio-Rodríguez [77]. Firstly, multilayer O/W emulsions were obtained using a mixture of non-ionic/cationic emulgents (Tween 80 / chitosan) and anionic/cationic emulgents (lecithin / chitosan). Subsequently, O/W emulsions were dried by PGSS-drying. Different operating parameters, such as emulsion formulation, nozzle geometry (wide and narrow), pre-expansion pressure (11-25.7 MPa), GPR (6-88) and expansion temperature (70-119 °C) were studied through 21 PGSS-drying runs. Spherical microparticles with fish oil loads up to 40 mg/g solid and encapsulation efficiencies up to 90 % were obtained.

The work by Rubio-Rodríguez [77] demonstrated that PGSS-drying may be a valuable process to produce fish oil microcapsules in food-grade coatings from fish oil-in-water emulsions. However, as Rubio-Rodríguez [77] concluded, further studies about formulation of O/W emulsions and its stability under SC-CO<sub>2</sub> would be required in order to optimize the PGSS-drying process in terms of yield and encapsulation efficiency. Besides, subsequent stability studies after storage would be also necessary in order to test if the microencapsulated *n*-3 PUFAs are



sufficiently protected against oxidation. Finally, a comparison among encapsulation efficiency and other properties (e.g., moisture, average particle size and distribution, morphology) of the particles obtained by PGSS-drying and conventional microencapsulation processes, mainly spray-drying but also others such as freeze-drying, would be also of interest in order to assess the competitiveness of the PGSS-drying process and its potential implementation at large scale. Chapter 4 of the present work (Results section) aims to fulfil these tasks.



## References

- [1] C.C. Akoh (Ed.), *Food Lipids, Chemistry, Nutrition, and Biotechnology*, 4th ed., CRC Press, Boca Raton, 2017.
- [2] D.E. Vance, J.E. Vance (Eds.), *Biochemistry of Lipids, Lipoproteins and Membranes*, 5th ed., Elsevier, San Diego, 2008.
- [3] A.P. Simopoulos, Omega-3 fatty acids in health and disease and in growth and development, *Am. J. Clin. Nutr.* 54 (1991) 438–463.
- [4] P.M. Kris-Etherton, W.S. Harris, L.J. Appel, Fish consumption, fish oil, omega-3 fatty acids, and cardiovascular disease, *Circulation*. 106 (2002) 2747–2757.
- [5] P.C. Calder, Mechanisms of action of (*n*-3) fatty acids, *J. Nutr.* 142 (2012) 592S–599S.
- [6] S. Kalmijn, L.J. Launer, A. Ott, J.C.M. Witteman, A. Hofman, M.M.B. Breteler, Dietary fat intake and the risk of incident dementia in the Rotterdam study, *Ann. Neurol.* 42 (1997) 776–782.
- [7] M.C. Morris, D.A. Evans, J.L. Bienias, C.C. Tangney, D.A. Bennett, R.S. Wilson, N. Aggarwal, J. Schneider, Consumption of fish and *n*-3 fatty acids and risk of incident Alzheimer disease, *Arch. Neurol.* 60 (2003) 940–946.
- [8] F. Calon, G.P. Lim, F. Yang, T. Morihara, B. Teter, O. Ubeda, P. Rostaing, A. Triller, N. Salem Jr., K.H. Ashe, S.A. Frautschy, G.M. Cole, Docosahexaenoic acid protects from dendritic pathology in an Alzheimer's disease mouse model, *Neuron*. 43 (2004) 633–645.
- [9] S.C. Larsson, M. Kumlin, M. Ingelman-Sundberg, A. Wolk, Dietary long-chain *n*-3 fatty acids for the prevention of cancer: A review of potential mechanisms, *Am. J. Clin. Nutr.* 79 (2004) 935–945.
- [10] J.R. Hibbeln, J.M. Davis, C. Steer, P. Emmett, I. Rogers, C. Williams, J. Golding, Maternal seafood consumption in pregnancy and neurodevelopmental outcomes in childhood (ALSPAC study): an observational cohort study, *Lancet*. 369 (2007) 578–585.
- [11] T.L. Psota, S.K. Gebauer, P. Kris-Etherton, Dietary omega-3 fatty acid intake and cardiovascular risk, *Am. J. Cardiol.* 98 (2006) 3–18.
- [12] K. Harnack, G. Andersen, V. Somoza, Quantitation of alpha-linolenic acid elongation to eicosapentaenoic and docosahexaenoic acid as affected by the ratio of *n*-6/*n*-3 fatty acids, *Nutr. Metab. (Lond)*. 6 (2009) 8.
- [13] A.P. Simopoulos, The importance of the ratio of omega-6/omega-3 essential fatty acids, *Biomed. Pharmacother.* 56 (2002) 365–379.



- [14] A.P. Simopoulos, A. Leaf, N. Salem, Workshop on the essentiality of and recommended dietary intakes for omega-6 and omega-3 fatty acids, *J. Am. Coll. Nutr.* 18 (1999) 487–489.
- [15] FAO - Food and Agriculture Organization of the United Nations, / WHO – World Health Organization, Interim summary of conclusions and dietary recommendations on total fat & fatty acids, Geneva, 2008.
- [16] European Food Safety Authority, Scientific opinion on dietary reference values for fats, including saturated fatty acids, polyunsaturated fatty acids, monounsaturated fatty acids, trans fatty acids, and cholesterol, *EFSA J.* 8 (2010) 1461.
- [17] N. Rubio-Rodríguez, S. Beltrán, I. Jaime, S.M. de Diego, M.T. Sanz, J.R. Carballido, Production of omega-3 polyunsaturated fatty acid concentrates: a review, *Innov. Food Sci. Emerg. Technol.* 11 (2010) 1–12.
- [18] D. Muir, T. Savinova, V. Savinov, L. Alexeeva, V. Potelov, V. Svetochev, Bioaccumulation of PCBs and chlorinated pesticides in seals, fishes and invertebrates from the White Sea, Russia, *Sci. Total Environ.* 306 (2003) 111–131.
- [19] S.E. Schober, T.H. Sinks, R.L. Jones, P.M. Bolger, M. McDowell, J. Osterloh, E.S. Garrett, R.A. Canady, C.F. Dillon, Y. Sun, C.B. Joseph, K.R. Mahaffey, Blood mercury levels in US children and women of childbearing age, 1999-2000, *J. Am. Med. Assoc.* 289 (2003) 1667–1674.
- [20] M.A. Moyad, An introduction to dietary/supplemental omega-3 fatty acids for general health and prevention: Part II, *Urol. Oncol. Semin. Orig. Investig.* 23 (2005) 36–48.
- [21] C. Dawczynski, R. Schubert, G. Jahreis, Amino acids, fatty acids, and dietary fibre in edible seaweed products, *Food Chem.* 103 (2007) 891–899.
- [22] J. Mataix, *Tablas de Composición de Alimentos*, 5th ed., Universidad de Granada, Granada, 2009.
- [23] M. Van Dijk, J. Vitek (Eds.), *Fish oil: Production, Consumption and Health Benefits (Nutrition and Diet Research Progress)*, 1st ed., Nova Science Publishers, Inc., New York, 2012.
- [24] I.H. Pike, A. Jackson, Fish oil: production and use now and in the future, *Lipid Technol.* 22 (2010) 59–61.
- [25] FAO - Food and Agriculture Organization of the United Nations, Fishery Industries Division, *The Production of Fish Meal and Oil*, FAO Fisheries Technical paper - 142, Food and Agriculture Organization of the United Nations, Rome, 1986.



- [26] M.L. Monte, M.L. Monte, R.S. Pohndorf, V.T. Crexi, L.A.A. Pinto, Bleaching with blends of bleaching earth and activated carbon reduces color and oxidation products of carp oil, *Eur. J. Lipid Sci. Technol.* 117 (2015) 829–836.
- [27] Á.G. Solaesa, S.L. Bucio, M.T. Sanz, S. Beltrán, S. Rebolleda, Characterization of triacylglycerol composition of fish oils by using chromatographic techniques, *J. Oleo Sci.* 63 (2014) 449–460.
- [28] Y. Ando, K. Nishimura, N. Aoyanagi, T. Takagi, Stereospecific Analysis of Fish Oil Triacyl-*sn*-glycerols, *J. Am. Oil Chem. Soc.* 69 (1992) 417–424.
- [29] C. Wijesundera, C. Ceccato, P. Watkins, P. Fagan, B. Fraser, N. Thienthong, P. Perlmutter, Docosahexaenoic acid is more stable to oxidation when located at the *sn*-2 position of triacylglycerol compared to *sn*-1(3), *J. Am. Oil Chem. Soc.* 85 (2008) 543–548.
- [30] FAO - Food and Agriculture Organization of the United Nations, GLOBEFISH Highlights, Issue 4/2017.
- [31] F. de Meester, R. Watson, S. Zibadi (Eds.), *Omega-6/3 Fatty Acids: Functions, Sustainability Strategies and Perspectives*, Humana Press, New York, 2013.
- [32] R. Ciriminna, F. Meneguzzo, R. Delisi, M. Pagliaro, Enhancing and improving the extraction of omega-3 from fish oil, *Sustain. Chem. Pharm.* 5 (2017) 54–59.
- [33] N. Rubio-Rodríguez, S.M. de Diego, S. Beltrán, I. Jaime, M.T. Sanz, J. Rovira, Supercritical fluid extraction of the omega-3 rich oil contained in hake (*Merluccius capensis*-*Merluccius paradoxus*) by-products: Study of the influence of process parameters on the extraction yield and oil quality, *J. Supercrit. Fluids.* 47 (2008) 215–226.
- [34] N. Rubio-Rodríguez, S.M. De Diego, S. Beltrán, I. Jaime, M.T. Sanz, J. Rovira, Supercritical fluid extraction of fish oil from fish by-products: A comparison with other extraction methods, *J. Food Eng.* 109 (2012) 238–248.
- [35] L.D. Lawson, B.G. Hughes, Human absorption of fish oil fatty acids as triacylglycerols, free acids, or ethyl esters, *Biochem. Biophys. Res. Commun.* 152 (1988) 328–335.
- [36] L.C. Boyd, M.F. King, B. Sheldon, A rapid method for determining the oxidation of *n*-3 fatty acids, *J. Am. Oil Chem. Soc.* 69 (1992) 325–330.
- [37] N. Ding, Y. Xue, X. Tang, Z.-M. Sun, T. Yanagita, C.-H. Xue, Y.-M. Wang, Short-term effects of different fish oil formulations on tissue absorption of docosahexaenoic acid in mice fed high- and low-fat diets, *J. Oleo Sci.* 62 (2013) 883–891.



- [38] S.L. Bucio, Á.G. Solaesa, M.T. Sanz, R. Melgosa, S. Beltrán, H. Sovová, Kinetic study for the ethanolysis of fish oil catalyzed by Lipozyme 435 in different reaction media, *J. Oleo Sci.* 64 (2015) 431–441.
- [39] Á.G. Solaesa, M.T. Sanz, R. Melgosa, S.L. Bucio, S. Beltrán, Glycerolysis of sardine oil catalyzed by a water dependent lipase in different *tert*-alcohols as reaction medium, *Grasas y Aceites.* 66 (2015) e102.
- [40] V.K. Mishra, F. Temelli, B. Ooraikul, Extraction and purification of  $\omega$ -3 fatty acids with an emphasis on supercritical fluid extraction-a review, *Food Res. Int.* 26 (1993) 217–226.
- [41] F. Shahidi, U.N. Wanasundara, Omega-3 fatty acid concentrates: nutritional aspects and production technologies, *Trends Food Sci. Technol.* 9 (1998) 230–240.
- [42] G.G. Haraldsson, B. Kristinsson, R. Sigurdardottir, G.G. Gudmundsson, H. Breivik, The preparation of concentrates of eicosapentaenoic acid and docosahexaenoic acid by lipase-catalyzed transesterification of fish oil with ethanol, *J. Am. Oil Chem. Soc.* 74 (1997) 1419–1424.
- [43] S. Uluata, D.J. McClements, E.A. Decker, How the multiple antioxidant properties of ascorbic acid affect lipid oxidation in oil-in-water emulsions, *J. Agric. Food Chem.* 63 (2015) 1819–1824.
- [44] E. Niki, Lipid peroxidation: Physiological levels and dual biological effects, *Free Radic. Biol. Med.* 47 (2009) 469–484.
- [45] H.H. Huss, Quality and quality changes in fresh fish. FAO Fisheries technical paper - 348, Food and Agriculture Organization of the United Nations, Rome, 1995.
- [46] A. Kamal-Eldin, N. V Yanishlieva, *n*-3 fatty acids for human nutrition: stability considerations, *Eur. J. Lipid Sci. Technol.* 104 (2002) 825–836.
- [47] C. Jacobsen, M.B. Let, N.S. Nielsen, A.S. Meyer, Antioxidant strategies for preventing oxidative flavour deterioration of foods enriched with *n*-3 polyunsaturated lipids: a comparative evaluation, *Trends Food Sci. Technol.* 19 (2008) 76–93.
- [48] S. Wada, X. Fang, The synergistic antioxidant effect of rosemary extract and  $\alpha$ -tocopherol in sardine oil model system and frozen-crushed fish meat, *J. Food Process. Preserv.* 195 (1992) 95–98.
- [49] E.N. Frankel, S.-W. Huang, E. Prior, R. Aeschbach, Evaluation of antioxidant activity of rosemary extracts, carnosol and carnosic acid in bulk vegetable oils and fish oil and their emulsions, *J. Sci. Food Agric.* 72 (1996) 201–208.



- [50] S.D. Bhale, Z. Xu, W. Prinyawiwatkul, J.M. King, J.S. Godber, Oregano and rosemary extracts inhibit oxidation of long-chain *n*-3 fatty acids in menhaden oil, *J. Food Sci.* 72 (2007) C504–C508.
- [51] D. Jimenez-Alvarez, F. Giuffrida, P.A. Golay, C. Cotting, A. Lardeau, B.J. Keely, Antioxidant activity of oregano, parsley, and olive mill wastewaters in bulk oils and oil-in-water emulsions enriched in fish oil, *J. Agric. Food Chem.* 56 (2008) 7151–7159.
- [52] R. Matsuno, S. Adachi, Lipid encapsulation technology - techniques and applications to food, *Trends Food Sci. Technol.* 4 (1993) 256–261.
- [53] Y.H. Cho, H.K. Shim, J. Park, Encapsulation of fish oil by an enzymatic gelation process using transglutaminase cross-linked proteins, *J. Food Sci.* 68 (2003) 2717–2723.
- [54] Y. Tan, K. Xu, L. Li, C. Liu, C. Song, P. Wang, Fabrication of size-controlled starch-based nanospheres by nanoprecipitation, *ACS Appl. Mater. Interfaces.* 1 (2009) 956–959.
- [55] M. Choi, U. Ruktanonchai, S. Min, J. Chun, A. Soottitantawat, Physical characteristics of fish oil encapsulated by  $\beta$ -cyclodextrin using an aggregation method or polycaprolactone using an emulsion-diffusion method, *Food Chem.* 119 (2010) 1694–1703.
- [56] J. Legako, N.T. Dunford, Effect of spray nozzle design on fish oil-whey protein microcapsule properties, *J. Food Sci.* 75 (2010) E394–E400.
- [57] R. Wang, Z. Tian, L. Chen, A novel process for microencapsulation of fish oil with barley protein, *Food Res. Int.* 44 (2011) 2735–2741.
- [58] S. Chatterjee, Z.M.A. Judeh, Encapsulation of fish oil with N-stearoyl O-butylglyceryl chitosan using membrane and ultrasonic emulsification processes, *Carbohydr. Polym.* 123 (2015) 432–442.
- [59] J. Yang, O.N. Ciftci, Encapsulation of fish oil into hollow solid lipid micro- and nanoparticles using carbon dioxide, *Food Chem.* 231 (2017) 105–113.
- [60] K.G.H. Desai, H.J. Park, Recent developments in microencapsulation of food ingredients, *Dry. Technol.* 23 (2005) 1361–1394.
- [61] A. Gharsallaoui, G. Roudaut, O. Chambin, A. Voilley, R. Saurel, Applications of spray-drying in microencapsulation of food ingredients: an overview, *Food Res. Int.* 40 (2007) 1107–1121.
- [62] S. Drusch, Y. Serfert, M. Scampicchio, B. Schmidt-Hansberg, K. Schwarz, Impact of physicochemical characteristics on the oxidative stability of fish oil microencapsulated by spray-drying, *J. Agric. Food Chem.* 55 (2007) 11044–11051.



- [63] S. Drusch, S. Berg, Extractable oil in microcapsules prepared by spray-drying: localisation, determination and impact on oxidative stability, *Food Chem.* 109 (2008) 17–24.
- [64] S.M. Jafari, E. Assadpoor, Y. He, B. Bhandari, Encapsulation efficiency of food flavours and oils during spray drying, *Dry. Technol.* 26 (2008) 816–835.
- [65] R. V Tonon, C.R.F. Grosso, M.D. Hubinger, Influence of emulsion composition and inlet air temperature on the microencapsulation of flaxseed oil by spray drying, *Food Res. Int.* 44 (2011) 282–289.
- [66] R. Morales-Medina, F. Tamm, A.M. Guadix, E.M. Guadix, S. Drusch, Functional and antioxidant properties of hydrolysates of sardine (*S. pilchardus*) and horse mackerel (*T. mediterraneus*) for the microencapsulation of fish oil by spray-drying, *Food Chem.* 194 (2016) 1208–1216.
- [67] K. Heinzelmann, K. Franke, B. Jensen, A.M. Haahr, Protection of fish oil from oxidation by microencapsulation using freeze-drying, *Eur. J. Lipid Sci. Technol.* (2000) 114–121.
- [68] K. Heinzelmann, K. Franke, J. Velasco, G. Márquez-Ruiz, Microencapsulation of fish oil by freeze-drying techniques and influence of process parameters on oxidative stability during storage, *Eur. Food Res. Technol.* 211 (2000) 234–239.
- [69] C. Chung, L. Sanguansri, M. Ann, *In vitro* lipolysis of fish oil microcapsules containing protein and resistant starch, *Food Chem.* 124 (2011) 1480–1489.
- [70] W. Klaypradit, Y.-W. Huang, Fish oil encapsulation with chitosan using ultrasonic atomizer, *LWT - Food Sci. Technol.* 41 (2008) 1133–1139.
- [71] P.J. García-Moreno, K. Stephansen, J. van der Krujjs, A. Guadix, E.M. Guadix, I.S. Chornakis, C. Jacobsen, Encapsulation of fish oil nanofibers by emulsion electrospinning: physical characterization and oxidative stability, *J. Food Eng.* 183 (2016) 39–49.
- [72] M. Türk (Ed.), *Particle Formation with Supercritical Fluids, Challenges and Limitations*, Vol. 6, 1st ed., Elsevier, 2014.
- [73] P.G. Jessop, W. Leitner, *Supercritical Fluids as Media for Chemical Reactions*, in: *Chem. Synth. Using Supercrit. Fluids*, Wiley-VCH Verlag GmbH, 1999: pp. 1–36.
- [74] G. Brunner, *Gas Extraction: an Introduction to Fundamentals of Supercritical Fluids and the Application to Separation Processes*, Steinkopff-Verlag Heidelberg, Springer, Darmstadt, New York, 1994.



- [75] S. Angus, B. Armstrong, K.M. de Reuck, *International Thermodynamic Tables of the Fluid State - 3*, IUPAC Project Centre, Imperial College, Pergamon Press, London, 1976.
- [76] Y.A. Çengel, M.A. Boles, *Thermodynamics: An Engineering Approach*, 8th ed., McGraw-Hill College, New York, 2015.
- [77] N. Rubio-Rodríguez, *Supercritical fluid technology for extraction, concentration and formulation of omega-3 rich oils. A novel strategy for valorization of fish by-products (PhD Thesis)*, University of Burgos, 2011.
- [78] L. Fiori, M. Volpe, M. Lucian, A. Anesi, M. Manfrini, G. Guella, From fish waste to omega-3 concentrates in a biorefinery concept, *Waste Biomass Valor.* 8 (2017) 2609–2620.
- [79] N. Imanishi, R. Fukuzato, S. Furuta, N. Ikawa, Supercritical fluid extraction of fish oil with carbon dioxide, *R & D Kobe Eng. Reports.* 39 (1989) 29–32.
- [80] C. Borch-Jensen, J. Mollerup, Phase equilibria of fish oil in sub- and supercritical carbon dioxide, *Fluid Phase Equilib.* 138 (1997) 179–211.
- [81] O.J. Catchpole, J.B. Grey, K.A. Noermark, Solubility of fish oil components in supercritical CO<sub>2</sub> and CO<sub>2</sub> + ethanol mixtures, *J. Chem. Eng. Data.* 43 (1998) 1091–1095.
- [82] A. Staby, J. Mollerup, Solubility of fish oil fatty acid ethyl esters in sub- and supercritical carbon dioxide, *J. Am. Oil Chem. Soc.* 70 (1993) 583–588.
- [83] Ö. Güçlü-Üstündağ, F. Temelli, Correlating the solubility behavior of fatty acids, mono-, di-, and triglycerides, and fatty acid esters in supercritical carbon dioxide, *Ind. Eng. Chem. Res.* 39 (2000) 4756–4766.
- [84] Ö. Güçlü-Üstündağ, F. Temelli, Correlating the solubility behavior of minor lipid components in supercritical carbon dioxide, *J. Supercrit. Fluids.* 31 (2004) 235–253.
- [85] M. Létisse, M. Rozières, A. Hiol, M. Sergent, L. Comeau, Enrichment of EPA and DHA from sardine by supercritical fluid extraction without organic modifier. I. Optimization of extraction conditions, *J. Supercrit. Fluids.* 38 (2006) 27–36.
- [86] S.L. Bucio, M.T. Sanz, S. Beltrán, R. Melgosa, Á.G. Solaesa, M.O. Ruiz, Study of the influence of process parameters on liquid and supercritical CO<sub>2</sub> extraction of oil from rendered materials: Fish meal and oil characterization, *J. Supercrit. Fluids.* 107 (2016) 270–277.
- [87] K. Ivanovs, D. Blumberga, Extraction of fish oil using green extraction methods: a short review, *Energy Procedia*, 2017: pp. 477–483.



- [88] J.-H. Lee, A.K.M. Asaduzzaman, J.-H. Yun, J.-H. Yun, B.-S. Chun, Characterization of the yellow croaker *Larimichthys polyactis* muscle oil extracted with supercritical carbon dioxide and an organic solvent, *Fish. Aquat. Sci.* 15 (2012) 275–281.
- [89] M.Z.I. Sarker, J. Selamat, A.S.M.A. Habib, S. Ferdosh, M.J.H. Akanda, J.M. Jaffri, Optimization of supercritical CO<sub>2</sub> extraction of fish oil from viscera of African Catfish (*Clarias gariepinus*), *Int. J. Mol. Sci.* 13 (2012) 11312–11322.
- [90] A.C. Aguiar, J. V Visentainer, J. Martínez, Extraction from striped weakfish (*Cynoscion striatus*) wastes with pressurized CO<sub>2</sub>: Global yield, composition, kinetics and cost estimation, *J. Supercrit. Fluids.* 71 (2012) 1–10.
- [91] S. Ferdosh, M.Z. Islam Sarker, N.N.N. Abd Rahman, J. Selamat, M.R. Karim, T.A. Razak, M.O. Abd Kadir, Fish oil recovery from viscera of indian mackerel (*Rastrelliger kanagurta*) by supercritical fluid: an optimization approach, *J. Chinese Chem. Soc.* 59 (2012) 1421–1429.
- [92] S. Hao, H. Hui, L. Li, X. Yang, J. Cen, W. Lin, Y. Wei, Extraction of fish oil from the muscle of sturgeon using supercritical fluids, *Adv. Mater. Res.* 655–657 (2013) 1975–1981.
- [93] S. Ferdosh, M.Z.I. Sarker, N.N.N.A. Rahman, M.J.H. Akand, K. Ghafoor, M.B. Awang, M.O.A. Kadir, Supercritical carbon dioxide extraction of oil from *Thunnus tonggol* head by optimization of process parameters using response surface methodology, *Korean J. Chem. Eng.* 30 (2013) 1466–1472.
- [94] B. Homayooni, M.A. Sahari, M. Barzegar, Concentrations of omega–3 fatty acids from rainbow sardine fish oil by various methods, *Int. Food Res. J.* 21 (2014) 743–748.
- [95] M.A. Gedi, J. Bakar, A.A. Mariod, Optimization of supercritical carbon dioxide (CO<sub>2</sub>) extraction of sardine (*Sardinella lemuru* Bleeker) oil using response surface methodology (RSM), *Grasas y Aceites.* 66 (2015).
- [96] Y. Wang, X. Ji, J. Huang, Q. Wang, Y. Chen, J. Xia, X. Su, The analysis of the effect of supercritical CO<sub>2</sub> extraction technology on volatile component of tuna oils, *J. Chinese Cereal. Oils Assoc.* 30 (2015) 74–78 and 100.
- [97] S. Ferdosh, Z.I. Sarker, N. Norulaini, A. Oliveira, K. Yunus, A.J. Chowdury, J. Akanda, M. Omar, Quality of tuna fish oils extracted from processing the by-products of three species of neritic tuna using supercritical carbon dioxide, *J. Food Process. Preserv.* 39 (2015) 432–441.
- [98] S. Ferdosh, M.Z.I. Sarker, N.N.N.A. Rahman, M.J.H. Akanda, K. Ghafoor, M.O.A. Kadir, Simultaneous extraction and fractionation of fish oil from tuna by-product using supercritical carbon dioxide (SC-CO<sub>2</sub>), *J. Aquat. Food Prod. Technol.* 25 (2016) 230–239.



- [99] M.M. Taati, B. Shabanpour, M. Ojagh, Extraction of oil from tuna by-product by supercritical fluid extraction (SFE) and comparison with wet reduction method, *AACL Bioflux*. 10 (2017) 1546–1553.
- [100] B. Ye, X. Wang, N. Tao, Q. Zhu, C. Hua, Extraction of oil and lecithin from Pacific saury (*Cololabis saira*) viscera by supercritical CO<sub>2</sub>, *J. Chinese Inst. Food Sci. Technol.* 15 (2015) 100–109.
- [101] I.A. Adeoti, K. Hawboldt, Experimental and mass transfer modelling of oil extraction from salmon processing waste using SC-CO<sub>2</sub>, *J. Supercrit. Fluids*. 104 (2017).
- [102] M. Haq, R. Ahmed, Y.-J. Cho, B.-S. Chun, Quality properties and biopotentiality of edible oils from atlantic salmon by-products extracted by supercritical carbon dioxide and conventional methods, *Waste Biomass Valor.* 8 (2017) 1953–1967.
- [103] S. Kuvendziev, K. Lisichkov, Z. Zeković, M. Marinkovski, Z.H. Musliu, Supercritical fluid extraction of fish oil from common carp (*Cyprinus carpio* L.) tissues, *J. Supercrit. Fluids*. 133 (2018) 528–534.
- [104] M. Goto, M. Sato, T. Hirose, Extraction of peppermint oil by supercritical carbon dioxide, *J. Chem. Eng. Jpn.* 26 (1993) 401–407.
- [105] J. Čmolík, J. Pokorný, Physical refining of edible oils, *Eur. J. Lipid Sci. Technol.* 102 (2000) 472–486.
- [106] B.M. Bhosle, R. Subramanian, New approaches in deacidification of edible oils - a review, *J. Food Eng.* 69 (2005) 481–494.
- [107] L.L. Lai, K.C. Soheili, W.E. Artz, Deacidification of soybean oil using membrane processing and subcritical carbon dioxide, *J. Am. Oil Chem. Soc.* 85 (2008) 189–196.
- [108] A. Kawashima, R. Iwakiri, K. Honda, Experimental study on the removal of dioxins and coplanar polychlorinated biphenyls (PCBs) from fish oil, *J. Agric. Food Chem.* 54 (2006) 10294–10299.
- [109] M. Jakobsson, B. Sivik, P.-A. Bergqvist, B. Strandberg, M. Hjelt, C. Rappe, Extraction of dioxins from cod liver oil by supercritical carbon dioxide, *J. Supercrit. Fluids*. 4 (1991) 118–123.
- [110] M. Jakobsson, B. Sivik, P.A. Bergqvist, B. Strandberg, C. Rappe, Counter-current extraction of dioxins from cod liver oil by supercritical carbon dioxide, *J. Supercrit. Fluids*. 7 (1994) 197–200.
- [111] O.J. Catchpole, J.B. Grey, K.A. Noermark, Fractionation of fish oils using supercritical CO<sub>2</sub> and CO<sub>2</sub> + ethanol mixtures, *J. Supercrit. Fluids*. 19 (2000) 25–37.



- [112] A. Kawashima, S. Watanabe, R. Iwakiri, K. Honda, Removal of dioxins and dioxin-like PCBs from fish oil by countercurrent supercritical CO<sub>2</sub> extraction and activated carbon treatment, *Chemosphere*. 75 (2009) 788–794.
- [113] C. Vaisali, S. Charanyaa, P.D. Belur, I. Regupathi, Refining of edible oils: a critical appraisal of current and potential technologies, *Int. J. Food Sci. Technol.* 50 (2015) 13–23.
- [114] H.R. Hobbs, N.R. Thomas, Biocatalysis in supercritical fluids, in fluorosolvents, and under solvent-free conditions., *Chem. Rev.* 107 (2007) 2786–820.
- [115] Ž. Knez, Enzymatic reactions in dense gases, *J. Supercrit. Fluids.* 47 (2009) 357–372.
- [116] G.R. Akien, M. Poliakoff, A critical look at reactions in class I and II gas-expanded liquids using CO<sub>2</sub> and other gases, *Green Chem.* 11 (2009) 1083.
- [117] T. Matsuda, Recent progress in biocatalysis using supercritical carbon dioxide., *J. Biosci. Bioeng.* 115 (2013) 233–41.
- [118] H. Gunnlaugsdottir, B. Sivik, Lipase-catalyzed alcoholysis of cod liver oil in supercritical carbon dioxide, *J. Am. Oil Chem. Soc.* 72 (1995) 399–405.
- [119] H. Gunnlaugsdottir, B. Sivik, Lipase-catalyzed alcoholysis with supercritical carbon dioxide extraction 1: Influence of flow rate, *J. Am. Oil Chem. Soc.* 74 (1997) 1483–1490.
- [120] H. Gunnlaugsdottir, A.Å. Karlsson, B. Sivik, Lipase-catalyzed alcoholysis with supercritical carbon dioxide extraction 2: Phase behavior, *J. Am. Oil Chem. Soc.* 74 (1997) 1491–1494.
- [121] J.V. Oliveira, D. Oliveira, Kinetics of the enzymatic alcoholysis of palm kernel oil in supercritical CO<sub>2</sub>, *Ind. Eng. Chem. Res.* 39 (2000) 4450–4454.
- [122] D. Oliveira, J.V. Oliveira, Enzymatic alcoholysis of palm kernel oil in n-hexane and SCCO<sub>2</sub>, *J. Supercrit. Fluids.* 19 (2001) 141–148.
- [123] S.-K. Shin, J.-E. Sim, H. Kishimura, B.-S. Chun, Characteristics of menhaden oil ethanolysis by immobilized lipase in supercritical carbon dioxide, *J. Ind. Eng. Chem.* 18 (2012) 546–550.
- [124] M. Lee, D. Lee, J. Cho, S. Kim, C. Park, Enzymatic biodiesel synthesis in semi-pilot continuous process in near-critical carbon dioxide, *Appl. Biochem. Biotechnol.* 171 (2013) 1118–1127.
- [125] A. Marty, W. Chulalaksananukul, J.S. Condoret, R.M. Willemot, G. Durand, Comparison of lipase-catalysed esterification in supercritical carbon dioxide and in n-hexane, *Biotechnol. Lett.* 12 (1990) 11–16.



- [126] A. Marty, W. Chulalaksananukul, R.M. Willemot, J.S. Condoret, Kinetics of lipase-catalyzed esterification in supercritical CO<sub>2</sub>, *Biotechnol. Bioeng.* 39 (1992) 273–280.
- [127] Z. -R. Yu, S.S.H. Rizvi, J.A. Zollweg, Enzymatic esterification of fatty acid mixtures from milk fat and anhydrous milk fat with canola oil in supercritical carbon dioxide, *Biotechnol. Prog.* 8 (1992) 508–513.
- [128] H. Gunnlaugsdottir, K. Wannerberger, B. Sivik, Alcoholysis and glyceride synthesis with immobilized lipase on controlled-pore glass of varying hydrophobicity in supercritical carbon dioxide, *Enzyme Microb. Technol.* 22 (1998) 360–367.
- [129] T.-J. Lin, S.-W. Chen, A.-C. Chang, Enrichment of *n*-3 PUFA contents on triglycerides of fish oil by lipase-catalyzed trans-esterification under supercritical conditions, *Biochem. Eng. J.* 29 (2006) 27–34.
- [130] T. Lin, S. Chen, Enrichment of *n*-3 polyunsaturated fatty acids into acylglycerols of borage oil via lipase-catalyzed reactions under supercritical conditions, *Chem. Eng. J.* 141 (2008) 318–326.
- [131] N. Ma, S. In, T. Zhao, D. Som, C.T. Kim, Y. Kim, I.H. Kim, S.I. Hong, T. Zhao, D.S. No, C.T. Kim, Y. Kim, I.H. Kim, Enrichment of docosahexaenoic acid from tuna oil via lipase-mediated esterification under pressurized carbon dioxide, *J. Supercrit. Fluids.* 87 (2014) 28–33.
- [132] M.-K. Roh, Y.D. Kim, J.-S. Choi, Transesterification of fish oil by lipase immobilized in supercritical carbon dioxide, *Fish. Sci.* 81 (2015) 1113–1125.
- [133] A.P.A. Corrêa, C.A. Peixoto, L.A.G. Gonçalves, F.A. Cabral, Fractionation of fish oil with supercritical carbon dioxide, *J. Food Eng.* 88 (2008) 381–387.
- [134] K. Zosel, Praktische Anwendungen der Stofftrennung mit überkritischen Gasen, *Angew. Chemie.* 90 (1978) 748–755.
- [135] W. Eisenbach, Supercritical Fluid Extraction: A Film Demonstration (Invited Lecture), *Berichte der Bunsengesellschaft Für Physikalische Chemie.* 88 (1984) 882–887.
- [136] W.B. Nilsson, E.J. Gauglitz Jr., J.K. Hudson, V.F. Stout, J. Spinelli, Fractionation of menhaden oil ethyl esters using supercritical fluid CO<sub>2</sub>, *J. Am. Oil Chem. Soc.* 65 (1988) 109–117.
- [137] W.B. Nilsson, E.J. Gauglitz, J.K. Hudson, Supercritical fluid fractionation of fish oil esters using incremental pressure programming and a temperature gradient, *J. Am. Oil Chem. Soc.* 66 (1989) 1596–1600.



- [138] U. Fleck, C. Tiegs, G. Brunner, Fractionation of fatty acid ethyl esters by supercritical CO<sub>2</sub>: High separation efficiency using an automated countercurrent column, *J. Supercrit. Fluids*. 14 (1998) 67–74.
- [139] V. Riha, G. Brunner, Separation of fish oil ethyl esters with supercritical carbon dioxide, *J. Supercrit. Fluids*. 17 (2000) 55–64.
- [140] G. Brunner, Fractionation of fats with supercritical carbon dioxide, *Eur. J. Lipid Sci. Technol.* 102 (2000) 240–244.
- [141] F. Sahena, I.S.M. Zaidul, S. Jinap, N. Saari, H.A. Jahurul, K.A. Abbas, N.A. Norulaini, PUFAs in fish: extraction, fractionation, importance in health, *Compr. Rev. Food Sci. Food Saf.* 8 (2009) 59–74.
- [142] M. Maschietti, A. Pedacchia, Supercritical carbon dioxide separation of fish oil ethyl esters by means of a continuous countercurrent process with an internal reflux, *J. Supercrit. Fluids*. 86 (2014) 76–84.
- [143] L. Fiori, M. Manfrini, D. Castello, Supercritical CO<sub>2</sub> fractionation of omega-3 lipids from fish by-products: plant and process design, modeling, economic feasibility, *Food Bioprod. Process.* 92 (2014) 120–132.
- [144] C.A. Pieck, C. Crampon, F. Charton, E. Badens, A new model for the fractionation of fish oil FAEEs, *J. Supercrit. Fluids*. 120 (2017) 258–265.
- [145] A. Bejarano, P.C. Simões, J.M. del Valle, Fractionation technologies for liquid mixtures using dense carbon dioxide, *J. Supercrit. Fluids*. 107 (2016) 321–348.
- [146] G. Brunner, Applications of supercritical fluids, *Annu. Rev. Chem. Biomol. Eng.* 1 (2010) 321–342.
- [147] L.T. Taylor, Supercritical fluid chromatography, *Anal. Chem.* 82 (2010) 4925–4935.
- [148] M. Perrut, R.M. Nicoud, H. Breivik, Processes for chromatographic fractionation of fatty acids and their derivatives, Patent US5719302A (1998).
- [149] G. Brunner, F. Reichmann, Process for recovering unsaturated fatty acids and derivatives thereof, Patent US5777141A (1998).
- [150] C.F. Poole (Ed.), *Supercritical Fluid Chromatography* 1st ed., *Handbooks in Separation Science*, Elsevier, 2017.
- [151] J.W. Tom, P.G. Debenedetti, Particle formation with supercritical fluids - a review, *J. Aerosol Sci.* 22 (1991) 555–584.
- [152] E.M. Phillips, V.J. Stella, Rapid expansion from supercritical solutions: application to pharmaceutical processes, *Int. J. Pharm.* 94 (1993) 1–10.



- [153] K. Oum, J.J. Harrison, C. Lee, D.A. Wild, K. Luther, T. Lenzer, On-line and *in situ* optical detection of particles of organic molecules formed by rapid expansion of supercritical solutions (RESS) of CO<sub>2</sub>, *Phys. Chem. Chem. Phys.* 5 (2003) 5467–5471.
- [154] J. Bleich, B.W. Müller, W. Waßmus, Aerosol solvent extraction system - a new microparticle production technique, *Int. J. Pharm.* 97 (1993) 111–117 .
- [155] E. Reverchon, G. della Porta, A. di Trolio, S. Pace, Supercritical antisolvent precipitation of nanoparticles of superconductor precursors, *Ind. Eng. Chem. Res.* 37 (1998) 952–958.
- [156] F.T. Karim, K. Ghafoor, S. Ferdosh, F. Al-Juhaimi, E. Ali, K.B. Yunus, M.H. Hamed, A. Islam, M. Asif, I.S.M. Zaidul, Microencapsulation of fish oil using supercritical antisolvent process, *J. Food Drug Anal.* 25 (2017) 654–666.
- [157] C. Prieto, L. Calvo, The encapsulation of low viscosity omega–3 rich fish oil in polycaprolactone by supercritical fluid extraction of emulsions, *J. Supercrit. Fluids.* 128 (2017) 227–234.
- [158] C. Prieto, C.M.M. Duarte, L. Calvo, Performance comparison of different supercritical fluid extraction equipments for the production of vitamin E in polycaprolactone nanocapsules by supercritical fluid extraction of emulsions, *J. Supercrit. Fluids.* 122 (2017) 70–78.
- [159] C. Prieto, L. Calvo, Supercritical fluid extraction of emulsions to nanoencapsulate vitamin E in polycaprolactone, *J. Supercrit. Fluids.* 119 (2017) 274–282.
- [160] E. de Paz, Á. Martín, A. Estrella, S. Rodríguez-Rojo, A.A. Matias, C.M.M. Duarte, M.J. Cocero, Formulation of  $\beta$ -carotene by precipitation from pressurized ethyl acetate-on-water emulsions for application as natural colorant, *Food Hydrocoll.* 26 (2012) 17–27.
- [161] V.S.S. Gonçalves, S. Rodríguez-Rojo, E. De Paz, C. Mato, T. Martín, M.J. Cocero, Production of water soluble quercetin formulations by pressurized ethyl acetate-in-water emulsion technique using natural origin surfactants, *Food Hydrocoll.* 51 (2015) 295–304.
- [162] G. Lévai, Á. Martín, A. Moro, A.A. Matias, V.S.S. Gonçalves, M.R. Bronze, C.M.M. Duarte, S. Rodríguez-Rojo, M.J. Cocero, Production of encapsulated quercetin particles using supercritical fluid technologies, *Powder Technol.* 317 (2017) 142–153.
- [163] E. Weidner, Z. Knez, Z. Novak, Process for preparing particles or powders, Patent WO1995021688A1 (1995).



- [164] E. Weidner, R. Steiner, Ž. Knez, Powder generation from polyethyleneglycols with compressible fluids, in: *Process Technology Proceedings*, 12 (1996) 223–228.
- [165] E. Weidner, High pressure micronization for food applications, *J. Supercrit. Fluids*. 47 (2009) 556–565.
- [166] Á. Martín, E. Weidner, PGSS-drying: Mechanisms and modeling, *J. Supercrit. Fluids*. 55 (2010) 271–281.
- [167] A.S.M. Tanbirul Haque, B.-S. Chun, Particle formation and characterization of mackerel reaction oil by gas saturated solution process, *J. Food Sci. Technol.* 53 (2016) 293–303.
- [168] D. Meterc, M. Petermann, E. Weidner, Drying of aqueous green tea extracts using a supercritical fluid spray process, *J. Supercrit. Fluids*. 45 (2008) 253–259.
- [169] Á. Martín, H.M. Pham, A. Kilzer, S. Kareth, E. Weidner, Micronization of polyethylene glycol by PGSS (Particles from Gas Saturated Solutions)-drying of aqueous solutions, *Chem. Eng. Process. Process Intensif.* 49 (2010) 1259–1266.
- [170] S. Varona, Á. Martín, M.J. Cocero, C.M.M. Duarte, Encapsulation of lavender essential oil in poly-( $\epsilon$ -caprolactones) by PGSS process, *Chem. Eng. Technol.* 36 (2013) 1187–1192.
- [171] E. de Paz, Á. Martín, M.J. Cocero, Formulation of  $\beta$ -carotene with soybean lecithin by PGSS (Particles from Gas Saturated Solutions)-drying, *J. Supercrit. Fluids*. 72 (2012) 125–133.
- [172] V.S.S. Gonçalves, J. Poejo, A.A. Matias, S. Rodríguez-Rojo, M.J. Cocero, C.M.M. Duarte, Using different natural origin carriers for development of epigallocatechin gallate (EGCG) solid formulations with improved antioxidant activity by PGSS-drying, *RSC Adv.* 6 (2016) 67599–67609.

Fish oil valorization using supercritical carbon dioxide technologies

# Objectives

## Objectives

The main objective of this work is to present new experimental information concerning the effect of relevant process parameters related to the valorization of fish by-products using supercritical carbon dioxide technologies.

Along the different chapters of the *Results* section, several aspects of the supercritical carbon dioxide technologies are evaluated in order to increase the knowledge in this field and make a contribution towards the understanding of this green technology when applied to biotransformation of fish by-products. One of the main aspects of this work is that it has been carried out with the purpose of being a comprehensive approach on the matter. In this sense, the work is comprised of both basic and applied research, and mainly focused on the lipase-catalyzed ethanolysis of fish oil triacylglycerides in supercritical carbon dioxide media. Additionally, it provides some insights into the formulation of fish oil concentrates as a solid powder with enhanced stability against oxidation.

Firstly, the effects of supercritical carbon dioxide exposure on several lipases that can be used in lipid biotransformations have been evaluated in order to select the most suitable catalyst for the ethanolysis of fish oil in SC-CO<sub>2</sub> media.

**Chapter 1** “*Effects of supercritical carbon dioxide treatment on four commercial lipases*” evaluates the influence of temperature, pressure, exposure time and depressurization steps on the activity of four commercial lipases treated with SC-CO<sub>2</sub>. Two free lipases (Palatase 20000 L and Lipozyme CALB L); and two immobilized lipases (Lipozyme RM IM and Lipozyme 435) have been studied. The analysis includes studies of the possible chemical, morphological and conformational modifications caused by SC-CO<sub>2</sub> treatment on the lipases as well as on their immobilization supports.

A second basic aspect of SC-CO<sub>2</sub> technology applied to the ethanolysis of fish oil is related to the experimental phase equilibria of the carbon dioxide + ethanol + fish



oil reaction system. Knowledge of the phase behavior of the reaction system may help in the selection of the most appropriate experimental conditions for the ethanolysis of fish oil in SC-CO<sub>2</sub>, as well as other applications involving these pseudo-ternary mixtures, such as supercritical extraction and fractionation, or particle formation techniques.

In **Chapter 2** “*Phase behavior of the pseudo-ternary system carbon dioxide + ethanol + fish oil at high pressures*”, the phase behavior of the pseudo-ternary mixture CO<sub>2</sub> + ethanol + fish oil in the temperature range 323.15-343.15 K and pressures from 10 MPa to 30 MPa has been determined by means of an analytical isothermal method with recirculation of the vapor phase. Experimental data were successfully correlated with the Peng-Robinson equation of state coupled with conventional two-parameter van der Waals mixing rules.

Once the most suitable catalyst and operating conditions have been investigated, applied studies about the kinetics of the ethanolysis reaction catalyzed by the commercial lipase Lipozyme RM IM is presented.

In **Chapter 3** “*Supercritical carbon dioxide as solvent in the lipase-catalyzed ethanolysis of fish oil: kinetic study*”, the effects of the initial molar ratio of substrates, pressure, and temperature on the reaction kinetics have been studied for the ethanolysis of fish oil in SC-CO<sub>2</sub> by Lipozyme RM IM. Experimental data have been satisfactorily correlated by a semi-empirical kinetic model based on the elementary reactions. Additionally, oxidation parameters of the reaction products have been determined and compared with those obtained at atmospheric pressure with conventional organic solvents and in solvent-free media. This way, optimal reaction conditions considering kinetic aspects and quality of the products can be determined.

Finally, the formulation of an omega-3 PUFA-enriched fish oil concentrate by the green technology Particles from Gas Saturated Solutions (PGSS)-drying has been explored.



**Chapter 4** “*Omega-3 encapsulation by PGSS-drying and conventional drying methods. Particle characterization and oxidative stability*” explores the potential benefits of SC-CO<sub>2</sub> technologies applied to particle formulation and encapsulation of heat-sensitive and easily oxidable compounds such as *n*-3 PUFAs, compared to other conventional precipitation methods. More specifically, the dried particles obtained by the PGSS-drying technology have been compared to those obtained by spray-drying and freeze-drying, which are commonly used in the pharmaceutical, cosmetic, and food industries to obtain dried powders from liquid solutions and dispersions.

Fish oil valorization using supercritical carbon dioxide technologies

# Results



## Results

The most outstanding results of this Thesis are presented as different chapters in this Results section. Each chapter corresponds to a scientific paper published in peer-reviewed journals during the course of the PhD. References to the original publications are provided in the front page.

Effects of supercritical carbon dioxide treatment on four commercial lipases .....	77
Phase behavior of the pseudo-ternary system carbon dioxide + ethanol+ fish oil at high pressures .....	121
Supercritical carbon dioxide as solvent in the lipase-catalyzed ethanolysis of fish oil: kinetic study .....	159
Omega-3 encapsulation by PGSS-drying and conventional drying methods. Particle characterization and oxidative stability .....	209

## Chapter 1

# Effects of supercritical carbon dioxide treatment on four commercial lipases

#*Candida antarctica* lipase B #*Rhizomucor miehei* lipase

#immobilized lipase #Lipozyme #enzyme activity #supercritical carbon dioxide

**Adapted from:**

R. Melgosa, M.T. Sanz, Á.G. Solaesa, S.L. Bucio, S. Beltrán, Enzymatic activity and conformational and morphological studies of four commercial lipases treated with supercritical carbon dioxide, *The Journal of Supercritical Fluids*. 97 (2015) 51–62.

DOI: <https://doi.org/10.1016/j.supflu.2014.11.003>



## Table of Contents

Tables.....	81
Figures .....	83
Abstract.....	85
Resumen.....	87
1. Introduction.....	89
2. Materials and methods .....	91
2.1. Enzymes and chemicals .....	91
2.2. Enzyme treatment under SC-CO <sub>2</sub> .....	96
2.3. Residual enzyme activity .....	97
2.4. Instrumentation .....	98
3. Results and discussion.....	99
3.1. Free enzymes .....	99
3.1.1. Residual activity.....	99
3.1.2. Conformational changes. Fluorescence emission spectra .....	103
3.2. Immobilized enzymes .....	105
3.2.1. Residual activity.....	105
3.2.2. Effect of water content on the residual activity .....	108
3.2.3. Conformational and morphological changes .....	111
Conclusion .....	115
References.....	117



## Tables

**Table 1-1.** Effect of exposure to subC-/SC-CO<sub>2</sub> on the residual activity (RA) of some free lipases. p (pressure), T (temperature), t (time), DR (depressurization rate).....92

**Table 1-2.** Effect of SC-CO<sub>2</sub> treatment on the residual activity (RA) of some immobilized lipases. p (pressure), T (temperature), t (time), DR (depressurization rate).....95

**Table 1-3.** Residual activities (% of initial activity) observed in the four commercial enzymes after SC-CO<sub>2</sub> treatment at the established conditions in each experience.....99

## Figures

- Figure 1-1.** Experimental apparatus for enzyme treatment under SC-CO<sub>2</sub>. 1: CO<sub>2</sub> cylinder; 2: syringe pump; 3: cryostat; 4: rupture disk; 5: vent valve; 6: inlet valve; 7: high pressure cell; 8: magnetic stirrer; 9: mechanical agitation; 10: thermostatic water bath. .... 96
- Figure 1-2.** Effect of the experimental conditions of the SC-CO<sub>2</sub> treatment on the residual activity of the studied lipases. Free Palatase 20000 L and Lipozyme CALB L, and immobilized Lipozyme RM IM and Lipozyme 435. a) effect of pressure (10-25 MPa); b) effect of temperature (35-70 °C); c) effect of exposure time (1-3 h); d) effect of depressurization steps (1-3). Lines are drawn to guide the eye. .... 101
- Figure 1-3.** Fluorescence emission spectra of the free lipase Palatase 20000 L before and after SC-CO<sub>2</sub> treatment under different experimental conditions. (For experimental conditions, see Table 1-3) ..... 104
- Figure 1-4.** Fluorescence emission spectra of the free lipase Lipozyme CALB L before and after SC-CO<sub>2</sub> treatment under different experimental conditions. (For experimental conditions, see Table 1-3). .... 104
- Figure 1-5.** Residual activity of Lipozyme RM IM *vs.* water content after SC-CO<sub>2</sub> treatment. Numbers indicate established conditions in each experience (see Table 1-3). .... 109
- Figure 1-6.** Residual activities of Lipozyme RM IM (red) and Lipozyme 435 (blue) after SC-CO<sub>2</sub> treatment and different amounts of added water. Empty symbols: treated samples from experience 2; full symbols: untreated samples. Dashed lines indicate the residual activity value of each treated lipase (experience 2) when no water was added. .... 110
- Figure 1-7.** FT-IR spectra of the studied immobilized lipases before and after SC-CO<sub>2</sub> treatment. Left: complete IR spectra (4000-400 cm<sup>-1</sup>); right: detail of the 1800-1500 cm<sup>-1</sup> region. Treated samples from experience 2. .... 112
- Figure 1-8.** SEM micrographs of Lipozyme RM IM. Left to right: 50x, 600x and 10000x. (a) untreated enzyme; (b) sample from experience 3; (c) sample from experience 9; (d) immobilization support alone (Duolite A568). .... 113



## Figures (*continued*)

**Figure 1-9.** SEM micrographs of Lipozyme 435. Left to right: 50x, 600x and 10000x. **(a)** untreated enzyme; **(b)** sample from experience 3; **(c)** sample from experience 9. ....114

## Abstract

This chapter investigates the effect of supercritical carbon dioxide (SC-CO<sub>2</sub>) treatment on four commercial lipases. The influence of experimental conditions: temperature (35-70 °C), pressure (10-25 MPa), exposure time (1-3 h) and depressurization steps (1-3) on the residual activity was studied.

Activity enhancement was verified for free enzymes (Palatase 20000 L and Lipozyme CALB L) treated at mild conditions; while the highest temperature and pressure and the longest exposure time assayed led to activity losses. On the other hand, either activity losses or no significant effect of the treatment in the enzyme activity were observed on immobilized enzymes (Lipozyme RM IM and Lipozyme 435).

Additional qualitative studies were performed: Fluorescence emission spectra showed changes in the conformational structure of both two free enzymes after SC-CO<sub>2</sub> treatment. Scanning electron micrographs showed morphological alterations in the immobilization supports of the treated enzymes; while infrared spectra did not show chemical modifications.

## Resumen

En el presente capítulo se investigan los efectos del tratamiento con dióxido de carbono supercrítico (CO<sub>2</sub>-SC) sobre cuatro lipasas comerciales. Se ha estudiado la influencia de las variables experimentales: temperatura (35-70 °C), presión (10-25 MPa), tiempo de exposición (1-3 h) y ciclos de despresurización (1-3) sobre la actividad residual de las enzimas.

Se ha verificado que la actividad de las enzimas libres (Palatase 20000L y Lipozyme CALB L) aumenta con tratamientos con CO<sub>2</sub>-SC en condiciones suaves; mientras que los tratamientos con temperaturas más altas y tiempos de exposición más largos producen bajadas de actividad. Por otro lado, las enzimas inmovilizadas (Lipozyme RM IM y Lipozyme 435) no han sido significativamente afectadas por el tratamiento con CO<sub>2</sub>-SC, si bien se ha reducido ligeramente su actividad en algunos casos.

Adicionalmente, se han realizado estudios cualitativos sobre el efecto del tratamiento con CO<sub>2</sub>-SC: el espectro de emisión fluorescente muestra cambios en la estructura conformacional de ambas enzimas libres tras el tratamiento con CO<sub>2</sub>-SC. Mediante microscopía electrónica de barrido se han observado alteraciones en la morfología de los soportes de las enzimas inmovilizadas, si bien no se han encontrado modificaciones químicas en el análisis del espectro infrarrojo.

## 1. Introduction

The utilization of enzymes as biocatalysts in many processes, either in their free or immobilized form, has become an increasingly important research field in recent years. Considerable attention has been paid to lipases, due to their high specificity in lipid biomodification and their selectivity towards fatty acid positions on the glycerol backbone [1].

Since the work of Zaks and Klibanov [2], organic solvents have been employed extensively in enzymatic reactions. However, they present serious environmental drawbacks and additional purification steps are needed to obtain the products of interest in a safe form. To cope with these issues, biochemical catalysis with lipases can be conducted in supercritical carbon dioxide (SC-CO<sub>2</sub>), a nontoxic, readily available, inexpensive, and easily removable solvent. In addition, the singular properties of supercritical fluids, such as liquid-like and tunable solvating power, and gas-like viscosity, diffusivity and superficial tension, have a positive effect on the reaction performance [3]. Additionally, fractionation of the reaction products is possible by coupling a series of separators after the reactor vessel.

The study of activity changes and the improvement of enzyme stability are important factors in the implementation of biocatalysis in supercritical systems. Activity changes can be observed when enzymes are treated with SC-CO<sub>2</sub>. In this work commercial lipases either in their free or immobilized form have been exposed to SC-CO<sub>2</sub> and activity and stability have been determined after SC-CO<sub>2</sub> treatment. Tables 1-1 and 1-2 summarize the effects of the exposure to pressurized CO<sub>2</sub> on the activity of free and immobilized lipases found in the literature. From these tables it can be concluded that activity changes may occur when enzymes are submitted to subcritical (subC-CO<sub>2</sub>) or SC-CO<sub>2</sub>.

The effects of subC-/SC-CO<sub>2</sub> on the activity of free lipases have been extensively studied (see Table 1-1). Free enzymes are less expensive than the immobilized preparations and, since proteins are not soluble in SC-CO<sub>2</sub>, they can be more easily



separated from the reaction products when compared to conventional biocatalysis. Other reason is that the enzymatic activity can be improved when free enzymes are exposed to sub/SC-CO<sub>2</sub>. Although some researchers reported that certain free enzymes can be inactivated when exposed to SC-CO<sub>2</sub> [4], other free lipases have been reported to increase their activity up to 860 % after incubation in sub/SC-CO<sub>2</sub> [5]. Changes in the conformational structure due to interactions between SC-CO<sub>2</sub> and enzyme residues that lead to an open, more active state of the enzyme [6–10] and/or extraction of water and impurities from the enzyme preparation [5,11] could explain this enhancement of the enzyme activity. The extent of the activity changes depends on the nature and source of the enzyme, as well as on the experimental conditions.

In the case of immobilized lipases submitted to pressurized CO<sub>2</sub>, the most studied are the one from *Mucor/Rhizomucor miehei* immobilized on a macroporous anion exchange resin and lipase B from *Candida antarctica* immobilized on a macroporous acrylic resin (Table 1-2). In general, activity of immobilized enzymes in SC-CO<sub>2</sub> is related to many factors, including the source and nature of the enzyme, the characteristics of the support, and the immobilization method. It has been reported that essential water in the enzyme microenvironment can be removed as a result of unfavorable partitioning between the support and the solvent, causing enzyme inactivation [12–14]. Other parameters such as pressure and temperature of the reaction system can also affect the enzyme activity [15,14,16]. In high pressure-batch stirred reactors, exposure time, depressurization rate, and the number of pressurization/depressurization steps can also affect enzyme activity and stability and must be considered [17].

The aim of this work is to investigate the influence of temperature, pressure, exposure time and depressurization steps on the activity of four commercial lipases treated with SC-CO<sub>2</sub>: two free lipases (Palatase 20000 L and Lipozyme CALB L); and two immobilized lipases (Lipozyme RM IM and Lipozyme 435). The analysis includes studies of the possible chemical, morphological and conformational

modifications caused by SC-CO<sub>2</sub> treatment. Fluorescence emission spectroscopy was applied in order to study the conformational changes that could have occurred in the structure of the free enzymes. Fourier transform-infrared spectroscopy (FT-IR) and scanning electron microscopy (SEM) were also used to respectively evaluate potential chemical and physical alterations in the immobilized enzymes.

## 2. Materials and methods

### 2.1. Enzymes and chemicals

Lipozyme RM IM and Palatase 20000 L were purchased from Sigma Aldrich (St. Louis, MO). Lipozyme 435 and Lipozyme CALB L were kindly provided by Novozymes (Bagsværd, Denmark).

Lipozyme RM IM is a lipase from *Rhizomucor miehei*, immobilized on Duolite A568 [18], a macro-porous hydrophilic granular weak base anion exchange resin, based on crosslinked phenol-formaldehyde polycondensate. The moisture content of Lipozyme RM IM was  $3.8 \pm 0.2$  g/100 g, determined by extraction with dry methanol during 24 h and further titration by Karl-Fischer method (Mitsubishi CA-20 automatic titrator). A similar humidity value ( $3.3 \pm 0.2$  g/100 g) was reported by Jenab *et al.* [19] by using a gravimetric method. Lipozyme 435 is a recombinant lipase from *Candida antarctica*, expressed on *Aspergillus niger*, and adsorbed onto Lewatit VP OC 1600 [18], a macro-porous hydrophobic resin presented in spherical beads and based on cross-linked methacrylic esters. The moisture content of Lipozyme 435 was  $0.7 \pm 0.2$  g/100 g, determined by the same Karl-Fischer titration method. Palatase 20000 L (free *R. miehei* lipase expressed on *A. oryzae*) and Lipozyme CALB L (free *C. antarctica* lipase expressed on *A. niger*) were provided in aqueous solution containing glycerol, sorbitol and other excipients and preservatives. Carbon dioxide (99.9 %) was supplied by Carbueros Metálicos S.A. (Spain). All other chemicals used were of analytical grade.

**Table 1-1.** Effect of exposure to subC-/SC-CO<sub>2</sub> on the residual activity (RA) of some free lipases. p (pressure), T (temperature), t (time), DR (depressurization rate).

Source	p, MPa	T, °C	t, h	Cycles	DR	Residual activity (RA) and other effects	Ref.
<i>Candida rugosa</i> (formerly <i>C. cylindracea</i> )							
LVII (solid powder)	8.3	50	15-150	1	--	RA = 97 % - 85 % (900 – 9000 min) Low RA (~ 20 %) when water was added at >1 % wt.	[20]
AY30 (aqueous solution)	5.1-15	20-65	1/cycle	30	--	RA ~ 45 % after 30 depressurizations at 20°C (liquid CO <sub>2</sub> ) RA ~ 65 % after 30 depressurizations at 65°C (SC-CO <sub>2</sub> ) RA was not affected by 20 T-induced phase transitions (65-20°C)	[21]
	15	35	1/cycle	1-30	--	RA ~ 100 ± 14 % - 72 ± 5 % (0-30 cycles)	
	15	75	1.5-24	1	--	RA ~ 76 ± 4 % - 56 ± 2 % (1.5-24 h)	
	15	25-105	1	1	--	RA ~ 100 ± 5 % - 36 ± 2 % (25-105 °C)	
AY30 (aqueous solution)	15, 30	40	22	1	--	Water added: no effect over a wide range (0-200 µL), no optimum RA = 92 % - ~ 85 % (30 and 15 MPa, 200 µL water, 400 mg lipase)	[22]
lipase from <i>C. cylindracea</i> (solid with 30% lactose)	15	75	24	1	--	RA ~ 110 ± 4	[21]
	15	75	60/cycle	30	--	RA ~ 103 ± 3	
L034P (solid powder)	30	40	24	1	'slow'	No change in the residual activity	[23]
Lip7 (lyophilized powder)	6-10	35-40	0.5-2.5	1	--	RA = 161 ± 4 % (6 MPa, 35°C, 0.5 h) - 180 ± 2 % (10 MPa, 40°C, 0.5 h) Changes in the secondary and tertiary structures.	[6]
CRL (aqueous solution)	5-20	35-45	0.17-0.67 (10-40 min)	1	2-10 MPa/min	RA = 122 ± 3 % (7 MPa, 45°C, 10 min) - 93 ± 3 % (20 MPa, 45°C, 10 min). Mild DR (2 MPa·min <sup>-1</sup> ) benefits RA. Changes in the secondary and tertiary structures.	[7]
CRL (solid powder)	6-15	40	0.67 (40 min)	1		RA = 119 ± 6 – 133 ± 8 (6 and 15 MPa)	[8]
<i>Candida antarctica</i>							
Lipozyme CALB L (aqueous solution)	6-10	35-40	0.33-2.5 (20-150 min)	1	--	RA = 82 ± 2 % (10 MPa, 40°C, 2.5 h) – 105 ± 4 (10 MPa, 40°C, 0.5 h). Changes in the secondary (far UV-CD spectra) and tertiary structures (fluorescence spectra)	[9]

**Table 1-1. Continued**

Source	p, MPa	T, °C	t, h	Cycles	DR	Residual activity (RA) and other effects	Ref.
<i>Pseudomonas sp.</i>							
lipase PS	15	35	1/cycle	1-30	--	RA ~ 100 ± 16 % - 70 ± 12 % (0 – 30 cycles)	[21]
(aqueous solution)	15	75	1.5-24	1	--	RA ~ 106 ± 4 % - 91 ± 17 % (90 – 1440 min)	
	15	25-105	1	1	--	RA ~ 100 ± 20 % - 22 ± 10 % (25 – 105 °C)	
<i>Pseudomonas fluorescens</i>							
L056P (powder)	30	40	24	1	'slow'	No change in the residual activity	[21]
(aqueous solution)	5-20	35-45	0.17-0.67 (10-40 min)	1	2-10 MPa/min	RA = 163 ± 4 % (20 MPa, 45°C, 40 min) - 106 ± 1 % (10 MPa, 45°C, 10 min). Medium DR (4 MPa·min <sup>-1</sup> ) benefits RA. Changes in the secondary and tertiary structures.	[7]
<i>Burkholderia cepacia</i> (formerly <i>P. cepacia</i> )							
PCL	5-20	35-45	0.17-0.67 (10-40 min)	1	4 MPa/min	RA = 96 % (5 MPa, 45°C, 10 min) - 130 % (15 MPa, 40°C, 25 min). Change in biodiesel conversion: 91 % (5 MPa, 45 °C, 40 min) – 116 % (5 MPa, 35°C, 10 min).	[10]
(solid powder)						Conformational changes (FT-IR and fluorescence emission spectra).	
(aqueous solution)	6-10	35-40	0.33-2.5 (20-150 min)	1	--	RA = 99 ± 2 % (6 MPa, 35°C, 20 min) – 116 ± 2 (10 MPa, 40°C, 30 min). Changes in the secondary (far UV-CD spectra) and tertiary structures (fluorescence spectra)	[9]
<i>Rhizopus javanicus</i>							
L036P (powder)	30	40	24	1	'slow'	No change in the residual activity	[23]
<i>Rhizopus niveus</i>							
L060P (powder)	30	40	24	1	'slow'	No change in the residual activity	[23]
<i>Rhizopus oryzae</i>							
(aqueous solution)	5-20	35-45	0.17-0.67 (10-40 min)	1	2-10 MPa/min	RA = 200 ± 7 % (15 MPa, 40°C, 25 min) – 77 ± 6% (7 MPa, 45°C, 10 min) Conformational changes (FT-IR and fluorescence emission). Positive effect of the DR	[7]

**Table 1-1. Continued**

Source	p, MPa	T, °C	t, h	Cycles	DR	Residual activity (RA) and other effects	Ref.
<i>Aspergillus niger</i> (aqueous solution)	15	75	24	1	--	No effect of enzyme purity on RA: $108 \pm 8\%$ - $97 \pm 4\%$	[21]
2 different purities	15	75	1/cycle	30	--	No effect of enzyme purity on RA: $92 \pm 9\%$ - $102 \pm 4\%$ No conformational changes (fluorescence intensity maxima)	
Porcine pancreas lipase PPL (solid powder)	15	35- 105	1-24	30		No effect of treatment on RA at $T < 65^\circ\text{C}$ . Positive effect of T and t on RA. Possibly because of extraction of water and fatty acid impurities. RA = 242.6 % at 15 MPa, 75°C and 1 h RA = 860 % at 15 MPa, 75°C and 24 h (no further increase after 50 h) RA = 191 % after 30 cycles at 15 MPa, 75°C, 1 h	[5]
L115P (powder)	30	40	24	1	'slow'	No change in the residual activity	[23]
PPL (solid powder)	15	75	24	1	--	RA varies with the influence of the chain length of the substrate. Activity increased with water added towards long chain triacylglycerols versus short chain	[11]

**Table 1-2.** Effect of SC-CO<sub>2</sub> treatment on the residual activity (RA) of some immobilized lipases. p (pressure), T (temperature), t (time), DR (depressurization rate).

Source (commercial name)	p, MPa	T, °C	t, h	Cycles	DR	Residual activity (RA) and other effects	Ref.	
<i>Mucor miehei</i> / <i>Rhizomucor miehei</i>	13-18	40-60	144 (6 d)	1	--	RA = 90 % - 80 % (13 MPa, 6 days, 40°C – 60°C) No effect of pressure in the range investigated Added water (0-2µL/mg enz.) promotes deactivation (13 MPa, 40°C, 1 day).	[24,25]	
	15	50	12 (5 d)	1-15	--	RA = 96 %. No loss of activity after several compression/decompression steps	[26]	
	(Lipozyme) <sup>a</sup>	30	40	4-24	1	--	Almost no loss of activity	
	(Lipozyme IM) <sup>a</sup>	8.6-8.9	35-37	4-12	1-3-5	4.5-89 bar·min <sup>-1</sup>	Exposure time had no effect. High DR decreased RA. Low DR and number of cycles increased activity, possibly because of extraction of inhibiting components in the immobilization matrix.	[27]
(Lipozyme IM 20) <sup>a</sup>	7.2-27.6	35-75	1-6	1	10-200 kg·m <sup>-3</sup> ·min <sup>-1</sup>	RA = 86.3 ± 2.5 % (7.2 MPa, 35°C, 6 h and 200 kg·m <sup>-3</sup> ·min <sup>-1</sup> ) RA = 99.5 ± 0.1 (7.2 MPa, 35°C, 1 h and 10 kg·m <sup>-3</sup> ·min <sup>-1</sup> )	[28]	
<i>Candida antarctica</i> lipase B  (Novozym 435) <sup>b</sup>	8-25	40-70	1-6	1	10-200 kg·m <sup>-3</sup> ·min <sup>-1</sup>	RA = 96 .5 % (8 MPa, 40°C, 60 min, 10 kgm <sup>-3</sup> min <sup>-1</sup> ) – 86 % (13.1 MPa, 40°C, 360 min, 10 kg·m <sup>-3</sup> min <sup>-1</sup> )	[29]	
	7.2-27.6	35-75	1-6	1-5	10-200 kg·m <sup>-3</sup> ·min <sup>-1</sup>	RA = 91.1 ± 0.9 % (27.6 MPa, 75°C, 6 h and 200 kg·m <sup>-3</sup> ·min <sup>-1</sup> ) RA = 98.7 ± 0.1 (7.2 MPa, 35°C, 1 h and 10 kg·m <sup>-3</sup> ·min <sup>-1</sup> ) Lower activity loss when compared with Lipozyme IM treated at the same conditions	[28]	
						RA decreased from 96 % after 1 cycle to 89.5 % after 5 cycles at 27.6 MPa, 75°C, 1 h and 10 kg·m <sup>-3</sup> ·min <sup>-1</sup> No physico-chemical modifications (FT-IR and thermogravimetric analyses) Morphological changes in the shape and the surface of the support (SEM)		
<i>Yarrowia lipolitica</i> <sup>c</sup> (non-commercial)	7.2-27.6	35-75	1-6	1	10-200 kg·m <sup>-3</sup> ·min <sup>-1</sup>	RA = 71.4 % (27.6 MPa, 75°C, 6 h and 10 kg·m <sup>-3</sup> ·min <sup>-1</sup> ) RA = 89.8 % (7.2 MPa, 35°C, 1 h and 10 kg·m <sup>-3</sup> ·min <sup>-1</sup> )	[30]	

(a): immobilized on a macroporous anionic resin (b): immobilized on a macroporous hydrophobic resin (c): immobilized on Accurel MP 1000 (hydrophobic).



## 2.2. Enzyme treatment under SC-CO<sub>2</sub>

A schematic diagram of the experimental apparatus used in the enzyme treatment is depicted in Fig. 1-1. It has been designed in our laboratory with a maximum operating pressure and temperature of 30 MPa and 80°C, respectively.

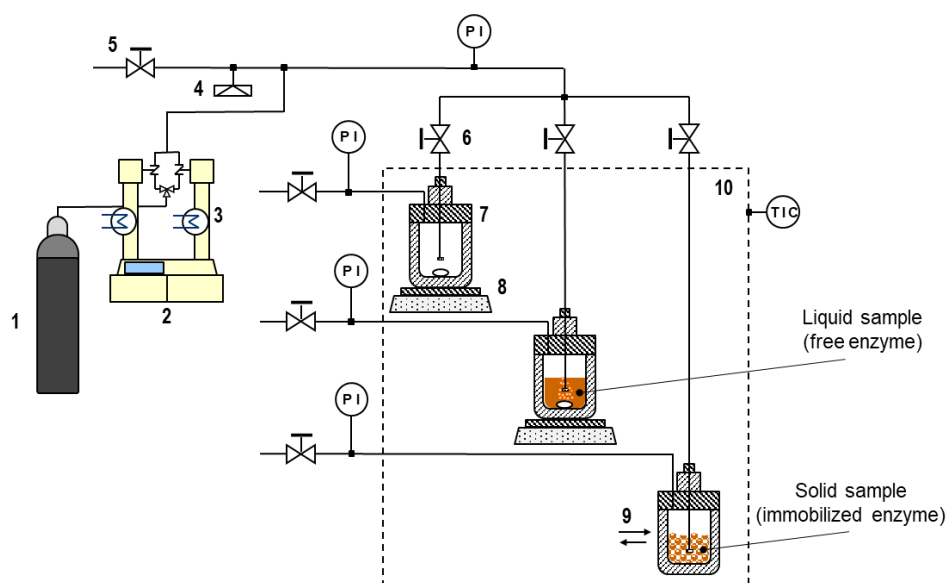


**Figure 1-1.** Experimental apparatus for enzyme treatment under SC-CO<sub>2</sub>. 1: CO<sub>2</sub> cylinder; 2: syringe pump; 3: cryostat; 4: rupture disk; 5: vent valve; 6: inlet valve; 7: high pressure cell; 8: magnetic stirrer; 9: mechanical agitation; 10: thermostatic water bath.

Basically, the high-pressure apparatus consists of a CO<sub>2</sub> reservoir, a high-pressure syringe pump with a pressure controller (ISCO 260 D) and a series of high pressure cells submerged in a thermostatic water bath. In the treatment of liquid free enzyme preparations, high pressure cells with an internal volume of approximately 10 mL have been employed. Immobilized enzymes were treated in high pressure cells with an internal volume of approximately 3 mL.

In a typical experiment, the enzyme preparation (5.0 mL of free enzyme or 0.5 g of immobilized enzyme) was charged into the high-pressure cell, which was then placed in the thermostatic water bath at the established temperature. Afterwards, the system was pressurized and maintained at constant temperature and pressure for a pre-established exposure time. Typically, the duration of the pressurization step was less than 0.5 min and accordingly was not included in the pressure holding time. Depressurization steps were performed at a constant decompression rate of  $240 \text{ kg m}^{-3} \text{ min}^{-1}$ .

Experiments were done in a temperature and pressure range commonly used in enzymatic reactions: temperature (T) from 35 to 75 °C and pressure (p) from 10 to 25 MPa. Exposure time (t) was extended from 1 to 6 h for all enzymes. Additionally, several depressurization steps (1-3) were carried out in the case of immobilized enzymes (Table 1-3).

### 2.3. Residual enzyme activity

The enzyme activity of free enzymes was determined as the initial rate in the hydrolysis reaction of the olive oil triglycerides [10]. In a typical assay, 1 mL of enzyme preparation was added to the substrate, consisting of 4 mL of 10 % homogenized olive oil and 5 mL of 50 mM phosphate buffer pH = 7.0. The reaction was carried out at 50 °C for 15 min. After incubation, 15 mL of a mixture of ethanol:acetone (1:1) was added to terminate the reaction. Liberated fatty acids were titrated with KOH 0.1 N in ethanol. As a blank control, the reaction mixture without the enzyme was titrated in the same way.

The enzyme activity of immobilized enzymes was determined as the initial rate in the esterification reaction of lauric acid with propanol at a molar ratio of 3:1, 60 % wt. hexane as reaction medium and enzyme concentration of 5 % wt. in relation to the substrates. At the beginning of the reaction, samples containing the mixture of lauric acid and propanol were collected and the lauric acid content was

determined by titration with KOH 0.1 N in ethanol by using an automatic titrator (Methrom Titrando 905). After the addition of the enzyme to the substrates, the mixture was kept at 50 °C for 15 min. Then, the lauric acid consumption was determined by the same experimental procedure.

In all cases, residual activity was calculated as the relationship between the enzyme activity after SC-CO<sub>2</sub> exposure and the initial enzyme activity, expressed as percentage (Eq. 1-1):

$$\text{residual activity} = \frac{\text{activity after SC-CO}_2 \text{ treatment}}{\text{initial activity}} \times 100 \% \quad (1-1)$$

All enzyme activity determinations were performed at least in triplicate.

#### 2.4. Instrumentation

The tertiary structure of the free enzymes was measured by fluorescence spectroscopy using a Varian Cary Eclipse spectrofluorimeter (Agilent Technologies) thermostated at 25 °C. The excitation wavelength was 280 nm, and the emission was read at 290-450 nm. All the spectra were scanned continuously with five replicates. All samples were diluted 10 times in pure water prior to analysis.

Infrared spectroscopy analyses were made to follow possible chemical alterations after exposure to SC-CO<sub>2</sub> since proteins absorb infrared wavelengths due to the peptide bond vibrations. Fourier transform-infrared spectroscopy (FT-IR) was performed in the 4000-400 cm<sup>-1</sup> range using a Thermo-Nicolet Nexus 670 FT-IR spectrophotometer. Scanning electron microscopy (SEM) was also performed to check possible changes in the morphological properties of the immobilized enzymes. Micrographs were obtained using a variable-pressure scanning electron microscope JEOL JSM-6460LV.

### 3. Results and discussion

#### 3.1. Free enzymes

##### 3.1.1. Residual activity

The experimental results obtained in the residual activity determination of the two free enzymes are showed in Table 1-3. The effect of pressure, temperature and exposure time is depicted in Figs. 1-2 a,b,c.

In general, SC-CO<sub>2</sub> treatment at mild conditions (experiences 1, 2, 4, and 6) promoted an increase in the residual enzyme activity of the two free lipases. In any case, the enzyme activity enhancement after SC-CO<sub>2</sub> treatment decreases as the operating pressure and temperature, as well as the exposure time increases.

**Table 1-3.** Residual activities (% of initial activity) observed in the four commercial enzymes after SC-CO<sub>2</sub> treatment at the established conditions in each experience.

exp.	Experimental conditions				Residual activity (%)*			
	p (MPa)	T (°C)	t (h)	dep. steps	Palatase 20000 L	Lipozyme CALB L	Lipozyme RM IM	Lipozyme 435
1	10				126 ± 2	104 ± 2	100 ± 1	97 ± 2
2	15	50	3	1	121 ± 4	107.5 ± 0.6	92 ± 2	82 ± 2
3	25				96 ± 3	97.3 ± 0.8	89 ± 1	86 ± 2
4	15	35	3	1	134 ± 2	112 ± 1	96.0 ± 0.6	95 ± 1
5		70			86 ± 3	80.9 ± 0.9	77 ± 2	74 ± 2
5a <sup>†</sup>	atm	70	3	1	-	-	69 ± 2	63 ± 2
6	15	50	1	1	135 ± 2	110 ± 2	94 ± 1	89.2 ± 0.7
7			6		112 ± 3	96 ± 1	87.4 ± 0.3	80 ± 1
8	15	50	3	2	-	-	91.6 ± 0.4	78 ± 1
9			3		-	-	88 ± 3	78 ± 1

\* residual activity = (activity after SC-CO<sub>2</sub> treatment / initial activity) x 100 %

<sup>†</sup> experience conducted in n-heptane



Treatment at the highest pressure studied in this work (exp. 3: 25 MPa, 50°C and 3 h) resulted in low activity losses of both two free enzymes (up to approximately 95 % initial activity). Palatase 20000 L gained activity even after 6 h exposed to SC-CO<sub>2</sub> at 15 MPa and 50°C (exp. 7) while a slight activity loss was observed for Lipozyme CALB L treated at the same conditions.

These results agree with those reported in the literature for other free lipases (Table 1-1). Activity of free lipases from *C. rugosa* after exposure to pressurized CO<sub>2</sub> has been extensively studied either in aqueous solution or as a powder but studies of lipases from other sources have been also reported in the literature (Table 1-1). In general, an increase or no change in lipase activity has been observed after exposure to pressurized CO<sub>2</sub> at mild conditions for lipases from different sources such as *C. rugosa*, *C. antarctica*, *Pseudomonas* sp., *Rhizopus* sp., *Aspergillus niger* and lipase from porcine pancreas. In their study of the effects of sub-/SC-CO<sub>2</sub> pretreatment on the activity of Lipozyme CALB L, Liu *et al.* [9] reported slightly lower activity enhancements when compared to those obtained in this work. A maximum of  $105 \pm 4$  % residual activity at 10 MPa, 40°C and 0.5 h was reported by Liu *et al.* [9], while in this work a maximum in the residual activity of  $112 \pm 1$  % was obtained at 15 MPa, 35°C and 3 h.

Liu *et al.* [9] also observed a negative effect of exposure time ( $82 \pm 2$  % initial activity at 10 MPa, 40°C and 2.5 h) while in this work Lipozyme CALB L maintained  $96 \pm 1$  % initial activity after 6 h at 15 MPa and 50°C. In the work by Liu *et al.* [9] no data about depressurization rate was reported, although other authors have pointed out that this parameter should not be neglected [7]. In the case of Palatase 20000 L, a maximum activity enhancement of  $135 \pm 2$  % was observed after SC-CO<sub>2</sub> treatment at 15 MPa, 50°C and 1 h. Compared to Lipozyme CALB L, Palatase 20000 L activity after SC-CO<sub>2</sub> treatment at the same conditions was enhanced in a higher extent. No references about the effect of the SC-CO<sub>2</sub> treatment on the activity of Palatase 20000 L or other free lipases from *R. miehei* were found in the literature.

The highest activity losses were found at the highest temperature assayed (exp. 5: 70°C, 15 MPa and 3 h). Therefore, they could be mainly attributed to thermal deactivation, possibly due to partial unfolding by breaking non-covalent interactions [7]. In any case, the residual activity of both free treated lipases remains above 80 %.

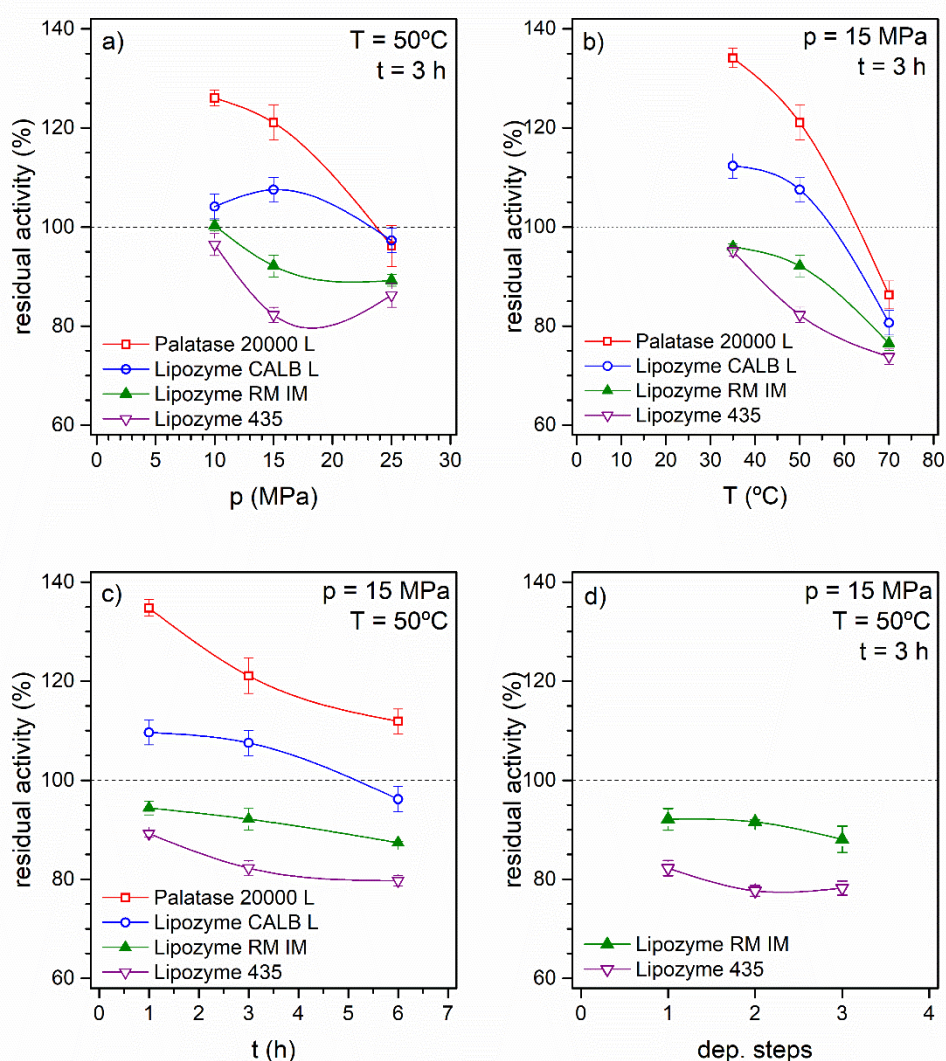


**Figure 1-2.** Effect of the experimental conditions of the SC-CO<sub>2</sub> treatment on the residual activity of the studied lipases. Free Palatase 20000 L and Lipozyme CALB L, and immobilized Lipozyme RM IM and Lipozyme 435. a) effect of pressure (10-25 MPa); b) effect of temperature (35-70 °C); c) effect of exposure time (1-3 h); d) effect of depressurization steps (1-3). Lines are drawn to guide the eye.



Palatase 20000 L was more thermostable than Lipozyme CALB L ( $86 \pm 2\%$  vs  $80.9 \pm 0.9\%$  initial activity, respectively). Gießauf *et al.* [19] reported a similar thermostability for lipase AY30 from *C. rugosa* treated with SC-CO<sub>2</sub> at 75°C, 15 MPa, and 1.5 h ( $76 \pm 4\%$  initial activity). However, no significant effect of SC-CO<sub>2</sub> treatment at the same conditions was found on the activity of lipase PS from *Pseudomonas* sp. and 2 different batches of lipase from *Aspergillus niger* [19]. They concluded that thermal stability of free enzymes depends on many factors such as the presence of unstable impurities or stabilizers [19]. Accordingly, Bauer *et al.* [20] related the activity loss of esterase EP10 from *Burkholderia gladioli* after SC-CO<sub>2</sub> treatment at 75 °C to the presence of impurities in the enzyme preparation. In the literature, it has been reported that SC-CO<sub>2</sub> could improve enzyme activity and stability by solubilization and removal of many impurities that can be present in free enzyme preparations like carbohydrates, fatty acids, and triglycerides, while the enzyme is generally insoluble in SC-CO<sub>2</sub> [5]. To evaluate this effect, protein concentration was determined by the Bradford method [31], finding that this value was not significantly affected ( $p < 0.05$ ) by the SC-CO<sub>2</sub> treatment in any of the experiences performed with both free enzyme preparations. These results are expected since water solubility in SC-CO<sub>2</sub> is low at the pressure and temperature conditions assayed in this work and also because it was assumed that commercial enzyme preparations were submitted to several purification steps during their production processes.

It has been also proposed that SC-CO<sub>2</sub> may interact with hydrophobic tryptophan (Trp) and tyrosine (Tyr) residues in the enzyme structure during the treatment [6–10]. Liu *et al* [6] proposed that, below a pressure threshold that depends on the enzyme nature and on the experimental conditions, CO<sub>2</sub> can interact with Trp and Tyr residues by means of weak interactions, promoting conformational changes that lead to a more accessible active site. However, above this threshold value, CO<sub>2</sub> interacts mainly chemically with these amino acids, affecting negatively the free enzyme activity [6]. This hypothesis could explain the activity enhancement

observed at mild conditions for both free lipases and the activity loss at the highest pressure and the longest exposure time in this study. The operating pressure threshold for both free lipases studied in this work is about 15 MPa. A similar value was found in the studies of the stability of free *C. rugosa* Lip7 after sub-/SC-CO<sub>2</sub> exposure [6].

### 3.1.2. Conformational changes. Fluorescence emission spectra

The hypothesis of SC-CO<sub>2</sub> induced conformational and activity changes has been studied by measuring the fluorescence emission spectra of both free lipases before and after SC-CO<sub>2</sub> treatment at different experimental conditions. Fluorescence spectroscopy is an available technique for studying the conformational structure of free enzymes, in which the intrinsic fluorescence at 280 nm of Trp and Tyr residues is influenced by the environment [32]. Therefore, differences in the intrinsic fluorescence intensity can indicate changes in the tertiary structure of the lipases. Results are presented in Figs. 1-3 and 1-4. From these figures, it can be observed that the fluorescence emission spectra of the SC-CO<sub>2</sub> treated enzymes and their respective untreated samples are significantly different, indicating that interactions between SC-CO<sub>2</sub> and Trp and Tyr residues have occurred and thus their microenvironments were significantly altered.

Samples from experiences 2 and 4 from Palatase 20000 L and experience 4 from Lipozyme CALB L showed higher fluorescence intensity maxima when compared to their respective untreated samples, indicating that the SC-CO<sub>2</sub> treatment had led the enzyme to adopt an open conformation in which the lid moves to uncover the active site [21]. In these conditions, enzyme substrates could easily reach the active site and the enzyme activity would be enhanced, as it was observed in the residual activity determinations (Table 1-3 and Fig. 1-2 a,b,c).

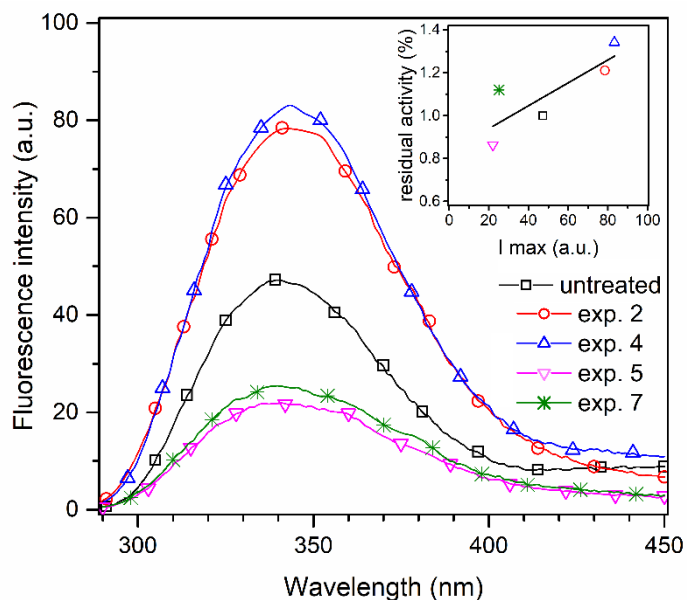


**Figure 1-3.** Fluorescence emission spectra of the free lipase Palatase 20000 L before and after SC-CO<sub>2</sub> treatment under different experimental conditions.  
 (For experimental conditions, see Table 1-3)

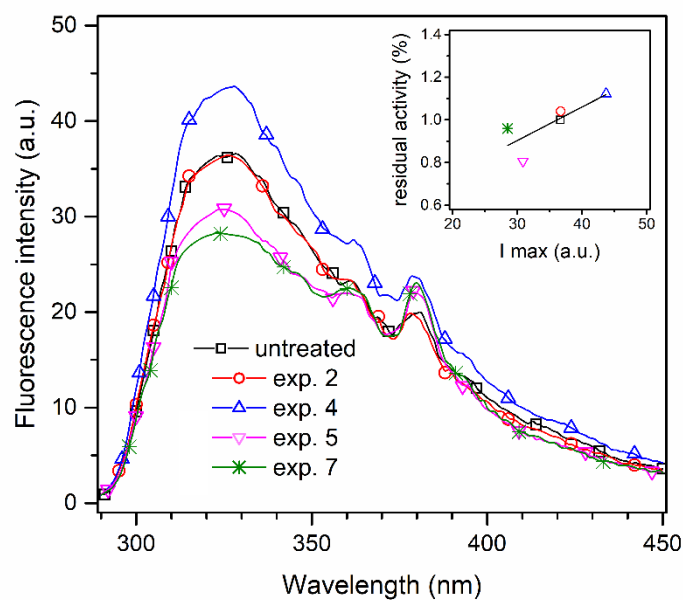


**Figure 1-4.** Fluorescence emission spectra of the free lipase Lipozyme CALB L before and after SC-CO<sub>2</sub> treatment under different experimental conditions.  
 (For experimental conditions, see Table 1-3).

On the other hand, samples from experiences 5 and 7 of both free enzymes showed lower fluorescence intensity maxima, which is in coincidence with a relatively low residual activity (Table 1-3 and Fig. 1-2 a,b,c). It seems that SC-CO<sub>2</sub> treatment at these conditions could have induced irreversible changes leading to an unfolded conformation in which Trp and Tyr residues have been transferred to a more hydrophobic environment. As it has been previously explained in section 3.1.1, some authors have suggested that, when a pressure threshold is reached [6], the interactions between SC-CO<sub>2</sub> and Trp and Tyr residues become stronger, affecting negatively the free enzyme activity.

As depicted in Figs. 1-3 and 1-4 (inset), the regression of the fluorescence intensity maxima of each sample versus their respective residual activity showed a linear dependence between these two parameters. The higher the fluorescence intensity maximum, the higher the residual activity. These results are contrary to the work of Chen *et al.* [7] with *C. rugosa* lipase, *P. fluorescens* lipase and *Rhizopus oryzae* lipase treated with sub-/SC-CO<sub>2</sub>, in which an initial increase of the residual activity with the fluorescence intensity maxima was found, but then a decrease of fluorescence occurred and samples with higher residual activity showed lower fluorescence intensity maxima [7]. It is also remarkable that Liu *et al.* [9] observed a decrease in the fluorescence intensity maxima of treated Lipozyme CALB L, even when the residual activity of the lipase was increased as a result of sub-/SC-CO<sub>2</sub> treatment.

## 3.2. Immobilized enzymes

### 3.2.1. Residual activity

The experimental results obtained in the residual activity determination of the immobilized enzymes are showed in Table 1-3 and Figs. 1-2 a-d. In general, it can be seen that SC-CO<sub>2</sub> treatment led to activity losses in all the experiments performed, except for Lipozyme RM IM in experience 1, in which no significant



effect of SC-CO<sub>2</sub> treatment in the residual activity was observed. Table 1-2 summarizes the effects of SC-CO<sub>2</sub> on the residual activity of some immobilized lipases found in the available literature. Comparing the results obtained with those from the literature (Table 1-2), a similar trend can be seen. Residual activity of the immobilized lipase from *R. miehei* ranged from 80 to 99.5 %, while for lipase from *C. antarctica* residual activity ranged from 86 to 98.7 %.

It must be highlighted that lipase from *R. miehei* either in its free (Palatase 20000 L) or in its immobilized form (Lipozyme RM IM) is more stable under the conditions assayed in this work than lipase B from *C. antarctica* in its free (Lipozyme CALB L) or immobilized form (Lipozyme 435, food grade) exposed to the same conditions. However, Oliveira et al. [28] found that lipase B from *C. antarctica* (Novozym 435, technical grade) presented lower activity losses when compared to lipase from *R. miehei* (Lipozyme IM) treated at the same conditions. Some authors have reported that the enzyme stability under SC-CO<sub>2</sub> could be related to the number of disulfide bonds that are present in the protein structure; however, both lipases have three disulfide bonds that stabilize the molecule [33,34].

Due to the relatively moderate pressure applied in most SC-CO<sub>2</sub> processes, the direct effect of pressure on enzyme inactivation can be considered small [3] and they may exist indirect effects that lead to activity losses on the immobilized enzymes. This way, it has been proposed that interactions between lipase amino groups and CO<sub>2</sub> can promote the formation of carbamates that contribute to the loss of enzyme activity [35].

Local changes of pH have been also suggested as a potential cause of enzyme inactivation due to absorption of CO<sub>2</sub> into the hydrated areas of the lipase [3,18]. However, Kamat *et al.* [12] concluded that pH changes were not the main reason for lowering enzyme activity, but the rapid release of CO<sub>2</sub> dissolved in the bound water of the enzyme and pressurization-depressurization steps could be responsible by means of structural changes in the enzyme, resulting in its inactivation.

As in the case of free enzymes, the highest activity losses ( $23 \pm 2$  % for Lipozyme RM IM and  $26 \pm 2$  % for Lipozyme 435) were found at the highest temperature studied in this work (exp. 5: 70 °C, 15 MPa and 3 h). To check the effect of the temperature in the residual activity of the free enzymes after exposure to conventional organic solvents, experience 5a was conducted in n-heptane at 70 °C, 3 h and atmospheric pressure (Table 1-3). Results obtained showed lower residual activity than that performed in SC-CO<sub>2</sub> at 15 MPa and the same time-temperature combination, indicating a protective effect of SC-CO<sub>2</sub> media in the enzyme thermostability.

For immobilized lipases, the effect of pressurization/depressurization cycles has been also studied since it is an important operating parameter in batch or packed bioreactors. Both immobilized lipases were exposed up to 3 pressurization-depressurization steps at 50 °C during 3 h of incubation. A slight decrease in lipase activity has been found by increasing the number of pressurization-depressurization steps from 1 to 3 (from  $92 \pm 2$  % to  $88 \pm 3$  % initial activity for Lipozyme RM IM and from  $82 \pm 2$  % to  $78 \pm 1$  % initial activity for Lipozyme 435). These results are in agreement with those reported by Oliveira *et al.* [28] who observed that activity of Novozym 435 decreased from 96 % to 89.5 % initial activity when submitted from 1 to 5 pressurization/depressurization cycles at 27.6 MPa, 75 °C and 1 h. Habulin *et al.* [36] also reported that proteinase from *Carica papaya* latex incubated in SC-CO<sub>2</sub> at 30 MPa and 50 °C and several depressurization cycles slightly decrease its activity during the first 10 cycles and, after that, residual activity of the proteinase treated by a fast depressurization method significantly decreased while the slowly depressurized proteinase maintained its residual activity for a longer period of time. It has been also reported that hydrolases with disulfide bonds have a lower degree of inactivation after several pressurization-depressurization steps than enzymes without them [19].

In this study, longer exposure times had greater negative effect on enzyme activity: 1 h of incubation at 15 MPa and 50 °C lead to activity loss of  $6 \pm 1$  % and



$11.8 \pm 0.7$  % for Lipozyme RM IM and Lipozyme 435, respectively; while extending the exposure time up to 6 h promoted  $12.6 \pm 0.3$  % and  $20 \pm 1$  % activity loss for Lipozyme RM IM and Lipozyme 435, respectively. In general, these activity losses could be attributed to the negative interactions that have been explained before, although extended in a longer period of time. Oliveira *et al.* [28] and Lanza *et al.* [29] also found a negative influence of the exposure time on the residual activity of Lipozyme IM [28] and Novozym 435 [28,29] after SC-CO<sub>2</sub> treatment in the same range of exposure time (1-6 h) and similar pressure and temperature conditions (35-75 °C; 7.2-27.6 MPa [28] and 40-70 °C; 8.0-25.5 MPa [29]). On the contrary, Aucoin *et al.* [27] reported no statistically significant influence of exposure time in the activity of Lipozyme IM 20 after 4, 8 and 12 h of treatment with SC-CO<sub>2</sub> at 8.6-8.9 MPa and 35-37 °C.

### 3.2.2. Effect of water content on the residual activity

As it has been explained, the enzyme activity loss after SC-CO<sub>2</sub> exposure depends on several parameters. One of the most important is the amount of water needed to maintain the native conformation of the enzyme and hence, its optimal functionality [13]. It is noticeable that SC-CO<sub>2</sub> can dissolve up to 0.3-0.5 g water/100 g, depending on the operating pressure and temperature [17]. This way, the essential water that is necessary to maintain the enzyme conformation and activity can be extracted and released together with the CO<sub>2</sub> during the depressurization step, causing enzyme denaturation and loss of activity [12–14].

For Lipozyme RM IM, titrable water was determined by Karl-Fischer before and after SC-CO<sub>2</sub> exposure. Fig. 1-5 shows the relationship between Lipozyme RM IM residual activity and the relative water loss. Experience 5 was excluded because the high activity loss could be mainly attributed to thermal inactivation. From the graph in Fig. 1-5, it can be seen that the loss of water after SC-CO<sub>2</sub> exposure and Lipozyme RM IM activity loss are likely correlated when no depressurization steps were

performed (dotted arrow). Nevertheless, the greatest loss of water from the enzyme took place after several pressurization/depressurization steps (experiences 8 and 9), although these water losses did not translate into further activity reduction.

In the case of Lipozyme 435, the initial titrable water was  $0.7 \pm 0.2$  g/100 g), which is much lower than Lipozyme RM IM. Water measurements after SC-CO<sub>2</sub> exposure were not reliable and not a clear correlation could be established between water and activity loss. In any case, lipase B from *C. antarctica* (CALB), of which Lipozyme 435 is an immobilized form, has been reported as a less water-sensitive lipase than others, either in its free or immobilized form [37]. Immobilized CALB treated with dry ethanol was still able to retain active conformation, suggesting that essential water molecules are kept in its structure [37]. However, activity losses have been found after SC-CO<sub>2</sub> treatment in this study. It could be possible that CO<sub>2</sub> molecules could enter inside the CALB active site, which is an elliptical and steep funnel, and due to its better transport properties compared to conventional solvents, such as ethanol, might have stripped out the essential water molecules. Conformational changes could have likely happened during SC-CO<sub>2</sub> exposure and in the pressurization and/or depressurization steps, negatively affecting Lipozyme 435 activity as it has been reported for Novozym 435 [27–29].

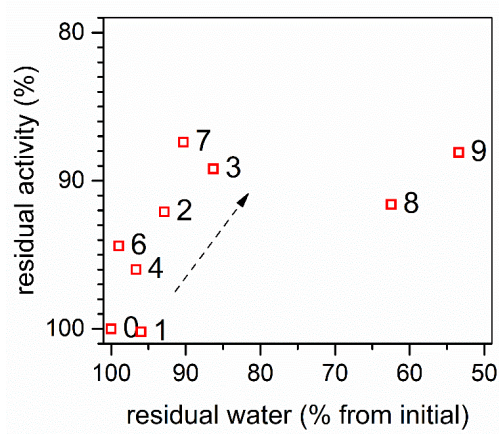


**Figure 1-5.** Residual activity of Lipozyme RM IM vs. water content after SC-CO<sub>2</sub> treatment. Numbers indicate established conditions in each experience (see Table 1-3).



To study the effect of water removal by SC-CO<sub>2</sub>, another set of residual activity determinations was carried out after adding different amounts of water to the reaction media (from 0 to 16 % wt. of enzyme). Results obtained are depicted in Fig. 1-6.

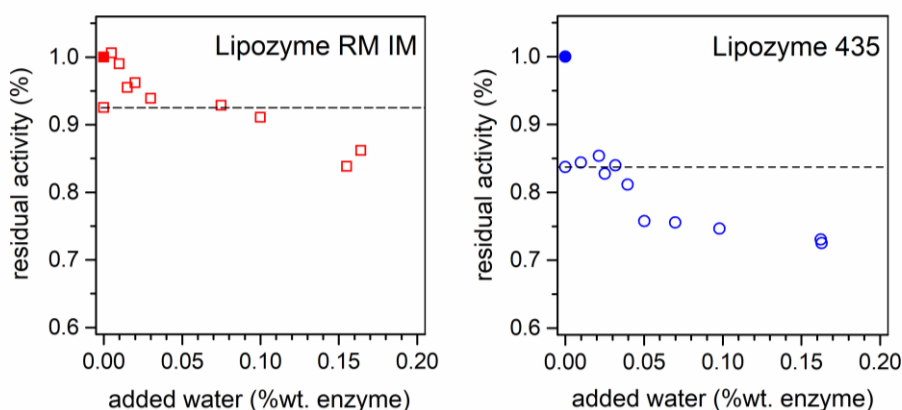


**Figure 1-6.** Residual activities of Lipozyme RM IM (red) and Lipozyme 435 (blue) after SC-CO<sub>2</sub> treatment and different amounts of added water. Empty symbols: treated samples from experience 2; full symbols: untreated samples. Dashed lines indicate the residual activity value of each treated lipase (experience 2) when no water was added.

Fig. 1-6 shows that Lipozyme RM IM was able to recover its initial activity when a low amount of water was added (around 0.5 - 1 % wt. of enzyme). However, the same was not true for Lipozyme 435. If we attend to the nature of the supports of both enzymes, the one of Lipozyme RM IM is hydrophilic, thus water can be easily adsorbed onto it. On the contrary, the hydrophobic character of the immobilization support of Lipozyme 435 might not allow the enzyme to recover its constitution water, and neither its enzymatic activity. In both enzymes, larger amounts of added water resulted in a decrease of the enzymatic activity. Since water is a reaction product, it is likely that this excess of free water slowed down the reaction by promoting the hydrolysis of the products. Conformational changes could also take place at high water concentrations [14] and, in the case of Lipozyme RM IM, mass transfer limitations could have occurred due to water adsorption onto the support, leading to pathway blockage and reduced solubility of the reactants [14].

### 3.2.3. Conformational and morphological changes

The conformational and morphological structures of SC-CO<sub>2</sub>-treated and untreated immobilized lipases were also investigated by FT-IR and SEM, respectively.

#### *i) Infrared spectra*

FT-IR analysis of the untreated and SC-CO<sub>2</sub>-treated immobilized lipases was performed in the range between 400 and 4000 cm<sup>-1</sup> (Fig. 1-7). In the protein FT-IR spectra, the major protein absorption bands due to the peptide group vibrations occur between 1900 and 1200 cm<sup>-1</sup> [38]. Different bands can be observed in this region: the amide I band (between 1600 and 1700 cm<sup>-1</sup>) is mainly associated with carbonyl stretching of the peptide. It consists of a group of overlapped signals, providing information about the secondary protein structure of the enzyme; the amide II band (1580-1510 cm<sup>-1</sup>) is due to the N-H bending with a contribution of the C-N stretching vibrations and the amide III region (1400-1200 cm<sup>-1</sup>), which has a weaker intensity [38,39].

No significant differences were found between the spectra of the untreated immobilized lipases and the spectra of the ones exposed to SC-CO<sub>2</sub>. These results are in coincidence with the works by Jenab *et al.* [19] and Oliveira *et al.* [28] and, based on them, no significant conformational changes in the secondary structure of the immobilized lipases were observed after enzyme treatment with SC-CO<sub>2</sub>.

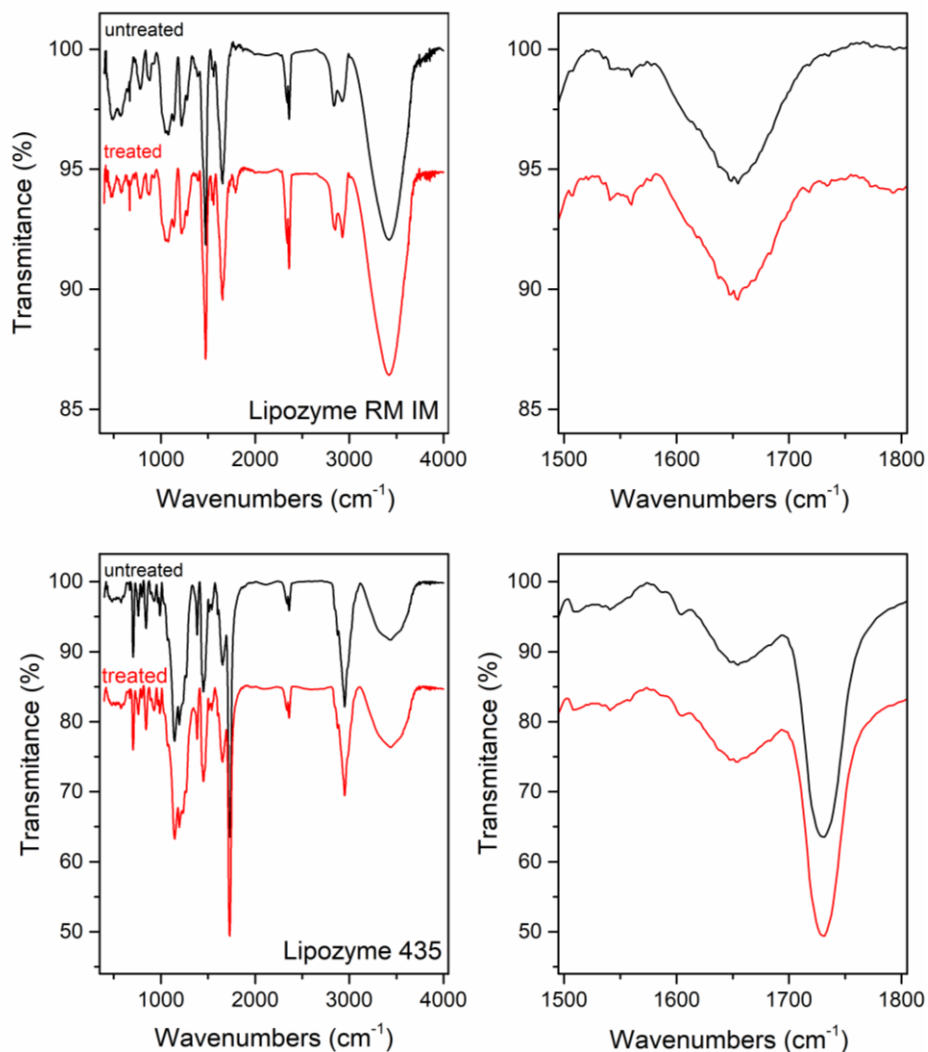


**Figure 1-7.** FT-IR spectra of the studied immobilized lipases before and after SC-CO<sub>2</sub> treatment. Left: complete IR spectra (4000-400 cm<sup>-1</sup>); right: detail of the 1800-1500 cm<sup>-1</sup> region. Treated samples from experience 2.

ii) *Scanning Electron Microscopy (SEM)*

Scanning Electron Microscopy (SEM) was used to investigate any potential morphological changes in both immobilized lipases. Micrographs from Lipozyme RM IM and Lipozyme 435 are shown in Figs. 1-8 and 1-9, respectively. Immobilization support of Lipozyme RM IM was also studied (Fig. 1-8d).

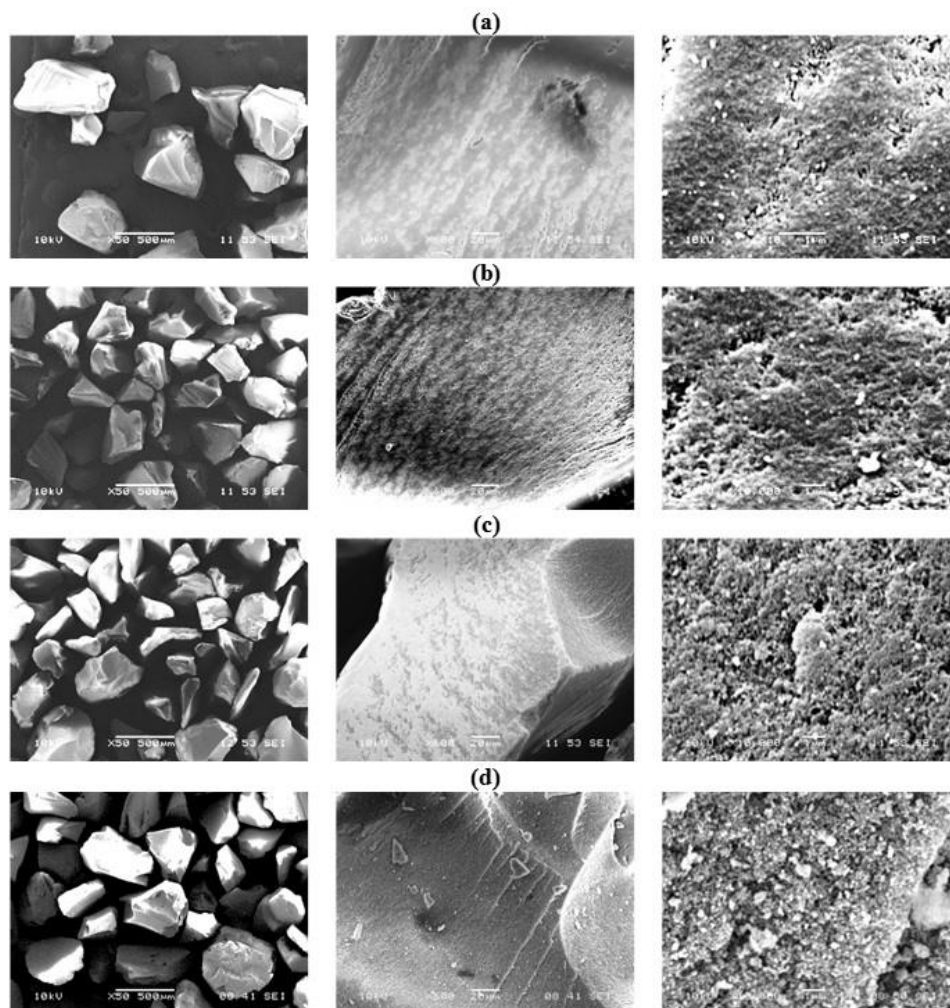


**Figure 1-8.** SEM micrographs of Lipozyme RM IM. Left to right: 50x, 600x and 10000x. (a) untreated enzyme; (b) sample from experience 3; (c) sample from experience 9; (d) immobilization support alone (Duolite A568).

Some authors have reported that SC-CO<sub>2</sub> can interact with the enzyme support, resulting in deformations such as plasticization and swelling [40]. In some cases, rapid depressurization can lead to the formation of cracks and holes in the surface of the immobilization support and increased porosity [28].

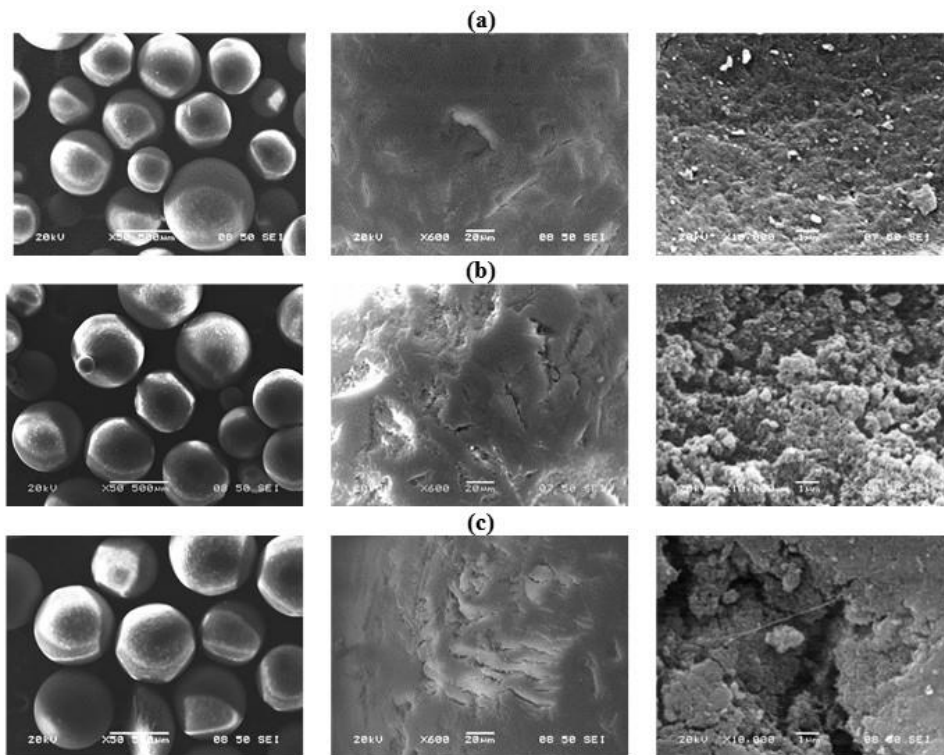


**Figure 1-9.** SEM micrographs of Lipozyme 435. Left to right: 50x, 600x and 10000x.  
(a) untreated enzyme; (b) sample from experience 3; (c) sample from exp. 9.

Recently, Jenab *et al.* [19] have observed structural changes in the SEM micrographs of Lipozyme RM IM and Lipozyme TL IM after SC-CO<sub>2</sub> treatment. Nevertheless, it was concluded that such changes could be attributed to mechanical stresses caused by magnetic stirring during SC-CO<sub>2</sub> exposure and not to pressurization-depressurization cycles [19]. In this study, external orbital agitation was used in the SC-CO<sub>2</sub> treatment of the immobilized enzymes instead of internal magnetic stirring; therefore, the support was not submitted to intense mechanical stress due to that means of stirring. However, several depressurization steps were conducted in this study, using a high depressurization rate (240 kg·m<sup>-3</sup>·min<sup>-1</sup>). As a consequence, a rough and cracked surface with an apparent increase of porosity can be appreciated after SC-CO<sub>2</sub> treatment in 10000x magnifications (Figs. 1-8 b,c and 1-9 b,c).

## Conclusion

In the present work, four commercial lipases: free Palatase 20000 L and Lipozyme CALB L, and immobilized Lipozyme RM IM and Lipozyme 435, were submitted to SC-CO<sub>2</sub> treatment. Based on the results obtained, it can be concluded that SC-CO<sub>2</sub> treatment at the experimental conditions in this study can affect the enzyme activity by means of conformational changes and structural alterations. It is also important to notice that the effect of the SC-CO<sub>2</sub> treatment strongly depends on the experimental conditions, the nature and the source of the enzyme and, mainly, whether the enzyme is presented in a free or immobilized form.

sub/SC-CO<sub>2</sub> treatment can improve the enzymatic activity of free lipases by means of interactions between SC-CO<sub>2</sub> and enzyme residues that lead to an open, more active conformation of the enzyme and/or extraction of water and impurities from the enzyme preparation.

In the case of immobilized enzymes, sub/SC-CO<sub>2</sub> treatment may cause swelling and other structural changes in the immobilization support, as well as extraction of water that could be essential for the enzyme activity. Therefore, the immobilization material and its behavior under sub/SC-CO<sub>2</sub> exposure, the hydrophobic or hydrophilic nature of the support and the potential water-dependency of the biocatalyst should be taken into account.

The results obtained in this work may help with the purpose of selecting the most appropriate biocatalyst and operation conditions to carry out biotransformations of lipids in SC-CO<sub>2</sub>, with the lowest activity loss, or, when possible, the highest activity improvement.

## References

- [1] K.E. Jaeger, T. Eggert, Lipases for biotechnology., *Current Opinion in Biotechnology*. 13 (2002) 390–7.
- [2] A. Zaks, A.M. Klibanov, Enzyme-catalyzed processes in organic solvents., *Proceedings of the National Academy of Sciences of the United States of America*. 82 (1985) 3192–3196.
- [3] K. Nakamura, Biochemical reactions in supercritical fluids, *Trends in Biotechnology*. 8 (1990) 288–292.
- [4] S. Damar, M.O. Balaban, Review of dense phase CO<sub>2</sub> technology: microbial and enzyme inactivation, and effects on food quality, *Journal of Food Science*. 71 (2006) 1–11.
- [5] A. Gießauf, T. Gamse, A simple process for increasing the specific activity of porcine pancreatic lipase by supercritical carbon dioxide treatment, *Journal of Molecular Catalysis B: Enzymatic*. 9 (2000) 57–64.
- [6] Y. Liu, D. Chen, L. Xu, Y. Yan, Evaluation of structure and hydrolysis activity of *Candida rugosa* Lip7 in presence of sub-/super-critical CO<sub>2</sub>, *Enzyme and Microbial Technology*. 51 (2012) 354–358.
- [7] D. Chen, C. Peng, H. Zhang, Y. Yan, Assessment of activities and conformation of lipases treated with sub- and supercritical carbon dioxide., *Applied Biochemistry and Biotechnology*. 169 (2013) 2189–2201.
- [8] Y. Liu, D. Chen, Y. Yan, Effect of ionic liquids, organic solvents and supercritical CO<sub>2</sub> pretreatment on the conformation and catalytic properties of *Candida rugosa* lipase, *Journal of Molecular Catalysis B: Enzymatic*. 90 (2013) 123–127.
- [9] Y. Liu, D. Chen, S. Wang, Effect of sub- and super-critical CO<sub>2</sub> pretreatment on conformation and catalytic properties evaluation of two commercial enzymes of CALB and Lipase PS, *Journal of Chemical Technology and Biotechnology*. 88 (2013) 1750–1756.
- [10] D. Chen, H. Zhang, J. Xu, Y. Yan, Effect of sub- and supercritical CO<sub>2</sub> treatment on the properties of *Pseudomonas cepacia* lipase., *Enzyme and Microbial Technology*. 53 (2013) 110–117.



- [11] C. Bauer, T. Gamse, R. Marr, Quality improvement of crude porcine pancreatic lipase preparations by treatment with humid supercritical carbon dioxide, *Biochemical Engineering Journal*. 9 (2001) 119–123.
- [12] S. V Kamat, E.J. Beckman, A.J. Russell, Enzyme activity in supercritical fluids, *Critical Reviews in Biotechnology*. 15 (1995) 41–71.
- [13] K. Rezaei, E. Jenab, F. Temelli, Effects of water on enzyme performance with an emphasis on the reactions in supercritical fluids., *Critical Reviews in Biotechnology*. 27 (2007) 183–195.
- [14] Ž. Knez, Enzymatic reactions in dense gases, *The Journal of Supercritical Fluids*. 47 (2009) 357–372.
- [15] Ž. Knez, M. Habulin, M. Primožič, Enzymatic reactions in dense gases, *Biochemical Engineering Journal*. 27 (2005) 120–126.
- [16] K. Rezaei, F. Temelli, E. Jenab, Effects of pressure and temperature on enzymatic reactions in supercritical fluids., *Biotechnology Advances*. 25 (2007) 272–280.
- [17] Z. Wimmer, M. Zarevúcka, A review on the effects of supercritical carbon dioxide on enzyme activity., *International Journal of Molecular Sciences*. 11 (2010) 233–253.
- [18] E. Séverac, O. Galy, F. Turon, P. Monsan, A. Marty, Continuous lipase-catalyzed production of esters from crude high-oleic sunflower oil., *Bioresource Technology*. 102 (2011) 4954–4961.
- [19] E. Jenab, F. Temelli, J.M. Curtis, Y.Y. Zhao, Performance of two immobilized lipases for interesterification between canola oil and fully-hydrogenated canola oil under supercritical carbon dioxide, *LWT - Food Science and Technology*. (2014) 263–271.
- [20] F. Kao, S.A. Ekhorutomwen, S.P. Sawan, Residual stability of lipase from *Candida rugosa* in hexane, supercritical CO<sub>2</sub>, and supercritical SF<sub>6</sub>, *Biotechnology Techniques*. 11 (1997) 849–852.
- [21] A. Gießauf, W. Magor, D.J. Steinberger, R. Marr, A study of hydrolases stability in supercritical carbon dioxide (SC-CO<sub>2</sub>), *Enzyme and Microbial Technology*. 24 (1999) 577–583.
- [22] C. Bauer, D.-J. Steinberger, G. Schlauer, T. Gamse, R. Marr, Activation and denaturation of hydrolases in dry and humid supercritical carbon dioxide (SC-CO<sub>2</sub>), *Journal of Supercritical Fluids*. 19 (2000) 79–86.

- [23] M. Habulin, Željko Knez, Activity and stability of lipases from different sources in supercritical carbon dioxide and near-critical propane, *Journal of Chemical Technology & Biotechnology*. 76 (2001) 1260–1266.
- [24] A. Marty, W. Chulalaksananukul, J.S. Condoret, R.M. Willemot, G. Durand, Comparison of lipase-catalysed esterification in supercritical carbon dioxide and in n-hexane, *Biotechnology Letters*. 12 (1990) 11–16.
- [25] A. Marty, W. Chulalaksananukul, R.M. Willemot, J.S. Condoret, Kinetics of lipase-catalyzed esterification in supercritical CO<sub>2</sub>, *Biotechnology and Bioengineering*. 39 (1992) 273–280.
- [26] T. Dumont, D. Barth, C. Corbier, G. Branlant, M. Perrut, Enzymatic reaction kinetic: comparison in an organic solvent and in supercritical carbon dioxide, *Biotechnology and Bioengineering*. 39 (1992) 329–333.
- [27] M.G. Aucoin, R.L. Legge, Effects of supercritical CO<sub>2</sub> exposure and depressurization on immobilized lipase activity, *Biotechnology Letters*. 23 (2001) 1863–1870.
- [28] D. Oliveira, A.C. Feihmann, A.F. Rubira, M.H. Kunita, C. Dariva, J.V. Oliveira, Assessment of two immobilized lipases activity treated in compressed fluids, *The Journal of Supercritical Fluids*. 38 (2006) 373–382.
- [29] M. Lanza, W.L. Priamo, J.V. Oliveira, C. Dariva, D. Oliveira, The effect of temperature, pressure, exposure time, and depressurization rate on lipase activity in SCCO<sub>2</sub>, *Applied Biochemistry and Biotechnology*. 113 (2004) 181–187.
- [30] D. de Oliveira, A.C. Feihmann, C. Dariva, A.G. Cunha, J. V. Bevilaqua, J. Destain, J.V. Oliveira, D.M.G. Freire, Influence of compressed fluids treatment on the activity of *Yarrowia lipolytica* lipase, *Journal of Molecular Catalysis B: Enzymatic*. 39 (2006) 117–123.
- [31] M.M. Bradford, A rapid and sensitive method for the quantitation of microgram quantities of protein utilizing the principle of protein-dye binding., *Analytical Biochemistry*. 72 (1976) 248–254.
- [32] J.R. Lakowicz, *Principles of fluorescence spectroscopy*, 3rd edition, Springer Science+Business Media, LLC, New York, 2006.
- [33] M. Arroyo, J.M. Sánchez-Montero, J.V. Sinisterra, Thermal stabilization of immobilized lipase B from *Candida antarctica* on different supports : Effect of water activity on enzymatic activity in organic media, *Enzyme and Microbial Technology*. 24 (1999) 3–12.



- [34] R.C. Rodrigues, R. Fernandez-Lafuente, Lipase from *Rhizomucor miehei* as a biocatalyst in fats and oils modification, *Journal of Molecular Catalysis B: Enzymatic*. 66 (2010) 15–32.
- [35] S. Kamat, G. Critchley, E.J. Beckman, A.J. Russell, Biocatalytic synthesis of acrylates in organic solvents and supercritical fluids: III. Does carbon dioxide covalently modify enzymes?, *Biotechnology and Bioengineering*. 46 (1995) 610–620.
- [36] M. Habulin, M. Primožič, Ž. Knez, Stability of proteinase from *Carica papaya* latex in dense gases, *The Journal of Supercritical Fluids*. 33 (2005) 27–34.
- [37] W. Piyatheerawong, Y. Iwasaki, X. Xu, T. Yamane, Dependency of water concentration on ethanolysis of trioleoylglycerol by lipases, *Journal of Molecular Catalysis B: Enzymatic*. 28 (2004) 19–24.
- [38] A. Natalello, D. Ami, S. Brocca, M. Lotti, S.M. Doglia, Secondary structure, conformational stability and glycosylation of a recombinant *Candida rugosa* lipase studied by Fourier-transform infrared spectroscopy., *The Biochemical Journal*. 385 (2005) 511–7.
- [39] S.E. Collins, V. Lassalle, M.L. Ferreira, FTIR-ATR characterization of free *Rhizomucor meihei* lipase (RML), Lipozyme RM im and chitosan-immobilized RML, *Journal of Molecular Catalysis B: Enzymatic*. 72 (2011) 220–228.
- [40] M. Habulin, M. Primožic, Ž. Knez, Supercritical fluids as solvents for enzymatic reactions, *Acta Chimica Slovenica*. 54 (2007) 667–677

## Chapter 2

# Phase behavior of the pseudo-ternary system carbon dioxide + ethanol + fish oil at high pressures

#phase equilibrium #supercritical carbon dioxide #ethanol #fish oil

#thermodynamic modelling #Peng-Robinson equation of state

**Adapted from:**

R. Melgosa, M.T. Sanz, Á.G. Solaesa, S. Beltrán, Phase behaviour of the pseudo-ternary system carbon dioxide + ethanol + fish oil at high pressures, *Journal of Chemical Thermodynamics*. 115 (2017) 106–113.

DOI: <https://doi.org/10.1016/j.jct.2017.07.032>

## Table of contents

Tables.....	125
Figures .....	127
Abstract.....	129
Resumen.....	131
1. Introduction.....	133
2. Experimental .....	135
2.1. Materials .....	135
2.2. Apparatus and procedure .....	137
3. Results and discussion.....	139
3.1. Experimental data .....	139
3.2. Data correlation.....	146
3.3. Thermodynamic consistency .....	152
Conclusion .....	153
References.....	155

## Tables

<b>Table 2-1.</b> Fatty acid composition of the fish oil [26].	136
<b>Table 2-2.</b> Vapor + Liquid phase compositions of the binary system CO <sub>2</sub> (1) + ethanol (2).	140
<b>Table 2-3.</b> Liquid + Liquid (L1+L2) and Vapor + Liquid (V+L2) phase compositions (weight fraction) of the pseudo-ternary system CO <sub>2</sub> (1) + ethanol (2) + fish oil (3) at T = 323.15 K and p = 10 MPa.	141
<b>Table 2-4.</b> Liquid + Liquid (L1+L2) and Vapor + Liquid (V+L2) phase compositions (weight fraction) of the pseudo-ternary system CO <sub>2</sub> (1) + ethanol (2) + fish oil (3) at T = 323.15 K and p = 30 MPa.	142
<b>Table 2-5.</b> Liquid + Liquid (L1+L2) and Vapor + Liquid (V+L1, V+L2) phase compositions (weight fraction) of the pseudo-ternary system CO <sub>2</sub> (1) + ethanol (2) + fish oil (3) at T = 343.15 K and p = 10 MPa.	143
<b>Table 2-6.</b> Molecular weight (MW), critical temperature (T <sub>c</sub> ), critical pressure (p <sub>c</sub> ), and acentric factor (ω) of the components of the pseudo-ternary system CO <sub>2</sub> + ethanol + fish oil.	148
<b>Table 2-7.</b> Estimated binary interaction parameters of the PR EoS vdW2 model for the pseudo-ternary system CO <sub>2</sub> + ethanol + fish oil at different temperature and pressure conditions in the different Liquid + Liquid (L1+L2) and Vapor + Liquid (V+L1, V+L2) 2-phase regions.	151



## Figures

- Figure 2-1.** Schematic diagram of the high-pressure apparatus used for the phase equilibrium measurements. 1: CO<sub>2</sub> inlet; 2: Fish oil and ethanol inlet; 3: high-pressure variable volume equilibrium view cell; 4: 6-way valve for light-phase sampling; 5: gear pump; 6: heavy-phase sampling valves; 7: rupture disk; 8: camera endoscope and video recorder; 9: venting valves; F: Coriolis mass flow meter. .... 137
- Figure 2-2.** Pressure-composition diagram of the binary system CO<sub>2</sub> + ethanol at T = 323.15 K (full symbols) and T = 343.15 K (hollow symbols). □, ■: experimental data obtained in this work; ●, ○: data from Lim *et al.* [9]; ▲, △: data from Joung *et al.* [12]. Continuous and dashed lines are calculated with PR EoS vdW2 model at T = 323.15 K and T = 343.15 K, respectively. .... 140
- Figure 2-3.** Phase diagram of the pseudo-ternary system CO<sub>2</sub> + ethanol + fish oil (T = 323.15 K, p = 10 MPa). -○-: experimental L1+L2 tie-line; -□-: experimental V+L2 tie-line; ☆: experimental monophasic mixture; ..... : PR EoS vdW2 model. .... 144
- Figure 2-4.** Phase diagram of the pseudo-ternary system CO<sub>2</sub> + ethanol + fish oil (T = 323.15 K, p = 30 MPa). -○-: experimental L1+L2 tie-line; -□-: experimental V+L2 tie-line; ☆: experimental monophasic mixture; ..... : PR EoS vdW2 model. .... 145
- Figure 2-5.** Phase diagram of the pseudo-ternary system CO<sub>2</sub> + ethanol + fish oil (T = 343.15 K, p = 10 MPa). -○-: experimental L1+L2 tie-lines; -△-: experimental V+L1 tie-lines; -□-: experimental V+L2 tie-lines; ..... : PR EoS vdW2 model. .... 146



## Abstract

This chapter provides experimental fluid phase equilibrium data of the pseudo-ternary mixture CO<sub>2</sub> + ethanol + fish oil, a system of interest in pharmaceutical and food-industry applications such as the production of omega-3 PUFA-enriched lipid derivatives at mild, non-oxidative conditions.

Experimental tie-lines were obtained by means of an analytical isothermal method with recirculation of the vapor phase. Measurements were carried out in the temperature range 323.15 K-343.15 K and at pressures from 10 MPa to 30 MPa. The Peng-Robinson equation of state coupled with the conventional van der Waals mixing rules with two adjustable parameters was used for experimental data correlation.



## Resumen

El presente capítulo recoge datos experimentales de equilibrio entre fases para el sistema pseudo-ternario dióxido de carbono ( $\text{CO}_2$ ) + etanol + aceite de pescado, un sistema de gran interés para aplicaciones farmacéuticas y alimentarias tales como la producción de derivados lipídicos enriquecidos en ácidos grasos poliinsaturados omega-3 en condiciones suaves y no oxidativas.

Las rectas de reparto experimentales se han obtenido mediante un método analítico isotérmico con recirculación de la fase vapor. Las medidas se han realizado en el rango de temperatura 323.15 K-343.15 K y presión desde 10 MPa hasta 30 MPa. Para la correlación de los datos experimentales se ha utilizado la ecuación de estado de Peng-Robinson con las reglas de mezcla convencionales de van der Waals y dos parámetros de ajuste



## 1. Introduction

Dense carbon dioxide is expected to play an important role as a reaction medium in ecologically friendly processing. Enzyme-catalyzed ethanolysis of lipid sources in supercritical carbon dioxide (SC-CO<sub>2</sub>) or CO<sub>2</sub>-expanded media can be used to improve the production of lipid derivatives, including concentrates of omega-3 polyunsaturated fatty acids (*n*-3 PUFAs) from fish oil [1,2]. However, the relatively low solubility of the reactants in SC-CO<sub>2</sub> limits the reaction performance in this medium; thus, a CO<sub>2</sub>-expanded media is preferred to minimize mass transfer limitations [3]. Understanding the phase behavior of the ethanol + fish oil substrate mixture with CO<sub>2</sub> would help in the selection of adequate ethanolysis conditions (pressure, temperature, ethanol-to-oil ratio, and amount of dissolved CO<sub>2</sub> in the reaction mixture). This knowledge can be also extended to other potential applications and may be of interest in the fish oil industry, since SC-CO<sub>2</sub> or CO<sub>2</sub>-expanded media can be used throughout all the *n*-3 PUFA concentration process, including the extraction of the fish oil [4], the refining step [5], the separation and fractionation of the reaction products [6,7], or the formulation of the final product by means of particle formation techniques [8].

Experimental data related with high-pressure phase equilibrium of the binary system CO<sub>2</sub> + ethanol is extensively reported in the literature [9–14]. Besides, ternary and higher systems comprising CO<sub>2</sub> and pure triglycerides, other lipid derivatives and their mixtures have been also investigated [15]. However, only a few data regarding the phase equilibrium of pseudo-ternary mixtures of CO<sub>2</sub>, ethanol, and edible oils can be found in the literature, and these data are usually related to the solubility of the lipid compounds in CO<sub>2</sub> with ethanol as a co-solvent [16].

Several publications have previously reported fluid phase equilibrium of pseudo-ternary mixtures of CO<sub>2</sub> + ethanol + vegetable oils. However, to our knowledge, this is the first work dealing with oils rich in *n*-3 PUFAs from animal sources, such as fish oil.

Geana and Steiner [17] reported fluid phase equilibrium data for the pseudo-ternary system CO<sub>2</sub> + ethanol + rapeseed oil in the temperature range 313 K-353 K and at pressures from 6 MPa to 12 MPa, satisfactorily correlating the phase behavior with the Peng-Robinson equation of state (PR EoS) [18] coupled with the conventional van der Waals mixing rules with two adjustable parameters (vdW2).

Ndiaye *et al.* [19] studied the fluid phase equilibria of binary and ternary mixtures involving CO<sub>2</sub>, ethanol, soybean oil, castor oil, and their fatty acid ethyl esters. The pseudo-ternary system CO<sub>2</sub> + ethanol + castor oil was studied at fixed ethanol-to-oil ratios, temperatures ranging from 313.15 K to 343.15 K and pressures from 2.13 MPa to 27.13 MPa. Experimental data were correlated both with PR EoS vdW2 and the Statistical Associating Fluid Theory (SAFT) [20] with one binary interaction parameter. Among these two models, the authors considered that SAFT EoS described better the phase behavior of the pseudo-ternary system, yet they pointed out at some deviations from their experimental results, such as the over-prediction of the cloud point pressure at high ethanol ratios [20].

Hernández *et al.* [21] investigated the fluid phase equilibrium behavior of the pseudo-ternary mixture CO<sub>2</sub> + ethanol + sunflower oil at two different conditions of temperature and pressure (313.15 K and 13 MPa; 333.15 K and 20 MPa). A group contribution equation of state (GC EoS) [22] was used to correlate the experimental data. Two different sets of parameters were adopted for the interaction between the triglyceride and the alcohol groups, one of them corresponding to the Liquid + Liquid (L1+L2) 2-phase region, and the other to the Vapor + Liquid (V+L2) 2-phase region.

More recently, Dalmolin *et al.* [23] studied the phase transitions in the system CO<sub>2</sub> + ethanol + rapeseed oil, at temperatures in the range 313.15 K-343.15 K and pressures up to 22.53 MPa. They found a 3-phase region with a Vapor + Liquid + Liquid (V+L1+L2) phase transition that occurred at higher pressures when increasing temperature, and satisfactorily explained their experimental results with the PR EoS vdW2 model.

In this work, the phase behavior of the pseudo-ternary mixture CO<sub>2</sub> + ethanol + fish oil in the temperature range from 323.15 K to 343.15 K and pressures from 10 MPa to 30 MPa has been determined by means of an analytical isothermal method with recirculation of the vapor phase (AnTVcir, as described by Dohrn and Brunner [24]). The main goal of the study involves a contribution towards understanding the phase behavior of systems containing CO<sub>2</sub>, ethanol, and oils rich in *n*-3 PUFAs. The knowledge obtained will be useful in the development of applications involving these pseudo-ternary mixtures, such as the previously mentioned enzymatic reactions, supercritical extraction and fractionation, and particle formation techniques.

## 2. Experimental

### 2.1. Materials

Fish oil was provided by AFAMSA S.A. (Pontevedra, Spain) being a mixture of tuna (*Thunnus* sp.) and sardine (*Sardina pilchardus*) refined oils. The fatty acid profile and free fatty acid content of the fish oil have been determined according to AOCS methods [25]. The fatty acid profile has been previously reported [26] and is also provided in Table 2-1. Free fatty acid content was found to be  $0.29 \pm 0.04$  % oleic acid. Density of fish oil was also measured in an Anton Paar DMA 5000 instrument, finding values of  $\rho^{323.15\text{ K}} = 906.53 \text{ kg}\cdot\text{m}^{-3}$  and  $\rho^{343.15\text{ K}} = 895.83 \text{ kg}\cdot\text{m}^{-3}$  ( $u(\rho) = \pm 0.05 \text{ kg}\cdot\text{m}^{-3}$ ).

Absolute ethanol (0.999 mass fraction) was purchased from Merck KGaA. Carbon dioxide (0.999 mass fraction in the liquid phase) was supplied by Air Liquide S.A. (Spain). Compounds have been used as provided by the manufacturers without further purification.

**Table 2-1.** Fatty acid composition of the fish oil [26].

Fatty acid		% wt.
myristic	C14:0	3.8
palmitic	C16:0	21.0
palmitoleic	C16:1 <i>n</i> -7	6.1
stearic	C18:0	6.0
oleic	C18:1 <i>n</i> -9	18.4
vaccenic	C18:1 <i>n</i> -7	3.0
linoleic cis (LA)	C18:2 <i>n</i> -6	2.4
$\alpha$ -linolenic (ALA)	C18:3 <i>n</i> -3	0.7
stearidonic	C18:4 <i>n</i> -3	0.9
eicosenoic	C20:1 <i>n</i> -9	2.1
eicosatrienoic	C20:3 <i>n</i> -3	2.0
eicosapentaenoic (EPA)	C20:5 <i>n</i> -3	6.9
docosapentaenoic (DPA)	C22:5 <i>n</i> -3	1.8
docosahexaenoic (DHA)	C22:6 <i>n</i> -3	24.9

Standard uncertainties are  $u(\% \text{ wt.}) = \pm 0.5$

The potential reactivity of fish oil in contact with ethanol could lead to some extent of trans-esterification and reaction products could be formed during phase equilibria measurements, mainly fatty acid ethyl esters (FAEE). Although reaction in the absence of catalysts is very slow, the presence of FAEE and other intermediate components was analyzed after phase equilibria measurements by NP-HPLC. Chromatographic method is reported elsewhere [27]. FAEE content was found less than 0.001 mole fraction and it was considered not to affect the phase equilibria.

Hydrolysis of the fish oil was also evaluated by means of the free fatty acid content [25], finding a maximum increase up to  $0.81 \pm 0.05$  % oleic acid at the highest studied temperature (343.15 K).

Fatty acid profile was also determined after phase equilibria measurements, finding no significant changes compared to the initial profile (Table 2-1). Additionally,

since fish oil is rich in polyunsaturated fatty acids (Table 2-1) it is very prone to oxidation. Therefore, primary oxidation was evaluated by means of peroxide value analysis [28] before and after phase equilibria measurements. Although PV slightly increased from  $2.0 \pm 0.2$  meq  $O_2/kg$  to  $3.5 \pm 0.1$  meq  $O_2/kg$ , oxidation products are minor components present in small amounts that would not affect the phase equilibria of the system.

## 2.2. Apparatus and procedure

A schematic diagram of the high-pressure apparatus used for fluid phase equilibrium measurements is shown in Fig. 2-1. It was built by Eurotechnica GmbH (Germany) and consists of an equilibrium cell made of stainless steel (SS-316) and equipped with a sapphire window for observing the content of the cell during measurements.

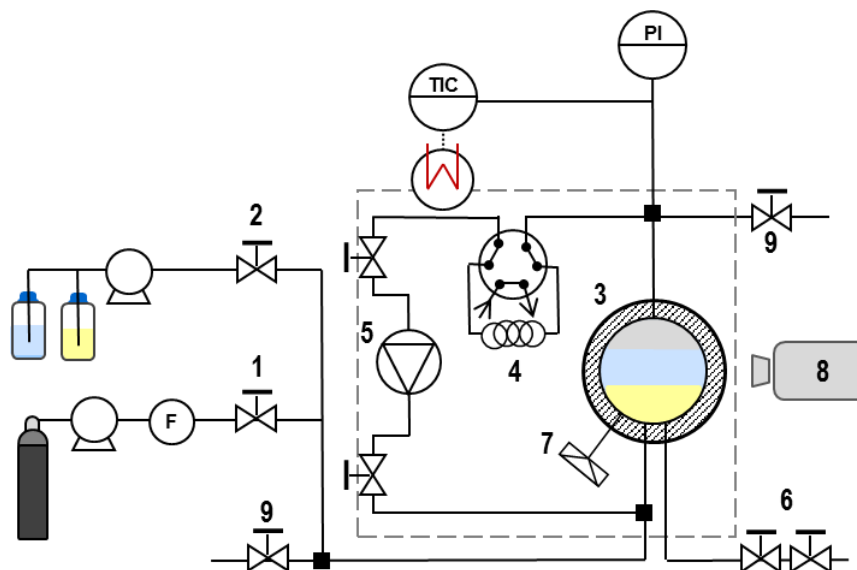


**Figure 2-1.** Schematic diagram of the high-pressure apparatus used for the phase equilibrium measurements. 1:  $CO_2$  inlet; 2: Fish oil and ethanol inlet; 3: high-pressure variable volume equilibrium view cell; 4: 6-way valve for light-phase sampling; 5: gear pump; 6: heavy-phase sampling valves; 7: rupture disk; 8: camera endoscope and video recorder; 9: venting valves; F: Coriolis mass flow meter.

Internal volume of the cell ranges from 40 to 70 mL, adjustable through a manual screw piston. The cell includes a pressure transducer and an immersed thermocouple, both calibrated and connected to a Data Acquisition System (DAS). The equipment was placed inside an oven that allowed temperature control of the system. Mixing of the components of the system was achieved by continuously taking the vapor phase and passing it back into the equilibrium cell through the liquid phase by means of a gear pump (Micropump IDEX). A 750  $\mu\text{L}$  loop that could be isolated by means of a 6-way valve (VICI) was placed in the recirculation path for sampling the vapor phase with minimal equilibrium disturbance. Besides, a micro-metering valve was connected to the bottom of the equilibrium cell through a 1/16" capillary for sampling the heavy phase. Pressure drop occurring when sampling the liquid phase was compensated by reducing the volume of the cell through the manual screw piston. Maximum specifications of the apparatus are  $p = 32 \text{ MPa}$  and  $T = 393 \text{ K}$ .

A typical experiment with the high-pressure variable-volume view cell began with the pre-heating of the system up to the desired temperature. When the temperature was achieved, the equilibrium cell was gently purged with low pressure  $\text{CO}_2$  to sweep the residual air inside the cell. Immediately afterwards, known volumes of fish oil and ethanol were introduced into the cell by means of a binary HPLC pump (Agilent 1200 Series). A certain amount of  $\text{CO}_2$  was then charged into the cell by using a high-pressure syringe pump (ISCO 260D). The exact amounts of fish oil and ethanol were calculated using their respective densities at room temperature, whereas the mass of  $\text{CO}_2$  charged into the cell was measured by a Coriolis mass flow meter (Rheonik RHE015). Once the cell was charged and the desired pressure was adjusted by actuating the manual screw piston, the gear pump was connected, and recirculation of the vapor phase was performed for at least 2 h to facilitate the mixing of the components and its distribution in the different phases of the system. The system was then let to stand for another 2 h at constant temperature and pressure. Phase separation was visually verified through the sapphire window and



samples from the vapor and liquid phases were taken by the 6-way and the micro-metering valve, respectively. Pressure variations up to  $\pm 0.1$  MPa were observed during sampling, while temperature change was not detected. Overall standard uncertainties in the equilibrium measurements were  $u(p) = \pm 0.15$  MPa,  $u(T) = \pm 0.1$  K, and  $u(w_i) = \pm 0.005$ ; being  $w_i$  the mass fraction of component  $i$ .

Samples were decompressed to atmospheric pressure and released  $\text{CO}_2$  was measured by means of a thermal mass flow meter (Bronkhorst F-110C). Ethanol and fish oil were separated from  $\text{CO}_2$  and collected in an ice-cooled glass trap. The amount of each component was determined by weighing the vials in a precision analytical balance (accurate to  $\pm 0.0001$  g) before and after evaporation of ethanol at  $T = 373.15$  K.

## 3. Results and discussion

### 3.1. Experimental data

In order to check the reliability of the apparatus and experimental procedure, preliminary measurements of the binary system  $\text{CO}_2$  + ethanol were carried out. Experimental high-pressure phase equilibria data of the  $\text{CO}_2$  + ethanol binary system is summarized in Table 2-2. The results obtained were compared with data taken from literature [9,12], finding a good agreement (Fig. 2-2).

**Table 2-2.** Vapor + Liquid phase compositions of the binary system CO<sub>2</sub> (1) + ethanol (2).

p / MPa	x <sub>1</sub>	y <sub>1</sub>	p / MPa	x <sub>1</sub>	y <sub>1</sub>
<b>T = 323.15 K</b>			<b>T = 343.15 K</b>		
4.67	0.2647	0.9840	7.01	0.2930	0.9679
5.12	0.2771	0.9859	8.05	0.3785	0.9656
5.34	0.3058	0.9819	9.04	0.4260	0.9614
5.78	0.3128	0.9837	9.98	0.4968	0.9484
7.07	0.4128	0.9814	10.98	0.6130	0.9432
7.69	0.4795	0.9739	11.50	0.6910	0.9060
7.96	0.5069	0.9764			
8.16	0.5455	0.9754			
8.44	0.6348	0.9740			
8.46	0.6279	0.9671			
8.51	0.6535	0.9679			
8.69	0.6875	0.9630			

Composition in mole fraction

Standard uncertainties are  $u(p) = \pm 0.15$  MPa,  $u(T) = \pm 0.1$  K, and  $u(w_i) = \pm 0.005$

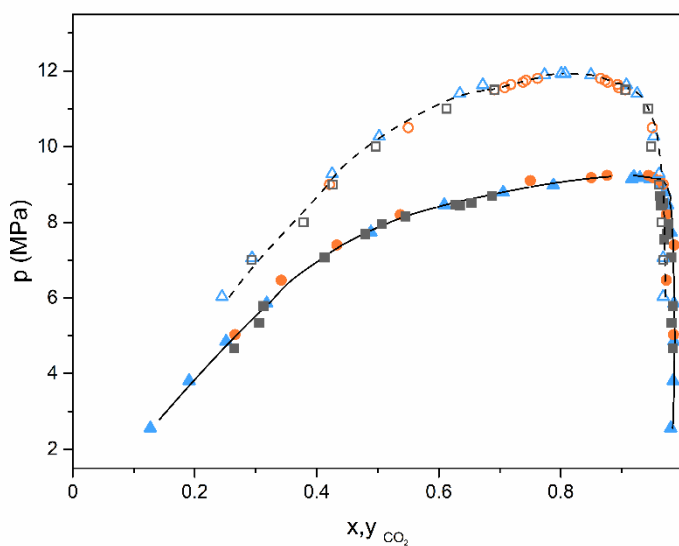


**Figure 2-2.** Pressure-composition diagram of the binary system CO<sub>2</sub> + ethanol at T = 323.15 K (full symbols) and T = 343.15 K (hollow symbols). □, ■: experimental data obtained in this work; ●, ○: data from Lim *et al.* [9]; ▲, △: data from Joung *et al.* [12]. Continuous and dashed lines are calculated with PR EoS vdW2 model at T = 323.15 K and T = 343.15 K, respectively.



Experimental high-pressure phase equilibrium data of the pseudo-ternary system CO<sub>2</sub> + ethanol + fish oil is listed in Tables 2-3, 2-4, and 2-5. Due to the large differences in molecular weight of the components of the system, compositions are expressed in terms of mass fraction instead of mole fraction.

**Table 2-3.** Liquid + Liquid (L1+L2) and Vapor + Liquid (V+L2) phase compositions (weight fraction) of the pseudo-ternary system CO<sub>2</sub> (1) + ethanol (2) + fish oil (3) at T = 323.15 K and p = 10 MPa.

heavy phase			light phase			type of phase eq.
w <sub>1</sub>	w <sub>2</sub>	w <sub>3</sub>	w <sub>1</sub>	w <sub>2</sub>	w <sub>3</sub>	
0.0000	0.2652	0.7348	0.0000	0.9256	0.0744	L1+L2
0.0423	0.2836	0.6741	0.0420	0.8692	0.0888	L1+L2
0.0761	0.2966	0.6273	0.0780	0.7957	0.1263	L1+L2
0.1012	0.3087	0.5901	0.1016	0.7638	0.1346	L1+L2
0.1696	0.3898	0.4406	0.1710	0.6176	0.2114	L1+L2
0.2247	0.0000	0.7754	0.9868	0.0000	0.0132	V+L2
0.2440	0.0272	0.7288	0.9580	0.0280	0.0140	V+L2
0.2776	0.0747	0.6478	0.9003	0.0751	0.0246	V+L2
0.3330	0.1181	0.5490	0.7924	0.1657	0.0419	V+L2
0.3622	0.1541	0.4837	0.7332	0.2193	0.0476	V+L2
0.3730	0.1710	0.4560	0.6949	0.2525	0.0526	V+L2
0.3804	0.1841	0.4355	0.6207	0.3010	0.0783	V+L2
0.2026	0.2224	0.5751	0.2024	0.2222	0.5754	homogeneous
0.2745	0.4691	0.2564	0.2747	0.4689	0.2564	homogeneous
0.3039	0.2838	0.4023	0.3030	0.2844	0.4026	homogeneous
0.4590	0.3640	0.1770	0.4593	0.3638	0.1769	homogeneous

Standard uncertainties are  $u(p) = \pm 0.15$  MPa,  $u(T) = \pm 0.1$  K, and  $u(w_i) = \pm 0.005$

Experimental results at  $T = 323.15$  K showed two different 2-phase regions for the two pressures investigated (10 MPa and 30 MPa). In one of them, two liquid phases could be distinguished, being the light and heavy phases rich with ethanol and oil, respectively (L1+L2). In the other 2-phase region, a light vapor phase rich with  $\text{CO}_2$  and a heavy liquid phase rich with fish oil (V+L2) were observed. Homogeneous monophasic mixtures were visually and analytically verified, samples taken from the top and bottom of the equilibrium cell were similar with differences smaller than the experimental uncertainty.

**Table 2-4.** Liquid + Liquid (L1+L2) and Vapor + Liquid (V+L2) phase compositions (weight fraction) of the pseudo-ternary system  $\text{CO}_2$  (1) + ethanol (2) + fish oil (3) at  $T = 323.15$  K and  $p = 30$  MPa.

heavy phase			light phase			type of phase eq.
$w_1$	$w_2$	$w_3$	$w_1$	$w_2$	$w_3$	
0.0000	0.2219	0.7781	0.0000	0.9066	0.0934	L1+L2
0.0649	0.3010	0.6341	0.0771	0.8185	0.1044	L1+L2
0.1550	0.4288	0.4162	0.1520	0.6654	0.1826	L1+L2
0.2559	0.0000	0.7441	0.9832	0.0000	0.0168	V+L2
0.2843	0.0674	0.6484	0.9089	0.0639	0.0272	V+L2
0.3073	0.1174	0.5753	0.8588	0.1131	0.0281	V+L2
0.3404	0.1401	0.5194	0.8252	0.1417	0.0331	V+L2
0.3844	0.1666	0.4490	0.7079	0.2367	0.0555	V+L2
0.4922	0.2338	0.2740	0.6089	0.3036	0.0875	V+L2
0.2926	0.2224	0.4851	0.2928	0.2219	0.4853	homogeneous
0.2919	0.4499	0.2582	0.2902	0.4488	0.2610	homogeneous
0.4528	0.416	0.1312	0.4481	0.4163	0.1356	homogeneous
0.5219	0.3261	0.1520	0.5198	0.328	0.1522	homogeneous

Standard uncertainties are  $u(p) = \pm 0.15$  MPa,  $u(T) = \pm 0.1$  K, and  $u(w_i) = \pm 0.005$



In the case of the phase equilibrium at  $T = 343.15$  K and  $p = 10$  MPa, three 2-phase regions (L1+L2, V+L1, and V+L2) and a 3-phase region (V+L1+L2) were observed. The appearance of the V+L1 region is consistent with the published phase equilibrium data of the binary system  $\text{CO}_2$  + ethanol at  $T = 343.15$  K [9,12].

**Table 2-5.** Liquid + Liquid (L1+L2) and Vapor + Liquid (V+L1, V+L2) phase compositions (weight fraction) of the pseudo-ternary system  $\text{CO}_2$  (1) + ethanol (2) + fish oil (3) at  $T = 343.15$  K and  $p = 10$  MPa.

heavy phase			light phase			type of phase eq.
$w_1$	$w_2$	$w_3$	$w_1$	$w_2$	$w_3$	
0.0000	0.2829	0.7171	0.0000	0.6497	0.3503	L1+L2
0.0363	0.2327	0.7310	0.0728	0.6418	0.2854	L1+L2
0.0618	0.2102	0.7280	0.1725	0.6291	0.1984	L1+L2
0.0890	0.1851	0.7259	0.3132	0.5677	0.1191	L1+L2
0.1157	0.1607	0.7236	0.4183	0.5088	0.0729	L1+L2
0.1624	0.1162	0.7214	0.4981	0.4199	0.0820	L1+L2
0.4854	0.5146	0.0000	0.9461	0.0539	0.0000	V+L1
0.4850	0.5014	0.0136	0.9239	0.0589	0.0172	V+L1
0.4870	0.4752	0.0378	0.9002	0.0680	0.0318	V+L1
0.1820	0.0000	0.8180	0.9796	0.0000	0.0204	V+L2
0.1843	0.0396	0.7761	0.9455	0.0325	0.0220	V+L2
0.1794	0.0717	0.7489	0.9143	0.0542	0.0315	V+L2
0.1814	0.0957	0.7229	0.9055	0.0607	0.0338	V+L2

Standard uncertainties are  $u(p) = \pm 0.15$  MPa,  $u(T) = \pm 0.1$  K, and  $u(w_i) = \pm 0.005$

Results obtained for the binary ethanol + fish oil tie-lines at  $T = 323.15$  K, and pressures of 10 MPa and 30 MPa (Figs. 2-3 and 2-4) are similar to those obtained by Bucio *et al.* in previous works at the same temperature and atmospheric pressure [26], indicating that, in the range investigated, pressure does not significantly affect phase equilibrium of this binary mixture. The composition of the two liquid phases in the L1+L2 region became more similar as more  $\text{CO}_2$  is dissolved. The same was true for the V+L2 region, where the compositions of the vapor and liquid phases in equilibrium tend to merge with increasing amounts of dissolved ethanol. A similar trend has been found for other pseudo-ternary mixtures of  $\text{CO}_2$  + ethanol + natural lipids, such as castor oil [19] and sunflower oil [21]. The homogeneous monophasic region at  $p = 30$  MPa appears to be slightly larger, although no strong effect of pressure on the phase behavior of the mixture at  $T = 323.15$  K can be observed.

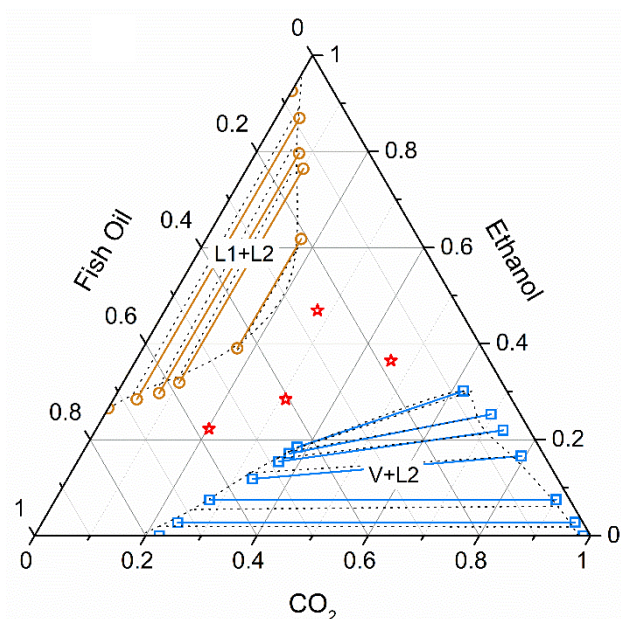


**Figure 2-3.** Phase diagram of the pseudo-ternary system  $\text{CO}_2$  + ethanol + fish oil ( $T = 323.15$  K,  $p = 10$  MPa). -○-: experimental L1+L2 tie-line; -□-: experimental V+L2 tie-line; ☆: experimental monophasic mixture; ····· : PR EoS vdW2 model.

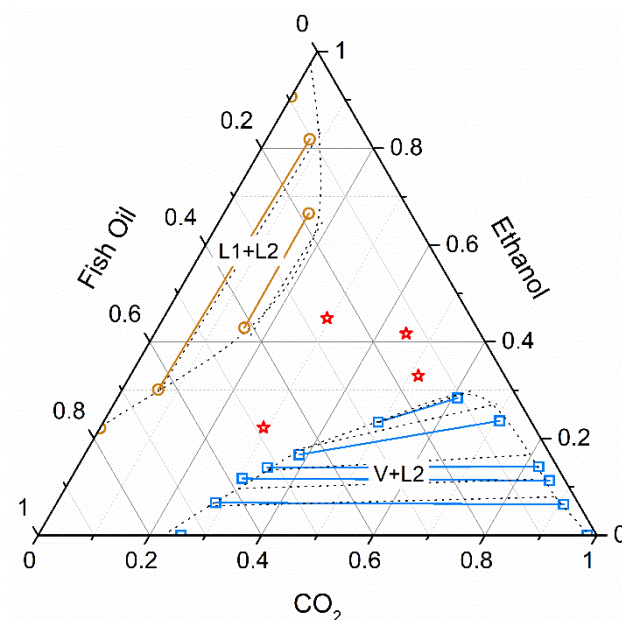


**Figure 2-4.** Phase diagram of the pseudo-ternary system  $\text{CO}_2$  + ethanol + fish oil ( $T = 323.15 \text{ K}$ ,  $p = 30 \text{ MPa}$ ). -○-: experimental L1+L2 tie-line; -□-: experimental V+L2 tie-line; ☆: experimental monophasic mixture; ····· : PR EoS vdW2 model.

From the phase diagram at  $T = 343.15 \text{ K}$  and  $p = 10 \text{ MPa}$  (Fig. 2-5), it can be observed that, starting from the binary sides of the phase diagram, increasing amounts of the third component made the tie-lines of the 2-phase regions approach the sides of the 3-phase region triangle. Inside this 3-phase region, theoretical mixtures split in a V+L1+L2 system, each phase with a composition defined by the vertices of the triangle.

Comparing the phase behavior at  $T = 343.15 \text{ K}$ ,  $p = 10 \text{ MPa}$  (Fig. 2-5) with the  $323.15 \text{ K}$  isotherm at the same pressure (Fig. 2-3), it is noticeable that the former presents a lower amount of  $\text{CO}_2$  dissolved in the liquid phase (V+L2 region), probably because of the temperature-driven increase in the  $\text{CO}_2$  vapor pressure. On the contrary, it can be observed that raising temperature from  $323.15$  to  $343.15 \text{ K}$  increases the solubility of fish oil in ethanol (L1+L2 region) from near  $0.075$  mass fraction up to  $0.35$  mass fraction, yet adding  $\text{CO}_2$  has a slight de-entraining effect at  $343.15 \text{ K}$  since the more  $\text{CO}_2$  is dissolved, the wider the tie-lines become.

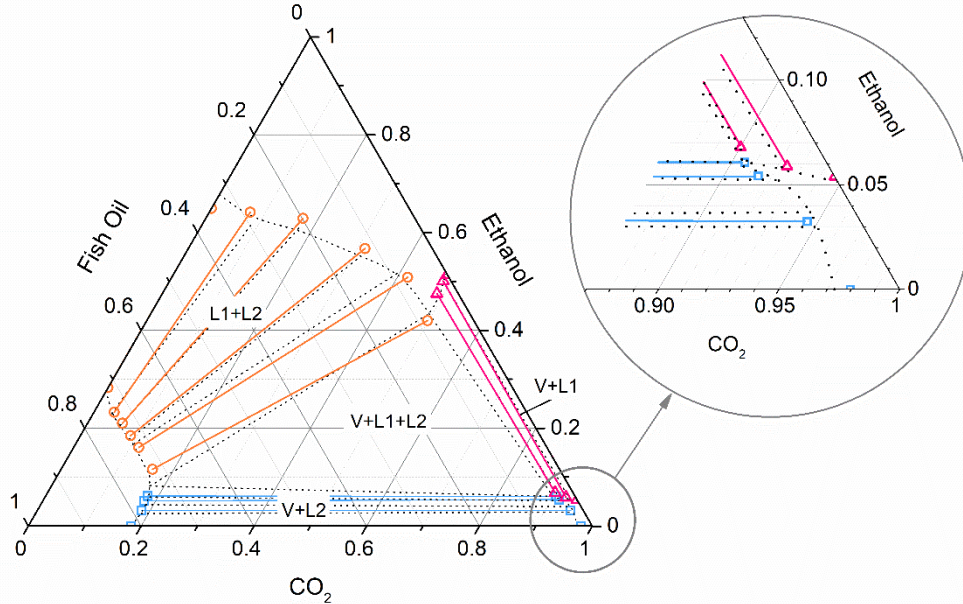


**Figure 2-5.** Phase diagram of the pseudo-ternary system CO<sub>2</sub> + ethanol + fish oil (T = 343.15 K, p = 10 MPa). -○-: experimental L1+L2 tie-lines; -△-: experimental V+L1 tie-lines; -□-: experimental V+L2 tie-lines; ·····: PR EoS vdW2 model.

### 3.2. Data correlation

In this work, fish oil has been treated as a pseudo-component, assuming that the different triacylglycerols present in the fish oil behave in a similar way, which has been previously verified [26]. Experimental phase equilibrium data of the pseudo-ternary mixture were correlated with the Peng-Robinson equation of state (PR EoS) in combination with the conventional van der Waals mixing rules with two adjustable parameters (vdW2).

PR EoS, was used as originally defined by Peng and Robinson [18]:

$$p = \frac{RT}{v-b} - \frac{a(T)}{v(v+b)+b(v-b)} \quad (2-1)$$



where the parameter  $a$  is related to the intermolecular attractive forces and  $b$  to the size of the molecules.

For a pure fluid, constant  $b$  takes the value:

$$b = 0.07780 \frac{RT_c}{P_c} \quad (2-2)$$

where  $T_c$  and  $p_c$  are the critical temperature and pressure of the pure fluid, respectively.

$a(T)$  is a function of temperature:

$$a(T) = a(T_c) \alpha(T) \quad (2-3)$$

where

$$a(T_c) = 0.45724 \frac{(RT_c)^2}{P_c} \quad (2-4)$$

and  $\alpha(T)$  depends on the temperature and acentric factor values of the compound. If  $T < T_c$ , the conventional expression from Peng-Robinson [18] is used:

$$\alpha(T) = \left(1 + \beta \left(1 - \sqrt{T/T_c}\right)\right)^2 \quad (2-5)$$

where  $\beta$  depends on the acentric factor  $\omega$  according to  $\beta = 0.37464 + 1.54226\omega - 0.26992\omega^2$  if  $\omega \leq 0.491$ ; and  $\beta = 0.379642 + 1.48503\omega - 0.164423\omega^2 + 0.016666\omega^3$  if  $\omega > 0.491$ .

Else, if  $T > T_c$ ,  $\alpha(T)$  is calculated as recommended in [29]:

$$\alpha(T) = \left(\exp\left(c \left(1 - (T/T_c)^d\right)\right)\right)^2 \quad (2-6)$$

with  $c$  and  $d$  defined as:

$$c = 1 - \frac{1}{d} \quad (2-7)$$

$$d = 1 + \frac{\beta}{2} \quad (2-8)$$

Binary mixture parameters are defined by the quadratic van der Waals mixing rules:

$$a = \sum_i \sum_j z_i z_j a_{ij} = \sum_i \sum_j z_i z_j (a_i a_j)^{0.5} (1 - k_{ij}) \quad (2-9)$$

$$b = \sum_i \sum_j z_i z_j b_{ij} = \sum_i \sum_j z_i z_j \frac{b_i + b_j}{2} (1 - l_{ij}) \quad (2-10)$$

here,  $z$  is either  $x$  or  $y$  and  $k_{ij}$ ,  $l_{ij}$  are adjustable binary interaction parameters. For a pure fluid,  $k_{ii} = l_{ii} = 0$ .

The molecular weight (MW), critical properties ( $T_C$  and  $p_C$ ) and acentric factor ( $\omega$ ) of the components of the system are listed in Table 2-6. Values for  $\text{CO}_2$  and ethanol were obtained from the literature [30] whereas group contribution methods were used to estimate the critical properties and the acentric factor of the pseudo-component fish oil [31,32].

**Table 2-6.** Molecular weight (MW), critical temperature ( $T_C$ ), critical pressure ( $p_C$ ), and acentric factor ( $\omega$ ) of the components of the pseudo-ternary system  $\text{CO}_2$  + ethanol + fish oil.

(pseudo-)component	MW (g/mol)	$T_C$ (K)	$p_C$ (MPa)	$\omega$	Ref.
$\text{CO}_2$	44.01	304.1	7.38	0.225	[30]
Ethanol	46.07	513.9	6.14	0.644	[30]
Fish Oil	902.03*	945.3 <sup>†</sup>	0.643 <sup>†</sup>	1.906 <sup>†</sup>	[31,32]

\*Calculated as a weighted average based on the reported fatty acid profile of the fish oil [26]

<sup>†</sup>Calculated by means of group contribution methods [31,32]



Binary interaction parameters  $k_{ij}$ ,  $l_{ij}$  in Eqs. 2-9 and 2-10 were estimated and fugacity coefficients  $\phi_i^V$  and  $\phi_i^L$  were calculated for each data set according to [18]. Simultaneously, the tie-line compositions that minimized the objective function (Eq. 2-11), satisfied the equilibrium isofugacity criterion ( $\phi_i^V y_i = \phi_i^L x_i$ ) for every component  $i$ , and the mass balances in each phase, were calculated by the Newton-Raphson method by fixing pressure, temperature, and composition of fish oil in the liquid phase.

A least-square objective function was defined as:

$$O.F. = \sum_{i=1}^{NC} \sum_{j=1}^{NP} (z_{ij}^{\text{exp}} - z_{ij}^{\text{calc}})^2 \quad (2-11)$$

where NC = number of components of the system, NP = number of experimental data points and  $z$  is either  $x$  or  $y$ . The superscripts exp and calc refer to experimental and calculated values.

Performance of PR EoS in combination with vdW2 mixing rules can be observed in Figs. 2-3, 2-4, and 2-5. The estimated binary interaction parameters for the PR EoS vdW2 model and the O.F. values (Eq. 2-11) are reported in Table 2-7. The CO<sub>2</sub> + ethanol interaction parameters ( $k_{12}$ ,  $l_{12}$ ) were estimated by correlating binary experimental data obtained in this work (Table 2-2) together with experimental data taken from literature at 323.15 K and 343.15 K [9,12] to the PR EoS vdW2 model, and were fixed in the calculations of the pseudo-ternary system. Experimental data points with deviations larger than 0.0001 from the calculations (according to Eq. 2-11 with  $j = 1$ ) were not considered. Results of this fitting are shown in Fig. 2-2.

The PR EoS vdW2 model was not fully capable of representing the different types of phase equilibrium (L1+L2, V+L1 and V+L2) when the same ethanol + fish oil interaction parameters ( $k_{23}$ ,  $l_{23}$ ) were applied in the correlation, thus different sets of binary interaction parameters were adopted for the ethanol + fish oil mixture in each of the 2-phase regions observed. This procedure is similar to the one followed by

Hernández *et al.*, who adopted different sets of parameters for the interaction between the triglyceride and the alcohol groups in the correlation of CO<sub>2</sub> + ethanol + sunflower oil phase equilibrium data with GC EoS [21]. The Peng-Robinson equation of state with Wong-Sandler mixing rules [33] (PR WS EoS) was also explored in order to overcome this deficiency. However, no significant improvement in the correlation of experimental data was achieved and therefore we chose the PR EoS vdW2 model due to its simplicity. As Hernández *et al.* [21] pointed out, it is likely that a more extensive set of binary ethanol + fish oil phase equilibrium data would be necessary.

For the V+L1 and V+L2 regions at T = 343.15 K and p = 10 MPa, only the first binary interaction parameter ( $k_{23}$ ) was included in the calculations, setting  $l_{23} = 0$ . As it can be seen in Fig. 2-5, this consideration leads to a good agreement between experimental and calculated data, possibly because of the low fractions of fish oil and ethanol in the V+L1 and V+L2 regions, respectively. As a general trend, the estimated values for the binary CO<sub>2</sub> + ethanol interaction parameters ( $k_{12}$  and  $l_{12}$ ) are similar to those reported in the literature [13,17,19,23]. In the case of the CO<sub>2</sub> + fish oil and ethanol + fish oil binaries, comparison is not an easy task, since interaction parameters for the PR EoS vdW2 model are scarcely reported in the literature, and parameters from different EoS and other mixing rules are not directly related. Geana and Steiner [17] also used the PR EoS vdW2 model to correlate the phase equilibria of the mixture CO<sub>2</sub> + ethanol + rapeseed oil in the temperature range 313 K-353 K and at pressures from 6 MPa to 12 MPa. The estimated interaction parameters for the CO<sub>2</sub> + oil and ethanol + oil binaries are of the same order as the ones obtained in this work. Differences could be attributed to the different fatty acid composition of the oils. Rapeseed oil is composed mainly by C18:1, C18:2 and C18:3 fatty acids [17], whereas fish oil mainly constituents are C16:0, C18:1 and C22:6 *n*-3 [26]. Similar values for these parameters can be also found in other available publications dealing with rapeseed oil [23] and other vegetable oils from castor and soybean [19].

**Table 2-7.** Estimated binary interaction parameters of the PR EoS vdW2 model for the pseudo-ternary system CO<sub>2</sub> + ethanol + fish oil at different temperature and pressure conditions in the different Liquid + Liquid (L1+L2) and Vapor + Liquid (V+L1, V+L2) 2-phase regions.

<b>T (K)</b>	<b>p (MPa)</b>	<b>type of phase eq.</b>	$k_{12}^a$	$k_{13}$	$k_{23}$	$l_{12}^a$	$l_{13}$	$l_{23}$	<b>O.F.</b>
323.15	10-30	L1+L2	0.0952	0.0695	-0.1026	-0.0248	0.0031	-0.0099	0.0631
		V+L2			0.0208			-0.1026	
343.15	10	L1+L2	0.0913	0.2268	-0.0821	-0.0103	-0.1005	-0.0118	0.0408
		V+L1			0.1400			- <sup>b</sup>	
		V+L2			-0.0355			- <sup>b</sup>	

<sup>a</sup> Estimated from binary experimental data obtained in this work and taken from literature [9,12].

<sup>b</sup> not considered ( $l_{23} = 0$ ).

### 3.3. Thermodynamic consistency

Thermodynamic consistency of experimental data has been tentatively tested by means of the method proposed by Valderrama and Faúndez [34] for high pressure gas-liquid equilibrium data including both phases, which in this work has been adapted to ternary mixtures at isobaric conditions. This method can be considered as a modeling procedure since a thermodynamic model that can accurately fit the experimental data must be first used to apply the consistency test [34]. The expression of the Gibbs-Duhem equation given in [34] at isothermal, isobaric conditions can be reduced to:

$$\sum_{i=1}^{NC} (z_i d \ln \phi_i) = 0 \quad (\text{isothermal, isobaric conditions } dT = 0, dp = 0) \quad (2-12)$$

which can lead to an expression similar to that given by Van Ness [35]:

$$\sum_{i=1}^{NC} d(z_i \ln \phi_i) - \sum_{i=1}^{NC} (\ln \phi_i dz_i) = 0 \quad (2-13)$$

By integrating both terms in the left side of Eq. 2-13 and designating the first by  $A_1$  and the second by  $A_2$ , experimental data can be considered as thermodynamically consistent when the criteria proposed by Wisniak *et al.* [36] is met (Eq. 2-16):

$$A_1 = \sum_{i=1}^{NC} \int d(z_i \ln \phi_i) \quad (2-14)$$

$$A_2 = \sum_{i=1}^{NC} \int (\ln \phi_i dz_i) \quad (2-15)$$

$$D = 100 \cdot \frac{\|A_1| - |A_2\|}{|A_1| + |A_2|} \leq 2 \quad (2-16)$$

Overall calculated deviations are  $D_{323.15 \text{ K}, 10 \text{ MPa}} = 0.457$ ,  $D_{323.15 \text{ K}, 30 \text{ MPa}} = 0.616$ , and  $D_{343.15 \text{ K}, 10 \text{ MPa}} = 0.104$ . Although area tests are usually not considered a sufficient condition of consistency, these positive results give an idea of the good quality of the phase equilibria data obtained in this work.



## Conclusion

Knowledge of the phase behavior of oils rich in  $n-3$  PUFAs with ethanol and  $\text{CO}_2$  rises as one of the fundamental aspects in the production of  $n-3$  PUFA concentrates at mild, non-oxidative conditions.

Experimental phase equilibrium data of the mixture  $\text{CO}_2$  + ethanol + fish oil is presented in this work at 3 different p-T combinations. Tie-lines of the pseudo-ternary diagram were obtained by means of an analytical isothermal method with recirculation of the vapor phase in a high-pressure variable-volume view cell. Results showed two 2-phase regions (L1+L2 and V+L2) at  $T = 323.15$  K for both pressures investigated (10 MPa and 30 MPa). An additional V+L1 and a 3-phase region (V+L1+L2) were observed at  $T = 343.15$  K and  $p = 10$  MPa.

Experimental data were correlated with the Peng-Robinson equation of state coupled with conventional two-parameter van der Waals mixing rules. The model successfully explained the experimental results, although different sets of binary ethanol + fish oil interaction parameters were required to adequately represent the different types of phase equilibrium. Experimental data can be considered as thermodynamically consistent according to the proposed area test.



## References

- [1] N. Rubio-Rodríguez, S. Beltrán, I. Jaime, S.M. de Diego, M.T. Sanz, J.R. Carballido, Production of omega-3 polyunsaturated fatty acid concentrates: A review, *Innovative Food Science and Emerging Technologies*. 11 (2010) 1–12.
- [2] R. Melgosa, M.T. Sanz, Á.G. Solaesa, E. de Paz, S. Beltrán, D.L. Lamas, Supercritical carbon dioxide as solvent in the lipase-catalyzed ethanolysis of fish oil: Kinetic study, *Journal of CO<sub>2</sub> Utilization*. 17 (2017) 170–179.
- [3] G.R. Akien, M. Poliakoff, A critical look at reactions in class I and II gas-expanded liquids using CO<sub>2</sub> and other gases, *Green Chemistry*. 11 (2009) 1083–1100.
- [4] N. Rubio-Rodríguez, S.M. De Diego, S. Beltrán, I. Jaime, M.T. Sanz, J. Rovira, Supercritical fluid extraction of fish oil from fish by-products: A comparison with other extraction methods, *Journal of Food Engineering*. 109 (2012) 238–248.
- [5] B.M. Bhosle, R. Subramanian, New approaches in deacidification of edible oils - A review, *Journal of Food Engineering*. 69 (2005) 481–494.
- [6] O.J. Catchpole, J.B. Grey, K.A. Noermark, Fractionation of fish oils using supercritical CO<sub>2</sub> and CO<sub>2</sub> + ethanol mixtures, *The Journal of Supercritical Fluids*. 19 (2000) 25–37.
- [7] A.P.A. Corrêa, C.A. Peixoto, L.A.G. Gonçalves, F.A. Cabral, Fractionation of fish oil with supercritical carbon dioxide, *Journal of Food Engineering*. 88 (2008) 381–387.
- [8] Á. Martín, S. Varona, A. Navarrete, M.J. Cocero, Encapsulation and co-precipitation processes with supercritical fluids: Applications with essential oils, *The Open Chemical Engineering Journal*. 5 (2010) 31–41.
- [9] J.S. Lim, Y.Y. Lee, H.S. Chun, Phase equilibria for carbon dioxide–ethanol–water system at elevated pressures, *The Journal of Supercritical Fluids*. 7 (1994) 219–230.
- [10] C.J. Chang, C.-Y. Day, C.-M. Ko, K.-L. Chiu, Densities and p-x-y diagrams for carbon dioxide dissolution in methanol, ethanol, and acetone mixtures, *Fluid Phase Equilibria*. 131 (1997) 243–258.

- [11] H. Chen, H. Chang, E.T.S. Huang, T. Huang, A new phase behavior apparatus for supercritical fluid extraction study, *Industrial and Engineering Chemistry Research*. 39 (2000) 4849–4852.
- [12] S.N. Joung, C.W. Yoo, H.Y. Shin, S.Y. Kim, K.P. Yoo, C.S. Lee, *et al.*, Measurements and correlation of high-pressure VLE of binary CO<sub>2</sub> – alcohol systems (methanol, ethanol, 2-methoxyethanol and 2-ethoxyethanol), *Fluid Phase Equilibria*. 185 (2001) 219–230.
- [13] Ž. Knez, M. Škerget, L. Ilič, C. Lütge, Vapor–liquid equilibrium of binary CO<sub>2</sub>–organic solvent systems (ethanol, tetrahydrofuran, ortho-xylene, meta-xylene, para-xylene), *The Journal of Supercritical Fluids*. 43 (2008) 383–389.
- [14] C. Secuianu, V. Feroiu, D. Gean, D. Geană, Phase behavior for carbon dioxide + ethanol system: Experimental measurements and modeling with a cubic equation of state, *The Journal of Supercritical Fluids*. 47 (2008) 109–116.
- [15] Ö. Güçlü-Üstündağ, F. Temelli, Solubility behavior of ternary systems of lipids in supercritical carbon dioxide, *The Journal of Supercritical Fluids*. 38 (2006) 275–288.
- [16] Ö. Güçlü-Üstündağ, F. Temelli, Solubility behavior of ternary systems of lipids, cosolvents and supercritical carbon dioxide and processing aspects, *The Journal of Supercritical Fluids*. 36 (2005) 1–15.
- [17] D. Geana, R. Steiner, Calculation of phase equilibrium in supercritical extraction of C54 triglyceride (rapeseed oil), *The Journal of Supercritical Fluids*. 8 (1995) 107–118.
- [18] D. Peng, D.B. Robinson, A new two-constant equation of state, *Industrial and Engineering Chemistry Fundamentals*. 15 (1976) 59–64.
- [19] P.M. Ndiaye, E. Franceschi, D. Oliveira, C. Dariva, F.W. Tavares, J.V. Oliveira, Phase behavior of soybean oil, castor oil and their fatty acid ethyl esters in carbon dioxide at high pressures, *The Journal of Supercritical Fluids*. 37 (2006) 29–37.
- [20] S.H. Huang, M. Radosz, Equation of state for small, large, polydisperse, and associating molecules: Extension to fluid mixtures, *Industrial and Engineering Chemistry Research*. 30 (1991) 1994–2005.



- [21] E.J. Hernández, G.D. Mabe, F.J. Señoráns, G. Reglero, T. Fornari, High-pressure phase equilibria of the pseudoternary mixture sunflower oil + ethanol + carbon dioxide, *Journal of Chemical and Engineering Data*. 53 (2008) 2632–2636.
- [22] S. Skjold-Jørgensen, Group contribution equation of state (GC-EOS): a predictive method for phase equilibrium computations over wide ranges of temperature and pressures up to 30 MPa, *Industrial and Engineering Chemistry Research*. 27 (1988) 110–118.
- [23] I. Dalmolin, A.A. Rigo, M.L. Corazza, P.M. Ndiaye, M.A.A. Meireles, E.A.C. Batista, J.V. Oliveira, Phase behaviour and thermodynamic modelling for the system (grape seed oil + carbon dioxide + ethanol) at high pressures, *Journal of Chemical Thermodynamics*. 68 (2014) 71–74.
- [24] R. Dohrn, G. Brunner, High-pressure fluid-phase equilibria: Experimental methods and systems investigated (1988-1993), *Fluid Phase Equilibria*. 106 (1995) 213–282.
- [25] Official Methods and Recommended Practices of the American Oil Chemists' Society, American Oil Chemists' Society, Champaign, IL (2011).
- [26] S.L. Bucio, A.G. Solaesa, M.T. Sanz, S. Beltrán, R. Melgosa, Liquid-liquid equilibrium for ethanolysis systems of fish oil, *Journal of Chemical Engineering Data*. 58 (2013) 3118–3124.
- [27] Á.G. Solaesa, M.T. Sanz, M. Falkeborg, S. Beltrán, Z. Guo, Production and concentration of monoacylglycerols rich in omega-3 polyunsaturated fatty acids by enzymatic glycerolysis and molecular distillation, *Food Chemistry*. 190 (2016) 960–967.
- [28] Official Methods of Analysis of the Association of Official Analytical Chemists. AOAC Official Method 965.33. Peroxide Value of Oils and Fats, AOAC International, Washington, DC (2002).
- [29] Y. Medina-Gonzalez, T. Tassaing, S. Camy, J.-S. Condoret, Phase equilibrium of the CO<sub>2</sub>/glycerol system: Experimental data by in situ FT-IR spectroscopy and thermodynamic modeling, *The Journal of Supercritical Fluids*. 73 (2013) 97–107.
- [30] B.E. Poling, M. Prausnitz, J.P. O'Connell, *The Properties of Gases and Liquids*, fifth ed., McGraw-Hill, New York, 2001.

- [31] L. Constantinou, R. Gani, J.P. O'Connell, Estimation of the acentric factor and the liquid molar volume at 298 K using a new group contribution method, *Fluid Phase Equilibria*. 103 (1995) 11–22.
- [32] L.P. Cunico, A.S. Hukkerikar, R. Ceriani, B. Sarup, R. Gani, Molecular structure-based methods of property prediction in application to lipids: A review and refinement, *Fluid Phase Equilibria*. 357 (2013) 2–18.
- [33] D.S.H. Wong, S.I. Sandler, A theoretically correct mixing rule for cubic equations of state, *American Institute of Chemical Engineers Journal*. 38 (1992) 671–680.
- [34] J.O. Valderrama, C.A. Faúndez, Thermodynamic consistency test of high pressure gas-liquid equilibrium data including both phases, *Thermochimica Acta*. 499 (2010) 85–90.
- [35] H.C. Van Ness, Exact forms of the unrestricted Gibbs-Duhem equation, *Chemical Engineering Science*. 10 (1959) 225–228.
- [36] J. Wisniak, J. Ortega, L. Fernández, A fresh look at the thermodynamic consistency of vapour-liquid equilibria data, *Journal of Chemical Thermodynamics*. 105 (2017) 385–395.

## Chapter 3

# Supercritical carbon dioxide as solvent in the lipase-catalyzed ethanolysis of fish oil: kinetic study

#omega-3 #lipase #ethanolysis

#supercritical carbon dioxide

**Adapted from:**

R. Melgosa, M.T. Sanz, Á.G. Solaesa, E. de Paz, S. Beltrán, D.L. Lamas, Supercritical carbon dioxide as solvent in the lipase-catalysed ethanolysis of fish oil: kinetic study, *Journal of CO<sub>2</sub> utilization*. 17 (2017) 170–179.

DOI: <https://doi.org/10.1016/j.jcou.2016.11.011>

## Table of contents

Tables.....	163
Figures .....	165
Abstract.....	167
Resumen.....	169
1. Introduction.....	171
2. Material and methods.....	173
2.1. Materials .....	173
2.2. Ethanolysis of fish oil in SC-CO <sub>2</sub> .....	174
2.3. Determination of the composition .....	175
2.4. Measurement of lipid oxidation .....	176
2.5. Kinetic model.....	177
3. Results and discussion.....	179
3.1. Effect of the initial substrate molar ratio .....	182
3.2. Pressure effect .....	188
3.3. Temperature effect .....	193
3.4. Comparison of supercritical carbon dioxide, <i>tert</i> -pentanol and solvent-free media .....	198
3.5. Lipid oxidation.....	199
Conclusion .....	203
References.....	205

## Tables

**Table 3-1.** Experimental conditions (initial molar ratio, MR; pressure, p; temperature, T) for the ethanolysis of fish oil by Lipozyme RM IM in SC-CO<sub>2</sub>. Initial reaction rate ( $r_0$ ) and yield of fatty acid ethyl esters at equilibrium conditions (Eq. FAEE yield) for each experience..... 181

**Table 3-2.** Effective forward ( $k_i^1$ ) and reverse ( $k_{-i}^1$ ) reaction rate constants, equilibrium constants ( $K_i$ ) and objective function (O.F.) values of the proposed kinetic model for the ethanolysis of fish oil by Lipozyme RM IM in SC-CO<sub>2</sub> at different initial molar ratio of substrates (MR). Reactions were performed at p = 10 MPa, T = 323.15 K, enzyme loading 5 % wt. of substrates. .... 187

**Table 3-3.** Values for the forward ( $k_i^0$ ) and reverse ( $k_{-i}^0$ ) pre-exponential constants, apparent activation volume of each forward ( $\Delta V_i^*$ ) and reverse ( $\Delta V_{-i}^*$ ) reaction step and values of the objective function (O.F.) of the proposed kinetic model for the ethanolysis of fish oil by Lipozyme RM IM in SC-CO<sub>2</sub> at 7.5 MPa and in the range 9-30 MPa. Reactions were performed at MR = 6:1, T = 323.15 K, enzyme loading 5 % wt. of substrates..... 192

**Table 3-4.** Values for the forward ( $k_i^0$ ) and reverse ( $k_{-i}^0$ ) pre-exponential constants, activation energy of each forward ( $E_i^a$ ) and reverse ( $E_{-i}^a$ ) reaction step and values of the objective function (O.F.) of the proposed kinetic model for the ethanolysis of fish oil by Lipozyme RM IM in SC-CO<sub>2</sub> in the range 323.15-343.15 K and at 353.15 K. Reactions were performed at MR = 6:1, p = 10 MPa, enzyme loading 5 % wt. of substrates..... 197

## Figures

- Figure 3-1.** Schematic diagram of the high-pressure apparatus used for the ethanolysis reactions in SC-CO<sub>2</sub>. 1: CO<sub>2</sub> reservoir; 2: syringe pump; 3: cryostat; 4: rupture disk; 5: high pressure batch stirred tank reactor; 6: thermostatic water bath; 7: magnetic stirrer; 8: sampling device. .... 174
- Figure 3-2.** Components profile in the ethanolysis of fish oil catalyzed by Lipozyme RM IM in SC-CO<sub>2</sub> medium. MR = 38:1, p = 10 MPa, T = 323.15 K and enzyme loading 5 % wt. of substrates. FAEE: fatty acid ethyl esters, TAG: triacylglycerides, DAG: diacylglycerides, MAG: monoacylglycerides, GLY: glycerol. Lines represent the fitting of the proposed kinetic model to the experimental data. .... 180
- Figure 3-3.** Effect of initial molar ratio of substrates (MR) on the FAEE yield in the ethanolysis of fish oil catalyzed by Lipozyme RM IM in SC-CO<sub>2</sub> medium. Experimental conditions: p = 10 MPa, T = 323.15 K and enzyme loading 5 % wt. of substrates. Lines represent the fitting of the proposed kinetic model to the experimental data. .... 183
- Figure 3-4.** Visual observation of the initial reaction mixture (MR = 6:1) at T = 323.15 K; left: 0.1 MPa, right: 10 MPa. .... 184
- Figure 3-5.** Equilibrium FAEE yield (%) vs. MR (ethanol :oil) in the ethanolysis of fish oil catalyzed by Lipozyme RM IM in SC-CO<sub>2</sub> medium. Solid line is from the non-linear regression of the experimental data (Eq. 3-9). **Inset:** Logarithmic relationship between initial reaction rate and MR. Dashed line is from the linear regression of the experimental data. Exp. conditions: p = 10 MPa, T = 323.15 K, enzyme loading 5 % wt. of substrates. .... 185
- Figure 3-6.** Effect of operating pressure (p) on the ethanolysis of fish oil catalyzed by Lipozyme RM IM in SC-CO<sub>2</sub> medium. Experimental conditions: MR = 6:1, T = 323.15 K and enzyme loading 5 % wt. of substrates. Lines represent the fitting of the proposed kinetic model to the experimental data. .... 188

## Figures (*continued*)

- Figure 3-7.** Equilibrium FAEE yield (%) ( $\Delta$ ) and  $\ln$  (initial reaction rate) ( $\circ$ ) vs. reduced operating pressure ( $p_r = p/p_c$ ) in the ethanolysis of fish oil catalyzed by Lipozyme RM IM in SC-CO<sub>2</sub> medium. Solid line is from the non-linear regression of the experimental data (Eq. 3-9). Dashed line is from the linear regression of the experimental data. Exp. conditions: MR = 6:1, T = 323.15 K, enzyme loading 5 % wt. of substrates. ....189
- Figure 3-8.** Effect of operating temperature (T) on the ethanolysis of fish oil catalyzed by Lipozyme RM IM in SC-CO<sub>2</sub> medium. Exp. conditions MR = 6:1, p = 10 MPa and enzyme loading 10 % wt. of substrates. Lines represent the fitting of the proposed kinetic model to the experimental data. ....194
- Figure 3-9.** Arrhenius plot for the ethanolysis of fish oil catalyzed by Lipozyme RM IM in SC-CO<sub>2</sub> medium. Lines are from the linear regression of the experimental data. Exp. Conditions: MR = 6:1, p = 10 MPa and enzyme loading 5 % wt. of substrates. ....195
- Figure 3-10.** Effect of solvent media on the ethanolysis of fish oil catalyzed by Lipozyme RM IM. Experimental conditions: MR = 6:1, T = 323.15 K and enzyme loading 5 % wt. of substrates (SC-CO<sub>2</sub> at 10 and 30 MPa, SF: solvent-free media and 20 % wt. of TP). ....198
- Figure 3-11.** Effect of the ethanolysis of fish oil catalyzed by Lipozyme RM IM on the acid value (AV) in different reaction media: SC-CO<sub>2</sub> at different operating pressure, SF (solvent-free media) and 20 % wt. of TP. Dashed line represents the recommended limit set by the FDA [39]. ....200
- Figure 3-12.** Effect of the ethanolysis of fish oil catalyzed by Lipozyme RM IM on the peroxide value (PV) in different reaction media: SC-CO<sub>2</sub> at different operating pressure, SF (solvent-free media) and 20 % wt. of TP. Dashed line represents the recommended limit set by the FDA [39]. ....201

## Abstract

In this chapter, supercritical carbon dioxide (SC-CO<sub>2</sub>) has been used as green solvent in the lipase-catalyzed ethanolysis of fish oil by Lipozyme RM IM at mild, non-oxidative conditions and with no solvent residues. The effect of experimental conditions, initial substrate ethanol/oil molar ratio (2-38), pressure (7.5-30 MPa), and temperature (323.15-353.15 K) on equilibrium conversion, reaction rate and oxidative status of the products has been studied.

No ethanol inhibition has been observed at high concentrations of ethanol, when putting in contact first the fish oil with the enzyme avoiding direct contact between the biocatalyst and ethanol. Operating pressure affected positively the reaction performance in the range investigated, which was verified by visual observation of the phase behavior of the initial reaction mixture showing an “expanded liquid phase” that might have helped to enhance reaction rate, and a gas phase. Raising temperature accelerated the reaction up to a limit (343.15 K), observing higher enzyme thermal stability than in other reaction media (313.15 K). However, lipid oxidation increases with temperature. Yields up to  $86 \pm 1$  % have been found at MR = 6:1, 30 MPa and 323.15 K.

Kinetic data have been correlated by using a mathematical model based on the elementary reactions of the 3-step transesterification. Kinetic rate constants, apparent activation volumes and energies are reported for the first time for a lipase-catalyzed ethanolysis reaction in SC-CO<sub>2</sub>.

## Resumen

En el presente capítulo se ha utilizado dióxido de carbono supercrítico (CO<sub>2</sub>-SC) como disolvente verde en la etanolisis de aceite de pescado catalizada por Lipozyme RM IM en condiciones suaves y no oxidativas. Se ha estudiado el efecto de las variables experimentales: relación inicial de sustratos etanol:aceite de pescado (2:1-38:1), presión (7.5-30 MPa) y temperatura de reacción (323.15-353.15 K) sobre la conversión de equilibrio, la velocidad inicial de reacción y el estado oxidativo de los productos de reacción.

La mezcla inicial de catalizador y aceite de pescado impide el contacto directo entre enzima y etanol, consiguiendo así evitar la inhibición del catalizador por efecto de altas concentraciones de etanol. En el rango investigado, la presión afecta positivamente al desarrollo de la reacción. Esto se ha verificado mediante la observación visual del equilibrio entre fases de la mezcla inicial de sustratos, en la que una “fase líquida expandida” posiblemente aumente la velocidad de reacción. El aumento de temperatura acelera la reacción hasta un máximo (343.15 K) a partir del cual comienza a observarse desactivación. En comparación con otros medios de reacción, el catalizador muestra mayor estabilidad térmica en CO<sub>2</sub>-SC. Sin embargo, la oxidación de los productos de reacción también aumenta con la temperatura. La máxima conversión observada ha sido de  $86 \pm 1$  % a MR = 6:1, 30 MPa y 323.15 K.

Los datos cinéticos se han correlacionado mediante un modelo matemático basado en los 3 pasos de la reacción de trans-esterificación de triglicéridos con etanol y sus reacciones elementales, obteniéndose por primera vez las constantes cinéticas y los volúmenes y energías de activación aparentes de una reacción de etanolisis catalizada por lipasas en CO<sub>2</sub>-SC.

## 1. Introduction

Fish oil is a natural source of omega-3 polyunsaturated fatty acids ( $n-3$  PUFAs) such as eicosapentaenoic acid (EPA, 20:5  $n-3$ ) and docosahexaenoic acid (DHA, 22:6  $n-3$ ). Health benefits of these compounds have been well established in the literature [1]. As a consequence, functional foods enriched with  $n-3$  PUFAs have been the type of functional food products whose production in Europe and USA has increased the most in the last years [2]. Nevertheless, in a recently published review it has been found that the excess of oxidation in commercial  $n-3$  PUFA supplements affects between 11-62% of the analyzed supplements [3]. Traditional methods for production of  $n-3$  PUFA concentrates from their natural sources have been recently reviewed, and a number of novel techniques have been proposed [2]. Among the latest, enzymatic modification of oils rich in  $n-3$  PUFAs in supercritical fluids (SCFs) rises as an alternative for obtaining less oxidized fish oil derivatives, compared to conventional methods.

Several studies have been carried out on enzymatic reactions in different SCF media. A comprehensive review on this subject was carried out by Knez [4], with references on different enzymatic reactions in dense gases, such as oxidation, hydrolysis, esterification and transesterification. Supercritical carbon dioxide (SC-CO<sub>2</sub>) is probably the most used SCF due to its benefits (non-toxic, non-flammable, readily available at high purities and low costs, and relatively mild critical conditions, easily separated from the reaction products by simple depressurization) that are appealing when choosing environmental replacement for organic solvents. Besides, by varying the temperature and pressure it allows the fractionation of the products.

Some previous studies of enzymatic ethanolysis of natural lipid sources in SC-CO<sub>2</sub> have been reported in the literature. Different immobilized lipases have been used as biocatalyst, such as the non-specific lipase Novozyme 435 from *Candida antarctica* [5-8] and the *sn*-1,3-regiospecific lipase Lipozyme TL-IM from

*Thermomuces lanuginosa* [9, 10]. In this work, Lipozyme RM IM from *Rhizomucor miehei*, a *sn*-1,3 specific lipase, has been used as biocatalyst. Ethanolysis of palm kernel oil in SC-CO<sub>2</sub> by the homologous Lipozyme IM was studied by Oliveira and Oliveira [7]. Although the biocatalyst was reported to be *sn*-1,3-specific, it did not behave as a regioselective lipase and considerable amounts of glycerol were found in the reaction products. Furthermore, the reaction conversion was followed in terms of glycerol production, not taking into account the reaction intermediates (di- and monoacylglycerides). Kondo *et al.* [11] carried out the synthesis of fatty acid ethyl esters (FAEEs) from SC-CO<sub>2</sub>-extracted canola oil in a continuous supercritical extraction-reaction (SFE-SFR) system by using Lipozyme RM IM as biocatalyst, observing a decrease in the FAEE production at high ethanol concentration.

Enzymatic reactions in SC-CO<sub>2</sub> can be affected by operating pressure in different ways. According to transition state theory and standard thermodynamics, operating pressure can affect the reaction rate constants. Besides, density-related changes in the physical parameters of SC-CO<sub>2</sub> may indirectly affect the enzyme catalytic activity, and thus the reaction performance [12]. Loss *et al.* [13] have recently reviewed different applications of supercritical fluids as alternative solvent for biocatalysis processes, concluding that there seems to be no “rule of thumb” for predicting the effect of pressure on enzyme activity in SC-CO<sub>2</sub>.

Direct effects of pressure on enzyme residual activity and stability of Lipozyme RM IM have been previously investigated, finding that almost no changes occurred in the range between 10 and 25 MPa at 323.15 K [14]. Different results have been found in the literature regarding the effect of pressure on Lipozyme RM IM-catalyzed reactions in SC-CO<sub>2</sub>. For instance, in the study of esterification of stearic acid with ethanol catalyzed by Lipozyme IM in SC-CO<sub>2</sub> in the range from 6 to 20 MPa at 323.15 K, Nakaya *et al.* [15] found an increase in esterification rate with an increase in pressure, but a maximum was found in the hydrolysis rate of the corresponding ethyl stearate. Laudani *et al.* [16] performed a detailed kinetic and thermodynamic study of the esterification of oleic acid with 1-octanol catalyzed by

Lipozyme RM IM in dense carbon dioxide. These authors reported a positive effect of increasing pressure from 8 to 10 MPa at 323.15 K. Further increase in pressure up to 30 MPa led to a decrease in reaction conversion from 84 % to 77 %. Therefore, the effect of pressure on enzyme activity in CO<sub>2</sub> is very dependent not only on the specific enzyme, but also on the reaction studied and the phase behavior of the system at different pressure and temperature conditions.

In this chapter, the effect of the initial molar ratio of substrates, pressure, and temperature on equilibrium yield and reaction rate has been studied for the ethanolysis of fish oil in SC-CO<sub>2</sub>, covering a wider range than previous works reported in the literature. Additionally, oxidation parameters of the refined fish oil and the reaction products obtained from the reactions in SC-CO<sub>2</sub> have been determined and compared with those obtained from reactions performed in conventional organic solvents and in solvent-free media at atmospheric pressure. This way, optimal reaction conditions considering kinetic aspects and quality of the products can be determined. Experimental data have been satisfactorily correlated by a simple semi-empirical kinetic model based on the elementary reactions that may occur in this system and taking into account reaction intermediates.

## 2. Material and methods

### 2.1. Materials

Lipozyme RM IM, a lipase from *Rhizomucor miehei* immobilized on a macroporous resin, was purchased from Novozymes A/S (Denmark). Refined fish oil was kindly provided by AFAMSA S.A. (Spain) being a mixture of tuna (*Thunnus* sp.) and sardine (*Sardina pilchardus*) oil. Fatty acid profile of the fish oil has been previously reported with a 24 % mol of docosahexaenoic acid (DHA) and 7 % mol of eicosapentaenoic acid (EPA) [17]. Absolute ethanol (99.9 %) was purchased from Merck KGaA. Carbon dioxide (99.9%) was supplied by Air Liquide S.A. (Spain). All other chemicals used in different analyses were of analytical or HPLC grade.

## 2.2. Ethanolysis of fish oil in SC-CO<sub>2</sub>

The ethanolysis reaction has been performed in a high-pressure batch stirred tank reactor (HP-BSTR) made of stainless steel (SS-316) with an internal volume of 100 mL. A schematic diagram of the high-pressure apparatus is shown in Fig. 3-1.

In a typical experiment, a weighed amount of enzyme (5.0 % wt. of substrates) was added into the reactor together with a known amount of fish oil. Subsequently, ethanol was added according to the established initial substrate molar ratio. This procedure was adopted in order to avoid direct contact of ethanol with the enzyme, which may cause inactivation of the catalyst. The reactor was then closed, connected to the pressure circuit and placed in a thermostatic water bath at the desired operating temperature. Subsequently, SC-CO<sub>2</sub> was fed into the reactor by means of a high-pressure pump (ISCO 260 D) up to the desired pressure, which was maintained by a digital pressure controller. A Bourdon pressure gauge also provided a secondary lecture. Once the established conditions have been reached, magnetic stirring was connected, and the reaction was initiated.

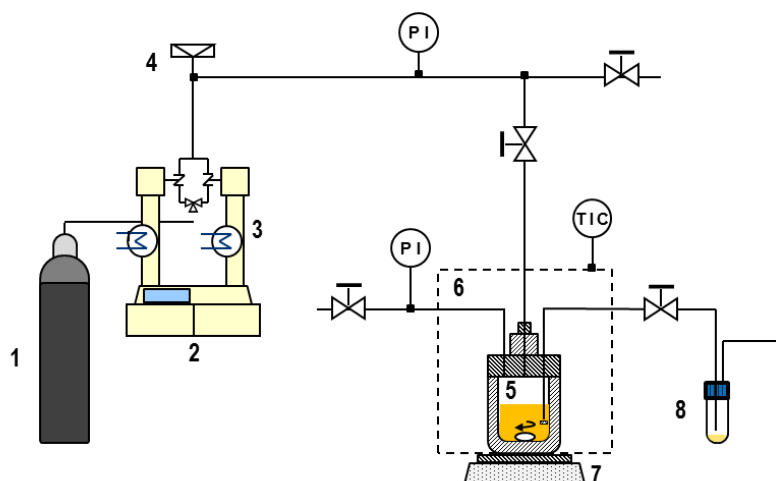


**Figure 3-1.** Schematic diagram of the high-pressure apparatus used for the ethanolysis reactions in SC-CO<sub>2</sub>. 1: CO<sub>2</sub> reservoir; 2: syringe pump; 3: cryostat; 4: rupture disk; 5: high pressure batch stirred tank reactor; 6: thermostatic water bath; 7: magnetic stirrer; 8: sampling device.

Operating temperature and pressure have been varied in the range between 323.15-353.15 K and 7.5-30 MPa, respectively. The effect of the initial substrate molar ratio has been studied in the range from 2:1 to 38:1 (ethanol:fish oil). Samples were taken periodically during 24 h through a siphoned capillary equipped with a microfilter made of sintered steel, which prevented the withdrawal of the enzyme from the reaction mixture. Samples were collected in glass screw-top vials immersed in a cold trap and stored at -18 °C up to analysis. Pressure drops up to 0.5 MPa were observed during the withdrawal of the samples, which were compensated by feeding fresh SC-CO<sub>2</sub> at the desired pressure into the reactor. According to the low mass of the samples (*ca.* 0.1 g) compared with the initial loading of the HP-BSTR, disturbances of the batch process were considered negligible.

### 2.3. Determination of the composition

Neutral lipid profile of the samples (fatty acid ethyl esters, FAEs; Monoacylglycerides, MAGs; diacylglycerides, DAGs; and unreacted triacylglycerides, TAGs) has been determined by normal phase HPLC. Chromatographic equipment, method and calibration procedure have been previously described in detail [18].

Chromatographic analysis of glycerol (GLY) content in the reaction samples was performed using High-Temperature Gas Chromatography (HTGC). Method and calibration procedure have been previously described [17]. GLY content in the reaction samples was also theoretically calculated by a balance of the glycerol backbone, as proposed by Sovová *et al.* for the enzymatic hydrolysis of blackcurrant oil in SC-CO<sub>2</sub> [19].

A modified expression of that from Sovová *et al.* [19] for an ethanolysis reaction gives:

$$n_{\text{GLY}}^t = (n_{\text{FAEE}} - n_{\text{DAG}} - 2 \cdot n_{\text{MAG}}) / 3 \quad (3-1)$$

where,  $n_{\text{FAEE}}$ ,  $n_{\text{DAG}}$ , and  $n_{\text{MAG}}$  are the FAEE, DAG and MAG mole content in the reaction samples, respectively; and  $n_{\text{GLY}}^t$  is the theoretical mole content of GLY. Theoretical calculation of GLY deviated less than 10% from experimental data, thus HT-GC determination of GLY and neutral lipid profile analysis were satisfactorily related.

Unreacted EtOH was theoretically calculated considering the reaction stoichiometry, in which the production of 1 mol of FAEE consumes 1 mol of EtOH, giving:

$$n_{\text{EtOH}}^t = n_{\text{EtOH}}^0 - n_{\text{FAEE}} \quad (3-2)$$

where  $n_{\text{EtOH}}^t$  is the theoretical remaining ethanol (mole content) and  $n_{\text{EtOH}}^0$  is the initial mole content of ethanol.

#### 2.4. Measurement of lipid oxidation

Determination of the peroxide value (PV), p-anisidine value (p-AnV), and acid value (AV) of the samples before and after the kinetic experiments have been performed in order to evaluate potential lipid oxidation processes during the ethanolysis reactions. The peroxide value, PV, measures the concentration of peroxides and hydroperoxides formed in the initial stages of lipid oxidation (primary oxidation). The p-anisidine value (p-AnV) is an estimation of the concentration of secondary oxidation products. Determination of the acid value (AV) has been also performed as an estimation of the hydrolytic rancidity of the fish oil and the reaction samples. All determinations were performed according to standard methods [20-22]. In the case of reaction samples, lipid fractions were obtained by means of evaporation of unreacted ethanol in a vacuum rotary evaporator (Heidolph).

## 2.5. Kinetic model

Lipase-catalyzed ethanolysis of triacylglycerides (TAG) of fish oil can be considered as a 3-step transesterification. At each step, one molecule of FAEE and a glyceride containing one fewer ester bond are obtained. Glycerides involved in the reaction are di- and monoacylglycerides (DAG and MAG), and glycerol (GLY) as the last product. Following the proposed model, the reaction takes place through the following steps (Eqs. 3-1 to 3-3):

1. Conversion of tri- to diacylglycerides:



2. Conversion of di- to monoacylglycerides:



3. Conversion of monoacylglycerides to glycerol:



To correlate the experimental kinetic data, a semi-empirical model based on the mass balance equations of all the species in the reaction system has been employed. Although the *sn*-1,3-specific catalyst cannot deacylate the *sn*-2 position of the acylglyceride, step 3 (Eq. 3-5) should be considered because isomerization of 2-MAG to 1(3)-MAG (acyl-migration) may occur. As the regioisomers 1,2- and 1,3-DAG; and 1(3)- and 2-MAG could not be distinguished with the applied analytical procedure, no difference was made between them in the model. Hydrolysis reaction has not been taken into account since no free fatty acids were detected (<0.1%) in the NP-HPLC analysis.

The kinetic equations involved in the ethanolysis system are the following:

$$d(n_{TAG}/n_{total})/dt = -k_1' \cdot x_{TAG} \cdot x_{EtOH} + k_{-1}' \cdot x_{DAG} \cdot x_{FAEE} \quad (3-6.1)$$

$$d(n_{DAG}/n_{total})/dt = k_1' \cdot x_{TAG} \cdot x_{EtOH} - k_{-1}' \cdot x_{DAG} \cdot x_{FAEE} - k_2' \cdot x_{DAG} \cdot x_{EtOH} + k_{-2}' \cdot x_{MAG} \cdot x_{FAEE} \quad (3-6.2)$$

$$d(n_{MAG}/n_{total})/dt = k_2' \cdot x_{DAG} \cdot x_{EtOH} - k_{-2}' \cdot x_{MAG} \cdot x_{FAEE} - k_3' \cdot x_{MAG} \cdot x_{EtOH} + k_{-3}' \cdot x_{GLY} \cdot x_{FAEE} \quad (3-6.3)$$

$$d(n_{GLY}/n_{total})/dt = k_3' \cdot x_{MAG} \cdot x_{EtOH} - k_{-3}' \cdot x_{GLY} \cdot x_{FAEE} \quad (3-6.4)$$

$$d(n_{FAEE}/n_{total})/dt = k_1' \cdot x_{TAG} \cdot x_{EtOH} - k_{-1}' \cdot x_{DAG} \cdot x_{FAEE} + k_2' \cdot x_{DAG} \cdot x_{EtOH} - k_{-2}' \cdot x_{MAG} \cdot x_{FAEE} + k_3' \cdot x_{MAG} \cdot x_{EtOH} - k_{-3}' \cdot x_{GLY} \cdot x_{FAEE} \quad (3-6.5)$$

$$d(n_{EtOH}/n_{total})/dt = -k_1' \cdot x_{TAG} \cdot x_{EtOH} + k_{-1}' \cdot x_{DAG} \cdot x_{FAEE} - k_2' \cdot x_{DAG} \cdot x_{EtOH} + k_{-2}' \cdot x_{MAG} \cdot x_{FAEE} - k_3' \cdot x_{MAG} \cdot x_{EtOH} + k_{-3}' \cdot x_{GLY} \cdot x_{FAEE} \quad (3-6.6)$$

$$n_{total} = n_{TAG} + n_{DAG} + n_{MAG} + n_{FAEE} + n_{GLY} + n_{EtOH} \quad (3-6.7)$$

The three reversible reactions have been considered as elementary reactions; therefore forward and reverse reactions are expected to follow a second order kinetic, being  $k_1'$ ,  $k_2'$  and  $k_3'$  the forward rate constant and  $k_{-1}'$ ,  $k_{-2}'$  and  $k_{-3}'$  the reverse rate constants for the lipase catalyzed reaction. Concentrations of reaction products are expressed as mole fraction. The effective forward and reverse rate constants,  $k_i'$  and  $k_{-i}'$ , have been simultaneously estimated except when varying the molar ratio, MR.

The differential equations were solved numerically with a fourth-order Runge-Kutta method and by reducing the experimental kinetic data minimizing the following objective function (O.F.):

$$\text{O.F.} = \left( \sum_{\text{all samples}} \sum_{i=1}^n (x_i^{\text{exp}} - x_i^{\text{calc}}) \right)^2 / n_{\text{samples}} \cdot 100 \quad (3-7)$$

by using the Simplex-Nelder-Mead method. The subscript  $i$  refers to the different components in the ethanolysis system. The subscripts “exp” and “calc” refer to the experimental and calculated mole fraction of the different components for each experimental kinetic data ( $n_{\text{samples}}$ ).

### 3. Results and discussion

In this section, the effect of various operating variables, such as pressure ( $p$ ), temperature ( $T$ ) and initial molar ratio of substrates ( $MR$ ) on the performance of the enzymatic ethanolysis of fish oil in  $SC\text{-CO}_2$  is presented. Besides, an evaluation of the oxidative and hydrolytic rancidity of the fish oil used as a substrate and of the reaction products obtained in different reaction media ( $SC\text{-CO}_2$ , *tert*-pentanol and solvent-free) is performed.

Fig. 3-2 shows the time course of the ethanolysis reaction of tuna and sardine oil by Lipozyme RM IM in  $SC\text{-CO}_2$  at  $MR = 38:1$ , 10 MPa and 323.15 K. From this figure, it can be seen that production of FAEE is very rapid at the beginning of the reaction and then it becomes slower, reaching a plateau at the equilibrium conversion.

Lipozyme RM IM is reported to act preferentially towards the *sn*-1,3 positions of the glycerol backbone, thus the reaction was supposed to stop at step 2 (Eq. 3-4) with accumulation of MAG and an almost negligible GLY production. However, Fig. 3-2 shows low concentration of MAG and a high production of GLY. A similar trend was observed in all the kinetic experiments. An explanation may be provided

considering the acyl-migration phenomenon, which may have been enhanced by the catalyst support, Duolite A568, which is a macroporous hydrophilic weak base anion resin, and it has been reported to promote acyl-migration [23]. Reaction time, temperature, solvents and water content in the medium may also play an important role in the acyl-migration phenomenon [24].

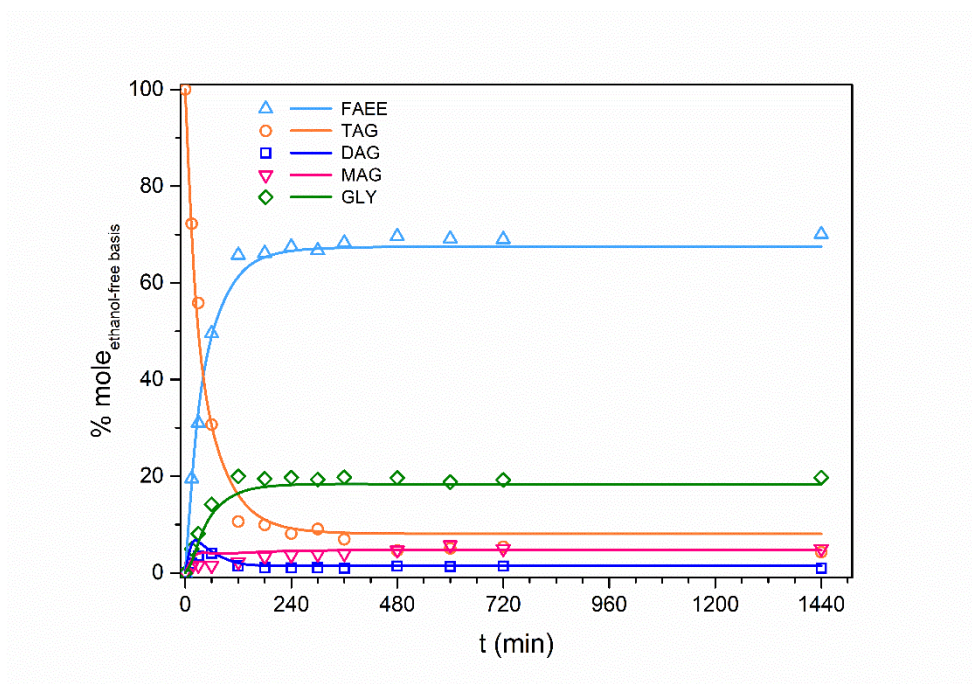


**Figure 3-2.** Components profile in the ethanolysis of fish oil catalyzed by Lipozyme RM IM in SC-CO<sub>2</sub> medium. MR = 38:1, p = 10 MPa, T = 323.15 K and enzyme loading 5 % wt. of substrates. FAEE: fatty acid ethyl esters, TAG: triacylglycerides, DAG: diacylglycerides, MAG: monoacylglycerides, GLY: glycerol. Lines represent the fitting of the proposed kinetic model to the experimental data.

In order to consider the presence of DAG and MAG intermediates in the reaction medium as well as the unreacted TAG, FAEE yield has been calculated as a fraction of all the lipid compounds detected:

$$\text{FAEE yield (\%)} = x_{\text{FAEE}} / (x_{\text{TAG}} + x_{\text{DAG}} + x_{\text{MAG}} + x_{\text{FAEE}}) \cdot 100 \quad (3-8)$$



Table 3-1 summarizes the results obtained in this work in terms of FAEE yield at equilibrium conditions and initial reaction rate in the experimental range investigated. Initial reaction rate, expressed as production of FAEE per mass of catalyst and reaction time, was calculated by linear regression of experimental data in the early stages of the kinetics, when a constant reaction rate can be observed.

**Table 3-1.** Experimental conditions (initial molar ratio, MR; pressure, p; temperature, T) for the ethanolysis of fish oil by Lipozyme RM IM in SC-CO<sub>2</sub>. Initial reaction rate ( $r_0$ ) and yield of fatty acid ethyl esters at equilibrium conditions (Eq. FAEE yield) for each experience.

Exp.	MR (ethanol:oil)	T (K)	p (MPa)	$r_0$ ( $\mu\text{mol}\cdot\text{g}_{\text{enz}}^{-1}\cdot\text{min}^{-1}$ )	Eq. FAEE yield* (%)
1	2:1	323.15	10	$34 \pm 2$	$57 \pm 3$
2	4:1	323.15	10	$43 \pm 5$	$70 \pm 2$
3	6:1	323.15	10	$71 \pm 5$	$82 \pm 2$
4	10:1	323.15	10	$79 \pm 3$	$84 \pm 1$
5	38:1	323.15	10	$130 \pm 10$	$86 \pm 1$
6	6:1	323.15	7.5	$51 \pm 7$	$51.4 \pm 0.3$
7	6:1	323.15	9	$67 \pm 6$	$80 \pm 3$
8	6:1	323.15	20	$110 \pm 10$	$82.1 \pm 0.7$
9	6:1	323.15	30	$210 \pm 20$	$86 \pm 1$
10	6:1	338.15	10	$110 \pm 10$	$82.3 \pm 0.5$
11	6:1	343.15	10	$160 \pm 20$	$82 \pm 1$
12	6:1	353.15	10	$64 \pm 5$	$75.0 \pm 0.3$

Catalyst loading: 5 % wt. of substrates

$$* \text{ FAEE yield (\%)} = x_{\text{FAEE}} / (x_{\text{TAG}} + x_{\text{DAG}} + x_{\text{MAG}} + x_{\text{FAEE}}) \cdot 100$$

### 3.1. Effect of the initial substrate molar ratio

Initial substrate molar ratio (MR) has been studied in the range from 2:1 to 38:1 (ethanol:fish oil) at 10 MPa, 323.15 K and enzyme loading of 5% wt. of substrates. Fig. 3-3 shows a positive effect of increasing MR on the FAEE yield in the covered range. Based on the mutual solubility data of the substrates (ethanol + oil), which have been previously investigated [17], experiments performed at MR = 10:1 and 38:1 form a two-phase reaction mixture at atmospheric pressure. However, initial reaction rate steadily increases when increasing MR (Table 3-1) in SC-CO<sub>2</sub> as reaction medium, thus no mass transfer limitations occurred. Visual observation of the ternary system in a High-Pressure View Cell (Eurotechnica GmbH) showed that the incorporation of SC-CO<sub>2</sub> promoted the reaction bulk to become homogeneous (Fig. 3-4), as it has been also observed by Ciftci and Temelli [25] in the system corn oil, methanol and CO<sub>2</sub>. Besides, the rapidly produced FAEE and the reaction intermediates may also act as mutual solvents.

Inhibition of Lipozyme RM IM by high concentration of low-molecular-weight alcohols has been reported in various studies and it has been attributed to a stripping effect of the essential water from the enzyme structure [26]. However, this phenomenon has not been observed in the MR range covered in this work (2:1-38:1 ethanol:oil). It could have been avoided by charging the catalyst and the fish oil together in the HP-BSTR, because fish oil surrounds the enzyme and ethanol would diffuse through the oil layer, not being at high concentration in the enzyme environment. An additional kinetic experiment (data not shown) showed that preventing the catalyst from being in direct contact with ethanol may be a suitable strategy to avoid inhibition. This additional experiment was performed at the same conditions as exp. 5 (MR = 38:1; T = 323.15; p = 10 MPa) except for the order of addition of the reactants. In this case, weighted quantities of fish oil and ethanol were placed together into the HP-BSTR. At this MR and atmospheric pressure, the system is partially immiscible [17]. Subsequently, the catalyst was added depositing in the interphase. Then, reaction was carried out as reported in the experimental

section for a typical experiment. However, maximum FAEE yield of this experiment was found to be as low as 6.50 % mole, showing that special care should be taken when loading the substrates and the catalyst.

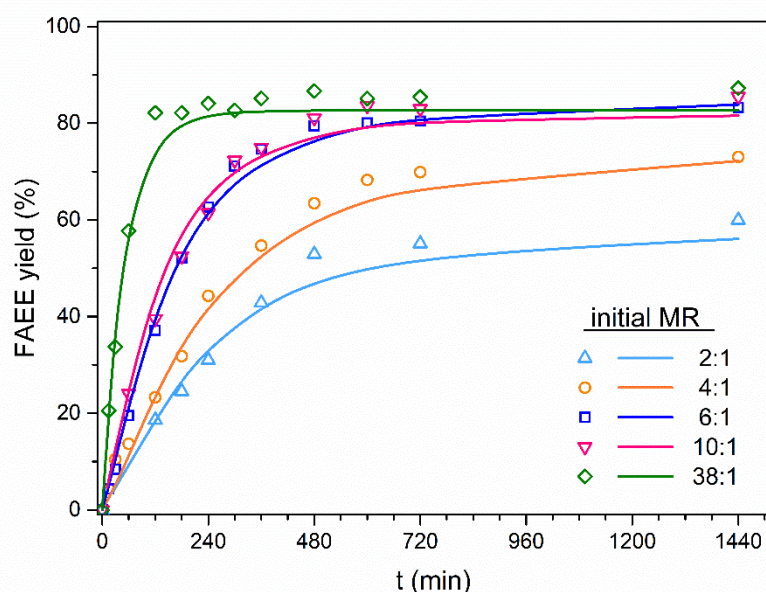


**Figure 3-3.** Effect of initial molar ratio of substrates (MR) on the FAEE yield in the ethanolysis of fish oil catalyzed by Lipozyme RM IM in SC-CO<sub>2</sub> medium. Experimental conditions: p = 10 MPa, T = 323.15 K and enzyme loading 5 % wt. of substrates. Lines represent the fitting of the proposed kinetic model to the experimental data.

In the literature, different results have been reported regarding the effect of ethanol on Lipozyme RM IM. Kondo *et al.* [11] found that FAEE production was inhibited by a large excess of ethanol in a continuous supercritical extractor-reactor, favouring an increase in the DAG content, the first reaction intermediate of TAG ethanolysis, at the highest concentration of ethanol studied (10% wt. of the CO<sub>2</sub> feed). On the other hand, several authors [27,28] have found appreciable conversion yields (around 80% wt.) in the ethanolysis of different natural lipid sources by Lipozyme RM IM in solvent-free media at MR higher than the stoichiometric (4:1 and 6:1 ethanol:oil). Oliveira and Oliveira [7] reported MR in the range 1:1 to 10:1

(ethanol:oil) as the variable that most positively affected the conversion yield of the enzymatic ethanolysis of palm kernel oil in SC-CO<sub>2</sub> by Lipozyme IM. They pointed at migration of ethanol to the vapor phase as the responsible for this positive effect and the lack of inhibition. However, it must be highlighted that the lipid substrate and the catalyst was firstly placed together into the reactor and then a pre-established amount of ethanol was introduced, following a similar experimental procedure as the one described in this work.

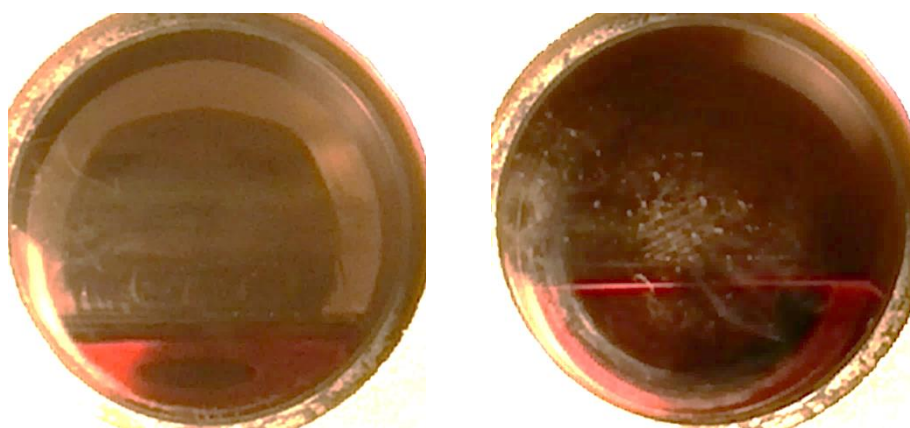


**Figure 3-4.** Visual observation of the initial reaction mixture (MR = 6:1) at T = 323.15 K; left: 0.1 MPa, right: 10 MPa.

The FAEE yield at equilibrium is represented as a function of MR in Fig. 3-5 a. From this figure, it can be noticed that the FAEE yield at equilibrium exhibits an asymptotic dependence on MR remaining practically constant at MR higher than 10:1. A similar expression of the one proposed by Chesterfield *et al.* for the ethanolysis of waste cooking oil [29] gives the following relationship for the FAEE yield at equilibrium and MR (Eq. 3-9)

$$\text{Eq. FAEE yield (\%)} = \frac{a}{1 + \exp\left(\frac{MR_0 - MR}{b}\right)} \quad (3-9)$$

Non-linear regression of experimental data was performed by using the Marquardt algorithm (Statgraphics) giving:  $a = 85.81\%$ , defined as the limiting equilibrium FAEE yield [29],  $b = 2.14$  and  $MR_0 = 0.518$  with  $R^2 = 0.982$ . Fig. 3-5 inset shows that a double-logarithmic relationship can be established between initial reaction rate and MR ( $\ln r_0 = 0.4644 \cdot \ln MR + 3.2461$ ;  $R^2 = 0.9463$ ).

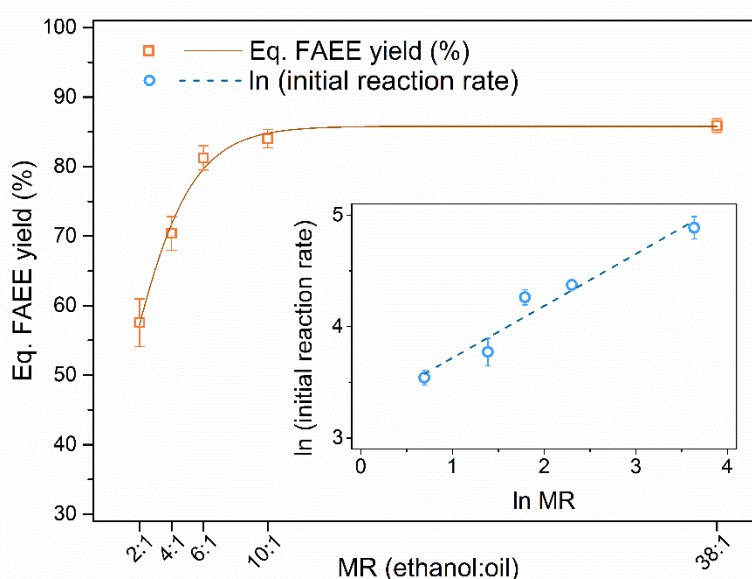


**Figure 3-5.** Equilibrium FAEE yield (%) vs. MR (ethanol :oil) in the ethanolysis of fish oil catalyzed by Lipozyme RM IM in SC-CO<sub>2</sub> medium. Solid line is from the non-linear regression of the experimental data (Eq. 3-9). **Inset:** Logarithmic relationship between initial reaction rate and MR. Dashed line is from the linear regression of the experimental data. Exp. conditions:  $p = 10$  MPa,  $T = 323.15$  K, enzyme loading 5 % wt. of substrates.

Table 3-2 lists the kinetic rate constants ( $k'_i$ ) calculated from the proposed model (Eqs. 3.6.1-3.6.7), as well as the value of the O.F. (Eq. 3-7) for the kinetic experiments performed at different MR. Equilibrium constants for each reaction step, evaluated as  $K_i = k'_i/k'_{-i}$ , are also reported. To our knowledge, this is the first time that kinetic rate constants are reported for the three steps of a lipase-catalyzed ethanolysis in SC-CO<sub>2</sub>.

As it can be observed from Table 3-2, the forward and reverse rate constants follow the order  $k'_3 > k'_2 > k'_1$  and  $k'_{-2} > k'_{-3} > k'_{-1}$ . An increase in MR leads to an increase in both the forward and the reverse rate constants. In the MR range studied, the forward rate constant of the third step (MAG to produce FAEE,  $k'_3$ ) is larger than the other two forward rate constants, being the initial breakdown of TAG the slowest step and therefore the rate-limiting step of the ethanolysis reaction.

This behavior has been also described in the literature for either acid or base-catalyzed transesterification [30]. It can be also noticed that equilibrium constants monotonously decreased with increasing MR due to the excess of ethanol employed. Besides, the equilibrium constant of the third reaction step,  $K_3$ , is one order of magnitude higher than those of the other two steps.

In the literature, different mechanisms have been proposed for lipase-catalyzed transesterification systems, most of them based on Ping-Pong Bi-Bi models [31]. Comparison with these studies is difficult since in most cases thermodynamic parameters are not provided. In this work, a simple model was adopted and surprisingly, leads to kinetic and equilibrium parameters of the same order as those reported by chemical-catalysis [30].

**Table 3-2.** Effective forward ( $k'_i$ ) and reverse ( $k'_{-i}$ ) reaction rate constants, equilibrium constants ( $K_i$ ) and objective function (O.F.) values of the proposed kinetic model for the ethanolysis of fish oil by Lipozyme RM IM in SC-CO<sub>2</sub> at different initial molar ratio of substrates (MR). Reactions were performed at p = 10 MPa, T = 323.15 K, enzyme loading 5 % wt. of substrates.

<b>MR</b> (etthanol:oil)	$k'_1$ (min <sup>-1</sup> )	$k'_{-1}$ (min <sup>-1</sup> )	$K_1^*$	$k'_2$ (min <sup>-1</sup> )	$k'_{-2}$ (min <sup>-1</sup> )	$K_2$	$k'_3$ (min <sup>-1</sup> )	$k'_{-3}$ (min <sup>-1</sup> )	$K_3$	<b>O.F.</b> †
<b>2:1</b>	0.0971	0.5998	0.1543	1.3972	2.4197	0.5511	3.7926	0.9194	4.1315	0.1704
<b>4:1</b>	0.1703	0.8898	0.1786	1.5682	4.0452	0.3684	5.3823	1.3874	4.0460	0.0592
<b>6:1</b>	0.4764	1.3465	0.4867	3.2605	5.9020	0.5290	7.4221	2.5333	2.6911	0.0309
<b>10:1</b>	0.5177	6.7735	0.0946	22.2968	164.8420	0.1426	11.5229	7.5545	2.1538	0.0137
<b>38:1</b>	3.5370	34.7671	0.0152	16.3786	158.3258	0.1178	27.8656	56.5390	0.2191	0.0047

\*  $K_i = k'_i/k'_{-i}$

† O.F. =  $\left( \sum_{\text{all samples}} \cdot \sum_{i=1}^n (x_i^{\text{exp}} - x_i^{\text{calc}})^2 \right) / n_{\text{samples}} \cdot 100$

### 3.2. Pressure effect

Pressure has been varied in the range from 7.5 to 30 MPa at fixed MR = 6:1 (ethanol:fish oil), 323.15 K and an enzyme loading of 5 % wt. of substrates. Table 3-1 shows that initial reaction rate steadily increases with pressure from 7.5 to 30 MPa, and FAEE yield at equilibrium increases from 51.4 % near the critical pressure (7.5 MPa) to 80 % at 9 MPa, showing a plateau around 81-85 % at higher pressures up to 30 MPa (Fig. 3-6). In the range investigated (7.5-30 MPa), no decay in the reaction performance was observed when increasing pressure.

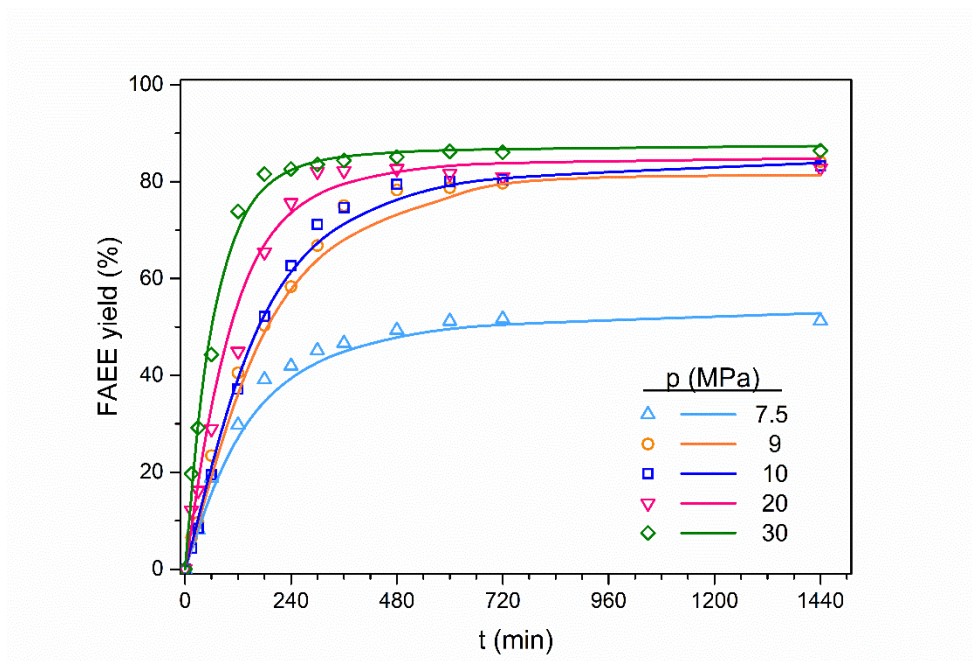


**Figure 3-6.** Effect of operating pressure ( $p$ ) on the ethanolsis of fish oil catalyzed by Lipozyme RM IM in SC-CO<sub>2</sub> medium. Experimental conditions: MR = 6:1, T = 323.15 K and enzyme loading 5 % wt. of substrates. Lines represent the fitting of the proposed kinetic model to the experimental data.

Fig. 3-7 shows that a semi-logarithmic relationship can be established between initial reaction rate and operating pressure (dashed line,  $\ln r_0 = 0.4220 \cdot \ln p_r + 3.6157$ ;  $R^2 = 0.9774$ ). Besides, a similar expression to the one proposed in Eq. 3-9 can be established to describe the effect of pressure on the equilibrium FAEE yield.

Operating pressure was expressed in terms of reduced pressure ( $p_r = p/p_c$ ). Non-linear regression was performed by using the Marquardt algorithm (Statgraphics) giving a limiting equilibrium FAEE yield of 83.47 %,  $b = 0.079$  and  $p_{r0} = 0.982$ , which gives  $p_0 = 7.22$  MPa, with  $R^2 = 0.973$ . The continuous line in Fig. 3-7 corresponds to this adjustment.

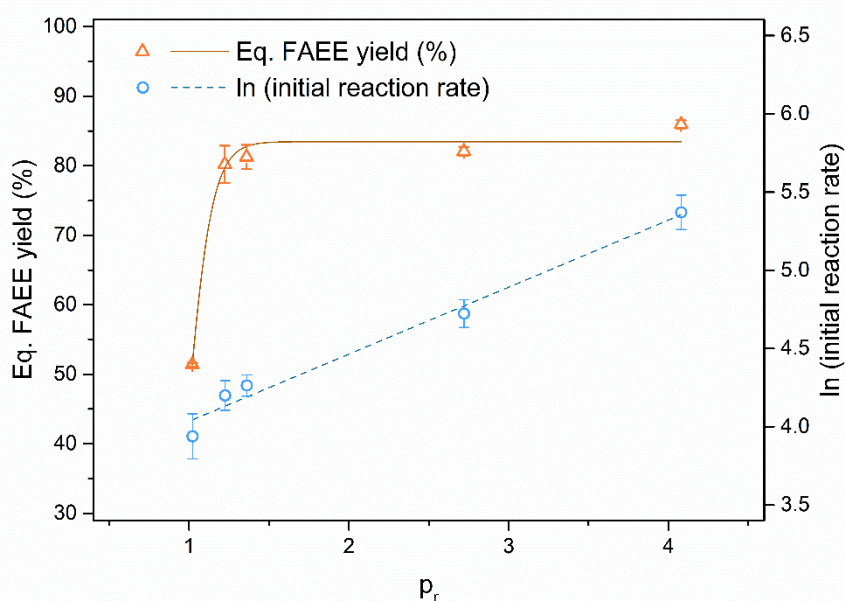


**Figure 3-7.** Equilibrium FAEE yield (%) ( $\Delta$ ) and  $\ln$  (initial reaction rate) ( $\circ$ ) vs. reduced operating pressure ( $p_r = p/p_c$ ) in the ethanolysis of fish oil catalyzed by Lipozyme RM IM in SC- $\text{CO}_2$  medium. Solid line is from the non-linear regression of the experimental data (Eq. 3-9). Dashed line is from the linear regression of the experimental data.

Exp. conditions: MR = 6:1,  $T = 323.15$  K, enzyme loading 5 % wt. of substrates.

The effect of operating pressure on the ethanolysis of fish oil by Lipozyme RM IM in SC- $\text{CO}_2$  could be explained considering the phase behavior of the fish oil/ethanol reaction mixture in SC- $\text{CO}_2$ . Visual observations of the initial reaction mixture at the different pressures assayed in this work showed that the reaction system consisted of an “expanded” liquid and a gas phase (Fig. 3-4). At the conditions studied in this work, solubility of  $\text{CO}_2$  in ethanol is high [32], whereas Borch-Jensen

and Mollerup [33] reported moderate solubility of CO<sub>2</sub> in fish oil at pressures from 6 to 65 MPa and temperatures from 293.15 to 393.2 K. At none of the temperatures, carbon dioxide and fish oil were completely miscible, but at each temperature, CO<sub>2</sub> solubility in fish oil was found to increase with increasing pressure [33]. This increase in CO<sub>2</sub> solubility with pressure may correspond to the increase in the reaction rate with pressure shown in Fig. 3-7, since CO<sub>2</sub> solvation results in a better mass transfer reaction medium due to an increase in diffusivity and a reduction of medium viscosity.

The different effects of pressure depending on the phase behavior of the system can be noted when comparing the results obtained in this work with those from the esterification of oleic acid with n-octanol in SC-CO<sub>2</sub> [16]. Phase behavior of the system oleic acid + n-octanol + CO<sub>2</sub> shows that CO<sub>2</sub> is highly soluble in the reaction mixture (oleic acid and ethanol) and the liquid phase can contain up to 70 % mole of CO<sub>2</sub> near the critical point of CO<sub>2</sub> [16]. Further increase in operating pressure promoted a decrease in conversion due to more CO<sub>2</sub> solvating in the reaction bulk and leading to dilution of the substrates. On the contrary, the mixture fish oil + ethanol can dissolve a much lower amount of CO<sub>2</sub> (30 % mole at MR = 6:1, 10 MPa and 323.15 K, according to analytical determination of the phase behavior in a high-pressure view cell [34]); therefore, dilution of the substrates at high pressure is not supposed to strongly affect the reaction performance in this system.

Oliveira and Oliveira [7] adopted a Taguchi experimental design to assess the influence of the process variables on the ethanolysis of palm kernel oil in SC-CO<sub>2</sub> catalyzed by Lipozyme IM. According to their results, Lipozyme IM was positively affected by pressure, although MR was the variable that more strongly affected the conversion. For this enzyme they found an optimum at 14.6 MPa. On the contrary, in the present work, no maximum in the pressure was found in the range from 7.5 to 30 MPa, although similar phase behavior could be expected for both reaction mixtures (fish oil + ethanol + CO<sub>2</sub> or palm kernel oil + ethanol + CO<sub>2</sub>).

The effect of pressure on the kinetic rate constants has been considered by using the transition-state theory and classical thermodynamics. Following this approach, the variation of the reaction rate constant  $k_i'$  with pressure for a bimolecular reaction  $A+B \rightleftharpoons M^* \rightleftharpoons \text{products}$  can be expressed as follows [12]:

$$\left. \frac{\partial \ln k}{\partial p} \right)_T = -\Delta V^*/RT \quad (3-10.1)$$

where  $k$  is the rate constant of the reaction expressed in pressure-independent concentration units,  $\Delta V^*$  is the apparent activation volume,  $T$  is the operating temperature and  $R$  is the gas constant. The direct integration of Eq 3-10.1 is not straightforward since activation volume changes with pressure [12]. However, within a small range of pressure it can be assumed that  $\Delta V^*$  does not change with pressure and Eq. 3-10.1 can be easily integrated, giving:

$$k_i' = k_i^0 \cdot \exp(-p \cdot \Delta V_i^* / RT) \quad (3-10.2)$$

where the subscript  $i$  refers to the different steps in the ethanolysis reaction. Following this expression, pre-exponential kinetic constants,  $k_i^0$ , and apparent activation volumes,  $\Delta V_i^*$ , have been simultaneously estimated for the experiments performed in the range 9-30 MPa. Results obtained are listed in Table 3-3. Kinetic parameters for the experiment performed at  $p = 7.5$  MPa were estimated separately because of the marked changes in the physical properties of the solvent near the critical region ( $p_r = 1.02$ ). In the pressure range 9-30 MPa, apparent activation volumes were negative ( $\Delta V_i^* < 0$ ) for all the reaction steps, which indicates that reaction rate constants will increase with increasing pressure. It can be observed that  $\Delta V^*$  for the first and third forward reaction steps are lower (or higher in absolute value) than the corresponding  $\Delta V^*$  for the reverse reaction, being these steps more sensitive to an increase in operating pressure.

**Table 3-3.** Values for the forward ( $k_i^0$ ) and reverse ( $k_{-i}^0$ ) pre-exponential constants, apparent activation volume of each forward ( $\Delta V_i^*$ ) and reverse ( $\Delta V_{-i}^*$ ) reaction step and values of the objective function (O.F.) of the proposed kinetic model for the ethanolysis of fish oil by Lipozyme RM IM in SC-CO<sub>2</sub> at 7.5 MPa and in the range 9-30 MPa. Reactions were performed at MR = 6:1, T = 323.15 K, enzyme loading 5 % wt. of substrates.

<b>p</b> <b>(MPa)</b>	$k_1^0$ <b>(min<sup>-1</sup>)</b>	$k_{-1}^0$ <b>(min<sup>-1</sup>)</b>	$\Delta V_1^*$ <b>(cm<sup>3</sup> mol<sup>-1</sup>)</b>	$\Delta V_{-1}^*$ <b>(cm<sup>3</sup> mol<sup>-1</sup>)</b>	$k_2^0$ <b>(min<sup>-1</sup>)</b>	$k_{-2}^0$ <b>(min<sup>-1</sup>)</b>	$\Delta V_2^*$ <b>(cm<sup>3</sup> mol<sup>-1</sup>)</b>	$\Delta V_{-2}^*$ <b>(cm<sup>3</sup> mol<sup>-1</sup>)</b>	$k_3^0$ <b>(min<sup>-1</sup>)</b>	$k_{-3}^0$ <b>(min<sup>-1</sup>)</b>	$\Delta V_3^*$ <b>(cm<sup>3</sup> mol<sup>-1</sup>)</b>	$\Delta V_{-3}^*$ <b>(cm<sup>3</sup> mol<sup>-1</sup>)</b>	<b>O.F.†</b>
<b>9 – 30</b>	0.2366	1.1770	-158.0394	-47.6628	1.5824	2.6906	-126.3835	-127.7673	3.0135	1.7217	-145.7125	-88.7143	0.0889
<b>7.5</b>	$k_1^* = 0.3099$		$k_{-1}^* = 43.1938$		$k_2^* = 2.3257$		$k_{-2}^* = 12.1366$		$k_3^* = 43.8870$		$k_{-3}^* = 45.9396$		0.0087

$$* k_i^* = k_i^0 \cdot \exp(-p \cdot \Delta V_i^* / RT)$$

$$\dagger \text{O.F.} = \left( \sum_{\text{all samples}} \cdot \sum_{i=1}^n (x_i^{\text{exp}} - x_i^{\text{calc}})^2 \right) / n_{\text{samples}} \cdot 100$$

On the contrary, the DAG to MAG conversion shows similar  $\Delta V^*$  values for the forward and reverse reactions, which suggest little influence of pressure in this step. Overall consideration of  $\Delta V^*$  values indicates that FAEE production may be favoured by increasing pressure, as it can be observed from the experimental results.

To our knowledge, no  $\Delta V^*$  values have been previously reported for lipase-catalyzed ethanolysis in SC-CO<sub>2</sub>. However, a similar  $\Delta V^*$  value of *ca.* -206 cm<sup>3</sup>·mol<sup>-1</sup> was reported by He *et al.* [35] for the transesterification of soybean oil without catalyst in sub- and supercritical methanol between 8.7 MPa and 36 MPa (553 K and MR methanol:soy bean oil = 42:1). In any case, Kamat *et al.* [12] stated that the use of  $\Delta V^*$  in enzyme-catalyzed reactions must be treated with caution, since changes in pressure will result in multiple variables being changed at a time which also influence the ability of the enzyme to catalyze a given reaction. Therefore  $\Delta V^*$  should not be used to compare the effects of pressure for catalyzed and uncatalyzed reactions. For an uncatalyzed reaction, data are only dependent of direct pressure-effects and no indirect effects of pressure are transmitted via the enzyme.

### 3.3. Temperature effect

To assess the effect of temperature on the kinetics of the ethanolysis of fish oil by Lipozyme RM IM in SC-CO<sub>2</sub>, operating temperature has been varied between 323.15 and 353.15 K. Initial substrate molar ratio (6:1 ethanol:fish oil), pressure (10 MPa) and enzyme loading (5% wt. of substrates) remained unchanged.

Fig. 3-8 shows that FAEE yield at equilibrium was similar in the temperature range from 323.15 to 343.15 K. This is probably because the heat of reaction is generally small for many transesterification systems; therefore, the equilibrium conversion observed for the ethyl esters is essentially temperature independent [36]. Raising temperature from 323.15 to 343.15 K resulted in an increase of the initial reaction rate (Table 3-1 and Fig. 3-8), probably because of a higher kinetic energy of the

molecules. Besides, lower viscosity and higher diffusivity of the solvent at higher temperatures may lead to lower mass transfer limitations [4]. The highest temperature assayed in this work (353.15 K) led to lower equilibrium FAEE yield (Table 3-1 and Fig. 3-9), which may be due to thermal deactivation of the catalyst.

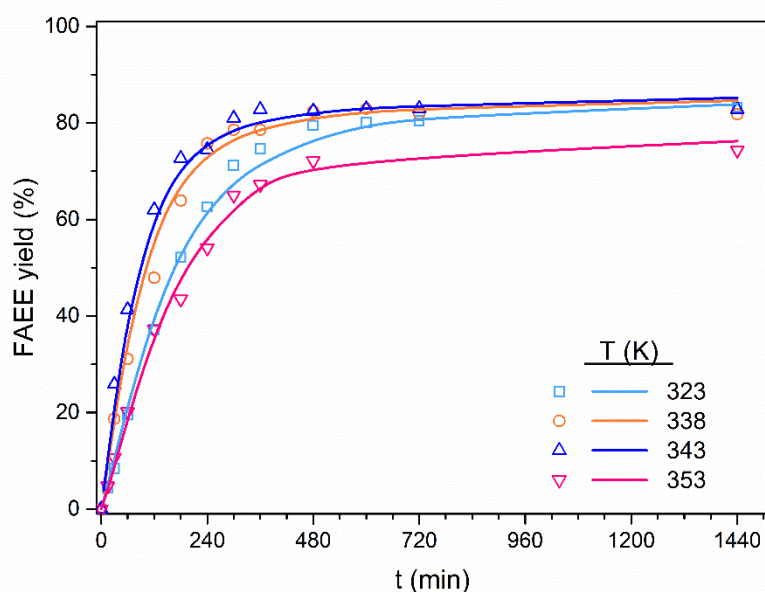


**Figure 3-8.** Effect of operating temperature ( $T$ ) on the ethanolysis of fish oil catalyzed by Lipozyme RM IM in SC- $\text{CO}_2$  medium. Exp. conditions MR = 6:1,  $p$  = 10 MPa and enzyme loading 10 % wt. of substrates. Lines represent the fitting of the proposed kinetic model to the experimental data.

The effect of temperature on initial reaction rate is shown in the Arrhenius plot (Fig. 3-9). From this figure, it can be seen that the Arrhenius dependence is no longer valid at temperatures higher than 343.15 K, probably because of the previously mentioned thermal deactivation of the catalyst. Similar results for thermal behavior of Lipozyme RM IM have been reported in the literature for the synthesis of *n*-octyl oleate in SC- $\text{CO}_2$  [16]. Conversion around 80 % was observed in the range 308.15-333.15 K at 10 MPa, whereas higher temperatures (343.15 and 353.15 K) led to lower conversion (around 65 %) yet slightly higher initial reaction rates, which may indicate that thermal deactivation is not immediate.

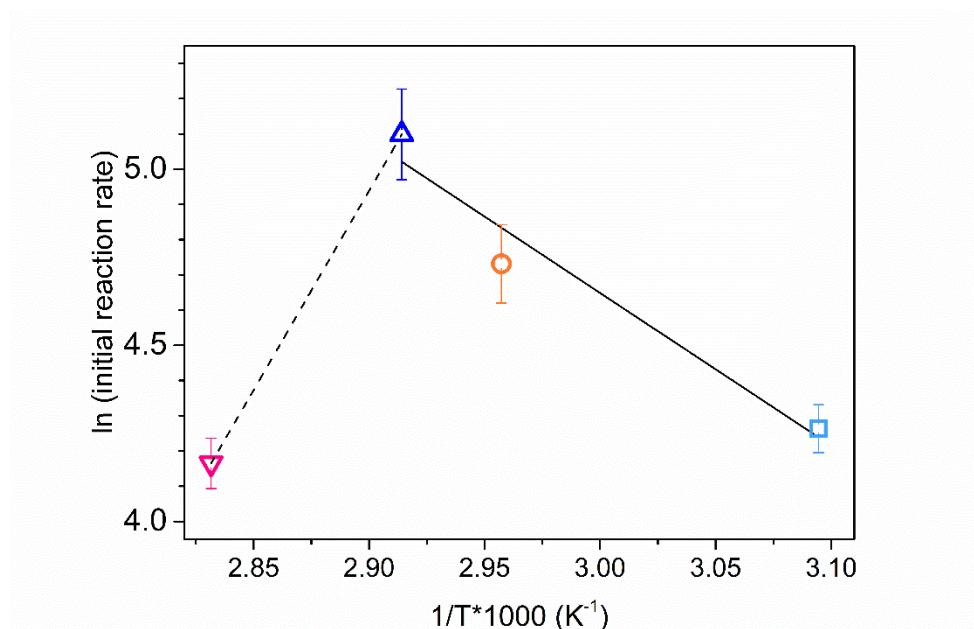


**Figure 3-9.** Arrhenius plot for the ethanolysis of fish oil catalyzed by Lipozyme RM IM in SC-CO<sub>2</sub> medium. Lines are from the linear regression of the experimental data. Exp. Conditions: MR = 6:1, p = 10 MPa and enzyme loading 5 % wt. of substrates.

Oliveira and Oliveira [7] reported  $T = 324$  K as the optimum temperature for the ethanolysis of palm kernel oil by Lipozyme IM in SC-CO<sub>2</sub>, whereas 313.15 K was found to be the optimum for the same reaction in n-hexane [8]. Recently, Calero *et al.* [28] have found the same operating temperature ( $T = 313.15$  K) as the optimum for the ethanolysis of sunflower oil by Lipozyme RM IM in solvent-free media (MR = 6:1) and different amounts of biocatalysts. According to the manufacturer of the catalyst, optimum activity temperature for Lipozyme RM IM catalyzed reactions is 313.15 K [37]. Based on these results, it could be concluded that higher thermal stability of the catalyst may be obtained in SC-CO<sub>2</sub> than in organic or solvent-free media [14,16,38]. In any case, it must be highlighted that optimum temperature in reactions involving easily oxidizable compounds such as *n*-3 PUFAs must consider not only the thermodynamic or kinetic criteria, but also the effect of operating temperature towards lipid oxidation, as it will be discussed in section 3.5.

The effect of temperature on the kinetic rate constants of the 3-step reaction has been described by the Arrhenius equation in the temperature range from 323.15 to 343.15 K:

$$k_i' = k_i^0 \cdot \exp(-E_i^a / RT) \quad (3-11)$$

where  $k_i^0$  is the preexponential factor,  $E_i^a$  is the activation energy of the reaction, T is the operating temperature and R is the gas constant. The subscript  $i$  accounts for the different steps of the ethanolysis reaction.

Combining this expression and the proposed kinetic model (Eqs. 3-3 to 3-6), experimental data from experiments performed at 323.15, 338.15, and 343.15 K were simultaneously and satisfactorily correlated. The experiment performed at 353.15 K has been excluded from the simultaneous fitting because of thermal inactivation of the catalyst. Estimated pre-exponential constants and activation energies for the ethanolysis of fish oil by Lipozyme RM IM in SC-CO<sub>2</sub> in the temperature range 323.15–343.15 K are listed in Table 3-4. It can be observed that the first forward step of the reaction, which is also the rate-limiting step, presented the highest estimated value for the activation energy and therefore the highest sensitivity to the reaction temperature.

**Table 3-4.** Values for the forward ( $k_i^0$ ) and reverse ( $k_{-i}^0$ ) pre-exponential constants, activation energy of each forward ( $E_i^a$ ) and reverse ( $E_{-i}^a$ ) reaction step and values of the objective function (O.F.) of the proposed kinetic model for the ethanalysis of fish oil by Lipozyme RM IM in SC-CO<sub>2</sub> in the range 323.15-343.15 K and at 353.15 K. Reactions were performed at MR = 6:1, p = 10 MPa, enzyme loading 5 % wt. of substrates.

<b>T</b> <b>(K)</b>	$k_1^0$ (min <sup>-1</sup> )	$k_{-1}^0$ (min <sup>-1</sup> )	$E_1^a$ (kJ mol <sup>-1</sup> )	$E_{-1}^a$ (kJ mol <sup>-1</sup> )	$k_2^0$ (min <sup>-1</sup> )	$k_{-2}^0$ (min <sup>-1</sup> )	$E_2^a$ (kJ mol <sup>-1</sup> )	$E_{-2}^a$ (kJ mol <sup>-1</sup> )	$k_3^0$ (min <sup>-1</sup> )	$k_{-3}^0$ (min <sup>-1</sup> )	$E_3^a$ (kJ mol <sup>-1</sup> )	$E_{-3}^a$ (kJ mol <sup>-1</sup> )	<b>O.F.</b> <sup>†</sup>
<b>323.15-343.15</b>	59947	85	31.83	10.10	718	1396	14.07	13.95	968	426	12.32	12.67	0.1085
<b>353.15</b>	$k_1' = 0.3583$		$k_{-1}' = 2.9463$		$k_2' = 2.7859$		$k_{-2}' = 9.9535$		$k_3' = 8.6937$		$k_{-3}' = 6.6718$		0.0608

$$* k_i' = k_i^0 \cdot \exp(-E_i^a / RT)$$

$$† \text{O.F.} = \left( \sum_{\text{all samples}} \cdot \sum_{i=1}^n (x_i^{\text{exp}} - x_i^{\text{calc}})^2 \right) / n_{\text{samples}} \cdot 100$$

### 3.4. Comparison of supercritical carbon dioxide, *tert*-pentanol and solvent-free media

Ethanolysis has been carried out at atmospheric pressure in *tert*-pentanol (TP) and in solvent-free medium (SF). For the kinetic performed in *tert*-pentanol, an optimized amount of solvent (20 % wt.) was added, based on the liquid-liquid equilibrium of the reaction system [17]. In the kinetic performed in SF medium, no solvent was added to the reaction system and ethanol acted simultaneously as solvent and reactant. Experiments were performed with the same enzyme concentrations as the experiments performed in SC-CO<sub>2</sub> (5 % wt. of substrates) and MR = 6:1 (ethanol:oil) and T = 323.15 K were chosen to compare the results. Fig. 3-10 allows comparison of the FAEE yields obtained in the different reaction media: TP and SF at atmospheric pressure and SC-CO<sub>2</sub> at two different operating pressures (10 and 30 MPa).

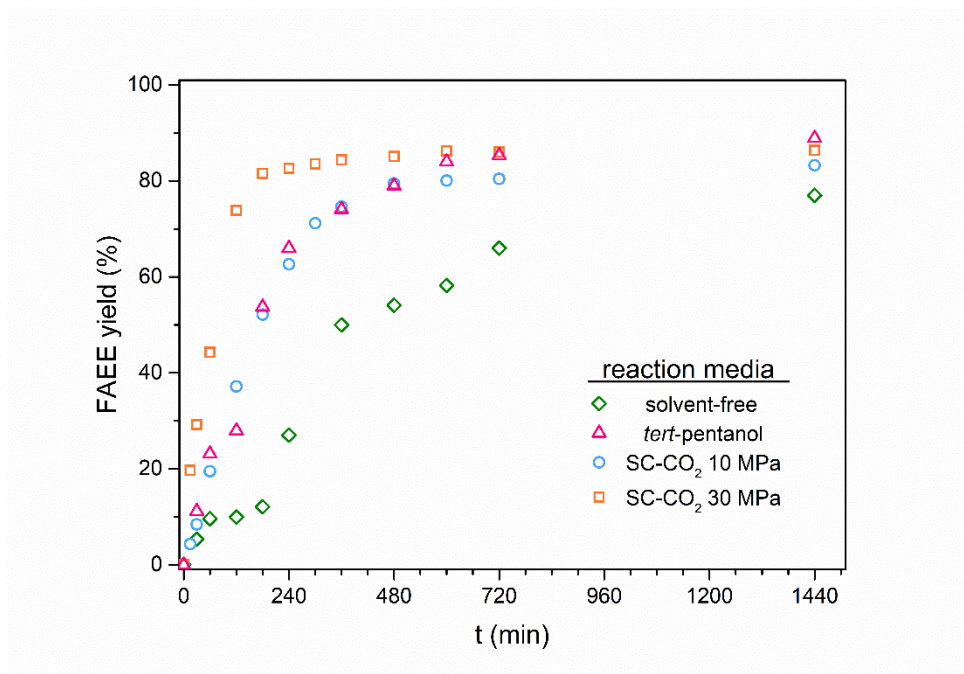


**Figure 3-10.** Effect of solvent media on the ethanolysis of fish oil catalyzed by Lipozyme RM IM. Experimental conditions: MR = 6:1, T = 323.15 K and enzyme loading 5 % wt. of substrates (SC-CO<sub>2</sub> at 10 and 30 MPa, SF: solvent-free media and 20 % wt. of TP).

SF medium presents the lowest reaction rate probably due to higher viscosities of the reaction mixture. Kinetic performance in TP is comparable to the results obtained in SC-CO<sub>2</sub> at 10 MPa. According to the results presented in Fig. 3-10, higher reaction rates are obtained when working in SC-CO<sub>2</sub> at 30 MPa than in TP. This proves that CO<sub>2</sub> dissolved in the reaction mixture plays an important role in the reaction performance by enhancing reaction rates due to better mass transfer properties.

### 3.5. Lipid oxidation

Peroxide (PV), p-Anisidine (p-AnV), and Acid (AV) Values have been determined for the supplied refined fish oil and for some of the reaction mixtures obtained after 24 h of reaction. AV and PV for the refined fish oil were  $0.56 \pm 0.01$  % oleic acid and  $4.99 \pm 0.01$  meq O<sub>2</sub> kg<sup>-1</sup>, respectively. AV fulfilled the guidance set by the FDA for food-grade triglycerides rich in *n*-3 PUFAs (1.0 % oleic acid), whereas PV is exactly on the recommended limit [39]. Results obtained for AV and PV after different reaction conditions are plotted in Figs. 3-11 and 3-12, respectively.

In general, at the same operating temperature ( $T = 323.15$  K) AV and PV in samples from the reactions in SC-CO<sub>2</sub> are lower than the ones from the reactions performed at atmospheric pressure, in which no significant difference is observed between organic solvent (*tert*-pentanol) and solvent-free media. Temperature is the parameter that most negatively affects the oxidation of the final mixture since both PV and AV increase with operating temperature. The highest values were obtained at 353.15 K, the highest T assayed in this work. Although higher reaction rates were obtained with an increase in temperature from 323.15 to 343.15 K, lipid oxidation increases with temperature. Therefore, the optimum operating temperature was the lowest temperature assayed in this work, 323.15 K. On the contrary, operating pressure affects in a lesser extent the AV and PV of the reaction samples in SC-CO<sub>2</sub> in the range investigated.

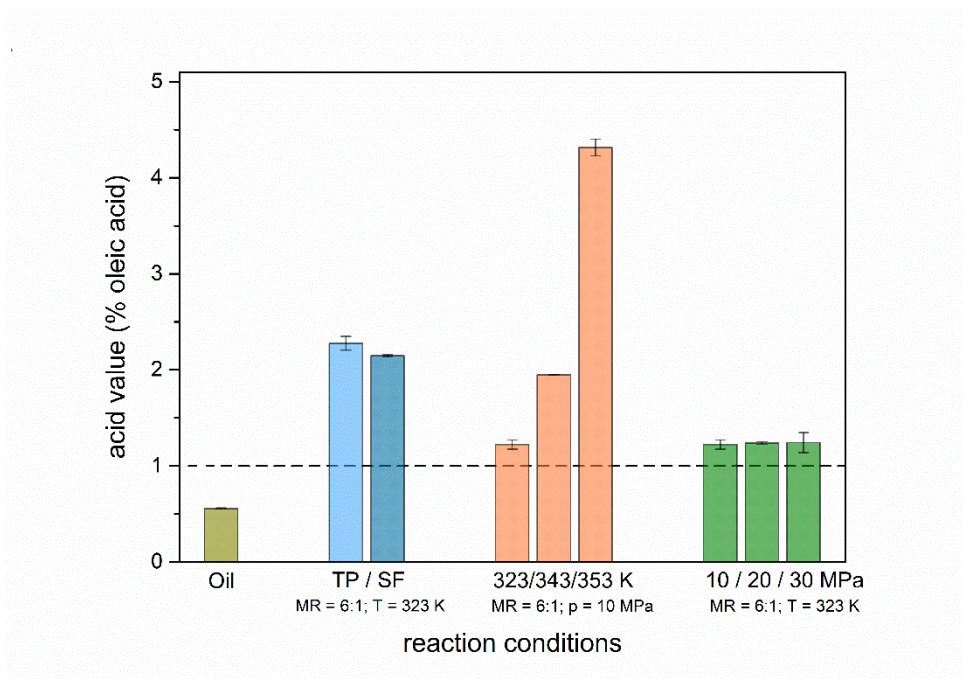


**Figure 3-11.** Effect of the ethanolsis of fish oil catalyzed by Lipozyme RM IM on the acid value (AV) in different reaction media: SC-CO<sub>2</sub> at different operating pressure, SF (solvent-free media) and 20 % wt. of TP. Dashed line represents the recommended limit set by the FDA [39].

p-AnV for the refined fish oil was found to be  $44 \pm 1$ . This value exceeds the limit recommended by the FDA [38]. Therefore the supplied fish oil was already partially oxidized. However, this value did not change significantly after the ethanolsis reaction either in SC-CO<sub>2</sub> or in conventional organic solvent (*tert*-pentanol) or solvent-free media. Indeed, p-AnV has been reported to be a good measurement of secondary oxidation processes, which are unlikely to happen in the short period of time in which the reaction took place.

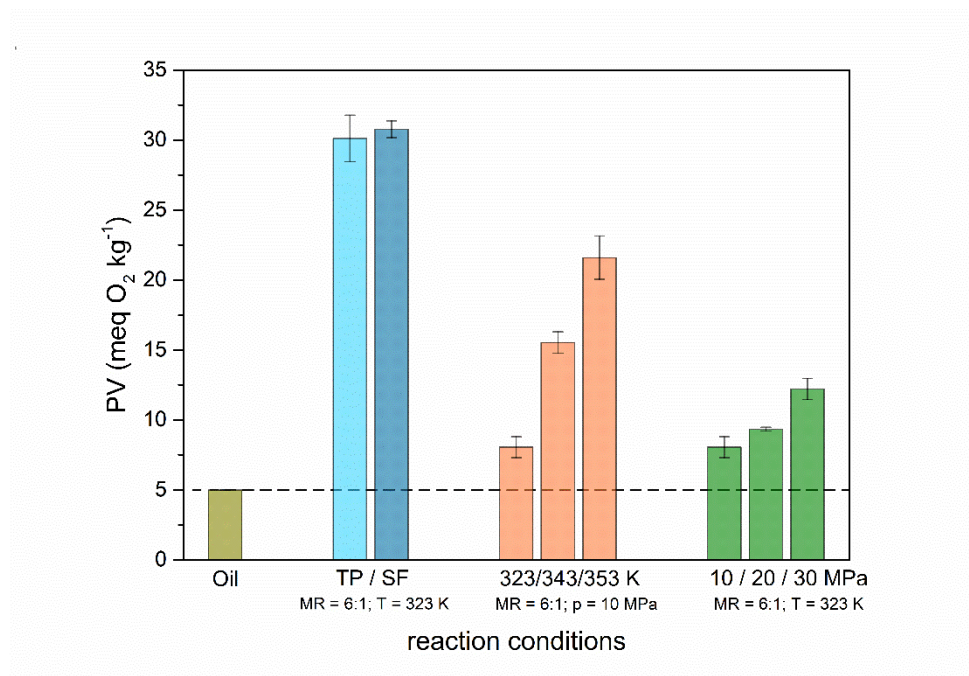


**Figure 3-12.** Effect of the ethanolysis of fish oil catalyzed by Lipozyme RM IM on the peroxide value (PV) in different reaction media: SC-CO<sub>2</sub> at different operating pressure, SF (solvent-free media) and 20 % wt. of TP. Dashed line represents the recommended limit set by the FDA [39].

To our knowledge, no other studies in the literature assessed lipid oxidation processes during enzymatic ethanolysis of fish oil in SC-CO<sub>2</sub>. Park *et al.* [40] determined PV and conjugated diene (CD) content of commercial salmon oil before and after enzymatically (Lipozyme IM) and chemically catalyzed ethanolysis at atmospheric pressure and hexane as the reaction media. They found that both methods increased PV and CD, yet little oxidation and isomerization of PUFAs were found when Lipozyme IM was used as the catalyst [39]. Results obtained in this work show that enzymatic ethanolysis of fish oil in SC-CO<sub>2</sub> can be considered a suitable method to obtain less oxidized reaction products compared to those obtained by enzymatic ethanolysis in conventional organic solvents or in solvent-free media at atmospheric pressure.

## Conclusion

SC-CO<sub>2</sub> has been used as a green solvent in the transesterification of fish oil by Lipozyme RM IM, providing an environmentally benign reaction medium. Advantages of using SC-CO<sub>2</sub> include replacing organic solvents, enhancing reaction kinetics by reducing mass transfer limitations and preventing oxidation due to displacement of oxygen. The latter is especially important when working with easily oxidizable compounds such as *n*-3 PUFAs.

Enzyme and phase behavior are key parameters to understand bioconversion in SC-CO<sub>2</sub>. The lipase showed higher thermal stability in SC-CO<sub>2</sub> reaction medium than in other conventional reaction media. Besides, no ethanol inhibition has been observed when avoiding high concentrations of ethanol in the enzyme environment. Operating pressure affected positively the reaction performance due to solvation of CO<sub>2</sub> in the reaction mixture, which reduces viscosity and improves diffusion coefficients. Lipase-catalyzed ethanolysis in SC-CO<sub>2</sub> has been shown as suitable method to obtain less oxidized *n*-3 PUFA FAEE compared to other reaction media.

Correlation of the kinetic data to a semi-empirical model showed that the rate-limiting step is the breakdown of triacylglycerides. Similar trends of kinetic and equilibrium parameters have been observed as those reported by chemical-catalysis.



## References

- [1] C. H. S. Ruxton, S. C. Reed, M. J. A. Simpson and K. J. Millington, The health benefits of omega-3 polyunsaturated fatty acids: a review of the evidence, *Journal of Human Nutrition and Dietetics*. 17 (2004) 449–459.
- [2] N. Rubio-Rodríguez, S. Beltrán, I. Jaime, S.M. de Diego, M.T. Sanz, J.R. Carballido, Production of omega-3 polyunsaturated fatty acid concentrates: a review, *Innovative Food Science & Emerging Technologies*. 11 (2010) 1–12.
- [3] B.B. Albert, D. Cameron-Smith, P.L. Hofman, W.S. Cutfield, Oxidation of marine omega-3 supplements and human health., *BioMed Research International*. 2013 (2013) 464921
- [4] Ž. Knez, Enzymatic reactions in dense gases, *The Journal of Supercritical Fluids*. 47 (2009) 357–372.
- [5] H. Gunnlaugsdottir, B. Sivik, Lipase-catalyzed alcoholysis of cod liver oil in supercritical carbon dioxide, *Journal of American Oil Chemists' Society*. 72 (1995) 399–405.
- [6] H. Gunnlaugsdottir, J. Mattias, B. Sivik, Process parameters influencing ethanolysis of cod liver oil in supercritical carbon dioxide, *The Journal of Supercritical Fluids*. 12 (1998) 85–93.
- [7] J.V. Oliveira, D. Oliveira, Kinetics of the Enzymatic Alcoholysis of Palm Kernel Oil in Supercritical CO<sub>2</sub>, *Industrial and Engineering Chemistry Research*. 39 (2000) 4450–4454.
- [8] D. Oliveira, J.V. Oliveira, Enzymatic alcoholysis of palm kernel oil in n-hexane and SCCO<sub>2</sub>, *The Journal of Supercritical Fluids*. 19 (2001) 141–148.
- [9] S.K. Shin, J.E. Sim, H. Kishimura, B.S. Chun, Characteristics of menhanden oil ethanolysis by immobilized lipase in supercritical carbon dioxide, *Journal of Industrial and Engineering Chemistry*. 18 (2012) 546–550.
- [10] M. Lee, D. Lee, J. Cho, S. Kim, C. Park, Enzymatic biodiesel synthesis in semi-pilot continuous process in near-critical carbon dioxide, *Applied Biochemistry and Biotechnology*. 171 (2013) 1118–1127.
- [11] M. Kondo, K. Rezaei, F. Temelli, M. Goto, On-line extraction - reaction of canola oil with ethanol by immobilized lipase in SC-CO<sub>2</sub>, *Industrial and Engineering Chemical Research*. 41 (2002) 5770–5774.

- [12] S. V Kamat, E.J. Beckman, A.J. Russell, Enzyme activity in supercritical fluids, *Critical Reviews in Biotechnology*. 15 (1995) 41–71.
- [13] R. Loss, L. Lerin, J.V. Oliveira, D. Oliveira, Lipase-Catalyzed Reactions in Pressurized Fluids, in: M.A.Z. Coelho, B.D. Ribeiro (Eds.), *White Biotechnology for Sustainable Chemistry*, The Royal Society of Chemistry, 2015: pp. 104–135.
- [14] R. Melgosa, M.T. Sanz, Á.G. Solaesa, S.L. Bucio, S. Beltrán, Enzymatic activity and conformational and morphological studies of four commercial lipases treated with supercritical carbon dioxide, *Journal of Supercritical Fluids*. 97 (2015) 51–62.
- [15] H. Nakaya, K. Nakamura, O. Miyawaki, Lipase-catalyzed esterification of stearic acid with ethanol, and hydrolysis of ethyl stearate, near the critical point in supercritical carbon dioxide, *Journal of the American Oil Chemists' Society*. 79 (2002) 23–27.
- [16] C.G. Laudani, M. Habulin, Ž. Knez, G. Della Porta, E. Reverchon, Lipase-catalyzed long chain fatty ester synthesis in dense carbon dioxide: Kinetics and thermodynamics, *Journal of Supercritical Fluids*. 41 (2007) 92–101.
- [17] S.L. Bucio, A.G. Solaesa, M.T. Sanz, S. Beltrán, R. Melgosa, Liquid-liquid equilibrium for ethanolysis systems of fish oil, *Journal of Chemical Engineering Data*. 58 (2013) 3118–3124.
- [18] Á.G. Solaesa, S.L. Bucio, M. T. Sanz, S. Beltrán, and S. Rebolleda, *Journal of Oleo Science*, 2014, **63**, 449–460.
- [19] H. Sovová, M. Zarevúcka, P. Bernášek and M. Stamenić, Kinetics and specificity of Lipozyme-catalysed oil hydrolysis in supercritical CO<sub>2</sub>, *Chemical Engineering Research and Design*. 86 (2008) 673–681.
- [20] Official Methods and Recommended Practices of the American Oil Chemists' Society, AOCs Official Method Cd 3d-63, American Oil Chemists' Society, Champaign, IL (2009).
- [21] Official Methods of Analysis of the Association of Official Analytical Chemists. AOAC Official Method 965.33. Peroxide Value of Oils and Fats, AOAC International, Washington, DC (2002).
- [22] Official Methods and Recommended Practices of the American Oil Chemists' Society, AOCs Official Method Cd 18-90, American Oil Chemists' Society, Champaign, IL (2011).



- [23] A. Millqvist Fureby, C. Virto, P. Adlercreutz, B. Mattiasson, Acyl group migrations in 2-monoolein, *Biocatalysis and Biotransformation*. 14 (1996) 89–111.
- [24] X. Xu, A. R. H. Skands, C. E. Høy, H. Mu, S. Balchen and J. Adler-Nissen, Production of specific-structured lipids by enzymatic interesterification: Elucidation of acyl migration by response surface design, *Journal of the American Oil Chemists' Society*. 75 (1998) 1179–1186.
- [25] O.N. Ciftci, F. Temelli, Continuous production of fatty acid methyl esters from corn oil in a supercritical carbon dioxide bioreactor, *Journal of Supercritical Fluids*. 58 (2011) 79–87.
- [26] W. Piyatheerawong, Y. Iwasaki, X. Xu, T. Yamane, Dependency of water concentration on ethanolysis of trioleoylglycerol by lipases, *Journal of Molecular Catalysis B: Enzymatic*. 28 (2004) 19–24.
- [27] V. Kumari, S. Shah, M.N. Gupta, Preparation of biodiesel by lipase-catalyzed transesterification of high free fatty acid containing oil from *Madhuca indica*, *Energy & Fuels*. 21 (2007) 368–372.
- [28] J. Calero, C. Verdugo, D. Luna, E.D. Sancho, C. Luna, A. Posadillo, F.M. Bautista, A.A. Romero, Selective ethanolysis of sunflower oil with Lipozyme RM IM, an immobilized *Rhizomucor miehei* lipase, to obtain a biodiesel-like biofuel, which avoids glycerol production through the monoglyceride formation., *New Biotechnology*. 31 (2014) 596–601.
- [29] D.M. Chesterfield, P.L. Rogers, E.O. Al-Zaini, A.A. Adesina, Production of biodiesel via ethanolysis of waste cooking oil using immobilised lipase, *Chemical Engineering Journal*. 207–208 (2012) 701–710.
- [30] A. Sivasamy, K.Y. Cheah, P. Fornasiero, F. Kemausuor, S. Zinoviev, S. Miertus, Catalytic applications in the production of biodiesel from vegetable oils, *ChemSusChem*. 2 (2009) 278–300.
- [31] B. Cheirsilp, A. H-Kittikun, S. Limkatanyu, Impact of transesterification mechanisms on the kinetic modeling of biodiesel production by immobilized lipase, *Biochemical Engineering Journal*. 42 (2008) 261–269.
- [32] J.S. Lim, Y.Y. Lee, H.S. Chun, Phase Equilibria for Carbon Dioxide-Ethanol- Water System at Elevated Pressures, *Journal of Supercritical Fluids*. 7 (1994) 219–230.
- [33] C. Borch-Jensen, J. Mollerup, Phase equilibria of fish oil in sub- and supercritical carbon dioxide, *Fluid Phase Equilibria*. 138 (1997) 179–211.

- [34] R. Melgosa, M.T. Sanz, Á.G. Solaesa, S. Beltrán, Phase behaviour of the pseudo-ternary system carbon dioxide + ethanol + fish oil at high pressures, *Journal of Chemical Thermodynamics*. 115 (2017) 106–113.
- [35] H. He, S. Sun, T. Wang, S. Zhu, Transesterification kinetics of soybean oil for production of biodiesel in supercritical methanol, *Journal of the American Oil Chemists' Society*. 84 (2007) 399–404.
- [36] S.L. Bucio, Á.G. Solaesa, M.T. Sanz, R. Melgosa, S. Beltrán, H. Sovová, Kinetic study for the ethanolysis of fish oil catalyzed by Lipozyme 435 in different reaction media, *Journal of Oleo Science*. 64 (2015) 431–441.
- [37] D. Oliveira, A.C. Feihmann, A.F. Rubira, M.H. Kunita, C. Dariva, J.V. Oliveira, Assessment of two immobilized lipases activity treated in compressed fluids, *The Journal of Supercritical Fluids*. 38 (2006) 373–382.
- [38] R.C. Rodrigues, R. Fernandez-Lafuente, Lipase from *Rhizomucor miehei* as a biocatalyst in fats and oils modification, *Journal of Molecular Catalysis B: Enzymatic*. 66 (2010) 15–32.
- [39] U.S. Department of Health and Human Services, U.S. Food and Drug Administration, Office of Food Additive Safety, GRAS Notice 000200, Silver Spring, MD (2006).
- [40] S.-B. Park, Y. Endo, K. Maruyama, K. Fujimoto, Enzymatic synthesis of ethyl ester of highly unsaturated fatty acids from fish oils using immobilized lipase, *Food Science and Technology Research*. 6 (2000) 192–195.

## Chapter 4

# Omega–3 encapsulation by PGSS-drying and conventional drying methods. Particle characterization and oxidative stability

#PGSS-drying #supercritical carbon dioxide

#ultrasound-assisted emulsification #microencapsulated fish oil

**Adapted from:**

R. Melgosa, Ó. Benito, M.T. Sanz, E. de Paz, S. Beltrán, Omega–3 encapsulation by PGSS-drying and conventional drying methods. Particle characterization and oxidative stability, Food Chemistry (submitted)

## Table of contents

Tables.....	213
Figures .....	215
Abstract.....	217
Resumen.....	219
1. Introduction.....	221
2. Materials and methods .....	224
2.1. Materials .....	224
2.2. Characterization of the <i>n</i> -3 PUFA concentrate .....	225
2.3. Ultrasound-assisted emulsification .....	226
2.4. PGSS-drying.....	226
2.5. Spray-drying .....	228
2.6. Freeze-drying.....	229
2.7. Characterization of the O/W Emulsion.....	229
2.7.1. Particle size analysis of the O/W emulsion.....	229
2.7.2. Emulsion stability .....	230
2.7.3. Density of the O/W emulsions.....	231
2.8. Characterization of the dried powders .....	231
2.8.1. Encapsulation efficiency.....	231
2.8.2. Particle size analysis of the dried powders .....	232
2.8.3. Moisture content .....	233
2.8.4. Scanning electron microscopy (SEM) .....	233
2.8.5. Differential scanning calorimetry (DSC).....	233
2.9. Measurement of lipid oxidation.....	234
2.9.1. Peroxide Value.....	234
2.9.2. TBARS analysis.....	234
2.10. Statistical analysis.....	236

## Table of contents (*continued*)

3. Results and discussion.....	236
3.1. Characterization of the <i>n</i> -3 PUFA concentrate .....	236
3.2. Emulsion stability .....	237
3.3. Density of the O/W emulsions .....	239
3.4. Particle Size Analysis.....	239
3.5. Encapsulation efficiency .....	242
3.6. Moisture content .....	244
3.7. Particle morphology (SEM) .....	244
3.8. Differential scanning calorimetry (DSC) .....	246
3.9. Oxidative stability of the dried powders .....	247
Conclusion .....	257
References.....	259

## Tables

<b>Table 4-1.</b> Characterization of the fish oil concentrate. ....	238
<b>Table 4-2.</b> Density of the original O/W emulsion and the reconstituted powders obtained by the different drying methods. Water:carrier:fish oil concentrate proportion was kept the same as the original (70:24:6 wt.).....	239
<b>Table 4-3.</b> Results obtained in the particle size analysis of the original O/W emulsion and the reconstituted powders obtained by the different drying methods. Water:carrier:fish oil concentrate proportion was kept the same as the original (70:24:6 wt.) .....	240
<b>Table 4-4.</b> Moisture content of the powders obtained by the different drying methods.....	244
<b>Table 4-5.</b> Peak temperatures of the thermal events observed in the PGSS-dried powder loaded with <i>n</i> -3 PUFA concentrate (PGSS-drying), the carrier alone (Hi-Cap™ 100), and the <i>n</i> -3 PUFA concentrate alone (Algatrium™ Plus). .....	247

## Figures

- Figure 4-1.** Schematic diagram of the PGSS-drying apparatus. VE-1: O/W emulsion vessel, VE-2: static mixer, VE-3: a) spraying tower, b) condenser, VE-4: CO<sub>2</sub> vessel, P-1: O/W emulsion pump, P-2: CO<sub>2</sub> pump, V-: process valve, E-: heat exchanger, R-: electrical resistance, PI: pressure indicator, TI(C): temperature indicator (and controller). .....227
- Figure 4-2.** Changes in the backscattering profile ( $\Delta$ BS) over time in the US-assisted O/W emulsion.....237
- Figure 4-3.** Particle size distribution plot of the original O/W emulsion and the reconstituted powders obtained by the different drying methods. Water:carrier:fish oil concentrate proportion was kept the same as the original (70:24:6 wt.).....241
- Figure 4-4.** Encapsulation efficiency of the powders obtained by the different drying methods. Powders were stored at 4°C in darkness and ambient oxygen concentration. Lines are drawn to guide the eye.....243
- Figure 4-5.** SEM micrographs of the dried powders. a) powder obtained by PGSS-drying, b) powder obtained by spray-drying; from left to right, 1500x, 5000x and 10000x magnifications. c) powder obtained by conventional freeze-drying (50x, 400x and 3000x). d) powder obtained by freeze-drying with liquid N<sub>2</sub>; (50x, 400x and 2000x). .....245
- Figure 4-6.** Peroxide Value (PV) of the *n*-3 PUFA concentrate (Algatrium™ Plus), the US-assisted O/W emulsions, and the particles obtained by the different drying methods right after drying. Samples were reconstituted the day of analysis keeping the original water:carrier:fish oil concentrate proportion (70:24:6 wt.).....248
- Figure 4-7.** PV evolution of the dried particles during storage at 4°C in darkness and ambient oxygen conditions. Samples were reconstituted the day of analysis keeping the original water:carrier:fish oil concentrate proportion (70:24:6 wt.). **Inset:** original PV of the *n*-3 PUFA concentrate (Algatrium™ Plus) and the US-assisted O/W emulsions.....251

## Figures (*continued*)

**Figure 4-8.** Thiobarbituric acid reactive substances (TBARS) content of the the *n*-3 PUFA concentrate (Algatrium™ Plus), the US-assisted O/W emulsions, and the particles obtained by the different drying methods right after drying. Samples were reconstituted the day of analysis keeping the original water:carrier:fish oil concentrate proportion (70:24:6 wt.). .....253

**Figure 4-9.** TBARS evolution of the dried particles during storage at 4°C in darkness and ambient oxygen conditions. Samples were reconstituted the day of analysis keeping the original water:carrier:fish oil concentrate proportion (70:24:6 wt.). **Inset:** TBARS of the *n*-3 PUFA concentrate (Algatrium™ Plus) and the original US-assisted O/W emulsions.....254

## Abstract

In this chapter, Particles from Gas-Saturated Solutions (PGSS)-drying has been used as a green alternative to encapsulate omega-3 polyunsaturated fatty acids (*n*-3 PUFAs) at mild, non-oxidative conditions. PGSS-drying has been compared to other conventional drying methods such as spray-drying and freeze-drying.

Encapsulation efficiencies (EE) as high as 98 % and spherical morphology were found for both PGSS- and spray-dried particles, whereas freeze-dried powders showed irregular morphology and EE ranging from 95.8 to 98.6 %.

Glass-transition and melting peaks of OSA-starch were observed in DSC analyses, as well as a cold-crystallization peak corresponding to the *n*-3 PUFA concentrate loaded in the PGSS-dried microparticles.

The oxidative status of the dried powders has been monitored over time through Peroxide Value (PV) and TBARS analyses. When compared to spray-drying, PGSS-dried microparticles showed lower primary and secondary oxidation after 28 days of storage at 4°C. The best primary oxidation results were obtained with the addition of ascorbic acid, which combined with the mild processing conditions of PGSS-drying, yielded a maximum of 2.5 meq O<sub>2</sub>/kg oil over 28 days of storage at 4 °C.

## Resumen

En el presente capítulo se han obtenido micropartículas de almidón modificado (OSA) con alto contenido de ácidos grasos poliinsaturados omega-3 (AGPI  $n-3$ ), mediante emulsificación asistida por ultrasonidos en combinación con secado mediante *PGSS (Particles from Gas-Saturated Solutions)-drying*. Con fines comparativos, también se han obtenido micropartículas mediante secado por pulverización y liofilización.

Las emulsiones obtenidas presentan una distribución de tamaños de gota estrechamente centrada alrededor de los 0.120  $\mu\text{m}$ . También son físicamente estables durante varios días. Se han obtenido eficacias de encapsulación (EE) de hasta 98 % y morfología esférica tanto con *PGSS-drying* como con secado por pulverización, mientras que las partículas liofilizadas son irregulares, con EE = 95.8-98.6 %. El análisis mediante *DSC* de las micropartículas obtenidas por *PGSS-drying* ha revelado picos de transición vítrea y de fusión del almidón modificado, así como un pico de cristalización fría perteneciente al concentrado de aceite de pescado.

El método *PGSS-drying* ofrece menores temperaturas de secado en una atmósfera intrínsecamente inerte, evitando la degradación oxidativa de los AGPI  $n-3$  durante el procesado. Así, en comparación con las partículas obtenidas mediante métodos de secado convencionales, las partículas obtenidas mediante *PGSS-drying* tienen menores valores de oxidación primaria y secundaria que las obtenidas mediante secado por pulverización. Además, estos valores se mantienen más bajos durante 28 días de almacenamiento a 4 °C. Los mejores resultados de oxidación primaria se han obtenido con la adición de ácido ascórbico en la fase continua de la emulsión, que en combinación con las condiciones suaves de procesado del método *PGSS-drying*, han resultado en un máximo de 2.5 meq O<sub>2</sub>/kg aceite a lo largo de 28 días de almacenamiento a 4 °C.

## 1. Introduction

An adequate intake of omega-3 polyunsaturated fatty acids ( $n-3$  PUFAs) is recommended in healthy diet guidelines due to their important benefits [1]. Long-chain  $n-3$  PUFAs, mainly eicosapentaenoic (EPA, 20:5  $n-3$ ) and docosahexaenoic (DHA, 22:6  $n-3$ ) acids are eicosanoid precursors, which are immunomodulatory molecules with a key role in the inflammatory response. EPA and DHA contribute to the normal brain, eye and cardiovascular functions in adults and help in the normal development of the eyes, brain and nervous system in children [2].

The perceived health benefits of these compounds have created a strong demand for EPA and DHA concentrates in the pharmaceutical and food industries. However,  $n-3$  PUFAs are unstable and very prone to oxidation, easily generating lipid hydroperoxides and free radicals under oxidative conditions. These species negatively affect sensory properties, since they can decompose into low-molecular-weight volatile compounds that are perceived as rancid, and what is more, they present potentially cytotoxic, carcinogenic and mutagenic effects [3,4] For these reasons,  $n-3$  PUFA concentrates are often encapsulated in order to protect them from light and oxygen during shelf life; and natural antioxidants such as tocopherols, phospholipids, ascorbic acid, or their mixtures are usually added [5,6].

Different encapsulation techniques can be used to encapsulate fish oil, such as emulsification, spray-drying, freeze-drying, coacervation, *in situ* polymerization, extrusion, or fluidized-bed coating [7]. Among these, the most widely used in the food and pharmaceutical industries is spray-drying, followed by freeze-drying. Freeze-drying is often applied to thermolabile and easily oxidizable compounds due to the protective low temperatures and vacuum conditions involved in the process. Its main drawback is the energy consumption, linked to the low temperature and high vacuum conditions as well as the long residence times required to completely dry the product, which in turn translate in high processing costs. On the contrary, spray-drying is a low-cost encapsulation technology which operates in a relatively simple and continuous way, thus it is commonly used at industrial scale [7].

One of the limitations of these drying techniques is that they require an aqueous feed solution, which constrains the wall material and the active compound to be water-soluble compounds. To overcome this limitation, an oil-in-water (O/W) emulsion can be prepared in order to disperse the lipid bioactive before drying. Ultrasound (US) assisted emulsification is a high-energy emulsification technique that has grown in importance among the pharmaceutical, cosmetic, and food industries, thanks to its versatility and the possibility of obtaining high quality food products with enhanced functional properties [8]. US-assisted emulsification can be applied to improve solubility, stability, and bioavailability of the dispersed bioactive compounds and, in particular, it can be used to obtain O/W emulsions with nanometric droplet size and narrow size distribution, as demonstrated in previous works [9]. Typically, US-assisted emulsification consists on applying low-frequency sound waves of 20-100 kHz through a metallic sonotrode immersed in the liquid medium, in order to generate disruptive forces that break down the macroscopic phases (coarse emulsion) to nanosized droplets. The nano-scale emulsions obtained present interesting functional properties [8] and, in the case of fish oil concentrates, an enhanced stability against oxidation [9].

Spray-drying also presents a second limitation linked to the high temperatures needed in the spray tower in order to completely dry the final product. This prevents the use of carrier materials with low melting temperature, such as polyethylene glycol (PEG) or soybean lecithin [10,11]; and what is more, exposes the bioactive compounds to adverse temperature conditions which may promote oxidative degradation.

Alternatively, supercritical fluids, and particularly supercritical carbon dioxide (SC-CO<sub>2</sub>), are a convenient medium to produce particles loaded with bioactive compounds. Carbon dioxide is an inert, non-toxic solvent, and is completely released from the product as a gas once back to atmospheric conditions. Besides, the accessibility of the supercritical state of carbon dioxide ( $T_C = 31.1$  °C;  $p_C = 73.8$  bar) and its advantageous physical properties (high density and diffusivity, and low

viscosity) make SC-CO<sub>2</sub> the solvent of choice in many particle formation processes. For a recent and comprehensive review on the applications and future developments in this field, the reader is referred to the book edited by Professor Turk [12]. Among the several proposed techniques, the Particles from Gas Saturated Solutions (PGSS) process overcomes the problems of solubility limitations and high gas consumption of other particle formation methods using SC-CO<sub>2</sub> [12]. This technique can be used for drying aqueous solutions, dispersions or, as in this work, O/W emulsions, in the so-called PGSS-drying process [12].

Basically, the PGSS-drying technique consists on mixing an aqueous solution with supercritical carbon dioxide upon saturation, and subsequently expanding the gas-saturated solution down to atmospheric pressure through a nozzle. This technique can be used as an alternative to conventional spray-drying, achieving a more efficient atomization due to the sudden vaporization of the dissolved CO<sub>2</sub> and the expansion of gas bubbles in the solution during depressurization from supercritical to atmospheric conditions. Both effects improve the atomization of the sprayed solution forming small droplets, thus reducing the particle size of the dried powder and enhancing the drying process [13,14]. Besides, the product is dried at low and homogeneous temperature because of the intense and deep cooling caused by the Joule-Thomson effect, which combined with the intrinsically inert ambient conditions due to oxygen displacement, prevent, or at least delay, oxidative degradation of the encapsulated bioactive compounds [13]. Operating conditions in the spraying tower, particularly temperature and gas-to-product ratio (GPR), must be taken into account in order to operate above the dew line of the carbon dioxide–water system [14], and ensure the complete drying of particles.

In this work, an *n*-3 PUFA enriched fish oil has been encapsulated by the alternative and green technology Particles from Gas Saturated Solutions (PGSS)-drying. The main goal of the study is to explore the potential benefits of supercritical carbon dioxide technologies applied to particle formulation and encapsulation of heat-sensitive and easily oxidizable compounds such as *n*-3 PUFAs, compared to other

conventional precipitation methods. This way, the PGSS-dried particles have been compared to those obtained by spray-drying and freeze-drying, which are commonly applied in the pharmaceutical, cosmetic, and food industries to dry aqueous solutions and dispersions. Characterization of the particles obtained by the different drying methods has been performed in terms of particle morphology, residual humidity, and particle size distribution of the reconstituted particles. Besides, encapsulation efficiency and oxidative stability (primary and secondary oxidation) of the encapsulated *n*-3 PUFA concentrate have been monitored over time in the particles formulated with each of the drying methods. Additionally, an antioxidant (ascorbic acid) has been added to some of the formulations as a strategy to enhance the oxidative stability of the encapsulated *n*-3 PUFA concentrate.

## 2. Materials and methods

### 2.1. Materials

Algatrium™ Plus, a concentrate of *n*-3 PUFAs from fish oil, was kindly donated by Brudy Technology S.L. (Spain). It has been stored at 4 °C in darkness and N<sub>2</sub> atmosphere. Hi-Cap™ 100, an octenyl-succinic-anhydride modified starch (OSA-starch) derived from waxy maize, was provided by Ingredion Inc. (Germany). Carbon dioxide (99.9%) was provided by Air Liquide S.A. (Spain). Ascorbic acid (L(+)-Ascorbic acid, AA) was purchased from Panreac AppliChem (Spain).

37% hydrochloric acid (HCl), diethyl ether, 1-butanol, 2-propanol, methanol, 2-thiobarbituric acid (TBA), and trichloroacetic acid (TCA) were provided by VWR Chemicals (Germany). Hexane, absolute ethanol, Iron(II) sulphate heptahydrate, and ammonium thiocyanate were purchased from Merck KGaA (Germany). 2,2,4-trimethylpentane (isooctane) and barium chloride dihydrate were supplied by Macron Fine Chemicals (France) and Panreac AppliChem (Spain), respectively. Cumene hydroperoxide and 1,1,3,3-tetraethoxypropane (TEP) standards were purchased from Sigma Aldrich (USA).

## 2.2. Characterization of the *n*-3 PUFA concentrate

Neutral lipid profile of the *n*-3 PUFA concentrate has been analyzed by normal-phase HPLC (NP-HPLC). Separation was carried out at room temperature in a Lichrospher Diol column (5 mm, 4 mm×250 mm) and detection was performed by evaporative light scattering (ELSD) (Agilent Technologies 1200 Series, USA) at 35 °C and 3.5 bar. Solvent gradient and calibration procedure have been reported elsewhere [15].

Fatty acid profile of the *n*-3 PUFA concentrate has been determined according to the AOAC Official Method [16] in a Hewlett Packard gas chromatograph (6890N Network GC System) equipped with an auto-sampler (7683B series) and a flame ionization detector (FID). The separation was carried out in a fused silica capillary column (Omegawax-320, 30 m×0.32 mm i.d.) with helium (1.8 mL/min) as carrier gas. Injection and detection temperatures, as well as ramp conditions have been previously reported [17]. Most of the fatty acids were identified by comparison of their retention times with those of chromatographic standards (Sigma Aldrich). As indicated by the AOAC method [16], an internal standard (methyl-tricosanoate, C23:0) was used for quantification purposes.

HPLC with diode array detection (HPLC-DAD) of the *n*-3 PUFA concentrate was carried out in order to detect tocopherol isomeric forms and other vitamin E analogs added to the *n*-3 PUFA concentrate, as their presence was reported by the provider. The analytical method is based on the IUPAC official method [18] with slight modifications, as reported in [17]. Separation was performed in an ACE 5 silica 250 mm × 4.6 mm column with 1 mL/min of hexane:2- propanol (99:1) as the mobile phase. An isocratic gradient was used, and the total run time was 15 min.  $\alpha$ -,  $\beta$ -,  $\gamma$ -, and  $\delta$ -tocopherols were monitored at  $\lambda = 296$  nm. For identification and quantification of each tocopherol isomer, a calibration curve with different amounts of the respective standard compound (Sigma Aldrich) was constructed.

### 2.3. Ultrasound-assisted emulsification

O/W emulsions were prepared following the procedure described by de Paz *et al.* [9]. The emulsion was formulated in a weigh proportion of 70:24:6 (water:carrier: *n*-3 PUFA concentrate), which was found to be the optimal in terms of obtaining the smallest droplet size [9]. The equipment used is a 20 kHz 750 W ultrasonic liquid processor Vibra-Cell 75043 (Sonics & Materials Inc.) with a Ø13 mm titanium alloy sonotrode. Experimental conditions have been also optimized in previous works [9]: amplitude was set at 100% and sound waves were delivered in pulses (5 s On/5 s Off) in order to avoid excessive heating of the sample, for a total processing time of 180 s. O/W emulsions were produced in batches of 100 g.

### 2.4. PGSS-drying

O/W emulsions were processed using the PGSS-drying technique in order to remove water and obtain a solid powder with the encapsulated *n*-3 PUFA concentrate loaded into the OSA-starch microparticles. Fig. 4-1 presents the schematic flow diagram of the PGSS-drying apparatus, in which CO<sub>2</sub> was fed by a membrane pump (LEWA) and preheated using a silicone bath before injection into the static mixer, where it was mixed with the O/W emulsion at the selected pressure and temperature. The CO<sub>2</sub> mass flow rate was measured with a Coriolis flow meter (Danfoss) with an accuracy of ± 0.1 kg CO<sub>2</sub>/h. Temperature before and after the static mixer was measured by means of Pt100 thermoresistances (accuracy of ± 0.1 K), being the later under PID control. Pressure in the CO<sub>2</sub> line and after the static mixer was measured with pressure transmitters (DESIN Instruments) with an accuracy of ± 0.05 MPa. Bourdon manometers (Nuova Firma) were installed to provide secondary lectures of the operating pressure.

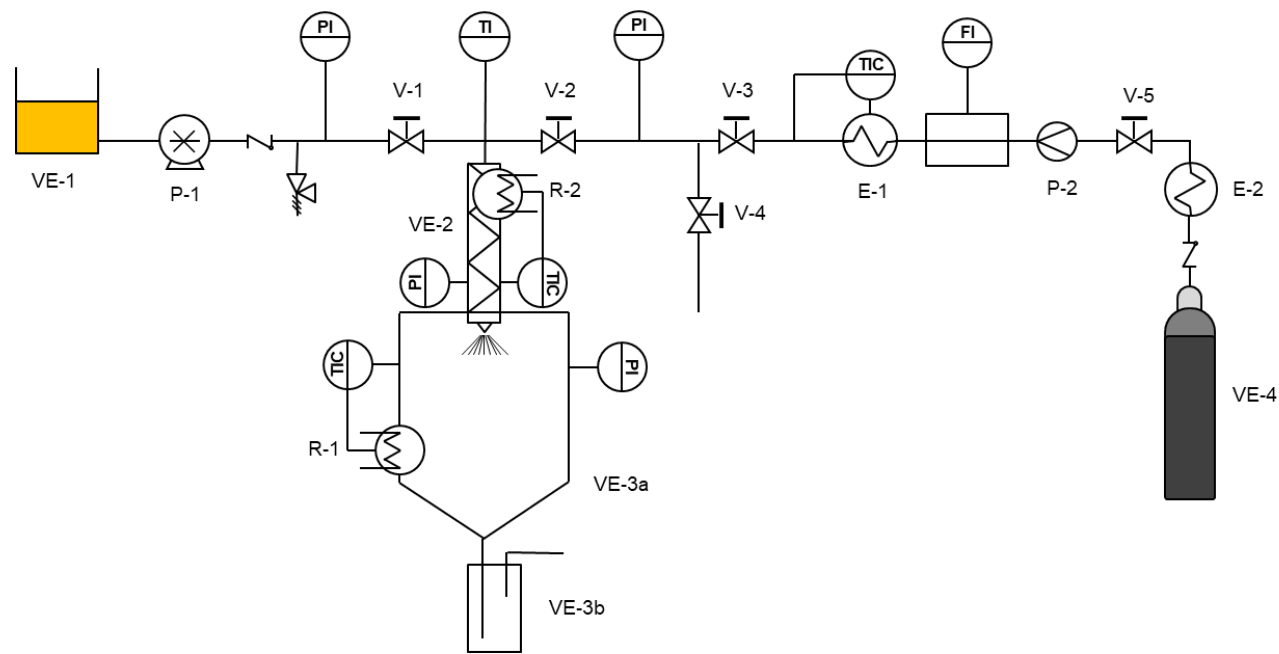


**Figure 4-1.** Schematic diagram of the PGSS-drying apparatus. VE-1: O/W emulsion vessel, VE-2: static mixer, VE-3: a) spraying tower, b) condenser, VE-4: CO<sub>2</sub> vessel, P-1: O/W emulsion pump, P-2: CO<sub>2</sub> pump, V-: process valve, E-: heat exchanger, R-: electrical resistance, PI: pressure indicator, TI(C): temperature indicator (and controller).

On the other hand, the O/W emulsion was pumped into the static mixer by a GILSON 305 piston pump (max. flow rate:  $25 \pm 0.1$  mL/min). The gas-saturated emulsion was then expanded into the spraying tower through a capillary nozzle with an internal diameter of 400  $\mu\text{m}$  (Spraying Systems Co., Ref.: PF1650-SS). The spraying tower was made of PVC and heated by electrical resistances. Temperature in the spray tower was also measured with a Pt100 probe and controlled using a PID.  $\text{CO}_2$  was vented off the spraying tower and passed through a water vapor condenser before final release. As security elements, a rupture disk, check valves, and a relief valve were installed at different points in the high-pressure circuit.

Typically, a PGSS-drying experiment began with the preheating of the system up to the desired temperature in the static mixer, which was fixed at 110 °C, and in the spraying tower, set at 55 °C. When the operating temperature in each vessel was achieved,  $\text{CO}_2$  was pumped up to the desired pressure, which was fixed at 10.0 MPa. Pressure and temperature conditions were chosen based on previous studies [19]. Once temperature and pressure conditions were stable, the emulsion pump was started at a flow rate such that the desired GPR, which was selected at 30 g/g, was obtained. After all the O/W emulsion was processed,  $\text{CO}_2$  was allowed to flow through the system at the same pressure and temperature conditions during 15 minutes in order to completely dry the particles. After that, the system was depressurized and particles were collected from the walls and bottom of the spraying tower and stored in darkness and refrigeration at 4 °C for subsequent analyses.

## 2.5. Spray-drying

Spray-drying is a conventional, well-known drying technique which is widely used in the pharmaceutical, cosmetic and food industries; thus, it was chosen to compare the characteristics of the powder that may be obtained conventionally to that obtained by the alternative PGSS-drying process. The spray-drying process was carried out in a commercial Buchi B-290 mini Spray-dryer. The O/W emulsion fed

to the spray-dryer was obtained following the procedure described in section 2.3. Operating conditions were: Inlet temperature 155 °C, which gave an outlet temperature of 100 °C; % pump was set at 8 %, which was equivalent to a mass flow of emulsion of 3.0 g/min. The emulsion was sprayed through a nozzle with 1.5 mm diameter and dried under a N<sub>2</sub> flow of 360 L/h.

## 2.6. Freeze-drying

O/W emulsions obtained by the US-assisted method described in section 2.3 were submitted to two different freezing methods: (1) conventional at -20 °C overnight, and (2) freezing with liquid nitrogen (N<sub>2</sub>) at -196 °C. Samples were then equilibrated for 2 h at -80 °C and submitted to freeze-drying in a Labconco Freeze Dry System at 1.5·10<sup>-4</sup> mbar during 48 h. These two different freezing methods were chosen in order to evaluate the effect of the freezing step, since the slower conventional freezing process is more likely to form large crystals of water, which could adversely affect the emulsion stability and structure, whereas the rapid freezing achieved with liquid N<sub>2</sub> could better preserve the physical structure of the emulsion.

## 2.7. Characterization of the O/W Emulsion

### 2.7.1. Particle size analysis of the O/W emulsion

The particle size (PS) of the O/W emulsion was measured by a Laser Diffraction (LD) equipment (Malvern Mastersizer 2000). Samples were dispersed in the suspension container with distilled water and measurement of the hydrodynamic diameter was carried out with gentle agitation in order to obtain a better dispersion of the particles. PS measurements are reported as relative volume distribution and defined by the mean diameter over volume (DeBroukere mean, D[4,3]) and as volume/surface mean diameter (Sauter mean, D[3,2]), as defined in Eqs. 4-1 and 4-2, respectively.

$$D[4,3] = \frac{\sum_1^n D_i^4 v_i}{\sum_1^n D_i^3 v_i} \quad (4-1)$$

$$D[3,2] = \frac{\sum_1^n D_i^3 v_i}{\sum_1^n D_i^2 v_i} \quad (4-2)$$

where  $D_i$  is the diameter of the  $i$ th particle.

The median particle size ( $d_{0.5}$ ), defined as the maximum particle diameter below which 50 % of the sample volume exists, is also reported. The span value, defined in Eq. 4-3, was also calculated.

$$\text{span} = \frac{d_{0.9} - d_{0.1}}{d_{0.5}} \quad (4-3)$$

where  $d_x$  is the maximum particle diameter below which  $x\%$  of the sample volume exists. Span values near to 1 indicate a narrow particle size distribution (PSD).

### 2.7.2. Emulsion stability

Physical stability of the O/W emulsion was analyzed by static multiple scattering in a vertical scan analyzer Turbiscan Lab Expert (Formulation Inc.) with ageing station AGS. By means of two optical sensors, the instrument measures the light transmitted through the emulsion ( $180^\circ$  from the incident light, transmission, T) and the light backscattered by the emulsion droplets ( $45^\circ$  from the incident light, backscattering, BS). The scanning process is made vertically along the glass cell from bottom to top, and the T/BS are each plotted as a function of the emulsion height in the glass cell. By monitoring the T/BS profiles at different time intervals, physical changes in the emulsion can be followed over time, which gives a detailed

overview of dispersion stability or instability. In the current work, the stability of the original emulsion was monitored at 4 h intervals for 24 days. Emulsion samples were kept in the ageing station at a constant temperature of 25 °C. As variations in T profiles were lower than 2%, only BS profiles at different storage times were analyzed in this study.

### 2.7.3. Density of the O/W emulsions

Density of original and reconstituted emulsions was measured in an Anton Paar DMA 5000 instrument at 25 °C. Each emulsion was measured at least in triplicate.

## 2.8. Characterization of the dried powders

### 2.8.1. Encapsulation efficiency

Encapsulation efficiency (EE) was determined according to the method described by Wang *et al.* [20] with some modifications. For the non-encapsulated oil determination, samples (*ca.* 1.0 g) of particles obtained by the different methods used in this work were suspended with 25 mL of hexane in a Falcon centrifuge tube, which was vortexed for 15 s at room temperature and centrifuged at 3000 rpm during 20 min. Immediately afterwards, the supernatant was taken and filtered, and its oil content was measured spectrophotometrically at  $\lambda = 286$  nm. The same procedure was repeated two additional times to extract the potentially remaining non-encapsulated oil. A calibration curve was previously constructed with known quantities of *n*-3 PUFA concentrate dissolved in hexane.

Total oil in the dried particles obtained by the different methods used in this work was determined following the AOAC Official Method [21]. Approximately 1.0 g of powder was weighed in a screw-capped glass tube and dissolved in 2 mL of ethanol. The mixture was vortexed for 15 s and 10 mL of 37% HCl were added.

Subsequently, each tube was tight-closed, vortexed again during 15 s and introduced in a water bath at 100 °C during 10 min. Digested samples were cooled down to ambient temperature and transferred to 50 mL Falcon centrifuge tubes, rinsing the glass tubes with 10 mL of ethanol. Afterwards, 25 mL of diethyl ether were added to the diluted samples, tubes were closed, and phases were mixed by inversion several times. Samples were centrifuged at 3000 rpm during 20 min and then 5 mL of the organic phase with the extracted oil were taken and transferred to tared round-bottom flasks in order to evaporate the solvent under vacuum (Heidolph rotary evaporator). Total oil in the samples was determined by mass difference of the initial clean round-bottom flask and that containing the extracted oil residue. Blanks with *ca.* 1.0 g of the carrier (Hi-Cap 100) were submitted to the same procedure for determination of fat traces, which were subtracted from the total oil content of the powders.

Encapsulation efficiency (EE) was calculated as defined in Eq. (4-4)

$$EE(\%) = \frac{TO - nEO}{TO} \cdot 100 \quad (4-4)$$

where TO is the total oil content and nEO is the non-encapsulated oil.

#### 2.8.2. Particle size analysis of the dried powders

Particle size analysis of the dried powders was carried out in a Malvern Mastersizer 2000 equipment, following the same procedure as in the original O/W emulsion (see section 2.7.1), yet firstly dissolving the dried powders in distilled water to obtain reconstituted emulsions. The original water:carrier:*n*-3 PUFA concentrate proportion (70:24:6 wt.) was maintained.

### 2.8.3. Moisture content

Moisture content of the dried particles was determined gravimetrically. Samples (*ca.* 0.5 g) of particles obtained by the different methods used in this work were weighed before and after drying in an oven at 120 °C until constant weight.

### 2.8.4. Scanning electron microscopy (SEM)

Morphology of the dried particles was observed in a Scanning Electron Detector microscope JEOL JSM-6460LV with Energy Dispersive X-ray (JEOL Ltd. Japan) operating at 20 kV. Samples were gold-sputtered and observed with magnifications of 1500, 5000 and 10000x for PGSS- and spray-dried particles, and 50, 400 and 2000 or 3000x for the freeze-dried powders.

### 2.8.5. Differential scanning calorimetry (DSC)

A TA Instruments Q200 differential scanning calorimeter with refrigerated cooling system (RCS90) and nitrogen purge gas was used. Melting point and enthalpies of indium were used for temperature and heat capacity calibration. Samples (*ca.* 10 mg) were placed in TA Tzero 40- $\mu$ L aluminum pans and closed with hermetic aluminum lids with pinhole. An empty pan closed with pin-holed lid was used as a reference. Starting temperature of the DSC analysis was set at 40 °C, which was held for 30 min. Then, the system was cooled down to -80 °C at 10 °C·min<sup>-1</sup>. After an isothermal period of 30 min, samples were heated from -80 °C to 350 °C at a constant heating rate of 10 °C·min<sup>-1</sup>. DSC thermograms were recorded and analyzed with the Advantage v. 5.5.20 software (TA Instruments).

## 2.9. Measurement of lipid oxidation

Oxidative status of the dried powders was determined in terms of primary oxidation (peroxide value, PV) and secondary oxidation (Thiobarbituric Acid Reactive Substances, TBARS). To observe the effect of each drying method, PV and TBARS of the fish oil concentrate and the O/W emulsions before drying were also measured.

For the dried powders, PV and TBARS were measured right after each drying method and monitored over a 28-day storage period. Dried powders were placed in closed containers and stored at 4 °C in darkness and ambient oxygen concentration. Samples were withdrawn at 7-day intervals and dissolved in distilled water to obtain reconstituted emulsions with the original water:carrier:*n*-3 PUFA concentrate proportion (70:24:6 wt.). PV and TBARS analyses were carried out as follows.

### 2.9.1. Peroxide Value

PV was measured spectrophotometrically with a Hitachi U-2000 apparatus and following the method described by Shanta *et al.* [22] with slight modifications. In brief, 10-50 mg of oil or 0.025-1.0 mL of emulsion, depending on the expected PV, were taken in a centrifuge tube and mixed with 1.5 mL of isooctane:2-propanol (3:1 v/v). The tube was vortexed for 15 s and centrifuged at 5000 rpm during 10 min. Immediately afterwards, 0.2 mL of the supernatant were transferred to a new centrifuge tube and 2.8 mL of methanol:1-butanol (2:1 v/v) were added. After vortexing for 15 s, 15 µL of 3.94 M ammonium thiocyanate, and 15 µL of a Fe<sup>2+</sup> solution were added. The Fe<sup>2+</sup> solution was obtained by mixing 0.132 M barium chloride in 0.4 M HCl and 0.144 M Iron(II) sulphate heptahydrate (1:1 v/v), centrifuging at 5000 rpm for 10 min, and taking the supernatant. Samples were vortexed again for 15 s and kept in darkness for 20 min. Blanks were prepared the same as above with 0.3 mL of distilled water instead of the oil or emulsion sample. Hydroperoxyde concentration was determined spectrophotometrically at  $\lambda = 510$  nm.

A calibration curve was constructed using known concentrations of cumene hydroperoxide, ranging from 0.13 to 3.28 mM. Results were expressed in milliequivalents of oxygen per kg of *n*-3 PUFA concentrate (meq O<sub>2</sub>/kg oil).

#### 2.9.2. TBARS analysis

TBARS present in the *n*-3 PUFA concentrate were determined following the method described by Ke and Woyewoda [23]. Briefly, 10 mg of *n*-3 PUFA concentrate were weighed in a screw-capped glass test tube. 5 mL of TBA work solution, which was prepared by mixing 0.04M 2-thiobarbituric acid in glacial acetic acid, chloroform, and 0.3M sodium sulphite (12:8:1 v/v), were also added to the screw-capped glass test tube. The mixture was vortexed for 15 s and incubated in a water bath at 95 °C during 45 min. After cooling down the test tubes under running cold water, 2.5 mL of 0.28M trichloroacetic acid were added to the samples, which were then mixed by inversion. Samples were then centrifuged at 2500 rpm for 10 min in order to separate the pink aqueous phase from the chloroform phase. Absorbance of the aqueous phase was measured at  $\lambda = 538$  nm in a Hitachi U-2000 spectrophotometer. Blanks were prepared the same as above, yet without the oil, and subtracted from the absorbance measurement.

TBARS analysis of the original and reconstituted O/W emulsions was carried out following the method described by Mei *et al.* [24] with slight modifications. Briefly, 0.025-1.0 mL of emulsion, depending on the expected oxidative status, were taken in screw-capped glass test tubes. Distilled water was used to complete to 1.0 mL if necessary. Subsequently, 2 mL of a TCA/TBA mixture – which was prepared by dissolving 7.5 g of TCA into 10 mL of 0.25M HCl, adding this solution to 0.1875 g of TBA and completing to volume with 0.25M HCl in a 50 mL volumetric flask – were added and the glass test tube was tightly closed, vortexed for 15 s and immersed in a water bath at 95 °C during 15 min. Then the vials were cooled down under running cold water and centrifuged at 5000 rpm during 10 min. Immediately

afterwards, the supernatant was collected and its absorbance measured in a Hitachi U-2000 spectrophotometer at  $\lambda = 538$  nm. Blank runs were also performed the same as above, but without adding the emulsion, and its absorbance subtracted from the measurements.

TBARS concentration in the emulsion and the *n*-3 PUFA concentrate samples was determined using a TEP standard curve with concentrations ranging from 2.5 to 20 nM. Results were expressed in mg malondialdehyde equivalents (MW = 72.06 g/mol) per kg of *n*-3 PUFA concentrate (mg MDA/kg oil).

## 2.10. Statistical analysis

All results reported in this work represent the average of at least three replicates. Statistical analyses were performed using Statgraphics Centurion XVII software. Statistical significance was determined by analysis of variance (ANOVA) using the Fisher's least significant difference test. Results were deemed as statistically significant when  $p < 0.05$ .

# 3. Results and discussion

## 3.1. Characterization of the *n*-3 PUFA concentrate

Results obtained in the characterization analysis are summarized in Table 4-1. As it can be seen from Table 4-1a, the fatty acid profile of the *n*-3 PUFA concentrate is constituted by more than 90 % *n*-3 PUFAs, being 73.49 % identified as DHA. Neutral lipid profile of the *n*-3 PUFA concentrate (Table 4-1b) also showed that more than the 75 % of the neutral lipids in the *n*-3 PUFA concentrate are in the form of triacylglycerides, with 21.6 % being in the form of fatty acid ethyl-esters. Traces of diacylglycerides and monoacylglycerides (1.2% and 0.7 %, respectively) were also found. The high content of triacylglycerides is an important feature of the *n*-3

PUFA concentrate, since these compounds are the natural form of food lipids and they may present better bioavailability and stability against oxidation [25]. Tocopherol analysis by HPLC-DAD revealed a racemic mixture of tocopherol added as antioxidant (again, this is in consonance with consumers preference for natural sources).  $\alpha$ -,  $\beta$ -,  $\gamma$ -, and  $\delta$ -tocopherol isomers were identified and quantified. Results are showed in Table 4-1c.

### 3.2. Emulsion stability

Physical stability of the O/W emulsion was analyzed by static multiple scattering. Changes in the backscattering profile ( $\Delta$ BS) were recorded every 4 h during 24 days of storage at 25 °C and plotted vs. time in Fig. 4-2. As shown in the figure,  $\Delta$ BS in the top-section reached 5% increment on day 2 and started to decrease in the lower section ( $|\Delta$ BS| > 2%) on day 5, indicating creaming destabilization due to phase separation and migration of the lighter oil droplets to the top zone. Moreover, a slight BS increase over time in the middle section of the glass cell can be seen (Fig. 4-2), indicating an increase in the emulsion droplet size over time.

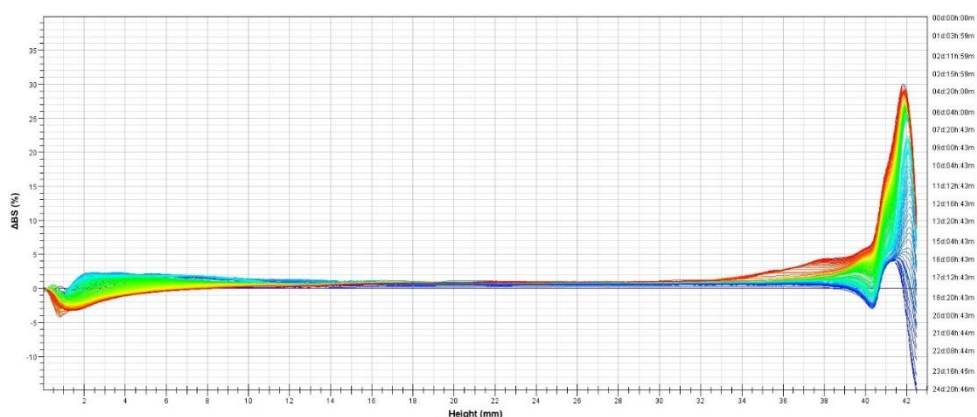


**Figure 4-2.** Changes in the backscattering profile ( $\Delta$ BS) over time in the US-assisted O/W emulsion.

**Table 4-1.** Characterization of the fish oil concentrate.

<b>a) Fatty acid profile (GC-FID)</b>		
<b>Trivial name</b>	<b>Formula</b>	<b>% wt.</b>
Palmitic	C16:0	0.17
Palmitoleic	C16:1 <i>n</i> -7	0.21
Stearic acid	C18:0	0.14
Oleic	C18:1 <i>n</i> -9	0.46
Vaccenic	C18:1 <i>n</i> -7	0.09
Linoleic (cis and trans)	C18:2 <i>n</i> -6	0.23
Gondoic	C20:1 <i>n</i> -9	0.16
Stearidonic	C18:4 <i>n</i> -3	0.19
Eicosatrienoic	C20:3 <i>n</i> -3	1.22
Eicosapentaenoic	C20:5 <i>n</i> -3 (EPA)	9.24
Cetoleic	C22:1 <i>n</i> -11	0.20
Docosadienoic	C22:2 <i>n</i> -6	3.04
Adrenic	C22:4 <i>n</i> -6	0.25
Docosapentaenoic <i>n</i> -6	C22:5 <i>n</i> -6	2.72
Docosapentaenoic <i>n</i> -3	C22:5 <i>n</i> -3	7.86
Docosahexaenoic	C22:6 <i>n</i> -3 (DHA)	73.49
Nervonic	C24:1	0.31

<b>b) Neutral lipid profile (NP-HPLC)</b>	
<b>Lipid class</b>	<b>% wt.</b>
Triacylglycerides	76.5
Diacylglycerides	1.2
Monoacylglycerides	0.7
Fatty acid ethyl-esters	21.6

<b>c) Tocopherol analysis (HPLC-DAD)</b>	
<b>Total (racemic, mg /g oil)</b>	<b>% wt.</b>
	2.19
<b>Isomeric form</b>	<b>% wt.</b>
$\alpha$ -tocopherol	53.2
$\beta$ -tocopherol	5.9
$\gamma$ -tocopherol	28.2
$\delta$ -tocopherol	12.7

Standard uncertainties are  $u(\% \text{ wt.})_{\text{GC-FID}} = \pm 0.1$ ;  $u(\% \text{ wt.})_{\text{NP-HPLC}} = \pm 0.5$ ;  $u(\% \text{ wt.})_{\text{HPLC-DAD}} = \pm 0.1$

### 3.3. Density of the O/W emulsions

Density measurements were carried out for the original emulsion as well as for the reconstituted dried powders. Results obtained are shown in Table 4-2. As it can be observed, no statistical difference ( $p < 0.05$ ) can be found between the densities of the original and reconstituted emulsions, being those the means of three independent measurements. Thus, an average value of  $1.091281 \text{ g}\cdot\text{cm}^{-3}$  was used for the volume-to-mass transformations.

**Table 4-2.** Density of the original O/W emulsion and the reconstituted powders obtained by the different drying methods. Water:carrier:fish oil concentrate proportion was kept the same as the original (70:24:6 wt.)

Emulsion	Density ( $\text{g}\cdot\text{cm}^{-3}$ )
Original	1.091282 <sup>a</sup>
PGSS-drying	1.091279 <sup>a</sup>
Spray-drying	1.091281 <sup>a</sup>
Freeze-drying (-20°C)	1.091283 <sup>a</sup>
Freeze-drying (liq N <sub>2</sub> )	1.091280 <sup>a</sup>
Average	$1.091281 \pm 2 \cdot 10^{-6}$

<sup>a</sup> Different upper-scripts denote statistically significant differences at  $p < 0.05$

### 3.4. Particle Size Analysis

Results from particle size analysis are reported in Table 4-3 for the original emulsion and the reconstituted powders. In general, similar values for D[4,3] and D[3,2] were found in all samples, barring the conventionally freeze-dried powder which showed significantly higher values for both D[4,3] and D[3,2], which means that the reconstituted emulsion from the conventionally freeze-dried powder presented larger mean diameters both in volumetric and surface basis, respectively.

Median particle size by volume ( $d_{0.5}$ ) of the emulsion is sub-micrometric, with  $d_{0.5} = 0.114 \text{ }\mu\text{m}$  and a D[4,3] and D[3,2] of  $0.144 \text{ }\mu\text{m}$  and  $0.114 \text{ }\mu\text{m}$ , respectively.

On the other hand, the drying methods proposed in this work slightly increased  $d_{0.5}$  after reconstitution, with the exception being the freeze-dried particles with liquid  $N_2$ , in which no statistically significant differences were found with the original emulsion. Still, most particle populations were around  $0.130 \mu\text{m}$  for particles obtained by PGSS-drying, freeze-drying and spray-drying methods. The span values followed a similar trend, with original < freeze-drying (liq  $N_2$ ) < spray-drying  $\approx$  freeze-drying ( $-20^\circ\text{C}$ ) < PGSS-drying. The higher span values in the reconstituted emulsions may be due to higher polydispersity.

**Table 4-3.** Results obtained in the particle size analysis of the original O/W emulsion and the reconstituted powders obtained by the different drying methods. Water:carrier:fish oil concentrate proportion was kept the same as the original (70:24:6 wt.)

Emulsion	D[4,3] <sup>*</sup>	D[3,2] <sup>†</sup>	$d_{0.5}$ ( $\mu\text{m}$ )	span <sup>‡</sup>
Original	0.144 <sup>a</sup>	0.114 <sup>a</sup>	0.114 <sup>a</sup>	1.150 <sup>a</sup>
PGSS-drying	0.227 <sup>b</sup>	0.116 <sup>a</sup>	0.134 <sup>b</sup>	2.197 <sup>d</sup>
Spray-drying	0.197 <sup>b</sup>	0.112 <sup>a</sup>	0.129 <sup>b</sup>	1.636 <sup>c</sup>
Freeze-drying ( $-20^\circ\text{C}$ )	0.567 <sup>c</sup>	0.121 <sup>b</sup>	0.131 <sup>b</sup>	1.772 <sup>c</sup>
Freeze-drying (liq $N_2$ )	0.146 <sup>a</sup>	0.107 <sup>a</sup>	0.118 <sup>a</sup>	1.291 <sup>b</sup>

$$^* D[4,3] = \frac{\sum_1^n D_{i,v_i}^4}{\sum_1^n D_{i,v_i}^3} ; ^\dagger D[3,2] = \frac{\sum_1^n D_{i,v_i}^3}{\sum_1^n D_{i,v_i}^2} ; ^\ddagger \text{span} = (d_{0.9} - d_{0.1})/d_{0.5}$$

<sup>a,b,c,d</sup> Different upper-scripts denote statistically significant differences at  $p < 0.05$

The particle size distribution plot (Fig. 4-3) revealed a bimodal size distribution for the O/W emulsion, possibly representing single and aggregated particles. Fig. 4-3 also reflects the increase in the median particle size and span values occurred after drying of particles by the different proposed methods (Table 4-3), with wider and lower peaks. The particle population around  $1 \mu\text{m}$  is also larger in the reconstituted emulsions when compared to the original (Fig. 4-3), indicating that some aggregation occurred after the formulation of particles and further reconstitution. A notable exception is the freeze-dried emulsion frozen with liquid nitrogen, in which the rapid and deep freezing process has possibly preserved its particle size

distribution more similar to the original (Fig. 4-3). In the case of the spray-dried and PGSS-dried particles, aggregation may have been caused by changes in the solution viscosity and surface tension during the drying process, which may result in the formation of larger droplets at the exit of the nozzle, which subsequently influence the final particle size [26]. In the PGSS-drying process, the extraction of water along the static mixer may also have an important effect in the emulsion viscosity and the surface tension of the oil droplets [11]. It is also noticeable that rehydrated particles obtained by conventional freeze-drying showed a small population (1.53 % vol.) of particles in the range around 5-35  $\mu\text{m}$  (Fig. 4-3). This is probably due to the growing of large water crystals during the slow conventional freezing process, which may have partially destabilized the O/W emulsion causing the release of the *n*-3 PUFA concentrate and the formation of large oil droplets after reconstitution.

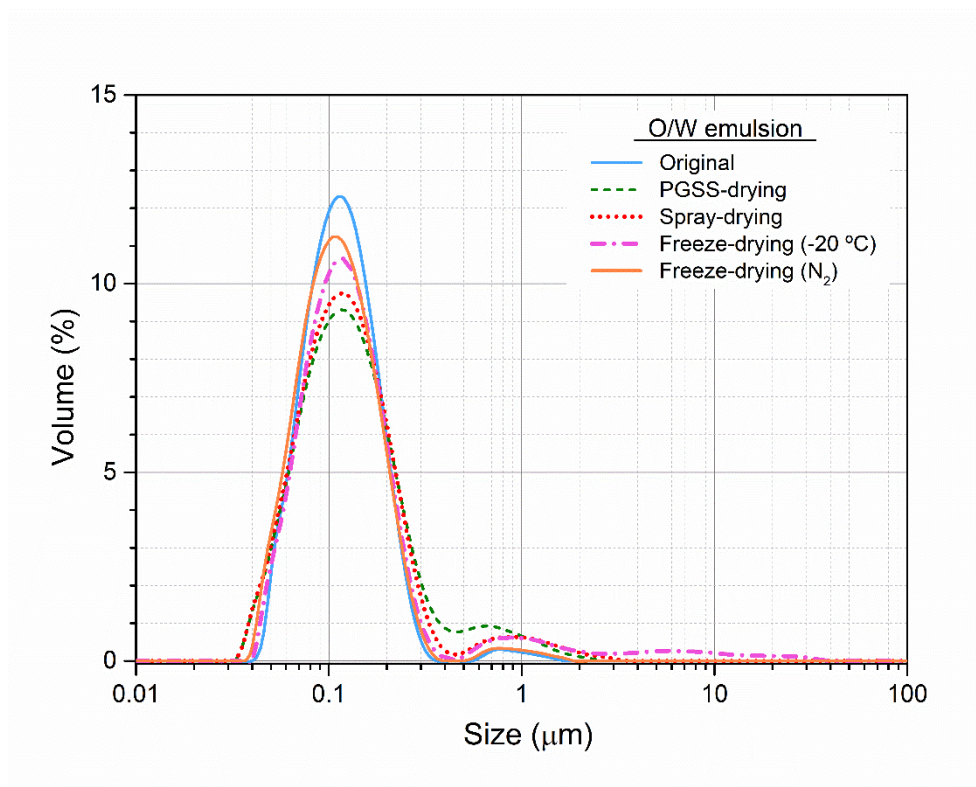


**Figure 4-3.** Particle size distribution plot of the original O/W emulsion and the reconstituted powders obtained by the different drying methods. Water:carrier:fish oil concentrate proportion was kept the same as the original (70:24:6 wt.)

### 3.5. Encapsulation efficiency

Encapsulation efficiency is one of the most important quality parameters in encapsulated fish oil and *n*-3 PUFA concentrates. The presence of free oil may adversely affect the physical properties of the final product, such as flowability and bulk density, and would also enhance lipid oxidation [20]. Fig. 4-4 presents the encapsulation efficiency of the powders loaded with Algatrium™ Plus obtained via the different drying methods proposed in this work.

Results showed high initial encapsulation efficiencies no matter the drying method used to obtain the powders (Fig. 4-4). It can be noticed that the powder obtained by freeze-drying with conventional -20°C freezing presents a slightly lower initial encapsulation efficiency, with  $EE = 95.8 \pm 0.2 \%$  (Fig. 4-4). As it has been previously mentioned, it is likely that partial destabilization of the emulsion and release of small amounts of *n*-3 PUFA concentrate may have happened, probably due to the mechanical and hygroscopic forces caused by the growing of large water crystals during the slow freezing process. By comparison, freeze-dried particles obtained with liquid nitrogen present the highest encapsulation efficiency with  $98.6 \pm 0.1 \%$  (Fig. 4-4), which reflects that the emulsion casting is preserved with a rapid and deep freezing step. Similar results have been also obtained by Lévai *et al.* [27] dealing with freeze-dried quercetin encapsulated in soybean lecithin. Still, more than 95 % of the total *n*-3 PUFA concentrate loading was encapsulated by conventional freeze-drying, and almost 98 % encapsulation efficiency was obtained by PGSS-drying ( $97.9 \pm 0.3 \%$ ), which is similar to the EE value of the spray-dried microparticles ( $97.5 \pm 0.1 \%$ ). Carneiro *et al.* [28] compared combinations of maltodextrin and Hi-Cap and other wall materials to encapsulate flaxseed oil by spray-drying, finding Hi-Cap as the best in terms of EE, with  $EE = 95.7 \%$ . Results obtained in this work are slightly higher than those reported in the literature in all cases except for conventionally freeze-dried particles, which is likely due to the optimized US-assisted emulsification process [9], together with the non-aggressive conditions in which the powders have been obtained.

Surface oil of the dried particles has been analyzed over time during 28 days of storage at 4°C in darkness and ambient oxygen concentration to check if some of the *n*-3 PUFA concentrate could have been released. As Fig. 4-4 shows, spray-dried particles released around 2% of the total encapsulated *n*-3 PUFA concentrate during the first 7 days and then the release continued at a lower rate, down to 94 % encapsulated oil after 28 days. In the case of the conventionally freeze-dried particles, a slight decrease in the encapsulated oil can be seen after the second week of storage; whereas for the PGSS- and freeze-dried particles frozen with liquid N<sub>2</sub>, no significant changes in the encapsulation efficiency were noted during the first 21 days and only a slight decrease started to occur after the fourth week of storage.

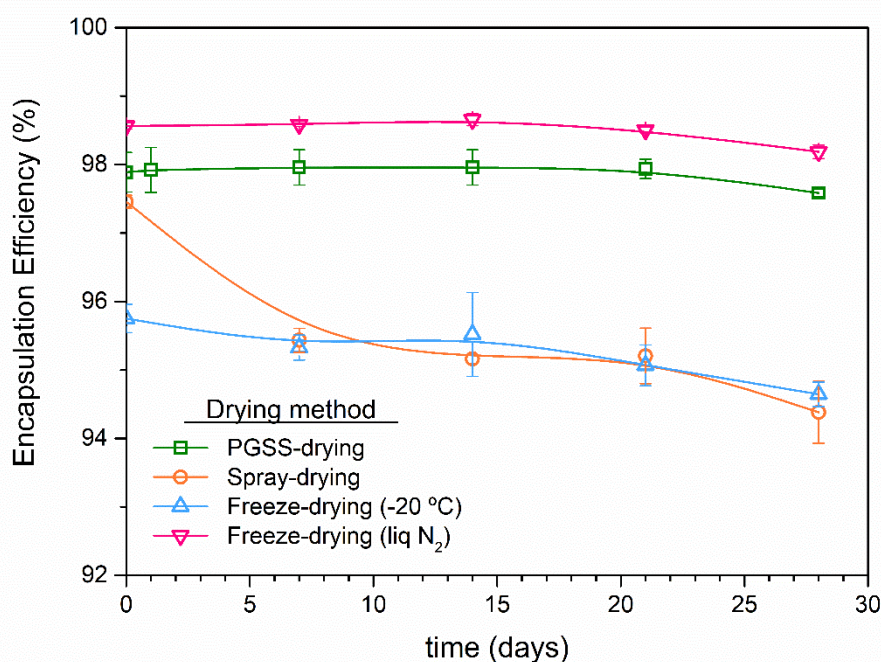


**Figure 4-4.** Encapsulation efficiency of the powders obtained by the different drying methods. Powders were stored at 4°C in darkness and ambient oxygen concentration. Lines are drawn to guide the eye.

### 3.6. Moisture content

Table 4-4 presents the moisture content of particles prepared with different drying methods. The spray-dried particles showed the highest residual humidity, whereas the PGSS-drying technique gave the lowest moisture value. Humidity values for the spray-dried particles found in this work are higher than those reported in the literature, which are usually around 1-3 % [28,29]. In the case of the freeze-dried particles, no significant difference in the final humidity was found ( $p < 0.05$ ), no matter the freezing method used (conventional at  $-20\text{ }^{\circ}\text{C}$  or with liquid nitrogen).

**Table 4-4.** Moisture content of the powders obtained by the different drying methods.

Drying method	Moisture (%)
PGSS-drying	$3.33 \pm 0.32^a$
Spray-drying	$5.60 \pm 0.20^c$
Freeze drying ( $-20^{\circ}\text{C}$ )	$4.66 \pm 0.05^b$
Freeze drying (liq $\text{N}_2$ )	$4.68 \pm 0.13^b$

<sup>a,b,c</sup> Different upper-scripts denote statistically significant differences at  $p < 0.05$

### 3.7. Particle morphology (SEM)

Visual morphology of the dried powders can be observed in the SEM micrographs depicted in Fig. 4-5. Both PGSS- and spray-dried particles present spherical morphology. For the PGSS-dried particles, diameters range from  $1.5\text{ }\mu\text{m}$  to  $5\text{ }\mu\text{m}$ , and some larger agglomerates around  $10\text{ }\mu\text{m}$  can be seen (Fig. 4-5 a). Fractured particles are also seen in some micrographs, showing a porous internal structure in which the  $n-3$  PUFA is probably encapsulated. Spray-dried particles show more variance in size, with small particles around  $1\text{ }\mu\text{m}$  together with some specimens larger than  $10-20\text{ }\mu\text{m}$  (Fig. 4-5 b). This variety in size has been also reported in the literature [28] and seems to be a typical characteristic of particles produced by this method.

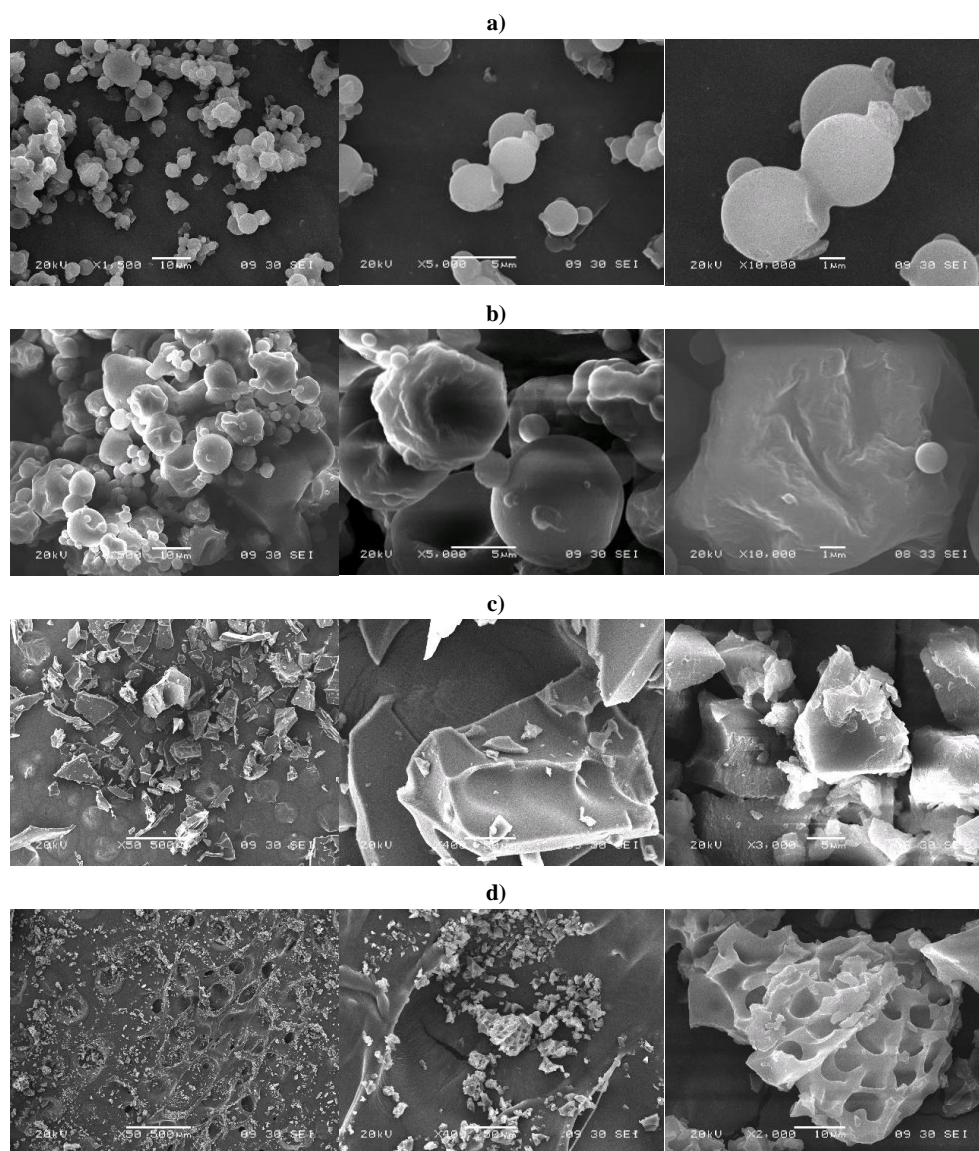


**Figure 4-5.** SEM micrographs of the dried powders. a) powder obtained by PGSS-drying, b) powder obtained by spray-drying; from left to right, 1500x, 5000x and 10000x magnifications. c) powder obtained by conventional freeze-drying (50x, 400x and 3000x). d) powder obtained by freeze-drying with liquid N<sub>2</sub>; (50x, 400x and 2000x).

Spray-dried particles also showed a rougher surface than PGSS-dried samples, with more imperfections or ‘teeth’. These surface depressions are associated to the collapse of the particle hollow core once the crust is formed during the initial stages of drying. Similar morphological characteristics have been also found in the literature [28].

In the case of the freeze-dried particles, larger and more irregular particles have been produced. Conventionally freeze-dried powder presents a flakey or scaly appearance, forming planar structures with some dimensions being larger than 100  $\mu\text{m}$  (Fig. 4-5 c). Some dents can be seen in the surface of several particles, probably corresponding to the voids left by water crystals after sublimation. In larger magnifications (3000x) a porous internal structure can be also appreciated, being the *n*-3 PUFA concentrate likely encapsulated inside these vesicles. In the case of the freeze-dried powder frozen with liquid  $\text{N}_2$  (Fig. 4-5 d), a powder finer than the conventionally frozen (Fig. 4-5 c) has been obtained. Some particles show an alveolar structure, which may have been formed by liquid nitrogen boiling during freezing of the O/W emulsion. These alveolar holes present diameters around 5-7.5  $\mu\text{m}$ .

### 3.8. Differential scanning calorimetry (DSC)

DSC runs of PGSS-dried particles, modified OSA-starch (Hi-Cap 100) used as a carrier, and fish oil concentrate revealed cold-crystallization, glass-transition (gelatinization) and melting peaks. The peak temperatures of these thermal events are summarized in Table 4-5. Endothermic peaks near 80 °C were observed in the PGSS-dried and Hi-Cap 100 samples, which probably correspond to the glass transition (gelatinization) of OSA-starch. A second endothermic peak was found around 220 °C in both PGSS-dried particles and Hi-Cap 100, which may be linked to the melting of OSA-starch. Similar glass-transition and melting temperatures have been reported in the literature for this polymer [30].

**Table 4-5.** Peak temperatures of the thermal events observed in the PGSS-dried powder loaded with *n*-3 PUFA concentrate (PGSS-drying), the carrier alone (Hi-Cap™ 100), and the *n*-3 PUFA concentrate alone (Algatrium™ Plus).

Sample	Peak temperature (°C)		
	Cold crystallization	Glass transition	Melting
PGSS-dried particles	-72.99	76.57	223.55
Hi-Cap™ 100	n.d.	78.83	217.05
Algatrium™ Plus	-71.42	n.d.	n.d.

In the lower temperature range, an exothermic cold-crystallization peak was noticeable for the fish oil concentrate and for the PGSS-dried particles, which may correspond to a lipid compound of the fish oil concentrate transitioning from liquid to solid state. This assumption can be corroborated by the studies of Tolstorebrov *et al.* [31], in which cold-crystallization peaks in the range -75 to -55 °C have been reported for some olein-, linolenin-, and linolein-containing tryacylglycerides, which are minority constituents of the fish oil concentrate (Table 4-2a). The slightly lower crystallization temperature observed in the PGSS-dried particles is probably linked to the particle shell offering external resistance to heat transfer to the encapsulated fish oil concentrate, thus delaying the cold crystallization event.

### 3.9. Oxidative stability of the dried powders

Peroxide value (PV) and thiobarbituric acid reactive substances (TBARS) have been systematically determined in the PGSS-dried powders with and without ascorbic acid (AA) during 28 days of storage at 4 °C and dark conditions.

In order to determine the initial oxidative status, PV and TBARS were measured in the *n*-3 PUFA concentrate and in the original emulsion right after US-assisted emulsification. With the purpose of comparing the different drying methods used in this work, PV and TBARS of the spray-dried and the freeze-dried particles were measured after formulation of the powders (day 0) and after 28 days of storage under

the same conditions as the PGSS-dried particles (4°C, darkness). Results obtained are summarized in Figs. 4-6 to 4-9.

Fig. 4-6 shows that PV increases from  $1.64 \pm 0.05$  meq O<sub>2</sub>/kg oil in the *n*-3 PUFA concentrate (Algatrium™ Plus) up to  $5.6 \pm 0.3$  meq O<sub>2</sub>/kg oil during the US-assisted emulsification process, which slightly surpasses the maximum limit of 5 meq O<sub>2</sub>/kg oil for fish oil concentrates intended for direct human consumption [32]. It is likely that the high energy input involved in the ultrasonication process promoted a temperature increase that may negatively affect the oxidative status of the *n*-3 PUFA concentrate [8]. As a strategy to prevent primary oxidation during US-assisted emulsification, 20 mM ascorbic acid (AA) was added to the emulsion formulation. AA concentration was selected based on Uluata *et al.* [3] studies on lipid oxidation in O/W emulsions.

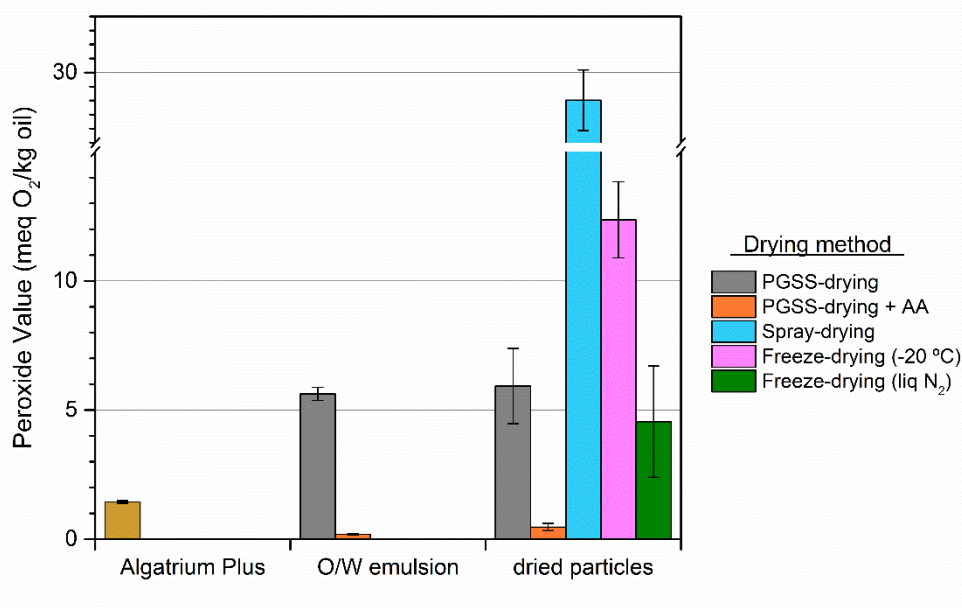


**Figure 4-6.** Peroxide Value (PV) of the *n*-3 PUFA concentrate (Algatrium™ Plus), the US-assisted O/W emulsions, and the particles obtained by the different drying methods right after drying. Samples were reconstituted the day of analysis keeping the original water:carrier:fish oil concentrate proportion (70:24:6 wt.).

As it can be seen in Fig. 4-6 (O/W emulsion), the antioxidant successfully protected the *n*-3 PUFA concentrate and even reduced the PV of the emulsion down to  $0.19 \pm 0.03$  meq O<sub>2</sub>/kg oil. This behavior has been also observed by Uluata *et al.* in O/W emulsions with AA [3] and it is likely related to AA's ability to inactivate free radicals such as lipid hydroperoxides. Other mechanisms can be also involved in the observed antioxidant activity, since AA can act as an oxygen scavenger thanks to the enediol group in carbons 2 and 3 [33,34], or even play a synergistic role by means of regenerating other antioxidants such as the tocopherol originally present in the *n*-3 PUFA concentrate [35]. However, it is not easy to determine which of these pathways is taking place in any given food system [3] and it is likely that all of them occur simultaneously.

If we focus on the PV results obtained after formulation of the dried particles (Fig. 4-6), it can be seen that PGSS-drying promoted a slight PV increase up to  $5.9 \pm 1.5$  meq O<sub>2</sub>/kg oil in the emulsion without AA, although this value is not significantly different ( $p < 0.05$ ) from the PV of the original emulsion. Furthermore, AA addition have a significant ( $p < 0.05$ ) effect on the PV of the PGSS-dried particles, since only a slight increase from  $0.19 \pm 0.03$  to  $0.5 \pm 0.1$  meq O<sub>2</sub>/kg oil was observed in the PGSS-dried particles with antioxidant (Fig. 4-6).

On the other hand, the spray-drying process yielded particles with much lower oxidative quality (PV =  $28.0 \pm 1.6$  meq O<sub>2</sub>/kg oil). As some authors have pointed out for the spray-drying process [36,37], it is likely that the rapid formation of the particle shell increased the resistance to evaporation of water trapped inside the particle core, promoting a rapid temperature increase in the particles and prolonging the *n*-3 PUFA exposure to high temperatures, thus promoting oxidation and increasing the PV after spray-drying formulation. The freeze-drying process with liquid nitrogen achieved good results, with PV =  $4.6 \pm 1.8$  meq O<sub>2</sub>/kg oil, which is not statistically different ( $p < 0.05$ ) from that of the original emulsion (Fig. 4-6). This result can be related to the freeze-drying process being a degradation-free technology, since the samples are not submitted to high processing temperatures and

processed in absence of light and in an almost inert atmosphere due to vacuum conditions. Unexpectedly, the conventionally frozen emulsion did overcome oxidation despite the favourable processing conditions ( $PV = 12.4 \pm 1.5$  meq  $O_2$ /kg oil) (Fig. 4-6). This is much likely due to oxygen contact during the conventional freezing step, in which the samples were held overnight at  $-20^\circ\text{C}$  under ambient oxygen concentration.

In view of the results (Fig. 4-6), we can infer that PGSS-drying is a suitable method to formulate dried particles loaded with *n*-3 PUFAs, more so if we combine the mild processing conditions with the addition of an antioxidant such as AA. As it has been previously stated, the short residence time of the O/W emulsion in the PGSS-drying system as well as the inert  $CO_2$  atmosphere prevent the loaded bioactive compounds from degradation [13] and as such, fish oil concentrate can be successfully protected from oxidation.

Oxidative stability of the PGSS-dried particles was monitored during 28 days of storage in darkness at  $4^\circ\text{C}$  (Fig. 4-7). Results obtained showed a sustained increase of primary oxidation, reaching values of  $PV = 25.2 \pm 0.7$  meq  $O_2$ /kg oil after 28 days of storage (Fig. 4-7). On the other hand, AA successfully protected the PGSS-dried particles from primary oxidation during storage, being the values found significantly lower ( $p < 0.05$ ) than those of the PGSS-dried particles without antioxidant. The highest PV was found after 14 days of storage and was  $2.5 \pm 0.5$  meq  $O_2$ /kg oil, still below the maximum allowable limit according to legislation, and remained with no significant changes ( $p < 0.05$ ) during the rest of the 28-day storage period, reaching a final value of  $2.2 \pm 0.3$  meq  $O_2$ /kg oil (Fig. 4-7).

Comparing the primary oxidation of the particles obtained by the different drying methods after 28 days of storage (Fig. 4-7), we can see the same trend as in the PV analysis after formulation, although PV increased in all samples. Freeze-dried particles frozen with liquid nitrogen maintained a relatively low PV of  $16.9 \pm 0.8$  meq  $O_2$ /kg oil, which is likely linked to the good encapsulation efficiency and the preservation of the physical structure of the emulsion thanks to the fast and deep-

cooling effect of liquid nitrogen. The same was not true for the conventionally freeze-dried particles, with PV =  $37.7 \pm 3.7$  meq O<sub>2</sub>/kg oil after 28 days of storage. Spray-dried particles showed the highest PV with  $66.0 \pm 0.4$  meq O<sub>2</sub>/kg oil after 28 days of storage. The higher oxidation rates of these two samples (spray-drying and conventional freeze-drying) are probably due to the high starting PV (Fig. 4-6) as well as their lower encapsulation efficiency, which implies more oil in the particle surface susceptible to oxidation. A similar encapsulation efficiency vs. oxidation rate inverse relationship has been observed by other authors [38].

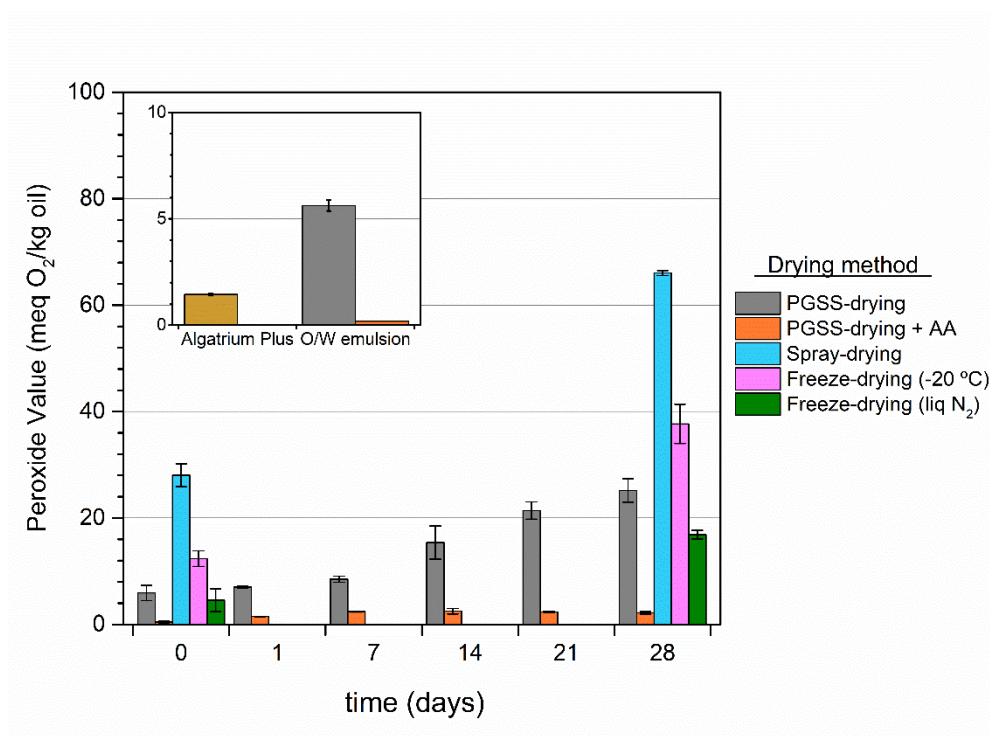


**Figure 4-7.** PV evolution of the dried particles during storage at 4°C in darkness and ambient oxygen conditions. Samples were reconstituted the day of analysis keeping the original water:carrier:fish oil concentrate proportion (70:24:6 wt.). **Inset:** original PV of the *n*-3 PUFA concentrate (AlgaTrium™ Plus) and the US-assisted O/W emulsions.

However, PGSS-dried and freeze-dried particles with liquid nitrogen exhibited high encapsulation efficiencies (up to 98%), and still encapsulated *n*-3 PUFA concentrate was not fully protected against primary oxidation (PV after 28 days =  $25.2 \pm 2.2$  and  $16.9 \pm 0.8$  meq O<sub>2</sub>/kg oil, respectively). This trend can be explained by taking into account not only the oxidation of the oil present in the particle surface, but also oxygen diffusion through the encapsulating material. It must be also pointed out that the fish oil concentrate used in this work is extremely rich in *n*-3 PUFAs, which are highly prone to oxidation. This highly sensitive-to-oxidation fatty acid profile may also offer an explanation to the higher oxidation rates obtained in this work compared to other studies, even with no accelerated storage [28,38].

Results of TBARS analysis are summarized in Figs. 4-8 and 4-9. Although there is no legal maximum limit for this parameter in food products, we can take the values of 10 μmol MDA equiv/kg fish and 1-2 μmol MDA equiv/g fat given in the FAO guidelines [39] as an orientative basis to evaluate rancidity of the *n*-3 PUFA concentrate (1 μmol MDA equiv/g fat corresponds to 72.06 mg MDA/kg oil). From Fig. 4-8 we can see that initial TBARS of the *n*-3 PUFA concentrate lay below this rancidity limit (TBARS =  $41.1 \pm 2.7$  mg MDA/kg oil). US-assisted emulsification slightly increased the TBARS value up to  $54.8 \pm 0.6$  mg MDA/kg oil in the formulation without AA, whereas the addition of AA yielded particles with TBARS =  $42.8 \pm 1$  mg MDA/kg oil (Fig. 4-8). In view of the results, AA addition successfully slowed down secondary oxidation during the ultrasonication step since no significant difference ( $p < 0.05$ ) between the AA-added emulsion and the *n*-3 PUFA concentrate was found (Fig. 4-8).

Among the dried powders (Fig. 4-8), spray-dried particles showed the highest secondary oxidative status with a TBARS value of  $88.5 \pm 6.0$  mg MDA/kg oil, which is above the FAO rancidity limit [39]. PGSS-drying process slightly increased TBARS up to  $59.4 \pm 4.4$  mg MDA/kg oil, whereas the addition of AA did not make any statistically significant difference ( $p < 0.05$ ). Both PGSS-drying with and without AA, and freeze-dried powder with liquid N<sub>2</sub> showed no statistically

significant differences with the original emulsion, which gives an idea of the protective effect of these drying methods against secondary oxidation. On the contrary, the conventionally frozen particles were not successfully protected, and TBARS increased up to  $74.5 \pm 3.5$  mg MDA/kg oil after the conventional freeze-drying process.

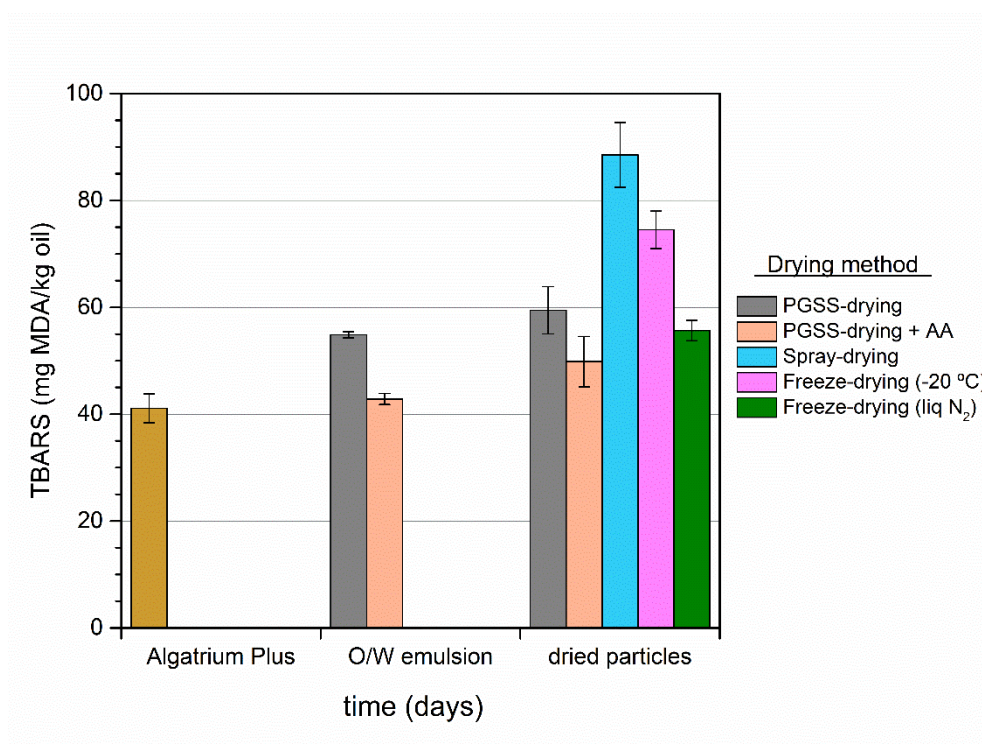


**Figure 4-8.** Thiobarbituric acid reactive substances (TBARS) content of the *n*-3 PUFA concentrate (Algatrium™ Plus), the US-assisted O/W emulsions, and the particles obtained by the different drying methods right after drying. Samples were reconstituted the day of analysis keeping the original water:carrier:fish oil concentrate proportion (70:24:6 wt.).

Secondary oxidation products were also monitored in the PGSS-dried particles during the 28-day storage period. In Fig. 4-9, we can see that TBARS in the PGSS-dried particles without AA did not significantly increase ( $p < 0.05$ ) up to the second week of storage, when TBARS value increased from  $69.2 \pm 1.4$  mg MDA/kg oil up to  $110.9 \pm 1.8$  mg MDA/kg oil, reaching a final value of  $141.0 \pm 1.9$  mg MDA/kg oil.

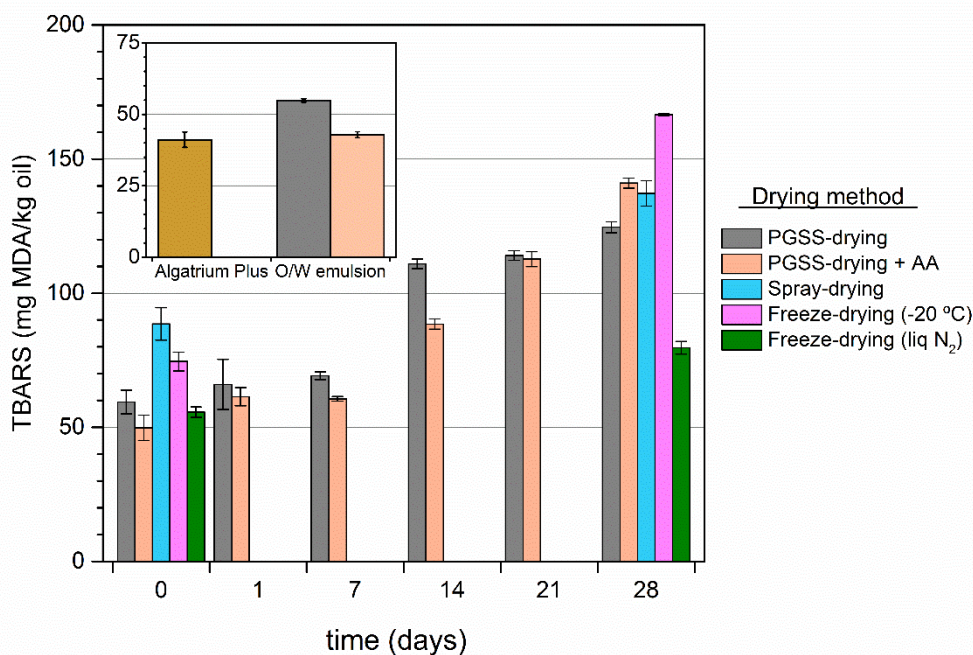


**Figure 4-9.** TBARS evolution of the dried particles during storage at 4°C in darkness and ambient oxygen conditions. Samples were reconstituted the day of analysis keeping the original water:carrier:fish oil concentrate proportion (70:24:6 wt.). **Inset:** TBARS of the *n*-3 PUFA concentrate (Alga-trium™ Plus) and the original US-assisted O/W emulsions.

On the other hand, AA addition delayed secondary oxidation for the first 14 days of storage, obtaining significantly lower ( $p < 0.05$ ) TBARS values than those of the control sample without antioxidant, yet increasing thereafter and even exceeding the control without AA after 28 days of storage (TBARS = 141.0 ± 1.9 mg MDA/kg oil). As previously mentioned, this behavior has been observed by other authors when studying the effect of ascorbic acid on lipid oxidation in O/W emulsions, especially in presence of transition metals such as iron and copper [3,24]. Uluata *et al.* [3] provide an explanation related to the ability of AA to reduce metal ions, making them more reactive towards peroxides and hydroperoxides. According to this proposed mechanism, reduced metallic species would decompose peroxides and

hydroperoxides into secondary oxidation products, increasing the observed TBARS and preventing the accumulation of primary oxidation intermediaries [3]. This behavior has been also observed in this work, although no metals were added to the O/W emulsion. However, it is possible that traces were present in the *n*-3 PUFA concentrate, enabling this hypothesis.

Additionally, it has been found that spray-dried and conventionally freeze-dried particles underwent secondary oxidation during the 28-day storage period, with final TBARS values of  $137.2 \pm 4.7$  mg MDA/kg oil and  $166.6 \pm 0.3$  mg MDA/kg oil, respectively (Fig. 4-9). Again, this high secondary oxidation status might be linked to the poorer encapsulation efficiency of those methods. On the other hand, freeze-dried particles frozen with liquid N<sub>2</sub> showed good stability against secondary oxidation during storage, maintaining a TBARS value of  $79.6 \pm 2.4$  during 28 days of storage at 4°C.

## Conclusion

Particles from Gas-Saturated Solutions (PGSS)-drying has been used to encapsulate omega-3 polyunsaturated fatty acids (*n*-3 PUFAs) into octenyl-succinic-anhydride (OSA) starch, obtaining a solid powder with high bioactive load (almost 20% wt.).

Spherical microparticles with an EE = 97.9 % have been produced by PGSS-drying. This is the highest EE reported in the literature for *n*-3 PUFA concentrates in OSA-starch. Similar morphologies and EE were obtained by conventional spray-drying. Freeze-dried particles showed irregular morphology. Conventional freezing negatively affected EE due to emulsion destabilization by mechanical and hygroscopic forces produced by large water crystals (EE = 95.8 %), which was overcome by fast freezing with liquid nitrogen (EE = 98.6%). DSC analysis of the PGSS-dried particles successfully identified cold crystallization of the *n*-3 PUFA concentrate as well as gelatinization and melting peaks of OSA-starch.

In comparison with conventional spray-drying, PGSS-drying offers lower drying temperature and an intrinsically inert atmosphere, which avoid oxidative degradation of *n*-3 PUFAs during processing, as demonstrated by the oxidative stability analyses. Conventional freeze-drying method yielded particles with low oxidative stability, whereas freezing with liquid N<sub>2</sub> resulted in a powder with oxidative stability comparable to PGSS-dried particles. Combined with the addition of natural antioxidants such as ascorbic acid, the PGSS-drying technique rises as a suitable method to formulate *n*-3 PUFAs in solid form and protect them against oxidation during shelf life.



## References

- [1] C.H.S. Ruxton, S.C. Reed, M.J.A. Simpson, K.J. Millington, The health benefits of omega-3 polyunsaturated fatty acids: A review of the evidence, *Journal of Human Nutrition and Dietetics*. 17 (2004) 449–459.
- [2] EFSA Panel on Dietetic Products Nutrition and Allergies (NDA), Scientific opinion on the substantiation of health claims related to eicosapentaenoic acid (EPA), docosahexaenoic acid (DHA), docosapentaenoic acid (DPA) *etc.*, *EFSA Journal*. 8 (2010) 1796.
- [3] S. Uluata, D.J. McClements, E.A. Decker, How the multiple antioxidant properties of ascorbic acid affect lipid oxidation in oil-in-water emulsions, *Journal of Agricultural and Food Chemistry*. 63 (2015) 1819–1824.
- [4] E. Niki, Lipid peroxidation: Physiological levels and dual biological effects, *Free Radical Biology and Medicine*. 47 (2009) 469–484.
- [5] J. Löliger, F. Saucy, Synergetic antioxidant mixture, Patent EP0326829B1, 1994.
- [6] M.Y. Baik, E.L. Suhendro, W.W. Nawar, D.J. McClements, E.A. Decker, P. Chinachoti, Effects of antioxidants and humidity on the oxidative stability of microencapsulated fish oil, *Journal of the American Oil Chemists' Society*. 81 (2004) 355–360.
- [7] A.M. Bakry, S. Abbas, B. Ali, H. Majeed, M.Y. Abouelwafa, A. Mousa, L. Liang, Microencapsulation of oils: a comprehensive review of benefits, techniques, and applications, *Comprehensive Reviews in Food Science and Food Safety*. 15 (2016) 143–182.
- [8] S. Abbas, K. Hayat, E. Karangwa, M. Bashari, X. Zhang, An overview of ultrasound-assisted food-grade nanoemulsions, *Food Engineering Reviews*. 5 (2013) 139–157.
- [9] E. de Paz, Ó. Benito, M.T. Sanz, R. Melgosa, Á.G. Solaesa, S. Beltrán, Formulation of highly rich omega-3 concentrate by ultrasounds emulsification: study of oxidation stability, *Journal of Food Engineering*. (*submitted*).
- [10] Á. Martín, H.M. Pham, A. Kilzer, S. Kareth, E. Weidner, Micronization of polyethylene glycol by PGSS (Particles from Gas Saturated Solutions)-drying of aqueous solutions, *Chemical Engineering and Processing*. 49 (2010) 1259–1266.

- [11] E. de Paz, Á. Martín, M.J. Cocero, Formulation of  $\beta$ -carotene with soybean lecithin by PGSS (Particles from Gas Saturated Solutions)-drying, *The Journal of Supercritical Fluids*. 72 (2012) 125–133.
- [12] M. Türk (Ed.), *Particle Formation with Supercritical Fluids, Challenges and Limitations*, Vol. 6, 1st ed., Elsevier, 2014.
- [13] E. Weidner, High pressure micronization for food applications, *The Journal of Supercritical Fluids*. 47 (2009) 556–565.
- [14] Á. Martín, E. Weidner, PGSS-drying: mechanisms and modeling, *The Journal of Supercritical Fluids*. 55 (2010) 271–281.
- [15] Á.G. Solaesa, M.T. Sanz, M. Falkeborg, S. Beltrán, Z. Guo, Production and concentration of monoacylglycerols rich in omega-3 polyunsaturated fatty acids by enzymatic glycerolysis and molecular distillation, *Food Chemistry*. 190 (2016) 960–967.
- [16] AOAC International, Official methods of analysis of the Association of Official Analytical Chemists. AOAC Official Method 2012.13. Determination of labeled fatty acids content in milk products and infant formula (2012).
- [17] S. Rebolleda, N. Rubio, S. Beltrán, M.T. Sanz, M.L. González-San José, Supercritical fluid extraction of corn germ oil: study of the influence of process parameters on the extraction yield and oil quality, *The Journal of Supercritical Fluids*. 72 (2012) 270–277.
- [18] W.D. Pocklington, A. Dieffenbacher, Determination of tocopherols and tocotrienols in vegetable oils and fats by high performance liquid chromatography, *Pure and Applied Chemistry*. 60 (1988) 877–892.
- [19] S. Varona, S. Rodríguez Rojo, Á. Martín, M.J. Cocero, A.T. Serra, T. Crespo, C.M.M. Duarte, Antimicrobial activity of lavandin essential oil formulations against three pathogenic food-borne bacteria, *Industrial Crops and Products*. 42 (2013) 243–250.
- [20] Y. Wang, W. Liu, X. Dong, C. Selomulya, Micro-encapsulation and stabilization of DHA containing fish oil in protein-based emulsion through mono-disperse droplet spray dryer, *Journal of Food Engineering*. 175 (2016) 74–84.
- [21] AOAC International, Official methods of analysis of the Association of Official Analytical Chemists. AOAC Official Method 925.32. Fat in eggs, acid hydrolysis method (2005).



- [22] N.C. Shantha, E.A. Decker, Rapid, sensitive, iron-based spectrophotometric methods for determination of peroxide values of food lipids, *Journal of AOAC International*. 77 (1994) 421–424.
- [23] P.J. Ke, A.D. Woyewoda, Microdetermination of thiobarbituric acid values in marine lipids by a direct spectrophotometric method with a monophasic reaction system, *Analytica Chimica Acta*. 106 (1979) 279–284.
- [24] L. Mei, D.J. McClements, J. Wu, E.A. Decker, Iron-catalyzed lipid oxidation in emulsion as affected by surfactant, pH and NaCl, *Food Chemistry*. 61 (1998) 307–312.
- [25] N. Rubio-Rodríguez, S. Beltrán, I. Jaime, S.M. de Diego, M.T. Sanz, J.R. Carballido, Production of omega-3 polyunsaturated fatty acid concentrates: a review, *Innovative Food Science & Emerging Technologies*. 11 (2010) 1–12.
- [26] S. Drusch, Y. Serfert, M. Scampicchio, B. Schmidt-Hansberg, K. Schwarz, Impact of physicochemical characteristics on the oxidative stability of fish oil microencapsulated by spray-drying, *Journal of Agricultural and Food Chemistry*. 55 (2007) 11044–11051.
- [27] G. Lévai, Á. Martín, A. Moro, A.A. Matias, V.S.S. Gonçalves, M.R. Bronze, C.M.M. Duarte, S. Rodríguez-Rojo, M.J. Cocero, Production of encapsulated quercetin particles using supercritical fluid technologies, *Powder Technology*. 317 (2017) 142–153.
- [28] H.C.F. Carneiro, R. V Tonon, C.R.F. Grosso, M.D. Hubinger, Encapsulation efficiency and oxidative stability of flaxseed oil microencapsulated by spray drying using different combinations of wall materials, *Journal of Food Engineering*. 115 (2013) 443–451.
- [29] S.A. Hogan, B.F. McNamee, E.D. O’Riordan, M. O’Sullivan, Emulsification and microencapsulation properties of sodium caseinate/carbohydrate blends, *International Dairy Journal*. 11 (2001) 137–144.
- [30] L. Yu, G. Christie, Measurement of starch thermal transitions using differential scanning calorimetry, *Carbohydrate Polymers*. 46 (2001) 179–184.
- [31] I. Tolstorebrov, T.M. Eikevik, M. Bantle, A DSC determination of phase transitions and liquid fraction in fish oils and mixtures of triacylglycerides, *Food Research International*. 58 (2014) 132–140.

- [32] Codex Alimentarius Commission, Standard for Fish Oils - Codex Stan 329-2017, Rome, Italy, 2017.
- [33] L.E. Johnson, Food technology of the antioxidant nutrients, *Critical Reviews in Food Science and Nutrition*. 35 (1995) 149–159.
- [34] M.-L. Liao, P.A. Seib, Chemistry of L-ascorbic acid related to foods, *Food Chemistry*. 30 (1988) 289–312.
- [35] D.W. Reische, D.A. Lillard, R.R. Eitenmiller, Antioxidants. In: C.C. Akoh and D.B. Min (Eds.), *Food Lipids: Chemistry, Nutrition and Biotechnology*, CRC Press, 2008, 413–422.
- [36] S. Drusch, S. Berg, Extractable oil in microcapsules prepared by spray-drying: localisation, determination and impact on oxidative stability, *Food Chemistry*. 109 (2008) 17–24.
- [37] H. Wang, F. Liu, L. Yang, Y. Zu, H. Wang, S. Qu, Y. Zhang, Oxidative stability of fish oil supplemented with carnosic acid compared with synthetic antioxidants during long-term storage, *Food Chemistry*. 128 (2011) 93–99.
- [38] J. Yang, O.N. Ciftci, Encapsulation of fish oil into hollow solid lipid micro- and nanoparticles using carbon dioxide, *Food Chemistry*. 231 (2017) 105–113.
- [39] H.H. Huss, *Quality and Quality Changes in Fresh Fish*. FAO Fisheries technical paper - 348, Food and Agriculture Organization of the United Nations, Rome, 1995.

Valorization of fish by-products using supercritical carbon dioxide technologies

## Conclusions and Future Challenges



## Conclusions and future challenges

Notwithstanding that each chapter contains its own conclusion, the following general concluding remarks can be established from the experimental studies carried out along this PhD Thesis and the results obtained.

- Production of omega-3 polyunsaturated fatty acids ( $n-3$  PUFAs) from fish oil, obtaining nutraceuticals and food supplements with high added value, constitutes a great opportunity for valorization of this by-product.
  - Development of industrially-feasible production methods that could yield less oxidized, highly purified  $n-3$  PUFAs, is a challenge for the pharmaceutical and food industries.
  - A biorefinery approach using supercritical fluid (SCF) technologies, combining the latest advances in supercritical fluid extraction and refining of fish oil, production, concentration and purification of  $n-3$  PUFAs, as well as formulation using SCF technologies, enables the possibility of obtaining  $n-3$  PUFAs without solvent residues at mild, non-oxidative conditions.
- Lipase-catalyzed ethanolysis of fish oil triacylglycerides in supercritical carbon dioxide (SC-CO<sub>2</sub>) is an attractive alternative to produce  $n-3$  PUFAs at mild and non-oxidative conditions, obtaining high reaction yields in short time. Reaction products are obtained in a chemical form (Fatty acid ethyl esters, FAEEs) that could be easily fractionated and purified by downstream SCF technologies.
- The catalytic activity of lipases can be affected by exposure to subcritical or supercritical carbon dioxide (sub/SC-CO<sub>2</sub>), mainly due to conformational changes and structural alterations. The extension of these changes strongly depends on the experimental conditions of the sub/SC-CO<sub>2</sub> treatment, the nature and source of the enzyme, and whether the enzyme is presented in a free or immobilized form.



- Together with the understanding of the effects of sub/SC-CO<sub>2</sub> on the biocatalyst activity, knowledge of the phase behavior of oils rich in *n*-3 PUFAs with ethanol and CO<sub>2</sub> at high pressures is another fundamental aspect for the correct design of the lipase-catalyzed ethanolysis of fish oil in SC-CO<sub>2</sub> process, since phase behavior can influence the reaction performance as well as the further fractionation and purification of the reaction products. Depending on the pressure, temperature, and amount of solvent (CO<sub>2</sub>), 2- or 3-phase mixtures consisting of one or two expanded liquid(s) and a gas phase, or a homogeneous supercritical phase can be obtained.
- Lipozyme RM IM from *Rhizomucor miehei* showed high activity in the ethanolysis of fish oil in SC-CO<sub>2</sub>. This solvent provided an environmentally benign reaction medium with no oxygen, which in turn yield less oxidized reaction products compared to other reaction media such as solvent-free or hexane. Lipozyme RM IM showed higher thermal stability in SC-CO<sub>2</sub> than in hexane. Besides, no dead-end inhibition due to ethanol has been observed.
- Formulation of *n*-3 PUFAs into a stable form and protected from oxidation is one of the major challenges of the omega-3 industry. Encapsulation technologies using SCF such as Particles from Gas-Saturated Solutions (PGSS)-drying are capable of encapsulate high loads of *n*-3 PUFAs at lower drying temperatures compared to spray drying and in an intrinsically inert atmosphere, which avoid oxidative degradation during processing.



Future challenges proposed are:

- Studying different alternatives to obtain structured lipids rich in  $n-3$  PUFAs through enzymatic catalysis in SC-CO<sub>2</sub> in TAG or partial acylglyceride (DAG and MAG) forms, which would be more desirable in terms of bioavailability and stability against oxidation. Different reactions such as hydrolysis, glycerolysis, and interestification, as well as other biocatalysts such as Lipozyme 435 from *Candida antarctica* would be explored.
- Implementing the continuous lipase-catalyzed modification of fish oil in SC-CO<sub>2</sub>, with extraction and further fractionation of the reaction products. This would include the design and construction of a continuous supercritical reactor and a series of separators, as well as studying the solubility of the reaction products (FAEE, DAG, MAG, and glycerol) in CO<sub>2</sub>.
- Optimizing the PGSS-drying process by exploring different emulsification methods such as high-pressure homogenization, using other encapsulating materials and/or adding natural antioxidants, in order to reduce the  $n-3$  PUFA oxidation during emulsification and improve the stability of the PGSS-dried microparticles during shelf life.
- Lastly, combining the points above together with the knowledge about supercritical extraction and refining of fish oil obtained in previous works (see refs. [17,33,34,77] of the Introduction), developing an integral and industrially-scalable process that would constitute a biorefinery aimed at the valorization of fish oil and the production of non-oxidized, highly purified  $n-3$  PUFA concentrates with better stability and bioavailability.

## Conclusiones y retos futuros

Si bien cada uno de los capítulos de la Tesis contiene sus propias conclusiones, los siguientes puntos se enumeran a modo de conclusiones generales extraídas del trabajo realizado y de los resultados obtenidos a lo largo de la Tesis Doctoral.

- La producción de ácidos grasos poliinsaturados omega-3 (AGPI  $n-3$ ) a partir de aceite de pescado para obtener alimentos funcionales, nutracéuticos y suplementos alimenticios con alto valor añadido constituye una gran oportunidad para la valorización de este subproducto.
  - El desarrollo y puesta en marcha a nivel industrial de métodos capaces de producir AGPI  $n-3$  con baja oxidación y alta pureza es un reto para las industrias farmacéutica y alimentaria.
  - La combinación, utilizando el enfoque global de biorrefinería, de los últimos avances en extracción y refinado de aceite de pescado mediante tecnologías de fluidos supercríticos (FSCs), así como la producción, concentración y purificación de AGPI  $n-3$  con FSCs, ofrece la posibilidad de obtener AGPIs  $n-3$  sin residuos de disolventes y en condiciones suaves y no oxidativas.
- La etanolisis de aceite de pescado catalizada por lipasas en dióxido de carbono supercrítico (CO<sub>2</sub>-SC) constituye una buena alternativa para la producción de AGPI  $n-3$  en condiciones suaves y no oxidativas, con altas conversiones y en tiempos de reacción cortos. Además, los productos de reacción se obtienen en una forma química (ésteres etílicos de ácidos grasos, EE) fácilmente manejable en los sucesivos pasos de fraccionamiento y purificación con FSCs.
- La actividad catalítica de las lipasas estudiadas puede verse afectada por la exposición al dióxido de carbono en condiciones sub- o supercríticas (CO<sub>2</sub>-sub/SC). Esto se debe principalmente a cambios conformacionales y alteraciones estructurales cuya extensión depende de las condiciones en las que se lleva a cabo el tratamiento con CO<sub>2</sub>-sub/SC, a la naturaleza y fuente de la enzima y a la inmovilización o no de la misma.

- Junto con los efectos del CO<sub>2</sub>-sub/SC sobre la actividad de los biocatalizadores empleados, el conocimiento del equilibrio entre fases de aceites ricos en AGPI *n*-3 con etanol y CO<sub>2</sub> a altas presiones es otro de los aspectos clave para el correcto diseño de los procesos de etanolisis de aceite de pescado catalizada por lipasas en CO<sub>2</sub>-SC. Esto se debe a que el equilibrio entre fases puede tener influencia sobre el rendimiento de la reacción, así como en los sucesivos procesos de fraccionamiento y purificación de los productos de reacción. Dependiendo de la presión, temperatura y proporción de disolvente (CO<sub>2</sub>), pueden encontrarse mezclas bi- o trifásicas constituidas por uno o dos líquidos expandidos y un gas; o bien un sistema monofásico constituido por una sola fase supercrítica homogénea.
- La lipasa Lipozyme RM IM de *Rhizomucor miehei* ha mostrado alta actividad en la etanolisis de aceite de pescado en CO<sub>2</sub>-SC. Este disolvente proporciona un medio de reacción ecológico y anóxico, lo que se traduce en productos de reacción sin residuos. La oxidación de los productos de reacción es menor si se emplea CO<sub>2</sub>-SC en lugar de disolventes convencionales como hexano o medio de reacción sin disolvente. Lipozyme RM IM presenta mayor estabilidad térmica en CO<sub>2</sub>-SC que en hexano. Además, no se ha observado inhibición del catalizador por etanol.
- La formulación de AGPI *n*-3 en forma estable y protegida frente a la oxidación es uno de los mayores retos a los que se enfrenta la industria de los omega-3. Los métodos de encapsulación que utilizan FSCs, tales como *Particles from Gas-Saturated Solutions (PGSS)-drying* ofrecen la posibilidad de encapsular altas cantidades de AGPI *n*-3 con temperaturas de secado más bajas comparadas con el secado por pulverización, y en una atmósfera intrínsecamente libre de oxígeno, lo cual evita la degradación oxidativa del producto durante el procesado.

Los retos futuros que se plantean tras la presente Tesis son:

- Estudiar diferentes alternativas de catálisis enzimática en CO<sub>2</sub>-SC para obtener lípidos estructurados ricos en AGPI *n*-3 en forma de TAG o de acilglicéridos parciales (DAG y MAG), las cuales son formas químicas más deseables en términos de biodisponibilidad y estabilidad frente a la oxidación. Pueden explorarse otras reacciones distintas de la etanolisis, tales como hidrólisis, glicerolisis o interesterificación; u otros biocatalizadores como Lipozyme 435 de *Candida antarctica*, que ha mostrado resultados prometedores en estudios preliminares sobre etanolisis de aceite de pescado en CO<sub>2</sub>-SC.
- Implementar el proceso en continuo de modificación de aceite de pescado catalizada por lipasas en CO<sub>2</sub>-SC, con posterior extracción y fraccionamiento de los productos de reacción. Incluyendo el diseño y construcción de un reactor supercrítico en continuo y varios separadores en serie, así como estudios de solubilidad de los productos de reacción (EE, DAG, MAG y glicerol) en CO<sub>2</sub>.
- Optimizar el proceso de *PGSS-drying*, explorando nuevos métodos de emulsificación como la homogeneización a alta presión, usando materiales encapsulantes de diferente naturaleza y/o añadiendo antioxidantes naturales, con el objetivo de reducir la oxidación de los AGPIs *n*-3 durante la emulsificación y mejorar la estabilidad de las micropartículas secas durante su vida útil.
- Por último, combinar los puntos anteriores junto con los conocimientos sobre extracción y refinado supercríticos de aceite de pescado obtenidos en trabajos previos (ver refs. [17,33,34,77] de la Introducción), desarrollando un proceso integral que pueda ser llevado a escala industrial, constituyendo así una biorrefinería para la valorización de aceite de pescado y la producción de concentrados de AGPI *n*-3 más estables y biodisponibles, con baja oxidación y alta pureza.

Fish oil valorization using supercritical carbon dioxide technologies

## Appendix Analytical Methods

## Table of Contents

Tables.....	277
Figures .....	279
1. Characterization of catalysts .....	283
1.1. Enzyme activity .....	283
1.2. Moisture content .....	287
1.3. Fluorescence spectrophotometry .....	289
1.4. FT-IR analysis of the chemical structure of the catalysts .....	290
1.5. Analysis of solid microstructure by Scanning Electron Microscope (SEM) .....	292
2. Characterization of fish oil, reaction products, and omega-3 concentrates .	294
2.1. Determination of free fatty acid content .....	294
2.2. Analysis of the fatty acid profile by GC-FID .....	296
2.3. Determination of the neutral lipids profile by NP HPLC-ELSD .....	300
2.4. Determination of peroxide value (PV).....	304
2.5. Determination of anisidine value .....	306
2.6. Analysis of Thiobarbituric Acid Reactive Substances (TBARS) .....	308
3. Characterization of O/W emulsions and microencapsulated omega-3 concentrates.....	311
3.1. Particle size analysis .....	311
3.2. Determination of peroxide value in O/W emulsions .....	314
3.3. Analysis of TBARS in O/W emulsions .....	316
3.4. Encapsulation efficiency .....	318
3.5. Moisture content .....	322
3.6. Analysis of thermal properties of the microparticles by Differential Scanning Calorimetry (DSC) .....	323
3.7. Analysis of solid microstructure by Scanning Electron Microscope (SEM) .....	324
References.....	325



## Tables

<b>Table A-1.</b> Temperature program used for the analysis of fatty acids by GC-FID.....	298
<b>Table A-2.</b> Retention times of standard lipid compounds identified by GC-FID.....	299
<b>Table A-3.</b> Binary solvent gradient used in neutral lipid analysis by HPLC-ELSD. ....	302
<b>Table A-4.</b> Calibration solutions of 1,1,3,3-tetraethoxypropane (TEP) for TBARS quantification in fish oil, reaction, and fish oil concentrate samples.....	310
<b>Table A-5.</b> Calibration solutions of 1,1,3,3-tetraethoxypropane (TEP) for TBARS quantification in O/W emulsions.....	315
<b>Table A-6.</b> Calibration solutions of 1,1,3,3-tetraethoxypropane (TEP) for TBARS quantification in O/W emulsions.....	317
<b>Table A-7.</b> Calibration solutions of fish oil concentrate for quantification of non-encapsulated oil. ....	320
<b>Table A-8.</b> Temperature program used for the DSC analysis. ....	324



## Figures

<b>Figure A-1.</b> Varian Cary Eclipse Fluorescence Spectrophotometer with Peltier-thermostated cell holder and temperature controller.....	289
<b>Figure A-2.</b> FT-IR equipment (adapted from <a href="http://www.ubu.es.../ft-ir">www.ubu.es.../ft-ir</a> ).....	290
<b>Figure A-3.</b> Scheme of a Scanning Electron Microscope (SEM) equipment (adapted from [5]).....	292
<b>Figure A-4.</b> JEOL JSM-6460LV Scanning Electron Microscope (adapted from <a href="http://www.ubu.es.../meh">www.ubu.es.../meh</a> ).....	293
<b>Figure A-5.</b> GC-FID equipment.....	296
<b>Figure A-6.</b> GC-FID chromatogram of fish oil.....	298
<b>Figure A-7.</b> NP HPLC-ELSD equipment.....	300
<b>Figure A-8.</b> HPLC-ELSD chromatogram of neutral lipid classes. Fatty acid ethyl esters (FAEE), triacylglycerides (TAG), free fatty acids (FFA), diacylglycerides (DAG), and monoacylglycerides (MAG).....	302
<b>Figure A-9.</b> Chemical reaction between an aldehydic compound and p-anisidine, producing a Schiff base with maximum absorption at $\lambda = 350$ nm. ....	306
<b>Figure A-10.</b> Reactions involved in TBARS analysis. (1) Hydrolysis reaction of 1,1,3,3-tetraethoxypropane (TEP) to yield malondialdehyde (MDA) and ethanol. (2) reaction of 2-thiobarbituric acid (TBA), and MDA to yield a pink-colored compound (TBA-MDA chromophore).....	309
<b>Figure A-11.</b> Particle size analysis by laser diffraction (adapted from <a href="http://www.malvern.com">www.malvern.com</a> ).....	311
<b>Figure A- 12.</b> Malvern Mastersizer 2000 apparatus with Hydro 2000SM dispersion unit.....	312
<b>Figure A-13.</b> Particle size vs. volume and cumulative volume. Median particle size, $d_{0.5}$ , represents the particle size value below which 50 % of the sample volume exists (adapted from [5]).....	313
<b>Figure A-14.</b> TA Instruments Q2000 DSC with RCS90 (adapted from <a href="http://www.tainstruments.com">www.tainstruments.com</a> ).....	323



This appendix is focused on the main analytical methods used in this work for characterization of the enzyme catalysts, the initial fish oil, the ethanolysis reaction products, the fish oil concentrate, the oil-in-water emulsions and the microencapsulated fish oil concentrate. The methods applied for the evaluation of the oxidative status of fish oil, reaction products, and fish oil concentrate samples are also included.

The main goal of this appendix is to expand the information about analytical methods, which have been briefly described in the chapters, to facilitate their understanding and further practical application. A systematic description of each method and its operational aspects is presented.

## 1. Characterization of catalysts

### 1.1. Enzyme activity

Residual activity was calculated as the ratio between the enzyme activity after SC-CO<sub>2</sub> exposure and the initial enzyme activity, expressed as percentage (Eq. A-1.1.1):

$$\text{residual activity (\%)} = \frac{\text{activity after SC-CO}_2 \text{ treatment}}{\text{initial activity}} \times 100 \quad (\text{A-1.1.1})$$

Methods used for determination of enzyme activity are described next for free (section 1.1.1) and immobilized lipases (section 1.1.2).

#### 1.1.1. Enzyme activity of free lipases

The enzyme activity of free enzymes was determined as the initial rate in the hydrolysis reaction of the olive oil triglycerides [1]. Free fatty acids (FFAs) liberated during the initial stages of the hydrolysis reaction were determined by potentiometric titration.

#### *Materials, reagents and solutions*

- 10 % homogenized olive oil. Prepared by mixing 1 part of olive oil and 9 parts of distilled water and vigorously shaking
- 50 mM phosphate buffer pH = 7.0.
- Commercial enzyme preparation (Palatase 20000 L, Lipozyme CALB L)
- Ethanol:acetone mixture (1:1)
- Standard KOH 0.1 N in ethanol. Prepared by dissolving 6.6 g of KOH (85 % wt.) in 1 L of ethanol and stored in a brown glass bottle before use. Standardization was performed using potassium phthalate monobasic as primary standard.
- Automatic potentiometric titrator Metrohm Titrand 905, with a combined pH electrode for non-aqueous acid-base titrations (LL solvotrode)
- Erlenmeyer flasks and stirring magnets



### *Hydrolysis reaction conditions*

4 mL of 10% homogenized olive oil, 5 mL of phosphate buffer, and 1 mL of enzyme preparation were mixed together and incubated at 50 °C for 15 min. To terminate the reaction, 15 mL of ethanol:acetone (1:1) were added. As a blank control, the reaction mixture without the enzyme was incubated in the same way.

### *Titration of liberated FFAs*

In this method, the free fatty acid content is determined from the amount of potassium hydroxide required to neutralize the reaction mixture. Liberated FFAs were titrated in a Metrohm Titrando 905 apparatus with KOH 0.1 N in ethanol until potentiometric equivalence point was detected. As a blank control, the reaction mixture without the enzyme was titrated in the same way.

### *Calculations*

Enzyme activity was expressed as lipase units, defined as the amount of enzyme that released 1 mmol fatty acid per minute under standard assay conditions (Eq. A-1.1.2).

$$\text{Free enz. activity (L.U.)} = 1000 \cdot \frac{(V_{\text{KOH}} - V_{\text{blank}}) \cdot N_{\text{KOH}}}{V_{\text{sample}} \cdot t} \cdot \text{PM}_{\text{oleic acid}} \quad (\text{A-1.1.2})$$

where  $V_{\text{KOH}}$  and  $N_{\text{KOH}}$  are the volume in mL and the normality of the standard potassium hydroxide solution, respectively.  $V_{\text{blank}}$  is the volume of KOH spent in the blank control (mL),  $V_{\text{sample}}$  is the total volume sample (25 mL), and  $t$  is the reaction time (15 min). Concentration of FFAs was expressed as oleic acid equivalents ( $\text{PM}_{\text{oleic acid}} = 282.5 \text{ g/mol}$ ).

### 1.1.2. Enzyme activity of Immobilized lipases

The enzyme activity of immobilized enzymes was determined as the initial rate of the esterification reaction of lauric acid (LA) with propanol.

#### *Materials, reagents and solutions*

- Lauric acid
- 2-propanol
- Hexane
- Commercial enzyme preparation (Lipozyme RM IM, Lipozyme 435)
- Disposable syringes and microfilters (0.45  $\mu\text{m}$ )
- Automatic potentiometric titrator Metrohm Titrand 905
- Standard KOH 0.1 N in ethanol. Prepared by dissolving 6.6 g of KOH (85 % wt.) in 1 L of ethanol and stored in a brown glass bottle before use. Standardization was performed using potassium phthalate monobasic as primary standard.
- Erlenmeyer flasks and stirring magnets

#### *Esterification reaction conditions*

LA was dissolved in propanol in a 3:1 mol:mol proportion. 60 % wt. hexane was added to the mixture to facilitate the esterification reaction. Initial FFA content of the substrate mixture was determined by potentiometric titration (Metrohm Titrand 905). The enzyme preparation was added in a 5 % wt. proportion in relation to the substrates, and the mixture was incubated at 50 °C for 15 min. Then, samples were collected and filtered to remove the catalyst, and the lauric acid consumption was determined by potentiometric titration (Metrohm Titrand 905).

#### *Determination of lauric acid (LA)*

In this method, the lauric acid content in the substrate mixture was determined through titration with potassium hydroxide in ethanol. An automatic titrator (Metrohm Titrand 905) was used to detect the potentiometric equivalence point.



### Calculations

Enzyme activity was expressed as lipase units, defined as the amount of enzyme required to esterify 1 mmol lauric acid per minute under standard assay conditions (Eq. A-1.1.3).

$$\text{Immobilized enz. activity (L.U.)} = 1000 \cdot \frac{(V_{\text{blank}} - V_{\text{KOH}}) \cdot N_{\text{KOH}}}{V_{\text{sample}} \cdot t} \cdot \text{PM}_{\text{lauric acid}} \quad (\text{A-1.1.3})$$

where  $V_{\text{KOH}}$  and  $N_{\text{KOH}}$  are the volume in mL and the normality of the standard potassium hydroxide solution, respectively.  $V_{\text{sample}}$  is the sample volume added (*ca.* 3 mL), and  $t$  is the reaction time (15 min).  $\text{PM}_{\text{lauric acid}} = 200.32 \text{ g/mol}$ .

## 1.2. Moisture content

Moisture content of the immobilized catalysts (Lipozyme RM IM, Lipozyme 435) was measured by extraction of water with methanol and subsequent titration following the Karl-Fisher method.

### *Material and equipment*

- Methanol
- Mitsubishi CA-20 Karl-Fischer titrator
- Karl-Fischer reagents: Aquamicon<sup>®</sup> CXU (cathode), Aquamicon<sup>®</sup> AX (anode)
- Disposable syringes, needles and septa

### *Analytical procedure*

An amount of sample (*ca.* 1 g) was weighed into a 20 mL glass vial and suspended in 10 mL methanol. Immediately afterwards, the glass vial was closed hermetically with a septum cap and placed on an orbital shaker overnight to allow water extraction. After that, an amount of methanol with the extracted water was taken with a syringe. A septum was placed in the needle tip to avoid ambient water contamination and the whole was accurately weighed in an analytical balance ( $\pm 0.0001$  g). The methanol was then injected into the anode solution of the Mitsubishi CA-20 apparatus and its water content was determined by Karl-Fisher titration. The empty syringe with the septum was weighed again and the exact sample mass was calculated by difference.

The analysis is based on a coulometric titration in which the sample is added to an electrolytic solution consisting of iodide ions, sulphur dioxide, a base, and methanol as solvent. Electrolytic oxidation causes the production of iodine, (Eq. A-1.2.1), resulting in an immediate Karl-Fischer reaction.





Following the Faraday's Law, the Iodine generated is directly related to the consumed electricity, and the water content can be determined immediately from the Coulombs required for electrolytic oxidation (1 mg of water = 10.71 C).

#### *Calculations*

The Karl-Fischer apparatus directly provides the water content of the injected sample (% moisture<sub>catalyst</sub>), expressed in % wt. Water content in the immobilized enzyme is determined according to Eq. A-1.2.2.

$$\% \text{ moisture} = \% \text{ moisture}_{\text{MeOH}} \cdot \frac{w_{\text{MeOH}}}{w_{\text{sample}}} \quad (\text{A-1.2.2})$$

where  $w_{\text{MeOH}}$  is the mass of methanol injected and  $w_{\text{sample}}$  is the mass of sample initially weighed.

### 1.3. Fluorescence spectrophotometry

Characterization of the tertiary structure of the free enzymes was performed by fluorescence spectroscopy. Fluorescence spectroscopy is an available technique for studying the conformational structure of free enzymes, in which the intrinsic fluorescence at 280 nm of Trp and Tyr residues is influenced by the environment [2]. Therefore, differences in the intrinsic fluorescence intensity can indicate changes in the tertiary structure of the lipases.

#### *Equipment*

A Varian Cary Eclipse fluorescence spectrophotometer (Agilent Technologies) with Peltier-thermostated cell holder and temperature controller was used for the spectrophotometric analyses (Fig. A-1).



**Figure A-1.** Varian Cary Eclipse Fluorescence Spectrophotometer with Peltier-thermostated cell holder and temperature controller.

#### *Experimental procedure*

Samples were diluted 10 times in distilled water prior to analysis. Measurements were performed at a constant temperature of 25 °C with excitation wavelength  $\lambda_{\text{exc}} = 280$  nm. Fluorescence emission spectra were read in the  $\lambda_{\text{emission}} = 290\text{-}450$  nm interval. All the spectra were scanned continuously with five replicates.

#### 1.4. FT-IR analysis of the chemical structure of the catalysts

Fourier Transform Infrared analysis aims to identify molecular structures. This instrumental analysis is based on the capability of molecular bonds to vibrate at a discrete energy level related to a certain infrared frequency, which allows to associate certain peaks in the IR spectra to specific molecular structures.

Since proteins absorb infrared wavelengths due to the peptide bond vibrations, Infrared spectroscopy analyses were made to follow possible chemical alterations in the protein structure after exposure to SC-CO<sub>2</sub>.

##### *Equipment and experimental procedure*

FT-IR was performed in the 4000-400 cm<sup>-1</sup> range using a Thermo-Nicolet Nexus 670 FT-IR spectrophotometer equipped with a one reflection ZnSe ATR crystal and a slip-clutch pressure applicator with 360 ° rotation. This module allowed to analyze both solid and liquid compounds within a pH range from 4 to 8 without sample pre-treatment (Fig. A-2).



**Figure A-2.** FT-IR equipment (adapted from [www.ubu.es.../ft-ir](http://www.ubu.es.../ft-ir)).



A little amount of sample was placed on the ZnSe ATR crystal previously cleaned and dry. In the case of solid samples, they were fixed by the slip-clutch pressure applicator. Subsequently, the sample was passed through a beam containing several infrared frequencies within a range from 400 to 4000  $\text{cm}^{-1}$ . The light absorbed at each frequency was detected as an interferogram and transformed to a FT-IR spectrum according to the Fourier transform algorithm.

#### *Data analysis*

FT-IR absorption was converted from % transmittance to absorbance according to Eq. A-1.4.1.

$$\text{Absorbance, } A = -\log(\text{Transmittance}) \quad (\text{A-1.4.1})$$

Potential changes in the chemical structure of the catalysts after SC-CO<sub>2</sub> exposure were monitored by comparison of their FT-IR spectra with that of the untreated catalysts. In the protein FT-IR spectra, the major protein absorption bands due to the peptide group vibrations occur between 1900 and 1200  $\text{cm}^{-1}$  [3]. Different bands can be observed in this region: the amide I band (between 1600 and 1700  $\text{cm}^{-1}$ ) is mainly associated with carbonyl stretching of the peptide. It consists of a group of overlapped signals, providing information about the secondary protein structure of the enzyme; the amide II band (1580-1510  $\text{cm}^{-1}$ ) is due to the N-H bending with a contribution of the C-N stretching vibrations and the amide III region (1400-1200  $\text{cm}^{-1}$ ), which has a weaker intensity [3,4].



### 1.5. Analysis of solid microstructure by Scanning Electron Microscope (SEM)

Scanning electron microscopy (SEM) is commonly used for imaging and characterization of solid microstructures. This instrumental technique produces a high-energy beam of electrons which is condensed and focused through magnetic lens as a fine spot. This spot impacts on the sample surface and interacts to the sample atoms, producing different signals such as secondary electrons or back-scattered electrons (BSE), which are detected and transformed in electronic signals that give a topographic image (Fig. A-3).

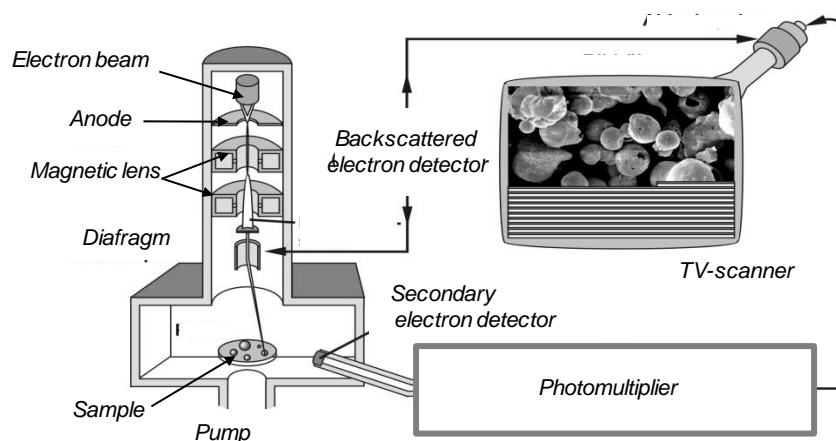


**Figure A-3.** Scheme of a Scanning Electron Microscope (SEM) equipment (adapted from [5]).

#### Equipment

The analysis of microstructure was ordered to the R&D Centre of the University of Burgos. The equipment used was a JEOL JSM-6460LV Field Emission Scanning Electron Microscope (FESEM) (Fig. A-4). This equipment was able to work with acceleration voltages from 0.2 to 30 kV and achieving different resolutions (1.0 nm at 20 kV, 2.5 nm at 1 kV or 5 nm at 0.2 kV). It also was provided of a high-vacuum turbo pump that allowed to obtain images from samples with low or null conductivity.



**Figure A-4.** JEOL JSM-6460LV Scanning Electron Microscope (adapted from [www.ubu.es.../meh](http://www.ubu.es.../meh)).

#### *Sample pre-treatment*

A small amount of sample was placed on a mounting carbon stub, which was then screw in a mounting plate and introduced in the SEM equipment. In order to achieve the electrical conductivity required for the electron beam to get a proper image, particles were previously sputtered with a thin layer of gold by using a gold coater (BioRad SC-500 sputter coater)

#### *Experimental procedure*

At least four SEM pictures were taken from each sample by changing the scale, magnification level, EHT voltage level of the electron beam or working distance from the sample to the beam tip.



## 2. Characterization of fish oil, reaction products, and omega-3 concentrates

### 2.1. Determination of free fatty acid content

Free fatty acid (FFA) content is defined as the fraction of fatty acids which is not attached to other molecules as in acylglycerides, wax esters or phospholipids. This parameter is related to the oil rancidity since free fatty acids came usually from the hydrolysis of acylglycerides due to the moisture, temperature and/or the action of lipases. In this work, the acid value of oils has been measured according to the AOCS Official Method [6]

#### *Analytical Method*

In this method, the free fatty acid content or acid value is determined from the amount of potassium hydroxide required to neutralize one gram of fat. This procedure has been the one used to determine FFA content in fish oil, reaction, or fish oil concentrate samples.

#### *Materials, reagents and solutions*

- Ethanol-ethyl ether mixture (1:1) used as oil solvent
- Standard KOH 0.1 N in ethanol. Prepared by dissolving 6.6 g of KOH (85 % wt.) in 1 L of ethanol and stored in a brown glass bottle before use.
- Potassium hydrogen phthalate ( $C_8H_5KO_4$ ) dried at 105 °C overnight and cooled down during 2 h, used as primary standard for standardization of KOH
- 80 mL beakers and stirring magnets
- Automatic potentiometric titrator Metrohm Titrando 905, with a combined pH electrode for non-aqueous acid-base titrations (LL solvotrode)



### *Experimental procedure*

#### *i) Standardization of titrant solution*

Standardization of KOH is necessary to obtain the actual normality of the titrant solution.  $\text{KIO}_3$  is used as primary standard. 200 mg of  $\text{C}_8\text{H}_5\text{KO}_4$  are accurately weighed in a beaker and dissolved in 50 mL of distilled water. Immediately afterwards, the mixture is titrated with KOH in the Metrohm Titrand 905 apparatus.

The correction factor  $f$  was calculated according to Eq. A-2.1.1.

$$f = \frac{m_{\text{C}_8\text{H}_5\text{KO}_4}}{V_{\text{KOH}} \cdot 20.423} \quad (\text{A-2.1.1})$$

where  $m_{\text{C}_8\text{H}_5\text{KO}_4}$  is the exact mass of  $\text{C}_8\text{H}_5\text{KO}_4$  in mg, and  $V_{\text{KOH}}$  is the volume of KOH needed for the titration, in mL.

#### *ii) Determination of total free fatty acid content*

1-2 g of sample was accurately weighed in an 80 mL beaker flask and dissolved in 50 mL of the ethanol-ethyl ether mixture. FFAs were titrated in a Metrohm Titrand 905 apparatus with KOH 0.1 N in ethanol until detection of the equivalence point.

### *Calculations*

Total free fatty acid content, expressed as % wt. of oleic acid, was calculated according to Eq. A-2.1.2, where  $V$  and  $N$  are the volume in mL and the normality of the standard potassium hydroxide solution, and  $w$  is the sample weight.

$$\% \text{FFA (oleic acid)} = \frac{V \cdot N \cdot 282.5}{10 \cdot w} \quad (\text{A-2.1.2})$$

## 2.2. Analysis of the fatty acid profile by GC-FID

The fatty acid profile of fish oil was quali- and quantitatively determined by gas chromatography (GC) following the official method proposed by the AOAC [7]. This method required a previous derivatization step based on the methylation of fatty acids by reaction of fish oil TAGs with a methanolic alkali solution, NaOH-MeOH, and boron trifluoride in methanol, BF<sub>3</sub>-MeOH. The resulting fatty acid methyl esters (FAMES) were separated in a GC equipment and detected in a flame ionization detector (FID). Identification of fatty acids was carried out by comparison of retention times of standard compounds, whereas quantification was performed using methyl-tricosanoate (C23:0) as internal standard (I.S.).

### *Material and equipment*

Gas chromatography was performed in a gas chromatograph (6890 N Network GC System, Hewlett Packard) equipped with an auto-sampler (7683B series) and a flame ionization (FID) detector (Fig. A-5). The column used was a fused silica capillary column (Omegawax<sup>TM</sup>-320, 30 m × 0.32 mm i.d.).

Oil derivatization was carried out in PYREX<sup>®</sup> glass tubes with leak-tight and Teflon-lined screw caps and a water bath was used for heating.



**Figure A-5.** GC-FID equipment.

### Reagents

- Isooctane solution of methyl tricosanoate (C23:0) (1 g / mL), used as I.S. It was prepared by accurately weighting 25 mg ( $\pm 0,1$  mg) of C23:0 methyl ester in a 25 mL volumetric flask and diluting with isooctane.
- Boron trifluoride (BF<sub>3</sub>) 12 % in methanol
- Sodium hydroxide (NaOH) 0.5 M in methanol, prepared by dissolving 2.0 g NaOH in 100 mL methanol.
- FAMES standards, dissolved in isooctane
- Sodium chloride (NaCl) saturated solution, prepared by dissolving 36 g NaCl in 100 mL of distilled water

### Experimental procedure

#### i) Sample preparation

Accurately, 1 mL of I.S. solution was added into a glass tube and evaporated in gentle stream of N<sub>2</sub>. When solvent was removed, 25 mg ( $\pm 0.1$  mg) of fish oil, reaction, or fish oil concentrate sample were weighed into the glass tube containing the solid internal standard, and 1.5 mL of NaOH-MeOH solution was added. The glass tube was blanketed with N<sub>2</sub>, capped, mixed and heated 5 minutes in a water bath at 100 °C\*. Then, it was cooled down and 2 mL BF<sub>3</sub>-MeOH were added. After mixing, the glass tube was again heated in the water bath at 100 °C for 30 minutes. Subsequently, the mixture was cooled, diluted with 1 mL of isooctane, and mixed in a vortex for 30 s. Immediately afterwards, the mixture was diluted in 5 mL of saturated NaCl solution, mixed and let to stand for phase separation. When that was clear, the upper organic layer was transferred into a glass vial for autosampler injection in the GC column.

---

\* **Note:** This step with methanolic NaOH is a mild methylation to disengage the fatty acids from the glycerol backbone and make them available for the strong methylation with BF<sub>3</sub>. Samples with TAGs, DAGs, and/or MAGs) require the complete derivatization process. In the case of FFA samples, the first step is not necessary. FAEE samples would not even require derivatization, although retention times of the compounds in the GC-FID could slightly change.



ii) Chromatographic method

1  $\mu$ L of derivatized sample was injected into the GC-FID apparatus using a split injection of (50:1). Injector temperature was set at 250 °C and helium, He, (1.8 mL / min) was used as carrier gas. The temperature program for the column is detailed in Table A-1. The FID detector was also heated at 250 °C. Flame was obtained by a mixture of hydrogen, H<sub>2</sub> (40 mL / min) and air (40 mL / min). Nitrogen, N<sub>2</sub>, (20 mL / min) was used as make-up gas. Control parameters and data analysis were carried out with a GC-Chemstation® Software (Agilent Tech.).

**Table A-1.** Temperature program used for the analysis of fatty acids by GC-FID.

	Rate (°C / min)	T set point (°C)	Hold time (min)
Initial		180	20
Ramp 1	1	200	1
Ramp 2	5	220	20

iii) Identification of the main chromatographic peaks

Several fatty acids usually present in common fish oil samples were identified by means of standard fatty acids methyl esters (FAMES) as it is shown in Fig. A-6. The retention times for each fatty acid are presented in Table A-2.

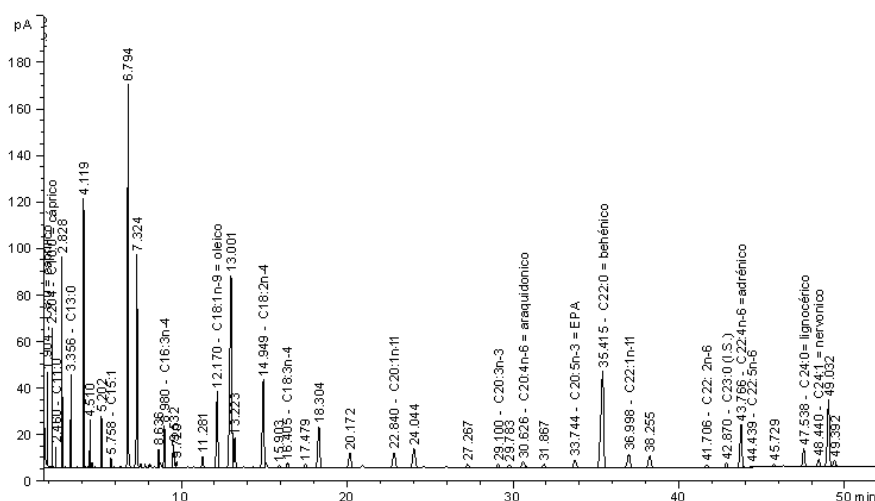


**Table A-2.** Retention times of standard lipid compounds identified by GC-FID

Type of fatty acid	Chemical formula	Common name	Retention time (min)
SFA	C14:0	Myristic acid	3.9
SFA	C16:0	Palmitic acid	6.4
MUFA	C16:1	Palmitoleic acid	7.0
SFA	C18:0	Stearic acid	11.5
MUFA	C18:1 <i>n</i> -9	Oleic acid	12.2
MUFA	C18:1 <i>n</i> -7	Vaccenic acid	12.5
PUFA	C18:2 <i>n</i> -6	Linoleic acid (LA)	14.1
PUFA	C18:3 <i>n</i> -6	$\gamma$ -linolenic acid (GLA)	15.4
PUFA	C18:3 <i>n</i> -3	$\alpha$ -linolenic acid (ALA)	17.1
PUFA	C18:4 <i>n</i> -3	Stearidonic acid	18.9
MUFA	C20:1 <i>n</i> -11	Gadoleic acid	22.9
PUFA	C20:3 <i>n</i> -6	dihomo- $\gamma$ -linolenic acid (DGLA)	27.7
PUFA	C20:3 <i>n</i> -3	Eicosatrienoic acid	29.1
PUFA	C20:5 <i>n</i> -3	Eicosapentaenoic acid (EPA)	33.8
MUFA	C22:1 <i>n</i> -11	Cetoleic	36.5
PUFA	C22:2 <i>n</i> -6	Docosadienoic	41.7
SFA (I.S.)	C23:0	Tricosanoic acid	42.9
PUFA	C22:4 <i>n</i> -6	Adrenic acid	43.8
PUFA	C22:5 <i>n</i> -6	Docosapentaenoic acid <i>n</i> -6 (DPA)	44.8
PUFA	C22:5 <i>n</i> -3	Docosapentaenoic acid <i>n</i> -3 (DPA)	46.5
PUFA	C22:6 <i>n</i> -3	Docosahexaenoic acid (DHA)	48.0

SFA: Saturated Fatty Acids, MUFA: Monounsaturated Fatty Acids, PUFA: Polyunsaturated Fatty Acids, I.S.: Internal Standard.

#### iv) Quantification of fatty acids

The amount of each fatty acid in the fish oil, reaction, or fish oil concentrate sample is quantified according to Eq. A-2.2.1, in which  $A_X$  is the area counts of each fatty acid, FA;  $A_{I.S.}$  is the area counts of internal standard;  $w_{I.S.}$  and  $w_{sample}$  are the internal standard and sample weights in mg, respectively;  $a_X$  is the slope of the calibration curve of each FAME standard; and  $CF_{FAME-FFA}$  is the ratio between the molecular weight of each FAME and that of the corresponding FFA in each case, which is necessary to express the result as mg of fatty acid (FA)/g oil rather than as FAME.

$$mg_{FA} / g_{oil} = \frac{A_X \cdot w_{I.S.}}{A_{I.S.} \cdot w_{sample} \cdot a_X \cdot CF_{FAME-FFA}} \cdot 1000 \quad (A-2.2.1)$$

### 2.3. Determination of the neutral lipids profile by NP HPLC-ELSD

Neutral lipids were quali- and quantitatively determined by Normal-Phase High Performance Liquid Chromatography (NP HPLC) with an Evaporative Light Scattering Detector (ELSD) according to the method proposed by Schaefer *et al.* [8] with slight modifications. The most recent version of the NP HPLC-ELSD methodology has been reported in [9]. In NP chromatography, the stationary phase is polar whereas the mobile phase is non-polar, thus the least polar compounds elute first from the separation column and the most polar elute later. It presents important advantages such as low system back pressure and easy solvent evaporation. Moreover, interaction forces not only depend on the polarity of the compound but also on steric factors, so structural isomers can be separated.

#### *Material and equipment*

High Performance Liquid Chromatography was performed in an Agilent 1200 system formed by a quaternary pump and an autoinjector (Fig A-7). Separations were carried out in a Lichrospher Diol-5  $\mu\text{m}$ ,  $4 \times 250$  mm column. Eluted compounds were detected in an evaporative light scattering detector (ELSD, Agilent 1200 series). Data were assessed by Agilent Chemstation<sup>®</sup> software.



**Figure A-7.** NP HPLC-ELSD equipment.

### *Reagents and standards*

Separation of neutral lipids was carried out by means of a binary gradient among two mobile phases:

- mobile phase A, composed by isooctane (HPLC grade)
- mobile phase B composed by a mixture of methyl *tert*-butyl ether (MTBE) and acetic acid (AcOH) (99.9 / 0.1 v).

Main lipid standards used for peak identification and method calibration where:

- FAEEs: ethyl-palmitate, ethyl-oleate
- TAGs: tripalmitine, trimiristin, triolein
- DAGs: dipalmitin, diolein (mix of both *sn*-1,3 and *sn*-1,2 isomers)
- MAGs: 1-monopalmitin, 1-monoolein, 2-monoolein, 1-monodocosahexaenoin
- FFAs: oleic acid, palmitic acid.

Additionally, other related standard compounds such as squalene, palmitil-palmitate, cholesteryl-palmitate,  $\alpha$ -tocopherol, and cholesterol were also used.

### *Experimental procedure*

#### *i) Sample preparation*

A known amount of fish oil, reaction, or fish oil concentrate sample was dissolved in *tert*-pentanol and diluted down to a vial concentration of 1 mg/mL (fish oil and fish oil concentrate samples) or 3-5 mg/mL (reaction samples). Diluted samples can be directly injected into the HPLC apparatus or previously filtered through a microfilter (0.45  $\mu$ m) if necessary.

#### *ii) Chromatographic method*

Neutral lipid separation was carried out at room temperature in the NP column. Flow rate was set at 1.0 mL/min with (A) isooctane, and (B) MTBE-AcOH (99.9 / 0.1 v). Separation was carried out in 47 minutes according to the binary solvent gradient presented in Table A-3. Detection was performed in the ELSD at 45 °C, using N<sub>2</sub> as nebulizer gas (3.5 bar and gain 7).



**Table A-3.** Binary solvent gradient used in neutral lipid analysis by HPLC-ELSD.

Accumulated time (min)	% Mobile Phase B
0	0
1	0
10	10
22	44
30	100
42	80
47	0

*iii) Identification of chromatographic peaks*

The chromatographic method developed aimed to separate different lipid families or classes (FAEEs, TAGs, DAGs, MAGs, and FFAs). Identification of each neutral lipid class and other related compounds was carried out by comparison of their retention time with those of the standard compounds. Fig. A-8 shows a HPLC chromatogram with the neutral lipid classes detected by this method.

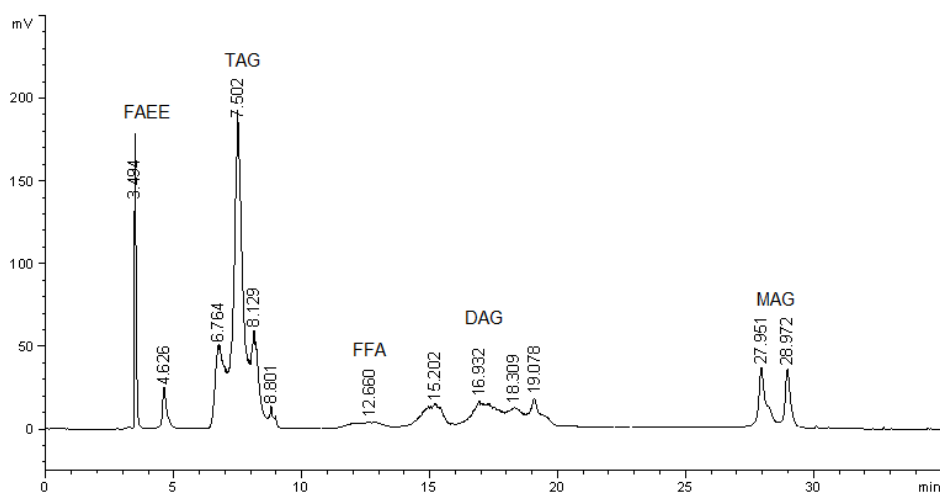


**Figure A-8.** HPLC-ELSD chromatogram of neutral lipid classes. Fatty acid ethyl esters (FAEE), triacylglycerides (TAG), free fatty acids (FFA), diacylglycerides (DAG), and monoacylglycerides (MAG).



#### iv) Quantification

Calibration has been performed by an external standard method with representatives of each group of compounds in concentration ranges depending on the lipid class. Calibration curves showed good correlation according to the exponential relationship described for an evaporative light scattering detector as it has been described in the literature [10]. Although ELSD parameters were optimized in order to enhance the sensitivity for all lipid-class representatives, different sensitivities were found for different lipid classes and for different compounds within the same class. This behavior has been also reported in the literature [8].

Regarding the standard compounds: ethyl-palmitate and ethyl-oleate were used for FAEE calibration; dipalmitin and diolein for DAG calibration; oleic and palmitic acids for FFA calibration; MAG class was calibrated with 1-monopalmitin, 1-monoolein, 2-monoolein, and 1-monodocosahexaenoin. In the case of TAGs, a mix of pure standards (trimiristin, tripalmitin, and triolein), showed an ELSD signal significantly different from that of the fish oil TAGs; therefore, the refined fish oil itself ( $\geq 99\%$  TAG) was used for the calibration of TAG. The calibration curves used in this work with quantification purposes are defined in Eqs. A-2.3.1-5.

$$\log(A_{\text{FAEE}}) = 1.6301 + 1.7442 \cdot \log(w_{\text{sample}}) \quad (\text{A-2.3.1})$$

$$\log(A_{\text{TAG}}) = 1.8427 + 1.8494 \cdot \log(w_{\text{sample}}) \quad (\text{A-2.3.2})$$

$$\log(A_{\text{FFA}}) = 2.1581 + 1.3377 \cdot \log(w_{\text{sample}}) \quad (\text{A-2.3.3})$$

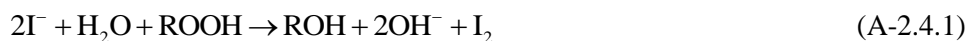
$$\log(A_{\text{DAG}}) = 2.8563 + 1.1330 \cdot \log(w_{\text{sample}}) \quad (\text{A-2.3.4})$$

$$\log(A_{\text{MAG}}) = 2.5272 + 1.5326 \cdot \log(w_{\text{sample}}) \quad (\text{A-2.3.5})$$

where  $w_{\text{sample}}$  is expressed in  $\mu\text{g}$ . The amount of each neutral lipid class in the oil sample, expressed as %wt., was determined by interpolation of the respective calibration curve.

## 2.4. Determination of peroxide value (PV)

Peroxide value (PV) is a measure of the peroxides and hydroperoxides generated during the early stage of lipid oxidation. These compounds can be determined indirectly with a redox titration in non-aqueous media, by measuring the amount of iodine,  $I_2$ , produced when the hydroperoxides, ROOH, contained in oil reacts with iodine ion,  $I^-$  (Eq. A-2.4.1).



In this work, the  $I_2$  generated in oil samples was measured by titration with sodium thiosulphate ( $Na_2S_2O_3$ ), according to AOAC Official Method [11].

### *Materials, reagents and solutions*

- Chloroform ( $CHCl_3$ )
- Glacial acetic acid (AcOH)
- Saturated aqueous solution of potassium iodide (KI), freshly prepared
- Aqueous solution of  $Na_2S_2O_3$  (0.01 N), used as titrant solution
- Potassium iodate ( $KIO_3$ ), dried at 180 °C overnight and cooled down during 2 h, used as primary standard for standardization of  $Na_2S_2O_3$
- Sulphuric acid ( $H_2SO_4$ ) solution (25 %)
- Automatic potentiometric titrator Metrohm Titrando 905, equipped with a Pt electrode
- 100 mL beakers, 250 mL Erlenmeyer flasks, and stirring magnets

### *Procedure*

#### *i) Standardization of titrant solution*

Standardization of  $Na_2S_2O_3$  is necessary to obtain the actual normality of the titrant solution.  $KIO_3$  is used as primary standard. 5 mg of  $KIO_3$  are accurately weighed in a beaker and dissolved in 80 mL of distilled water. After that, 0.8 mL of KI solution and 10 mL of  $H_2SO_4$  are added. Immediately afterwards, the mixture is titrated with  $Na_2S_2O_3$  in the Metrohm Titrando 905 apparatus.



The correction factor  $f$  was calculated according to Eq. A-2.4.2.

$$f = \frac{m_{\text{KIO}_3}}{V_{\text{Na}_2\text{S}_2\text{O}_3} \cdot 0.3567} \quad (\text{A-2.4.2})$$

where  $m_{\text{KIO}_3}$  is the exact mass of  $\text{KIO}_3$  and  $V_{\text{Na}_2\text{S}_2\text{O}_3}$  is the volume of  $\text{Na}_2\text{S}_2\text{O}_3$  needed for the titration, in mL.

#### ii) Determination of peroxide value

A certain amount of fish oil, reaction, or fish oil concentrate sample (*ca.* 1 g) was weighed in an Erlenmeyer flask and dissolved in 10 mL of chloroform. Then, 15 mL of glacial acetic acid and 1 mL of saturated KI aqueous solution were added. The closed flask was agitated during 1 min and then stored preserved of light during 5 min. After that, the mixture was diluted by adding 75 mL of distilled water and transferred to a 100 mL beaker with stirring magnet for titration with  $\text{Na}_2\text{S}_2\text{O}_3$  in the Metrohm Titrando 905 apparatus. The Pt electrode must be immersed in the aqueous phase. Slight stirring is necessary to release all the iodine from the solvent phase.

Blank runs were performed the same as above, yet without sample. Low values for blanks are recommended (less than 0.05 mL of  $\text{Na}_2\text{S}_2\text{O}_3$ ). Both blank and sample are analyzed in triplicate.

#### Calculations

The peroxide value (PV), expressed as milliequivalents of  $\text{O}_2$  per kg of sample, was determined according to Eq. A-2.4.3, where  $V_S$  and  $V_B$  are the titrant volumes in mL for blank and sample, respectively;  $N$  is the normality of  $\text{Na}_2\text{S}_2\text{O}_3$  solution,  $f$  is the titrant factor (Eq. A-2.4.2) and  $m$  is the weight of sample in g.

$$\text{PV} = \frac{(V_S - V_B) \cdot N \cdot f}{m} \cdot 1000 \quad (\text{A-2.4.3})$$

## 2.5. Determination of anisidine value

The anisidine value (AV) is a measure of the non-volatile carbonyl compounds, mainly 2-alkenals, resulting from secondary lipid oxidation processes. In this work, AV has been measured according to AOCS Official Method [12], which is based on the reductive amination reaction that takes place between *p*-anisidine and aldehydic compounds such as 2-alkenals. This reaction leads to the formation of a Schiff base (Fig. A-9), which presents a high absorption at  $\lambda = 350$  nm.

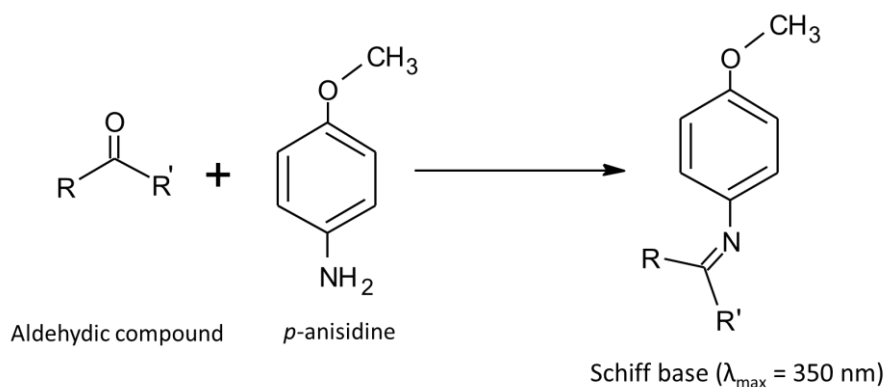


**Figure A-9.** Chemical reaction between an aldehydic compound and *p*-anisidine, producing a Schiff base with maximum absorption at  $\lambda = 350$  nm.

### *Material, reagents and solutions*

- *Tert*-pentanol
- Glacial acetic acid (AcOH)
- *p*-Anisidine solution (0.25 % w/v in AcOH), freshly prepared.
- Absorbance measurements were carried out in a UV-Vis spectrophotometer (Hitachi U-2000).



### *Experimental procedure*

A sample solution (A) was prepared by dissolving 0.5 g of fish oil, reaction, or fish oil concentrate sample in 25 mL of *tert*-pentanol, which was used instead of hexane due to poor solubility of some reaction products. The absorbance of this solution was measured at  $\lambda = 350$  nm using *tert*-pentanol as blank. Then, solution B was prepared by mixing 5 mL of solution A with 1 mL of *p*-anisidine solution, shaken and stored protected from light for 10 min. The absorbance of this solution was also measured at  $\lambda = 350$  nm using a mixture of 5 mL *tert*-pentanol and 1 mL of *p*-anisidine solution as blank.

### *Calculations*

Anisidine value (AV) was determined according to Eq. A-2.5.1, where  $A_A$  and  $A_B$  are the absorbances at  $\lambda = 350$  nm of sample A and sample B, respectively; and  $m$  is the exact sample weight.

$$AV = \frac{(1,2 \cdot A_B - A_A)}{m} \cdot 25 \quad (\text{A-2.5.1})$$

## 2.6. Analysis of Thiobarbituric Acid Reactive Substances (TBARS)

Thiobarbituric acid reactive substances (TBARS) are those compounds formed during secondary lipid oxidation processes that react with 2-thiobarbituric acid (TBA), forming a pink-colored complex with strong absorbance at  $\lambda = 538$  nm. TBARS are often referred to as malondialdehyde (MDA), one of the main secondary oxidation products formed by decomposition of oxidized unsaturated fatty acids. TBARS in fish oil, reaction products, and fish oil concentrate samples were analyzed following the spectrophotometric method described by Ke and Woyewoda [13].

### *Material, reagents and solutions*

- Glacial acetic acid (AcOH)
- 0.04 M 2-thiobarbituric acid in AcOH (TBA stock solution)
- Chloroform
- 0.3 M sodium sulphite ( $\text{Na}_2\text{SO}_3$ ) aqueous solution
- TBA work solution. Prepared by mixing TBA stock solution, chloroform and  $\text{Na}_2\text{SO}_3$  solution at 12:8:1 v. (max. 30 min before analysis).
- 0.28 M trichloroacetic acid (TCA) aqueous solution
- 10 mM 1,1,3,3-tetraethoxypropane (TEP) aqueous solution, used as standard for construction of the calibration curve.
- UV-Vis spectrophotometer (Hitachi U-2000).
- Water bath and centrifuge

### *Experimental procedure*

#### *i) Calibration*

A calibration curve was constructed using a primary 0.1 mM TEP aqueous solution (TEP work solution). Although TBARS are expressed as MDA, TEP is commonly used as standard due to its better stability. At mild acid conditions, TEP is hydrolyzed to MDA at 1:1 stoichiometric ratio, and MDA reacts with TBA forming a pink-colored compound (Fig. A-10).

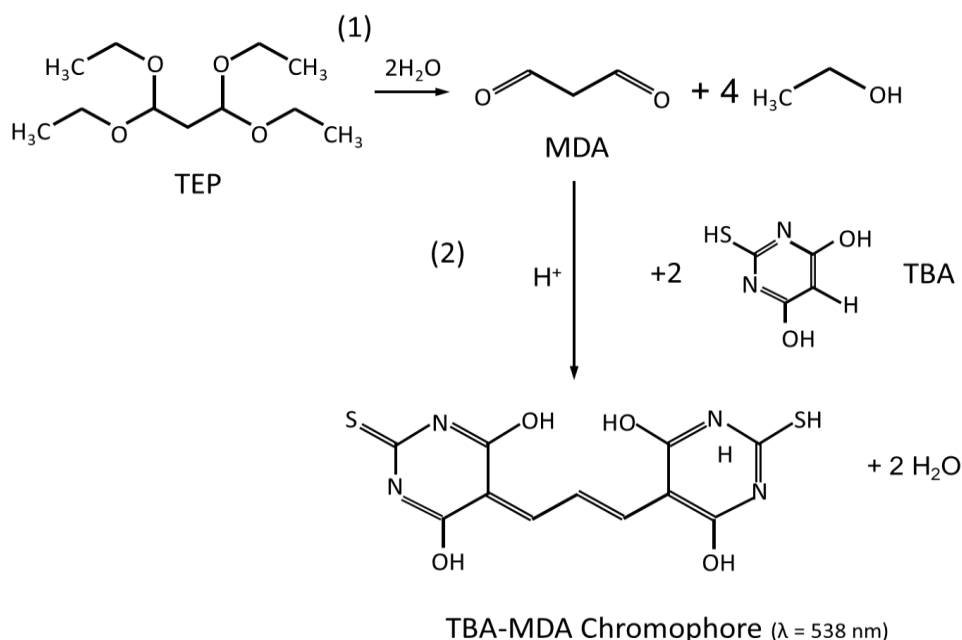


**Figure A-10.** Reactions involved in TBARS analysis. (1) Hydrolysis reaction of 1,1,3,3-tetraethoxypropane (TEP) to yield malondialdehyde (MDA) and ethanol. (2) reaction of 2-thiobarbituric acid (TBA), and MDA to yield a pink-colored compound (TBA-MDA chromophore).

Each calibration standard was prepared by pipetting known quantities of TEP work solution in a screw-capped glass test tube and diluting with distilled water when necessary, according to Table A-4. Subsequently, 5 mL of TBA work solution were added. After tight-closing the tubes and vortexing for 15 s, they were incubated in a water bath at 95 °C during 45 min. Then, the test tubes were cooled down under running cold water and 2.5 mL of TCA were added to each tube. After mixing by inversion several times, samples were centrifuged at 2500 rpm for 10 min in order to separate the pink aqueous phase from the chloroform phase. Immediately afterwards, the supernatant was taken, and its absorbance measured at  $\lambda = 538 \text{ nm}$ .

**Table A-4.** Calibration solutions of 1,1,3,3-tetraethoxypropane (TEP) for TBARS quantification in fish oil, reaction, and fish oil concentrate samples.

	TEP work solution ( $\mu\text{L}$ )	H <sub>2</sub> O ( $\mu\text{L}$ )	[TEP] <sub>final</sub> (nmol)
STD-0	0	200	0
STD-1	25	150	2.5
STD-2	50	100	5
STD-3	100	50	10
STD-4	150	25	15
STD-5	200	0	20

Each TEP concentration should be at least duplicated. Experimental calibration curve used in this work is defined in Eq. A-2.6.1.

$$\text{Abs}_{\lambda=538 \text{ nm}} = 0.0256 \cdot [\text{TEP}] \text{ (nmol)} + 0.0186; \quad (R^2 = 0.9846) \quad (\text{A-2.6.1})$$

#### ii) Determination of TBARS

TBARS analysis in samples was performed the same as in the calibration standard, yet with 10 mg of fish oil, reaction, or fish oil concentrate sample instead. Blank runs were also carried out without any sample.

#### Calculations

TBARS content in the samples, expressed as mg malonaldehyde (MDA)/kg, was calculated according to Eq. A-2.6.2, where Abs is the absorbance of the sample against blank;  $a$  and  $b$  are the slope and intercept of the calibration curve (Eq. A-2.6.1), respectively;  $m$  is the exact sample weight (g); and  $MW_{\text{MDA}}$  is the molecular weight of malondialdehyde (72.06 g/mol).

$$\text{TBARS} = 1000 \cdot \frac{(Abs - b) \cdot MW_{\text{MDA}}}{a \cdot m \cdot 1000} \quad (\text{A-2.6.2})$$

### 3. Characterization of O/W emulsions and microencapsulated omega-3 concentrates

#### 3.1. Particle size analysis

Particle size and particle size distribution of microencapsulated omega-3 concentrates were determined via laser diffraction (LD) method according to the official method proposed by ISO standards [14].

This technique is based on the fact that particles passing through a laser beam are able to scatter light at a certain angle. The scattered angle increases logarithmically as particle size decreases, whereas the intensity of scattered light decreases with the cross-sectional area of the particle (Fig. A-11).

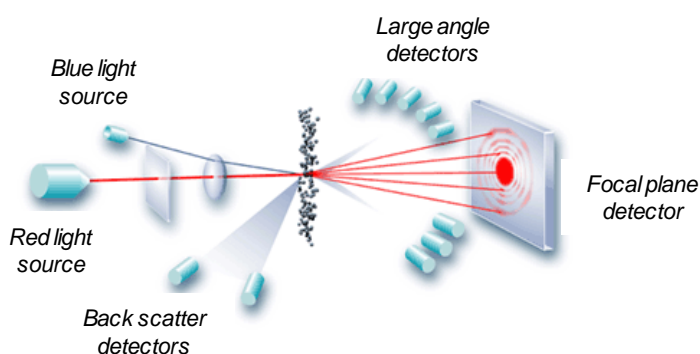


**Figure A-11.** Particle size analysis by laser diffraction (adapted from [www.malvern.com](http://www.malvern.com)).

#### *Equipment*

The measurements of particle size were carried out in a Malvern Mastersizer 2000 (Fig A-12) composed by a laser beam, which provides a source of coherent and intense light at a fixed wavelength, and a series of detectors, which measure the intensity of the scattered light over a wide range of angles. The equipment also presents a Hydro 2000SM dispersion unit, which allows a better dispersion of the particles by means of gentle agitation. Control of the apparatus and data analysis were performed with Malvern Mastersizer 2000 Software SOPs.



**Figure A- 12.** Malvern Mastersizer 2000 apparatus with Hydro 2000SM dispersion unit.

#### *Experimental procedure*

A certain amount of microencapsulated omega-3 concentrate in O/W emulsion form was placed in the dispersion unit. Then, the agitation was connected in order to disperse the particles in distilled water. This dispersion was passed through a focused laser beam (wave length = 10 mm), which is scattered by the particles at a certain angle. The intensity of the scattered light, which is inversely proportional, is measured by the detector as depicted in Fig. A-11.

#### *Calculations and data analysis*

Data analysis was carried out by the Mastersizer 2000 Software SOPs, which gives particle size related to volume frequency or to cumulative volume. Particle size *vs.* volume frequency allows to determine if the particle size distribution is normal, which indicates that there is not particle agglomeration. Particle size *vs.* cumulative volume allows to estimate the median particle size expressed as  $d_{0.5}$ , which is defined as the maximum particle diameter below which 50 % of the sample volume exists (Fig A-13).

Besides, the Malvern software SOPs calculates different parameters related to particle size of the measured dispersion, such as mean diameter over volume (D[4,3]) and volume/surface mean diameter (D[3,2]), which are defined in Eqs. A-3.1.1 and A-3.1.2, respectively.

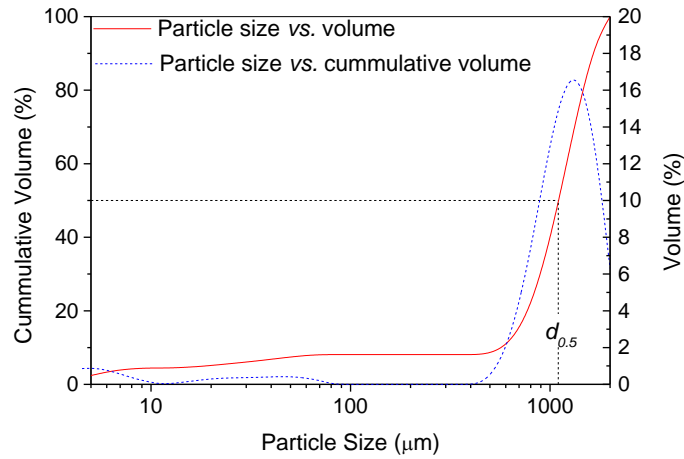


**Figure A-13.** Particle size vs. volume and cumulative volume. Median particle size,  $d_{0.5}$ , represents the particle size value below which 50 % of the sample volume exists (adapted from [5]).

$$D[4,3] = \frac{\sum_1^n D_i^4 v_i}{\sum_1^n D_i^3 v_i} \quad (\text{A-3.1.1})$$

$$D[3,2] = \frac{\sum_1^n D_i^3 v_i}{\sum_1^n D_i^2 v_i} \quad (\text{A-3.1.2})$$

where  $D_i$  is the diameter of the  $i$ th particle.

The span value, defined in Eq. A-3.1.3, was also calculated.

$$\text{span} = \frac{d_{0.9} - d_{0.1}}{d_{0.5}} \quad (\text{A-3.1.3})$$

where  $d_x$  is the maximum particle diameter below which  $x$  % of the sample volume exists. Span values near to 1 indicate a narrow particle size distribution (PSD).

### 3.2. Determination of peroxide value in O/W emulsions

Peroxide value (PV) in O/W emulsions (original or obtained from reconstitution of dried particles) was determined spectrophotometrically at  $\lambda = 510$  nm, following the method developed by Shanta *et al.* [15] for PV analysis in aqueous media, with slight modifications.

#### *Materials, reagents and solutions*

- Cumene hydroperoxide solution, used as standard ( $C_0 = 500 \mu\text{g/mL}$ )
- Isooctane:2-propanol solution (3:1 v/v)
- Methanol:1-butanol solution (2:1 v/v)
- 0.4 M Hydrochloric acid (HCl)
- 0.132 M barium chloride solution in 0.4 M HCl.
- 0.144 M Iron(II) sulphate heptahydrate aqueous solution
- $\text{Fe}^{2+}$  work solution. Mix equal volumes of 0.132 M barium chloride and Iron(II) sulphate heptahydrate solutions, centrifuge at 5000 rpm for 10 min and take the supernatant
- 3.94 M ammonium thiocyanate
- UV-Vis spectrophotometer Hitachi U-2000
- Vortex, water bath and centrifuge
- Falcon centrifuge tubes, screw-capped glass test tubes

#### *Experimental Procedure*

##### *i) Calibration*

A calibration curve was constructed using known concentrations of cumene hydroperoxide, ranging from 20 to 500  $\mu\text{g/mL}$ , as indicated in Table A-5. 0.3 mL of each standard solution were taken into centrifuge tubes and added of 1.5 mL of isooctane:2-propanol. The tube was vortexed for 15 s and centrifuged at 5000 rpm during 10 min. Immediately afterwards, 0.2 mL of the supernatant were transferred to a new centrifuge tube and 2.8 mL of methanol:1-butanol were added. After



vortexing for 15 s, 15  $\mu\text{L}$  of 3.94M ammonium thiocyanate and 15  $\mu\text{L}$  of  $\text{Fe}^{2+}$  work solution were added. Samples were vortexed again for 15 s and kept in darkness for 20 min. Immediately afterwards, absorbance was measured at  $\lambda = 510 \text{ nm}$ .

**Table A-5.** Calibration solutions of 1,1,3,3-tetraethoxypropane (TEP) for TBARS quantification in O/W emulsions.

	Take (mL) ; from	Complete to (mL) with $\text{H}_2\text{O}$	[cumene hydroperoxide] ( $\mu\text{g}/\text{mL}$ )	$m_{\text{POOH}}$ ( $\mu\text{g}$ )
<b>C<sub>0</sub></b>	-	-	500	6
<b>C<sub>1</sub></b>	20 ; C <sub>0</sub>	25	400	15
<b>C<sub>2</sub></b>	12.5 ; C <sub>1</sub>	25	200	30
<b>C<sub>3</sub></b>	5 ; C <sub>1</sub>	25	100	60
<b>C<sub>4</sub></b>	2.5 ; C <sub>1</sub>	25	50	120
<b>C<sub>5</sub></b>	10 ; C <sub>4</sub>	25	20	150

The calibration curve used in this work is defined in Eq. A-3.2.1.

$$\text{Abs}_{\lambda=510 \text{ nm}} = 0.009188 \cdot m_{\text{POOH}}; \quad (R^2 = 0.9983) \quad (\text{A-3.2.1})$$

where  $m_{\text{POOH}}$  is the mass of hydroperoxides in the sample, in  $\mu\text{g}$ .

#### ii) Determination of peroxide value

0.025-1.0 mL of O/W emulsion, depending on the expected PV, were submitted to the experimental procedure described above for the calibration solutions. Blank runs were also performed with 0.3 mL distilled water instead of sample.

#### Calculations

The peroxide value (PV), expressed as milliequivalents of oxygen per kg of oil (meq  $\text{O}_2/\text{kg}$  oil), was determined according to Eq. A-3.2.2, where  $\text{Abs}_{\lambda=510 \text{ nm}}$  is the absorbance of the sample against blank;  $a$  and  $b$  are the slope and intercept of the calibration curve (Eq. A-3.2.1), respectively;  $m_{\text{oil}}$  is the exact oil content in the sample (g); and  $\text{MW}_{\text{cumene hydroperoxide}} = 152.2 \text{ g/mol}$ .

$$\text{PV} = \frac{(\text{Abs}_{\lambda=510 \text{ nm}} - b)}{a \cdot m_{\text{oil}} \cdot \text{MW}_{\text{cumene hydroperoxide}}} \quad (\text{A-3.2.2})$$

### 3.3. Analysis of TBARS in O/W emulsions

TBARS analysis of the original and reconstituted O/W emulsions was carried out following the method described by Mei *et al.* [16] with slight modifications. The analysis is based on the same principles as the TBARS analysis in fish oil, reaction, or fish oil concentrate samples (section 2.6).

#### *Material, reagents and solutions*

- 0.25 M Hydrochloric acid (HCl)
- Trichloroacetic acid (TCA) solution (0.75g/mL) in 0.25 M HCl.
- 2-thiobarbituric acid (TBA)
- TCA/TBA mixture. Weight 0.1875 g TBA and dissolve with TCA solution. Complete to volume with 0.25 M HCl in a 50 mL volumetric flask
- 0.5 mg/mL 1,1,3,3-tetraethoxypropane (TEP) aqueous solution, used as standard for construction of the calibration curve.
- UV-Vis spectrophotometer (Hitachi U-2000)
- Falcon® centrifuge tubes, screw-capped glass test tubes
- Vortex, water bath and centrifuge

#### *Experimental procedure*

##### *i) Calibration*

TEP standard solutions with concentrations ranging from 0.192 to 7.5 µg/mL were obtained according to Table A-6. 1.0 mL of each standard solution was taken in screw-capped glass test tubes. Subsequently, 2 mL of a TCA/TBA mixture were added and the glass test tube was tightly closed, vortexed for 15 s and immersed in a water bath at 95 °C during 15 min. Then the vials were cooled down under running cold water and centrifuged at 5000 rpm during 10 min. Immediately afterwards, the supernatant was collected, and its absorbance measured in a Hitachi U-2000 spectrophotometer at  $\lambda = 538$  nm.



**Table A-6.** Calibration solutions of 1,1,3,3-tetraethoxypropane (TEP) for TBARS quantification in O/W emulsions.

	Take (mL) ; from	Complete to (mL) with H <sub>2</sub> O	[TEP] (μg/mL)
<b>STD-0</b>	-	-	500*
<b>STD-1</b>	0.750 ; STD-0	50	7.5
<b>STD-2</b>	10 ; STD-1	25	3.0
<b>STD-3</b>	10 ; STD-2	25	1.2
<b>STD-4</b>	10 ; STD-3	25	0.48
<b>STD-5</b>	10 ; STD-4	25	0.192

\*not measured

The calibration curve used in this work is defined in Eq. A-3.3.1.

$$\text{Abs}_{\lambda=538 \text{ nm}} = 0.2397 \cdot [\text{TEP}] (\mu\text{g/mL}) - 0.0041; (R^2 = 0.9997) \quad (\text{A-3.3.1})$$

#### ii) Determination of TBARS

TBARS analysis in O/W emulsions was performed the same as in the calibration procedure, yet with 0.025-1.0 mL of emulsion instead, depending on the oxidative status of the sample, and completing up to 1.0 mL with distilled water if necessary. Blank runs were also carried out with 1.0 mL of distilled water only.

#### Calculations

TBARS content in the samples, expressed as mg malonaldehyde (MDA)/kg oil, was calculated according to Eq. A-3.3.2, where  $\text{Abs}_{\lambda=538 \text{ nm}}$  is the absorbance of the sample against blank;  $a$  and  $b$  are the slope and intercept of the calibration curve (Eq. A-3.3.1), respectively;  $m_{\text{oil}}$  is the exact oil content in the sample (g); and  $\text{MW}_{\text{MDA}}$  and  $\text{MW}_{\text{TEP}}$  are the molecular weights of malondialdehyde and 1,1,3,3-tetraethoxypropane (72.06 and 220.31 g/mol, respectively).

$$\text{TBARS} = \frac{(\text{Abs}_{\lambda=538\text{nm}} - b)}{a \cdot m_{\text{oil}}} \cdot \frac{\text{MW}_{\text{MDA}}}{\text{MW}_{\text{TEP}}} \quad (\text{A-3.3.2})$$

### 3.4. Encapsulation efficiency

Encapsulation efficiency (EE) of the fish oil microparticles was determined according to the method described by Wang *et al.* [17] with some modifications. EE can be defined as the amount of encapsulated bioactive, related to the total bioactive load in the particle. In this work, the encapsulated omega-3 concentrate has been calculated as the difference between total omega-3 concentrate in the microparticle and the non-encapsulated omega-3 concentrate present in the particle surface (Eq. (A-3.5.1)).

$$EE(\%) = \frac{TO - nEO}{TO} \cdot 100 \quad (A-3.5.1)$$

where TO is the total oil content and nEO is the non-encapsulated oil. Total oil and non-encapsulated oil were analyzed separately as described in sections 3.5.1 and 3.5.2, respectively.

#### 3.4.1. Total oil

Total oil is defined as the amount of oil removed with an organic solvent after destroying the coating material. In this case, since the coating material is mainly composed by a polysaccharide (octenyl-succinic-anhydride-modified starch), the method followed to determine the total oil content was an acid digestion, according to AOAC Official Method [18].

#### *Material and reagents*

- Absolute ethanol
- Hydrochloric acid 37 %
- Diethyl ether
- Screw-capped glass tubes
- 50 mL conical Falcon® centrifuge tubes
- Round-bottom flasks
- Centrifuge, vortex, rotary evaporator, and water bath



### Procedure

Approximately 1.0 g of particles was weighed in a screw-capped glass tube and dissolved in 2 mL of ethanol. The mixture was vortexed for 15 s and 10 mL of 37 % HCl were added. Subsequently, each tube was tight-closed, vortexed again during 15 s and introduced in a water bath at 100 °C during 10 min. Digested samples were cooled down to ambient temperature and transferred to 50 mL Falcon centrifuge tubes, rinsing the glass tubes with 10 mL of ethanol. Afterwards, 25 mL of diethyl ether were added to the diluted samples, tubes were closed, and phases were mixed by inversion several times. Samples were centrifuged at 3000 rpm during 20 min and then 5 mL of the organic phase with the extracted oil were taken and transferred to tared round-bottom flasks in order to evaporate the solvent under vacuum (Heidolph rotary evaporator). After that, the round-bottom flask with the oil residue was weighed again. Blanks with *ca.* 1.0 g of the carrier were submitted to the same procedure for determination of fat traces, which were subtracted from the total oil content of the powders.

### Calculations

Total oil in the samples, expressed as mg / g solid, was determined by mass difference of the initial clean round-bottom flask and that containing the extracted oil residue (Eq. A-3.5.2).

$$TO = \frac{V_1}{V_2} \frac{(m_f - m_0)}{m_s} 1000 \quad (\text{A-3.5.2})$$

where  $m_0$  is the weight (g) of the empty round-bottom flask,  $m_f$  is the weight of the flask with the oil residue (g),  $m_s$  is the weight of solid sample (g),  $V_1$  is the total amount of organic solvent added (mL), and  $V_2$  is the amount of the organic solvent aliquot taken to the glass vessel (mL).



### 3.4.2. Non-encapsulated oil

Non-encapsulated oil in oil microcapsules is defined as the fraction of total oil that is removed by washing the solid with an organic solvent such as hexane. Since the oil extracted by the organic solvent is too low to be determined gravimetrically, it was measured by UV-Vis spectrometry taking in to account the absorbance of fish oil at  $\lambda = 286$  nm, which is due to the presence of unsaturated compounds.

#### *Material and reagents*

- Hexane
- 50 mL conical Falcon® centrifuge tubes
- disposable syringes and microfilters (0.45  $\mu\text{m}$ )
- UV-Vis spectrophotometer (Hitachi U-2000)
- Centrifuge

#### *Experimental procedure*

##### *i) Calibration*

Calibration solutions were prepared from a primary organic solution of the fish oil concentrate used in encapsulation experiments in hexane (0.005 g/mL) (M-1) according to Table A-7.

**Table A-7.** Calibration solutions of fish oil concentrate for quantification of non-encapsulated oil.

	<b>Take (mL) from</b>	<b>Complete to (mL) with hexane</b>	<b>[Fish oil concentrate] (mg/mL)</b>
S-1	0.1 ; M-1	5	1.000
S-2	0.15 ; M-1	10	0.75
S-3	2.5 ; S-1	5	0.50
S-4	2.5 ; S-3	5	0.25
S-5	2.5 ; S-4	5	0.125
S-6	2.5 ; S-5	5	0.0625



Each fish oil concentrate concentration should be at least duplicated. Experimental calibration curve used in this work is defined in Eq. A-3.5.3.

$$\text{Abs}_{\lambda=286 \text{ nm}} = 1.0655 \cdot [\text{fish oil concentrate}] + 0.0548; \quad (R^2 = 0.9995) \quad (\text{A-3.5.3})$$

#### ii) Removal of the non-encapsulated fish oil

Accurately, 1 g of solid sample was weighed in a 50 mL conical Falcon® tube and suspended in 25 mL of hexane. The mixture was vortexed for 15 s and centrifuged during 20 minutes at 3000 rpm. After that, the hexane was taken with a disposable syringe and filtered through a microfilter (0.45 μm) for measurement at  $\lambda = 286 \text{ nm}$  in the UV-Vis spectrophotometer.

#### Calculations

Non-encapsulated fish oil concentrate in the particles, expressed as mg oil/g solid, was calculated according to Eq. A-3.5.4, where  $\text{Abs}_{\lambda=286 \text{ nm}}$  is the absorbance of the sample against blank;  $a$  and  $b$  are the slope and intercept of the calibration curve (Eq. A-3.5.3), respectively;  $V_{\text{hexane}}$  is the amount of hexane used to wash the particles (mL); and  $m$  is the exact sample weight (g).

$$\text{nEO} = \frac{(\text{Abs}_{\lambda=286 \text{ nm}} - b) \cdot V_{\text{hexane}}}{a \cdot m} \quad (\text{A-3.5.4})$$



### 3.5. Moisture content

Moisture content, defined as the loss in mass of the sample on heating at 105 °C, was determined by the AOAC Official Methods 934.01 [19].

#### *Material and equipment*

- Drying oven
- Aluminium dishes
- Analytical balance ( $\pm 0.0001$  g).

#### *Analytical procedure*

An amount of sample (1 to 3 g) was weighed into a pre-weighed aluminium dish and dried in an oven at 100 – 105 °C for at least 16 - 18 hours until constant weight. After that, it was cooled to room temperature in a desiccator and weighed again. The determination was carried out in triplicate.

#### *Calculations*

Moisture content, expressed as % wt., was determined according to Eq. A-3.6.1, where  $w_o$  is the weight of the empty covered aluminum dish;  $w_1$  is the weight of dish + sample before drying and  $w_2$  is the weight of dish + sample after drying.

$$\% \text{moisture} = \frac{m_1}{m_o} = \frac{(w_2 - w_1)}{(w_1 - w_o)} \cdot 100 \quad (\text{A-3.6.1})$$

### 3.6. Analysis of thermal properties of the microparticles by Differential Scanning Calorimetry (DSC)

Differential scanning calorimetry (DSC) is a thermoanalytical technique in which the difference in the amount of heat required to increase the temperature of a sample against a reference is measured as a function of temperature. The basic principle underlying this technique is that when the sample undergoes a physical transformation (e.g., crystallization, glass transition, melting, vaporization), more or less heat will need to flow to it in order to maintain the set-point temperature and temperature ramp.

#### *Equipment*

A TA Instruments Q2000 differential scanning calorimeter with refrigerated cooling system (RCS90) and nitrogen purge gas was used (Fig. A-14). Conventional or modulated DSCs can be performed in this apparatus. In modulated DSC, a sinusoidal temperature oscillation is overlaid on the linear temperature ramp, allowing to measure heat flow simultaneously with, and independently of, changes in heat capacity. Total heat flow signal contains the sum of all thermal transitions, as in standard DSC. The reversing heat flow contains glass transition and melting transitions, while the non-reversing heat flow contains kinetic events like curing, volatilization, melting, and decomposition.



**Figure A-14.** TA Instruments Q2000 DSC with RCS90 (adapted from [www.tainstruments.com](http://www.tainstruments.com)).

### *Calibration*

Melting point and enthalpies of indium were used for temperature and heat capacity calibration.

### *Experimental procedure*

Samples (*ca.* 10 mg) were placed in TA Tzero 40- $\mu$ L aluminum pans and closed with hermetic aluminum lids with pinhole. An empty pan closed with pin-holed lid was used as a reference. Holding temperatures and temperature ramps for the analysis are summarized in Table A-8.

**Table A-8.** Temperature program used for the DSC analysis.

	<b>Rate (<math>^{\circ}</math>C / min)</b>	<b>T set point (<math>^{\circ}</math>C)</b>	<b>Hold time (min)</b>
Initial		40	30
Ramp 1	10	-80	30
Ramp 2	10	350	15

### *Data analysis*

DSC thermograms were recorded and analyzed with the Advantage v. 5.5.20 software (TA Instruments). The software allows to process DSC thermograms and set peak characteristics (onset, mid, inflection and end temperatures), and calculate enthalpies of transitions by integrating the peak corresponding to a given transition.

## 3.7. Analysis of solid microstructure by Scanning Electron Microscope (SEM)

Scanning electron microscopy (SEM) of the dried microparticles was carried out in the R&D Centre of the University of Burgos, following the procedure described in section 1.5.



## References

- [1] D. Chen, H. Zhang, J. Xu, Y. Yan, Effect of sub- and supercritical CO<sub>2</sub> treatment on the properties of *Pseudomonas cepacia* lipase., *Enzyme Microb. Technol.* 53 (2013) 110–117.
- [2] J.R. Lakowicz, *Principles of fluorescence spectroscopy*, 3rd edition, Springer Science + Business Media, LLC, New York, 2006.
- [3] A. Natalello, D. Ami, S. Brocca, M. Lotti, S.M. Doglia, Secondary structure, conformational stability and glycosylation of a recombinant *Candida rugosa* lipase studied by Fourier-transform infrared spectroscopy., *Biochem. J.* 385 (2005) 511–517.
- [4] S.E. Collins, V. Lassalle, M.L. Ferreira, FTIR-ATR characterization of free *Rhizomucor meiheii* lipase (RML), Lipozyme RM IM and chitosan-immobilized RML, *J. Mol. Catal. B Enzym.* 72 (2011) 220–228.
- [5] N. Rubio-Rodríguez, *Supercritical fluid technology for extraction, concentration and formulation of omega-3 rich oils. A novel strategy for valorization of fish by-products (PhD Thesis)*, University of Burgos, 2011.
- [6] American Oil Chemist' Society, *AOCS Official Method Cd 3d-63. Acid value* (2009).
- [7] AOAC International, *Official methods of analysis of the Association of Official Analytical Chemists. AOAC Official Method 2012.13. Determination of labeled fatty acids content in milk products and infant formula* (2012).
- [8] A. Schaefer, T. Kuchler, T.J. Simat, H. Steinhart, Migration of lubricants from food packagings. Screening for lipid classes and quantitative estimation using normal-phase liquid chromatographic separation with evaporative light scattering detection, *J. Chromatogr. A.* 1017 (2005) 107–116.
- [9] Á.G. Solaesa, M.T. Sanz, M. Falkeborg, S. Beltrán, Z. Guo, Production and concentration of monoacylglycerols rich in omega-3 polyunsaturated fatty acids by enzymatic glycerolysis and molecular distillation, *Food Chem.* 190 (2016) 960–967.
- [10] N.C. Megoulas, M.A. Koupparis, Twenty years of evaporative light scattering detection, *Crit. Rev. Anal. Chem.* 35 (2005) 301–316.
- [11] AOAC International, *Official methods of analysis of the Association of Official Analytical Chemists. AOAC Official Method 965.33 Peroxide Value of Oils and Fats* (2002).
- [12] American Oil Chemist' Society, *AOCS Official Method Cd 18-90. p-Anisidine value*, (2011).



- [13] P.J. Ke, A.D. Woyewoda, Microdetermination of thiobarbituric acid values in marine lipids by a direct spectrophotometric method with a monophasic reaction system, *Anal. Chim. Acta.* 106 (1979) 279–284.
- [14] International Standards Organization, ISO Standard 13320:2009, Particle size analysis -- Laser diffraction methods, (2009).
- [15] N.C. Shantha, E.A. Decker, Rapid, sensitive, iron-based spectrophotometric methods for determination of peroxide values of food lipids, *J. AOAC Int.* 77 (1994) 421–424.
- [16] L. Mei, D.J. McClements, J. Wu, E.A. Decker, Iron-catalyzed lipid oxidation in emulsion as affected by surfactant, pH and NaCl, *Food Chem.* 61 (1998) 307–312.
- [17] Y. Wang, W. Liu, X. Dong, C. Selomulya, Micro-encapsulation and stabilization of DHA containing fish oil in protein-based emulsion through mono-disperse droplet spray dryer, *J. Food Eng.* 175 (2016) 74–84.
- [18] AOAC International, Official methods of analysis of the Association of Official Analytical Chemists. AOAC Official Method 925.32. Fat in eggs, acid hydrolysis method (2005).
- [19] AOAC International, Official methods of analysis of the Association of Official Analytical Chemists. AOAC Official Method 934.01 Moisture in Animal Feed (1998).

# *Curriculum Vitae*

## **Rodrigo Melgosa Gómez**

Born in August 24th, 1989 in Burgos (Spain)

Location: Burgos

e-mail: [r.melgosa89@gmail.com](mailto:r.melgosa89@gmail.com)

Scopus Author ID: [55933027100](https://orcid.org/0000-0003-2130-2422)

ORCID: <http://orcid.org/0000-0003-2130-2422>

ResearcherID: [I-4538-2015](https://orcid.org/0000-0003-2130-2422)

### Profile

Agricultural Engineer (2010) and BSc in Food Science and Technology (2013) by the University of Burgos, obtaining in both degrees the Special End of Studies Prize upon graduation. After receiving my MSc in Food Safety and Biotechnology by the University of Burgos (2014), I started PhD studies in the program “Advances in Food Science and Biotechnology”, in the University of Burgos.

I carried out my end-of-BSc and MSc Projects in the Chemical Engineering Section of the University of Burgos, hired as research assistant (2013-2014). Since the beginning of my PhD studies, I benefit from a pre-doctoral grant financed by the Ministry of Economy and Competitiveness of Spain (Ref.: BES-2013-063937).

I am part of the research group Industrial and Environmental Biotechnology (BIOIND). We have published the results of our research in 13 scientific papers and presented them in national and international scientific meetings.

### Education

---

<b>2014-2018</b>	PhD student in “Advances in Food Science and Biotechnology”, University of Burgos, Spain
<b>2013-2014</b>	MSc in Food Safety and Biotechnology University of Burgos, Spain
<b>2010-2013</b>	BSc in Food Science and Technology University of Burgos, Spain
<b>2007-2010</b>	AS in Agricultural Engineering University of Burgos, Spain

---

## Employment

---

<b>2014-2018</b>	PhD fellowship in the Department of Biotechnology and Food Science, University of Burgos, Spain (Ref.: BES-2013-063937)
<b>2013-2014</b>	Research Assistant in the Department of Biotechnology and Food Science, University of Burgos, Spain (Ref.: CTQ2012-39131-C02-01)
<b>2012-2013</b>	Research Scholar in IGMO S.L., Burgos (Spain)

---

## Short research visits

---

<b>2016</b> (4 months)	Matís Ohf. (Reykjavík, Iceland)
<b>2014</b> (3 weeks)	University of Strathclyde, Glasgow, Scotland (UK) Socrates Course: Process Intensification by High Pressure Technologies (PIHPT) – Actual Strategies for Energy and Resources Conservation

---

## Publications compiled in the PhD Thesis

1. R. Melgosa, Ó. Benito, M.T. Sanz, E. de Paz, S. Beltrán, Omega-3 encapsulation by PGSS-drying and conventional drying methods. Particle characterization and oxidative stability, *Food Chemistry* (*submitted*)
2. R. Melgosa; M.T. Sanz; Á.G. Solaesa; S. Beltrán. Phase behaviour of the pseudo-ternary system carbon dioxide + ethanol + fish oil at high pressures. *Journal of Chemical Thermodynamics*. 115, pp. 106–113. 2017
3. R. Melgosa; M. Teresa Sanz; A.G. Solaesa; E. de Paz; S. Beltrán; D.L. Lamas. Supercritical carbon dioxide as solvent in the lipase-catalyzed ethanolysis of fish oil: kinetic study. *Journal of CO<sub>2</sub> Utilization*. 17, pp. 170–179. 2017.
4. R. Melgosa; M.T. Sanz; Á.G. Solaesa; S.L. Bucio; S. Beltrán. Enzymatic activity and conformational and morphological studies of four commercial lipases treated with supercritical carbon dioxide. *The Journal of Supercritical Fluids*. 97, pp. 51–62. 2015.

## Co-authored publications

5. A.E. Illera; M.T. Sanz; O. Benito-Román; S. Varona; S. Beltrán; R. Melgosa; A.G. Solaesa. Effect of thermosonication batch treatment on enzyme inactivation kinetics and other quality parameters of cloudy apple juice. *Innovative Food Science and Emerging Technologies*. 47, pp. 71–80. 2018.
6. A.E. Illera; M.T. Sanz; S. Beltrán; R. Melgosa; A.G. Solaesa; M.O. Ruiz. Evaluation of HPCD batch treatments on enzyme inactivation kinetics and selected quality characteristics of cloudy juice from Golden delicious apples. *Journal of Food Engineering*. 221, pp. 141–150. 2018.
7. Á.G. Solaesa; M.T. Sanz; R. Melgosa; S. Beltrán. Substrates emulsification process to improve lipase-catalyzed sardine oil glycerolysis in different systems. Evaluation of lipid oxidation of the reaction products. *Food Research International*. 100, pp. 572–578. 2017.
8. H. Briongos; A.E. Illera; M.T. Sanz; R. Melgosa; S. Beltrán; A.G. Solaesa. Effect of high pressure carbon dioxide processing on pectin methylesterase activity and other orange juice properties. *LWT-Food Science and Technology*. 74, pp. 411–419. 2016.
9. Á.G. Solaesa; M.T. Sanz; S. Beltrán; R. Melgosa. Kinetic study and kinetic parameters of lipase-catalyzed glycerolysis of sardine oil in a homogeneous medium. *Cuihua Xuebao/Chinese Journal of Catalysis*. 37(4), pp. 596–606. 2016.
10. S.L. Bucio; M.T. Sanz; S. Beltrán; R. Melgosa; Á.G. Solaesa; M.O. Ruiz. Study of the influence of process parameters on liquid and supercritical CO<sub>2</sub> extraction of oil from rendered materials: Fish meal and oil characterization. *The Journal of Supercritical Fluids*. 107, pp. 270–277. 2016.
11. Á.G. Solaesa; M.T. Sanz; R. Melgosa; S.L. Bucio; S. Beltrán. Glycerolysis of sardine oil catalyzed by a water dependent lipase in different *tert*-alcohols as reaction medium. *Grasas y Aceites*. 66(4), e102. 2015.
12. S.L. Bucio; Á.G. Solaesa; M.T. Sanz; R. Melgosa; S. Beltrán; H. Sovová. Kinetic study for the ethanolysis of fish oil catalyzed by Lipozyme<sup>®</sup> 435 in different reaction media. *Journal of Oleo Science*. 64(4), pp. 431–441. 2015.
13. S.L. Bucio; A.G. Solaesa; M.T. Sanz; S. Beltrán; R. Melgosa. Liquid-liquid equilibrium for ethanolysis systems of fish oil. *Journal of Chemical and Engineering Data*. 58(11), pp. 3118–3124. 2013.

### Oral communications

R. Melgosa, M.T. Sanz, Á.G. Solaesa, S. Beltrán, “Modificación enzimática de aceite de pescado en CO<sub>2</sub> supercrítico” in *II Jornadas de Doctorandos de la Universidad de Burgos*. December 2015, Burgos (Spain).

R. Melgosa, M.T. Sanz, Á.G. Solaesa, S. Beltrán, “Valorization of fish oil to obtain omega-3 rich concentrates through biocatalysis in supercritical carbon dioxide media” in *11th International Symposium on Supercritical Fluids*. October 2015, Seoul (Republic of Korea).

R. Melgosa, M.T. Sanz, Á.G. Solaesa, A.V. Merchán, D.L. Lamas, S. Beltrán, “Fish oil ethanolysis by Lipozyme RM IM in supercritical CO<sub>2</sub>” in *VIII reunión de Expertos en Tecnologías de Fluidos Comprimidos (FLUCOMP)*. September 2015, Cádiz (Spain).

### Poster presentations

R. Melgosa, M.T. Sanz, Á.G. Solaesa, S. Beltrán, “High-pressure phase equilibria of the pseudo-ternary system CO<sub>2</sub> + ethanol + fish oil” in *16th European Meeting on Supercritical Fluids*. April 2017, Lisbon (Portugal).

R. Melgosa, M.T. Sanz, Á.G. Solaesa, S. Beltrán, “Enzymatic modification of fish oil in supercritical carbon dioxide” in *15th European Meeting on Supercritical Fluids*. May 2016, Essen (Germany).

R. Melgosa, M.T. Sanz, Á.G. Solaesa, A.V. Merchán, D.L. Lamas, S. Beltrán, “Fish oil ethanolysis by Lipozyme RM IM in supercritical CO<sub>2</sub>” in *10th European Congress of Chemical Engineering*. Sept-Oct 2015, Nice (France).

R. Melgosa, M.T. Sanz, S. Beltrán, “Efecto del tratamiento con CO<sub>2</sub> supercrítico sobre la actividad de distintas lipasas” and R. Melgosa, M.T. Sanz, S. Beltrán, Á.G. Solaesa, S.L. Bucio, “Etanolisis enzimática de aceite de pescado en CO<sub>2</sub> supercrítico” in *VII reunión de Expertos en Tecnologías de Fluidos Comprimidos (FLUCOMP)*. June 2014, Barcelona (Spain).

R. Melgosa, M.T. Sanz, S. Beltrán, “Evaluation of the residual activity of immobilized and free lipases treated with supercritical carbon dioxide” and R. Melgosa, M.T. Sanz, S. Beltrán, Á.G. Solaesa, S.L. Bucio, “Lipase catalyzed ethanolysis of fish oil in supercritical carbon dioxide” in *14th European Meeting on Supercritical Fluids*. May 2014, Marseille (France).

R. Melgosa, M.T. Sanz, S. Beltrán, “Evaluación de la estabilidad enzimática y de la influencia de la presión y la temperatura sobre reacciones enzimáticas en dióxido de carbono supercrítico” in *XXXIV Reunión Bienal Real Sociedad Española de Química (RSEQ)*. September 2013, Santander (Spain).